



Electrochemical Dissolution and Passivation Phenomena of Gold Cyanidation from Roasted Ore In the Presence of Iron Oxides

Thèse

Ahmet Deniz Bas

**Doctorat en génie des matériaux et de la métallurgie
Philosophiæ doctorat (Ph. D.)**

Québec, Canada

© Ahmet Deniz Bas, 2017

**Electrochemical Dissolution and Passivation
Phenomena of Gold Cyanidation from Roasted
Ore In the Presence of Iron Oxides**

Thèse

Ahmet Deniz Bas

Sous la direction de :

Edward Ghali, directeur de recherche

Résumé

Cette thèse de doctorat est divisée en des études sur l'or pur; la corrosion galvanique; et la polarisation de l'or en présence d'oxydes de fer contenus dans un minerai d'or grillé. La dissolution de l'or diminue en présence de magnétite et, augmente en présence d'hématite et de maghémite. Des produits de corrosion et des couches adsorbées ralentissent la dissolution d'or. Pour les études sur l'or pur, une augmentation du pH de 10 à 11 a réduit de 35 fois la densité de courant, alors qu'elle a augmentée de 32 fois en diminuant l'agitation de 100 à 60 tr/min. Les études potentiostatiques, à trois potentiels anodiques, montrent que l'augmentation de la concentration de cyanure, du pH, et du potentiel diminuent la densité de courant. Des films d'oxydes d'or ont été identifiés par XPS. La mesure du bruit électrochimique est un outil prometteur pour estimer la vitesse de corrosion in situ.

Pendant les tests de corrosion galvanique, utilisés en mode ampèremètre zéro-résistance, les électrodes minérales testées ont eu un effet négatif sur la lixiviation de l'or selon l'ordre décroissant : magnétite, magnétite-hématite avec des surfaces égales, et minerai d'or grillé. Cependant, la maghémite et l'hématite ont eu un effet positif. La concentration d'ions solubles et la vitesse de diffusion pourraient retarder ou favoriser la dissolution. L'argent a été identifié par XPS sur la surface de l'or, suggérant, une passivation partielle.

À partir des études de polarisation potentiodynamique, l'hématite, en tant que composé système "combiné d'anode Au-hématite", favorise le courant de corrosion anodique de 12%, alors que la magnétite abaisse le courant (de 11%). Les études de deux cellules séparées ont été réalisées pour révéler l'influence des ions solubles dans la dissolution de l'or. Le balayage du potentiel circuit ouvert jusqu'à vers des valeurs cathodiques en présence d'oxygène atmosphérique et de cyanure montre des vitesses de corrosion, déduites des pentes de Tafel, sont proches des à valeurs industrielles. La vitesse de lixiviation de l'or diminue de 40% en présence de pulpe de magnétite, alors que celle-ci augmente, respectivement de 25% et 10% pour l'hématite et la maghémite. MEB-EDX confirment l'effet négatif de la magnétite par la présence d'une forte accumulation d'oxydes de fer sur la surface de l'or. De faibles quantités d'or ont été identifiées sur les particules de magnétite par XPS. La séparation magnétique des résidus de cyanuration a été suivie la caractérisation électrochimique du concentré et des rejets.

Abstract

This Ph.D. thesis is divided into studies using pure gold; galvanic corrosion; and gold polarization in presence of iron oxides of roasted gold ore. Gold dissolution decreases in the presence of magnetite, and increases in the presence of hematite, and maghemite. The corrosion products and adsorbed layers lead to a slowdown of gold dissolution. For pure gold study, increasing pH from 10 to 11 results in a current density lower by 35 times, while it increases by 32 times with decreasing agitation from 100 to 60 rpm. At three anodic potentials, potentiostatic studies show that increasing cyanide concentration, pH, and potential decrease the current density. Au oxides have been identified by XPS. Electrochemical noise measurement is promising tool with its in-situ corrosion rate estimation.

In galvanic corrosion studies, employing zero-resistance ammeter (ZRA) mode, the tested mineral electrodes show a negative effect on gold leaching in decreasing order: magnetite, magnetite-hematite with equal surfaces, and roasted gold ore. However, maghemite and hematite show a positive effect. Concentration of soluble ions and diffusion rate could retard or promote gold dissolution. Silver has been identified by XPS on gold surface suggesting partial passivation.

In potentiodynamic polarization studies, hematite, as a part of the combined “Au-hematite anode” system promotes anodic corrosion current by 12%, while magnetite shows negative effect (11%). Two separate container tests have been considered to examine the influence of soluble ions on gold dissolution. Scanning from open circuit potential to more cathodic values in presence of atmospheric oxygen and cyanide shows corrosion rates obtained from Tafel slopes close to industrial practice. Gold leach rate decreases by 40% with magnetite slurry, whereas it increased by 25% and 10% for hematite and maghemite, respectively. SEM-EDS findings have confirmed the negative effect of magnetite due to the high accumulation of iron oxides on the gold surface. Low amounts of gold in magnetite particles are identified by XPS. Magnetic separation of leach tailings has been followed by electrochemical characterisation of the concentrate and the residues.

Table of Contents

Résumé	iii
Abstract	iv
Table of Contents	v
List of Tables	ix
List of Figures	x
Acknowledgements	xvi
Foreword	xviii
Chapter 1 Introduction.....	1
1.1 State of the Technology.....	2
1.2 Scientific Problem and Objectives of This Project.....	2
1.3 Description of the Strategy Adapted to This Ph.D. Thesis.....	3
1.4 Key Contributions of This Ph.D. Project.....	5
Chapter 2 Critical Review of Electrochemical Dissolution of Gold	9
Résumé	11
Abstract	12
2.1 Leaching and Types of Gold Ores.....	13
2.2 Electrochemical Dissolution of Gold	14
2.3 Passivation Phenomenon and Inhibition of Gold Dissolution.....	15
2.4 Electrochemical Methods Used in Gold Dissolution Studies.....	17
2.4.1 Potentiodynamic polarization	19
2.4.2 Cyclic Voltammetry (CV)	24
2.4.3 Potentiostatic and Galvanostatic Polarization Methods	25
2.4.4 Galvanic Corrosion by Zero Resistance Ammeter	26
2.4.5 Electrochemical Noise Measurement (ENM).....	26
2.4.6 Scanning Reference Electrode Technique (SRET).....	28
2.4.7 Electrochemical Impedance Spectroscopy (EIS).....	28
2.5 Electrochemical Studies of Gold Cyanidation.....	29
2.5.1 Pure Gold Studies	29
2.5.2 Sulphidic Gold Ore Studies	33
2.5.3 Oxidised Gold Ores Studies	35
2.6 Interpretation of Electrochemical Findings	38

2.6.1 Practical Implications	38
2.6.2 The Mechanism of Dissolution Slowdown During Cyanidation.....	43
Chapter 3 Electrochemical Behaviour of Pure Gold in Cyanide Solutions.....	48
Résumé	49
Abstract	50
3.1 Introduction	51
3.2 Experimental Conditions	53
3.2.1 Ore Sample and Roasted Gold Ore Electrode Preparation	53
3.2.2 Cyclic Voltammetry, Potentiodynamic, and Potentiostatic Tests Procedures.....	53
3.2.3 Electrochemical Noise (EN) Measurement Test Procedure	54
3.2.4 Procedure of Surface Characterization Test	55
3.3 Results and Discussion	55
3.3.1 CV without Agitation and Potentiodynamic Tests	55
3.3.2 Effect of pH on Anodic Behaviour of Gold.....	62
3.3.3 Potentiostatic Tests at Different Anodic Potentials	64
3.3.4 Electrochemical Noise Measurements (ENM)	65
3.3.5 Surface Characterization.....	72
3.4 Conclusions	73
3.5 Acknowledgements	74
Chapter 4 Galvanic Interactions Between Gold and Iron Oxide Electrodes in Cyanide Solutions	75
Résumé	76
Abstract	77
4.1 Introduction	78
4.2 Experimental.....	79
4.2.1 Ore Sample	79
4.2.2 Material and Preparation of Electrodes	80
4.2.3 Electrochemical Test Procedure	81
4.3 Results	81
4.3.1 Peak Determination by Cyclic Voltammetry (CV)	81
4.3.2 Galvanic Dissolution of Gold	83
4.4 Conclusions	93
4.5 Acknowledgements	94
Chapter 5 Electrochemical Behaviour of Roasted Gold Ore During Cyanidation	95

Résumé	96
Abstract	97
5.1 Introduction	98
5.2 Experimental Conditions	100
5.2.1 Roasted Gold Ore Sample	100
5.2.2 Material and Preparation of Electrodes	100
5.2.3 Electrochemical Test Procedures	101
5.2.4 Conventional Cyanide Leaching	104
5.3 Results and Discussion	104
5.3.1 Dissolution Behaviour of Gold at Open Circuit Potentials (OCP)	104
5.3.2 Potentiodynamic Polarization of Au, RGO, and Oxide Mineral Electrodes	112
5.3.3 Effect of Leaching Parameters on Anodic Polarization of RGO Electrode	114
5.3.4 Corrosion Rate of Au, RGO, and Combined Disc Electrodes	120
5.4 Conclusions	125
5.5 Acknowledgements	127
Chapter 6 Electrochemical Interactions Between Gold and Iron Oxide Minerals	128
Résumé	129
Abstract	130
6.1 Introduction	131
6.2 Experimental Conditions	133
6.2.1 Material and Preparation of Electrodes	133
6.2.2 Electrochemical Procedures	134
6.3 Results and Discussion	136
6.3.1 Potentiodynamic Cathodic Polarization of Gold and Roasted Gold Ore	136
6.3.2 Combined Anode Electrode Polarization (CAP) System	138
6.3.3 Interpretation of Electrochemical Findings	143
6.4 Conclusions	153
6.5 Acknowledgements	155
Chapter 7 Influence of Iron Oxide Slurries on the Dissolution of Gold Electrode	156
Résumé	157
Abstract	158
7.1 Introduction	160
7.2 Experimental Conditions	162

7.2.1 Ore Sample and Iron Oxide Minerals	162
7.2.2 Electrochemical and Leaching Test Procedures	163
7.2.3 Magnetic Separation Tests.....	164
7.3 Results and Discussion	164
7.3.1 The Influence of Cyanidation on the Open Circuit Potential (OCP) of Au.....	164
7.3.2 Corrosion Rate of Au by Cathodic Polarization and Conventional Leaching	166
7.3.3 SEM-EDS, and XPS studies.....	171
7.3.4 Cyanidation of RGO and Gold Recovery from Magnetic Concentrate.....	173
7.3.5 Electrochemical Characterization of the Magnetic Concentrate and Tailings.....	177
7.3.6 Influence of Iron Oxides on Gold Dissolution	182
7.4 Conclusions	184
7.5 Acknowledgements	185
Chapter 8 Conclusions and Recommendations	186
8.1 Evaluation of Dissolution and Passivation Phenomena.....	187
8.2 Recommendations for Future Studies.....	191
References	192
Appendix A Passive Behaviour of Gold in Sulphuric Acid Medium.....	209
Appendix B Electrochemical Study of Gold Cyanidation in the Presence of Roasted Gold Ore and Its Associated Oxide Minerals.....	211
Appendix C Complimentary Activities during the Doctoral Formation	213
Appendix D Scientific Publications	214

List of Tables

Table 2.1 A brief summary of the electrochemical methods used for gold cyanidation (<i>continue on the next page</i>).	18
Table 2.2 Gold anodic dissolution profiles at different conditions (Nicol, 1980).	21
Table 2.3 Comparison of the polarization potential range from some selected papers.	23
Table 2.4 Comparison of the peak current densities.	31
Table 2.5 Comparison of dissolution rates of gold from some selected papers.	39
Table 2.6 Gold deportment results of carbon-in-leach tailings and the techniques used to analyse forms of gold (Total assayed gold = 3.4 g/L) (Dimov and Hart, 2014).	45
Table 5.1 Corrosion potentials of different electrodes in absence and in presence of gold ore slurry in 0.04 M NaCN solution, pH 10.5 at 25 °C.	105
Table 5.2 Dissolution rate (calculated from cathodic Tafel polarization slope) of electrodes (pure gold (Au) electrode with a surface of 1 cm ² , roasted gold ore (RGO) electrode with a surface area of 4.9 cm ²) (* ¹ is calculated by extrapolating Tafel slope to OCP for comparison).	122
Table 6.1 Important electrochemical terms on gold polarization with disc electrodes.	145
Table 7.1 Open Circuit Potential (OCP) (V/SHE) of electrodes for 2 minutes prior and after 4 h of leaching.	165
Table 7.2 Corrosion rates of Au in different conditions (Pure Au electrode: 0.25 cm ²).	166
Table 7.3 Influence of lead nitrate on the cyanidation of roasted gold ore, pH: 10.5, NaCN: 0.01 M, 24 h.	173
Table 7.4 Conductivities of iron oxide minerals (Barroso-Bogeat et al., 2014).	183

List of Figures

Fig. 1.1 A representative illustrations of the strategy adapted.	3
Fig. 1.2 A representative illustration of the methodology and approach adapted in this thesis	8
Fig. 2.1 Gold processing routes of the top 20 global gold producers in 2011 (Adams, 2016).	14
Fig. 2.2 Cathodic and anodic Tafel polarization diagram (ASTM G3-89, 2006).....	20
Fig. 2.3 Hypothetical polarization diagram for a passivable system with anodic and cathodic branches (ASTM G3-89, 2006).	20
Fig. 2.4 Comparison of the gold anodic dissolution profiles (Nicol, 1980).	21
Fig. 2.5 Anodic (as function of cyanide concentration) and cathodic curves for gold dissolution (adapted from Kudryk and Kellogg, 1954).	44
Fig. 2.6 Polarization curves showing passivation of the anodic reaction from the work of Mills (1951), retrieved and adapted from Cathro and Walkley (1961).	44
Fig. 2.7 Superposition of reduction curves for ferric ion and of the anodic polarization curve of Type 410 stainless steel in M H ₂ SO ₄ . Curve (1) 0.01 M Fe ³⁺ at 55 cm/sec, (2) 0.066 M Fe ³⁺ at 55 cm/sec, and (3) 0.066 M Fe ³⁺ at 100 cm/sec. In case (3) the limiting diffusion current density for the ferric ion is greater than the critical current density for the steel and the ferric ion therefore passivates the steel (adapted from Scully, 1966).	47
Fig. 3.1 Cyclic voltammetry of pure gold electrode (Au, 1 cm ²) in the first two cycles (CV I and II) without agitation (dotted arrow indicates the return) in 0.04 M NaCN solution in oxygen-free conditions at pH 10.5.	56
Fig. 3.2 Effect of NaCN concentration on anodic potentiodynamic behaviour of gold electrode (Au, 1 cm ²) (NaCN: 0.005 - 0.2 M, pH 10.5, T: 25°C, scan rate: 0.166 mV/s and argon bubbling).	57
Fig. 3.3 Potentiodynamic and cyclic voltammetry test of pure gold electrode (Au, 1 cm ²) at 100 rpm agitation in 0.04 M NaCN solution in oxygen-free conditions at pH 10.5.	60
Fig. 3.4 Influence of oxygen on anodic potentiodynamic behaviour of pure gold (Au, 1 cm ²) and compared to roasted gold ore electrode (RGO, 4.9 cm ²) in solution with atmospheric oxygen, 100 rpm agitation in 0.04 M NaCN solution (pH 10.5), T: 25°C, scan rate: 0.166 mV/s).	61
Fig. 3.5 Effect of pH on the anodic potentiodynamic behaviour of gold electrode (Au 1 cm ²) in 0.04 M NaCN solution at 100 rpm agitation (pH: 10-12), T: 25°C, scan rate: 0.166 mV/s) (** 60 rpm agitation).	62

Fig. 3.6 Corrosion (dissolution) rates (i_{corr}) of RGO (4.9 cm ²) after 0.166 mV/s scan rate at different pH values (10.5-11.5) in 0.04 M NaCN electrolyte at 100 rpm agitation in duplicates (1. run and 2. run).	63
Fig. 3.7 Effect of potential (1 and 1.4 V) on current changes in different cyanide concentrations (0.04 and 0.1 M) using potentiostatic test (pH 10-11, T: 25°C, scan rate: 0.166 mV/s, Argon bubbling) (a: pH 10 at 1 V 0.04M NaCN; b: pH 10 at 1.4 V 0.04M NaCN; c: pH 11 at 1 V 0.04M NaCN; d: pH 11 at 1.4 V 0.04M NaCN; e: pH 11 at 1 V in 0.1M NaCN; f: pH 11 at 1.4 V in 0.1M NaCN).	64
Fig. 3.8 Potential (a) and current (b) noise recorded during 24 h immersion of gold electrode in three concentrations of NaCN (0.01, 0.04 and 0.1 M) at pH 10.5.	66
Fig. 3.9 Instantaneous measured $1/R_n$ for gold (Au 1 cm ²) immersed in three concentrations of NaCN (0.01, 0.04 and 0.1 M) and roasted gold ore (RGO 4.9 cm ²) for comparison in 0.04 M NaCN at pH 10.5.	67
Fig. 3.10 Recorded potential noise (a) and current noise (b) decay in time for two polarized gold electrodes under potentiostatic conditions at 1 and 1.4 V during 16 h immersion in NaCN solution (0.04 M).	69
Fig. 3.11 Potential noise (...) and current noise (—) for two polarized gold electrodes under potentiostatic conditions applying one active potential (a) 0.3 V and two passive potentials (b) 1 V and (c) 1.4 V immersed in NaCN solution (0.04 M) after 16h.	71
Fig. 3.12 X-ray photoelectron Spectroscopy (XPS) surface analysis for gold electrode after 2 h potentiostatic in 0.1 M NaCN at 25°C, argon bubbling and magnetically stirring at 100 rpm.	72
Fig. 4.1 Fe-oxides identified by SEM analysis from the received roasted gold ore sample.....	80
Fig. 4.2 Cyclic voltammetry (CV) of different electrodes; (a) Au (pure gold), (b) RGO (roasted gold ore), (c) Mag (magnetite), (d) Hem (hematite) disc electrodes in 0.04 M NaCN solution at pH 10.5 with scan rate of 10 mV/s, argon bubbling onto the surface of electrolyte at 25 °C.....	82
Fig. 4.3 Potentiodynamic cathodic polarization of gold (Au), and roasted gold ore (RGO) with scan rate of 0.166 mV/s at pH 10.5, 100-rpm agitation, atmospheric oxygen, 25 °C..	84
Fig. 4.4 The influence of agitation speed on the galvanic potential (a) and current (b) between gold (Au) and roasted gold ore (RGO) electrodes, pH 10.5, 25 °C, cyanide conc. 0.01 M, 25 °C, saturated atmospheric oxygen, Au electrode surface area 0.25 cm ² , RGO area 4.9 cm ²	85

Fig. 4.5 XPS surface image showing the presence of Ag on the surface of Au electrode after galvanic coupled with Au and RGO.	86
Fig. 4.6 Galvanic couple potential and ZRA vs. time at 100 rpm agitation, pH 10.5, 0.01 M cyanide conc., saturated atmospheric oxygen, 25 °C, (a) RGO (roasted gold ore electrode 4.9 cm ²) and Mag (magnetite disc electrode 4.9 cm ²); (b) RGO (roasted gold ore electrode 4.9 cm ²) and Hem (hematite disc electrode 4.9 cm ²).	87
Fig. 4.7 The influence of agitation speed on the galvanic potential (a) and current (b) between gold (Au) and magnetite electrodes, pH 10.5, 25 °C, cyanide conc. 0.01 M, 25 °C, saturated atmospheric oxygen, Au electrode surface area 0.25 cm ² , Mag area 4.9 cm ²	88
Fig. 4.8 SEM (a) and EDS (b) images of Au electrode surface after galvanic coupling with Mag disc electrode, pH 10.5 at 100-rpm, cyanide conc. 0.01 M, 25 °C, saturated atmospheric oxygen, Au electrode surface area 0.25 cm ² , Mag area 4.9 cm ²	89
Fig. 4.9 The influence of agitation speed on the galvanic potential (a) and current (b) between gold (Au) and maghemite (Mgh) electrodes, pH 10.5, 25 °C, cyanide conc. 0.01 M, 25 °C, saturated atmospheric oxygen, Au electrode surface area 0.25 cm ² , Mgh area 4.9 cm ²	91
Fig. 4.10 The influence of agitation speed on the galvanic potential (a) and current (b) between gold (Au) and MagHem-ES electrodes, pH 10.5, cyanide conc. 0.01 M, 25 °C, saturated atmospheric oxygen, Au electrode surface area 0.25 cm ² , MagHem-ES area 4.9 cm ²	91
Fig. 4.11 The influence of agitation speed on the galvanic potential (a) and current (b) between gold (Au) and hematite (Hem) electrodes, pH 10.5, cyanide conc. 0.01 M, 25 °C, saturated atmospheric oxygen, Au electrode surface area 0.25 cm ² , Hem area 4.9 cm ²	92
Fig. 5.1 Schematic illustration of Scanning Reference Electrode Technique (SRET) set-up (CE: counter electrode; RE: reference electrode; WE: working electrode).....	103
Fig. 5.2 Instantaneous measured corrosion rate ($1/R_p$) for roasted gold ore and pure gold electrodes immersed in NaCN (0.04 M) solution by ENM after potentiodynamic polarization followed by potentiostatic test (2h) in absence of agitation, pH 10.5, 25 °C.	108
Fig. 5.3 3-D SRET potential images at different immersion times in 0.04M NaCN solution at pH 10.5 and 25°C for (a) Au at 1h, (b) Au at 8 h, (c) Au at 16 h; (d) RGO at 1h, (e) RGO at 8 h and (f) RGO at 16 h.....	110

Fig. 5.4 QEMF corrosion cell vs. immersion time in 0.04M NaCN solution at pH 10.5 and 25°C for pure gold (Au) and roasted gold ore (RGO) disc electrodes.	111
Fig. 5.5 Potentiodynamic cathodic polarization of different electrodes with scan rate of 0.166 mV/s in 0.04M NaCN electrolyte at 100 rpm agitation at atmospheric oxygen, pH 10.5, 25 °C (Au** indicates the cathodic polarization by scanning from -300 mV to E_{corr}).....	112
Fig. 5.6 Potentiodynamic anodic polarization of different electrodes with scan rate of 0.166 mV/s in 0.04M NaCN electrolyte at 100 rpm agitation, pH 10.5, 25 °C (Au: 1 cm ² ; other electrodes 4.9 cm ²).....	113
Fig. 5.7 Effect of NaCN concentration on the polarization of RGO with scan rate of 0.166 mV/s at pH 10.5 at 100 rpm agitation, 25 °C.	115
Fig. 5.8 Effect of pH on the anodic polarization of RGO electrode at 0.166 mV/s scan rate in 0.04 M NaCN electrolyte at the agitation of 100 rpm, 25 °C.	117
Fig. 5.9 Effect of agitation (1: 100 rpm; 2: 250 rpm; and 3: 400 rpm) on the anodic polarization curve of pure gold (Au) electrode with scan rate of 0.166 mV/s in 0.04 M NaCN solution, pH 10.5, 25 °C.....	118
Fig. 5.10 Effect of agitation (100, 250 and 400 rpm) on the anodic polarization curve of RGO with scan rate of 0.166 mV/s in 0.04 M NaCN solution, pH 10.5, 25 °C.....	120
Fig. 5.11 Effect of agitation (100, 250 and 400 rpm) on the cathodic polarization curve of RGO with scan rate of 0.166 mV/s in 0.04 M NaCN solution, pH 10.5, 25 °C.....	122
Fig. 5.12 (a) Surface image of Au electrode after combined with RGO electrode test showing the brownish-red colour; (b) SEM image of Au electrode surface.	125
Fig. 6.1 Schematic illustration of one container (OC) electrochemical set-up for combined anode electrode polarization (CAP) tests (1: Au as working electrode; 2: mineral electrode; 3: counter electrode; 4: reference electrode; 5: pH meter; 6: slurry; 7: NaCN electrolyte; 8: magnetic bar (4 x 1 cm ²)).....	135
Fig. 6.2 The influence of oxygen and cyanide on cathodic potentiodynamic polarization of pure gold (0.25 cm ²) (a) and roasted gold ore (b) electrodes (4.9 cm ²) at 0.166 mV/s scan rate in 0.01 M NaCN electrolyte at pH 10.5 at 100 rpm agitation, 25 °C.....	137
Fig. 6.3 Effect of roasted gold ore (RGO) on gold dissolution either in one or two containers (a) in the absence of slurry, (b) in the presence of slurry (35%), in 0.01 M NaCN solution, atmospheric oxygen, pH 10.5, at 100 rpm magnetic agitation at 0.166 mV/s scan rate, 25. °C	139

Fig. 6.4 Effect of hematite (Hem) on gold dissolution either in one or two containers (a) in the absence of slurry, (b) in the presence of slurry (35%) in 0.01 M NaCN solution, atmospheric oxygen, pH 10.5, 100 rpm magnetic agitation at 0.166 mV/s scan rate, 25 °C.140

Fig. 6.5 Effect of maghemite (Mgh) on gold dissolution either in one or two containers (a) in the absence of slurry, (b) in the presence of slurry (35%) in 0.01 M NaCN solution, atmospheric oxygen, pH 10.5, 100 rpm magnetic agitation at 0.166 mV/s scan rate, 25 °C.141

Fig. 6.6 Effect of magnetite (Mag) on gold dissolution either in one or two containers (a) in the absence of slurry, (b) in the presence of slurry (35%), in 0.01 M NaCN solution, atmospheric oxygen, pH 10.5, 100 rpm magnetic agitation, 0.166 mV/s scan rate, 25 °C.143

Fig. 6.7 Anodic profile of RGO/Au combined anode polarization in two containers in the presence of slurry in 0.01 M NaCN solution, atmospheric oxygen, pH 10.5, at 100 rpm magnetic agitation at 0.166 mV/s scan rate, 25 °C.....144

Fig. 6.8 The influence of the treatment of tailings of first slurry test as a new feed slurry on the dissolution behaviour of gold for RGO/Au combined anode polarization in two separate containers in 0.01 M NaCN solution, atmospheric oxygen, pH 10.5, at 100 rpm magnetic agitation at 0.166 mV/s scan rate, 25 °C.....146

Fig. 6.9 The influence of slurry in two separated containers (TC) for RGO and Au electrode combined polarization in 0.01 M NaCN solution, atmospheric oxygen, pH 10.5, at 100 rpm magnetic agitation at 0.166 mV/s scan rate, 25 °C.....147

Fig. 6.10 The influence of magnetic pre-treatment on RGO and Au electrode combined polarization in one container in 0.01 M NaCN solution, atmospheric oxygen, pH 10.5, at 100 rpm magnetic agitation at 0.166 mV/s scan rate, 25 °C.....148

Fig. 6.11 Effect of NaCN concentration on anodic polarization of Au connected to MagHem-ES electrode at 0.166 mV/s scan rate at 100 rpm agitation, pH 10.5, 25 °C.149

Fig. 6.12 (a) Scanning electron microscopy (SEM), (b) Energy-dispersive X-ray spectroscopy (EDS) of black zone; and (c) EDS of grey zone around black one; on Au electrode after polarization test connected to MagHem-ES at 0.166 mV/s scan rate in 0.4 M NaCN solution, atmospheric oxygen, pH 10.5, at 100 rpm magnetic agitation, 25 °C.151

Fig. 6.13 Effect of agitation on anodic polarization of Au connected to MagHem-ES electrode in 0.01 M NaCN solution at 0.166 mV/s scan rate, 25 °C.153

Fig. 7.1 Corrosion rate of Au in 0.01 M NaCN, with a pH of 10.5 and 100-rpm agitation at 25 °C; cathodic polarization curves in different conditions.	167
Fig. 7.2 The influence of soluble species on the dissolution kinetics of gold (mg) after 4 h in 0.01 M NaCN, with a pH of 10.5, under 100-rpm agitation, at 25 °C by MP-AES.	170
Fig. 7.3 SEM images of coatings on the pure Au electrode after 4 h of leaching; (a) pure Au in a slurry of RGO (x 5000); (b), (c), and (d) pure Au in a slurry of Magnetite (x 100), (x 500); (x 10000), respectively; (e) EDS profile (after the magnetite test) showing Fe-Ox.....	172
Fig. 7.4 XPS profile of magnetite particles (survey spectrum and Au 4f/2 spectrum).....	173
Fig. 7.5 Processing route for maghemite-rich magnetic concentrates.....	174
Fig. 7.6 Atomic (%) of elements ($\pm 5\%$) in the magnetic concentrate and magnetic tails by XPS.	175
Fig. 7.7 SEM images of the magnetic concentrate (a) and magnetic tails (b). (The light-white phase is Fe-Ox, and the grey phase is Ca and Si).	176
Fig. 7.8 XRD profiles of the magnetic concentrate and magnetic tails (Mgh: Maghemite; Hem: Hematite; Qtz: Quartz; Cal: Calcite; Dol: Dolomite; Gp: Gypsum).	176
Fig. 7.9 Potentiodynamic cathodic polarization of roasted gold ore (RGO), magnetic concentrate (Mag Conc), magnetic tailings (Mag Tails), synthetic maghemite (Synth Mgh), and pure gold (Au) electrodes with a scan rate of 0.166 mV/s in 0.01 M NaCN electrolyte saturated with atmospheric oxygen at 100-rpm agitation, a pH of 10.5, and 25 °C (Au: 0.25 cm ² ; other electrodes: 4.9 cm ²); (a) polarization from the open circuit potential to the cathodic potential; (b) polarization from the cathodic potential to the open circuit potential.....	179
Fig. 7.10 The influence of oxygen concentration (atmospheric and bubbled (dotted line)) on the potentiodynamic cathodic polarization of synthetic maghemite (Synth Mgh) (a), roasted gold ore (RGO) (b), and magnetic tails (c) electrodes from the open circuit potential to the cathode potential with a scan rate of 0.166 mV/s in 0.01 M NaCN electrolyte at 100-rpm agitation, a pH of 10.5, and 25°C.	181
Fig. 7.11 Potentiodynamic anodic polarization of roasted gold ore (RGO), magnetic concentrate (MagConc), Magnetic tails (Mag Tails), synthetic maghemite, and pure gold (Au) electrodes with a scan rate of 0.166 mV/s in 0.01 M NaCN electrolyte saturated with atmospheric oxygen at 100-rpm agitation, a pH of 10.5, and 25 °C (Au: 0.25 cm ² ; other electrodes: 4.9 cm ²).....	182

Acknowledgements

First and foremost, I would like to express my sincere thanks and appreciation to my supervisor, Professor Edward Ghali, for his guidance and support. It has been an honour to be his student. I appreciated all the time he took to share his ideas with me, making my Ph.D. study enjoyable and productive. His dedication and diligence will always remain an inspiration in my future endeavours. He has always been supportive and given me the freedom to explore alternative paths during the course of my Ph.D. As a mentor, his contributions to my professional development are priceless.

I would like to acknowledge Dr. Fariba Safizadeh, Dr. Wei Zhang, and Dr. Liliana Gavril for their support, assistance, and contribution during this work. Special thanks are likewise expressed to Dr. Yeonuk Choi, of Barrick Gold Corporation, for his invaluable comments and ideas which serve as a strong link to the industrial practice. Mr. Georges Houlachi, of Hydro Québec, is gratefully acknowledged for his encouragement and professional advice for my career. I also thank Prof. Fathi Habashi for his encouragement in exploring different aspects of metallurgical subjects, and also for his help to find me this Ph.D. project.

Special thanks are extended to the Natural Sciences and Engineering Research Council of Canada (NSERC), Barrick Gold Corporation, and Hydro-Québec for their financial support through the R&D NSERC Program. Professional technical participations of Mrs. Vicky Dodier, Dr. Alain Adnot, Mr. André Ferland, Mr. Jean Frenette, Mr. Daniel Marcotte, and Mr. Christian Jalbert are gratefully acknowledged. My friends at Laval University Nabil Sorour, Chaoran Su, Ramzi Ishak, François K. Kadiavi, Jonathan F. Marcoux, and Michael Neil are gratefully appreciated for their friendships and help.

“To my mother, father, and brother, from Salihpaşalar, for strongly encouraging me to pursue my dreams in Canada”

“There is a crack in everything, that’s how the light gets in”
L. C.

Foreword

This thesis is composed of eight chapters and presented as articles in insertion form. The objectives, methodology, and experimental approach are presented in Chapter 1. Following, Chapter 2 provides a literature review to this thesis which is inspired from the review paper entitled “A review on electrochemical dissolution and passivation of gold during cyanidation in presence of sulphides and oxides” co-authored by Ahmet Deniz Bas, Edward Ghali, and Yeonuk Choi, and *submitted to Hydrometallurgy Journal*. Chapters 3, 4, 5, 6, and 7 present the results of this project in the form of scientific articles, and Chapter 8 highlights the general discussion and recommendations for future studies. This project was supervised by Prof. Edward Ghali and Dr. Yeonuk Choi.

Chapter 3: Active and passive behaviours of gold in cyanide solutions

Authors: Ahmet Deniz Bas^{a*}, Fariba Safizadeh^a, Wei Zhang^a, Edward Ghali^a, Yeonuk Choi^b

^aDepartment of Mining, Metallurgical and Materials Engineering, Laval University, Quebec, Canada, G1V 0A6

^bBarrick Gold Corporation, Suite 3700, 161 Bay Street P.O. Box 212, Toronto, Ontario, Canada, M5J 2S1

Journal: Trans. Nonferrous Met. Soc. China, 25, 10, 3442-3453. Elsevier.

DOI: [10.1016/S1003-6326\(15\)63981-4](https://doi.org/10.1016/S1003-6326(15)63981-4)

I did all the experimental measurements and analysis along with paper writing and presentation. The scientific revision was done by Dr. Fariba Safizadeh, Dr. Wei Zhang, Prof. Edward Ghali, and Dr. Yeonuk Choi.

The electrochemical behaviour of gold in sulphuric acid medium has also been considered as comparison to that in cyanide medium. In this regard, another article entitled “**Passive Behaviour of Gold in Sulphuric Acid Medium**” co-authored by Wei Zhag, Ahmet Deniz Bas, Edward Ghali, Yeonuk Choi, has been published in *Trans. Nonferrous Met. Soc. China*, Elsevier, 25, 6, 2037-2046. DOI: [10.1016/S1003-6326\(15\)63813-4](https://doi.org/10.1016/S1003-6326(15)63813-4). However, only its abstract was given in the **Appendix A** since this paper is considered as complimentary to Chapter 3 which is mainly presented as full manuscript on cyanide.

Chapter 4: A study of electrochemical interactions between gold and its associated oxide minerals

Authors: Ahmet Deniz Bas^{a*}, Edward Ghali^a, Yeonuk Choi^b

^aDepartment of Mining, Metallurgical and Materials Engineering, Laval University, Quebec, Canada, G1V 0A6

^bBarrick Gold Corporation, Suite 3700, 161 Bay Street P.O. Box 212, Toronto, Ontario, Canada, M5J 2S1

This article has been published in *54th Annual Conference of Metallurgists (COM 2015)*, The Metallurgy and Materials Society of CIM, The LUCY ROSATO Memorial Symposium, Toronto, Canada, August 23-26, paper no 8897.

In this work, the influence of iron oxide minerals on gold dissolution during galvanic corrosion either in one and two separate containers has been investigated. The experimental measurements and analysis along with paper writing were performed by the first author. The scientific revision was done by Prof. E. Ghali, and Dr. Y. Choi.

The electrochemical behaviour of gold in sulphuric acid medium has also been considered as compared to that in cyanide medium. In this regard, another article entitled “**Electrochemical study of gold cyanidation in the presence of roasted gold ore and its associated oxide minerals**” co-authored by Ahmet Deniz Bas, Edward Ghali, and Yeonuk Choi, and it has been published in *55th Annual Conference of Metallurgists (COM 2016)*, Electrometallurgy 2016 Symposium, Proceedings of XXVIII IMPC-Quebec, Canada, September 11-15, paper no 842. However, only its abstract was given in the **Appendix B** since this paper is considered as complimentary to Chapter 4 which is mainly presented as full manuscript.

Chapter 5: Electrochemical dissolution of roasted gold ore in cyanide solutions

Authors: Ahmet Deniz Bas^{a*}, Liliana Gavril^a, Wei Zhang^a, Edward Ghali^a, Yeonuk Choi^b

^aDepartment of Mining, Metallurgical and Materials Engineering, Laval University, Quebec, Canada, G1V 0A6

^bBarrick Gold Corporation, Suite 3700, 161 Bay Street P.O. Box 212, Toronto, Ontario, Canada, M5J 2S1

Journal: *Hydrometallurgy*, 156, 188-198. DOI: [10.1016/j.hydromet.2015.07.003](https://doi.org/10.1016/j.hydromet.2015.07.003)

In this work, the electrochemical dissolution behaviour of roasted gold ore as function of leaching parameters has been highlighted, and optimal conditions for roasted gold ore studies have also been investigated. The experimental measurements and analysis along with paper writing were performed by the first author. The manuscript was revised by Dr. L. Gavril, Dr. W. Zhang, Prof. E. Ghali, and Dr. Y. Choi.

Chapter 6: A study of the electrochemical dissolution and passivation phenomenon of roasted gold ore in cyanide solutions

Authors: Ahmet Deniz Bas^{a*}, Wei Zhang^a, Edward Ghali^a, Yeonuk Choi^b

^aDepartment of Mining, Metallurgical and Materials Engineering, Laval University, Quebec, Canada, G1V 0A6

^bBarrick Gold Corporation, Suite 3700, 161 Bay Street P.O. Box 212, Toronto, Ontario, Canada, M5J 2S1

Journal: *Hydrometallurgy*, 158, 1-9. DOI: [10.1016/j.hydromet.2015.09.020](https://doi.org/10.1016/j.hydromet.2015.09.020)

In this work, the influence of iron oxide minerals on gold dissolution has been examined by Combined Anode Electrodes Polarization, as a new approach. The experimental measurements and analysis along with paper writing were performed by the first author. The manuscript was revised by Dr. Wei Zhang, Prof. E. Ghali, and Dr. Yeonuk Choi.

Chapter 7: Leaching and electrochemical dissolution of gold in the presence of iron oxide minerals associated with roasted gold ore

Authors: Ahmet Deniz Bas^{a*}, Fariba Safizadeh^a, Edward Ghali^a, Yeonuk Choi^b

^aDepartment of Mining, Metallurgical and Materials Engineering, Laval University, Quebec, Canada, G1V 0A6

^bBarrick Gold Corporation, Suite 3700, 161 Bay Street P.O. Box 212, Toronto, Ontario, Canada, M5J 2S1

Journal: *Hydrometallurgy*, 166, 143-153. DOI: [10.1016/j.hydromet.2016.10.001](https://doi.org/10.1016/j.hydromet.2016.10.001)

In this work, the implication of electrochemical findings in conventional cyanidation has been tested by considering cathodic Tafel slope only as a new approach. The experimental measurements and analysis along with paper writing were performed by the first author. The manuscript was revised by Dr. Fariba Safizadeh, Prof. E. Ghali, and Dr. Yeonuk Choi.

Finally, **Chapter 8** provides general conclusions for this thesis as well as few recommendations for future work plan.

Chapter 1

Introduction

1.1 State of the Technology

It is worth mentioning that due to the rapid depletion of free-milling types of gold ores, it is accepted worldwide that there is an increasing trend for the treatment of refractory gold ores which often require oxidation, such as roasting, as a pre-treatment process prior to cyanidation. As a result, in recent years, the treatment of oxidised gold ores by electrochemical methods and conventional cyanidation is therefore becoming essential for R&D, and for the mining industry. Up to now, almost all the electrochemical studies of gold ores have been performed using sulphidic ones, and there is a paucity for the electrochemical studies of oxidised gold ores. Usually, oxide gold ores do not present any issue (easy to leach and low reagent consumption). Although many studies have been carried out on the anodic behaviour of gold using cyclic voltammetry, potentiodynamic, and ZRA (zero-resistance ammeter) mode galvanic corrosion tests, there is still a doubt on gold passive phenomenon. These advancements in the processing of gold ores have shown the importance and necessity of electrochemical characterisation studies for oxidised and more complex gold ores.

1.2 Scientific Problem and Objectives of This Project

During cyanidation of gold, in some conditions, the dissolution rate of gold could slow down which results in longer retention times and/or poor gold extractions. It is a big problem for the mining industry. In this Ph.D. project, oxidised/roasted gold ore sample from Barrick Gold Corporation (BGC) is used to examine the electrochemical dissolution of roasted gold ore. At BGC cyanidation plant, ~ 90% of gold is leached from the roasted gold ore whereas an 10% rest in the leach residue. Passivation could be responsible for this unrecovered gold. It is worth noting that passivation of gold could be due to adsorbed species, corrosion products (precipitates), and/or combinations of both mechanisms (thereof, as our hypothesis). The influence of gold carrier iron oxide minerals such as hematite (Fe_2O_3), magnetite (conducting mineral) (Fe_3O_4), and also maghemite (has the same structure as magnetite, that is spinel ferrite and is also ferromagnetic; $\gamma\text{-Fe}_2\text{O}_3$) on gold leaching was examined in a systematic way as in freely corroding mode at open circuit potential (OCP) or in the presence of imposed potentials. Based on these statements, the

main objective of this project is to provide a detailed knowledge of electrochemical dissolution behaviour of roasted (oxidised) gold ores and to establish the optimal leaching conditions for roasted gold ore, as far as possible. Concurrently, providing an appropriate understanding of the passivation phenomenon of gold is one of the objectives. Hence, the questions below reflect the objectives of my Ph.D. thesis:

- (i) What are the main dissolution characteristics of pure gold and gold ores?
- (ii) How does the passive behaviour of gold change under passive conditions?
- (iii) Is the passivation a surface product or an adsorbed layer or both?
- (iv) What is the influence of iron oxide on gold dissolution? How do they affect galvanic interactions and passivation phenomenon of gold?
- (v) What causes the slowdown of gold dissolution rate?
- (vi) What are the optimal dissolution conditions for roasted gold ore(s)?

1.3 Description of the Strategy Adapted to This Ph.D. Thesis

Based on the above questions, the scientific approach of this Ph.D. thesis is shown in [Fig. 1.1](#).

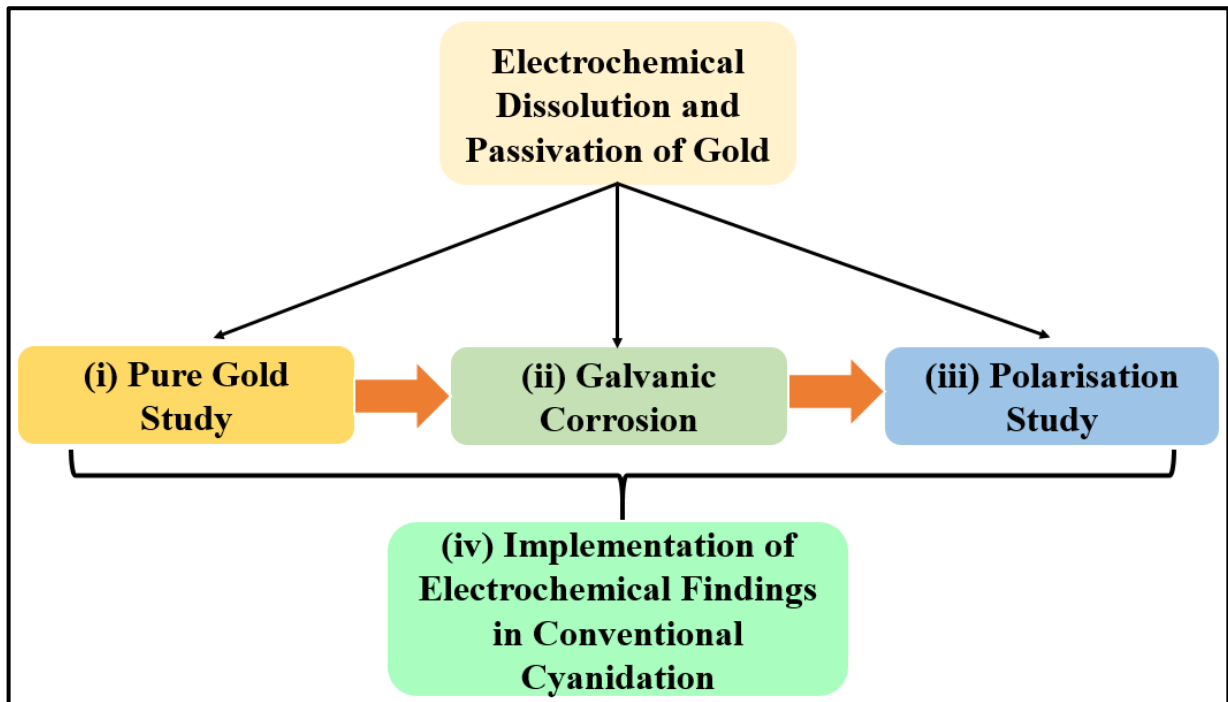


Fig. 1.1 A representative illustrations of the strategy adapted.

a) Active and passive behaviours of gold, when it is under passive conditions, have been examined as a function of leaching parameters. This would give more information about the characteristics of passivation of gold's surface.

b) As complimentary to the conventional electrochemical methods, more recent ones have been considered to study the active and passive behaviour of gold in cyanide solutions. In this case, Electrochemical Noise Measurement (ENM) with its in-situ corrosion rate feature, and Scanning reference electrode technique (SRET), monitoring the real-time changes of anodes and cathodes, have been used. It is also important to note that, to the best of our knowledge, there is no previous work on gold leaching using these methods.

c) Electrochemical interactions between gold and its associated oxide minerals individually (hematite, magnetite, and maghemite) are examined with imposed potentials using combined anode electrodes polarization (CAP), as a new approach, as function of leaching parameters in a systematic way. In this case, gold and iron oxide electrodes are electrically connected to each other, as working electrode, and platinum is used as counter electrode.

d) Galvanic interactions and passivation phenomena without imposed potentials, as in practice, either in the absence or in the presence of slurry of roasted gold ore at Zero Resistance Ammeter (ZRA) mode are investigated.

e) Electrochemical dissolution of roasted gold ore electrode is examined as function of leaching parameters to obtain the optimal conditions for roasted gold ores. To identify the dominating effect in between galvanic interactions and passivation phenomenon on gold dissolution, one and two separate containers tests are considered. These tests have been performed for CAP and ZRA conditions. It is assumed that in two separate containers, the passivation of gold surface could be eliminated whereas both galvanic interactions and passivation phenomenon are potentially present in one container.

f) Since hematite and magnetite are the major iron oxides in roasted gold ore sample, a new electrode named "MagHem-ES", which has equal surfaces of magnetite and hematite in

one electrode, is developed to examine the concurrent effects of these minerals on the dissolution rate of gold.

g) The influence of maghemite on gold dissolution is examined. Maghemite is critical due to its non-porosity, therefore the unrecovered gold is mainly associated and captured by maghemite. Additionally, its effect on gold dissolution could be different and should be evaluated when gold is in free contact with maghemite.

h) Generally, it has been accepted that the intersection of anodic and cathodic curves gives the corrosion rate of the metal. However, our preliminary results have shown that the intersection does not represent the actual leach rate of gold. Another approach close to the conventional cyanidation results should be found. Then, a new approach is proposed such as considering only cathodic Tafel slope by extrapolating to open circuit potential.

i) After the cyanidation of roasted gold ore, leach tailings are collected for further characterisation. Then, leach tailings are subjected to magnetic separation tests to have magnetic and non-magnetic parts containing gold. For a better understanding, electrochemical behaviours of these parts are evaluated by performing anodic and cathodic polarisation tests. Additionally, cathodic polarisation tests are considered both scanning from OCP to more cathodic potentials, and from more cathodic potentials to OCP for better understanding. Further, the influence of oxygen concentration is examined in polarisation tests. Throughout this project, XPS, and SEM-EDS are considered to detect the surface species on gold. Thus, a detailed anodic dissolution profile of roasted gold ore could be established.

1.4 Key Contributions of This Ph.D. Project

Until now, the treatment of oxidised, e.g. roasted gold ores, has received relatively less attention than the sulphidic ones (Adams, 2016). Recently, it can be admitted that the handling of oxidised gold ores is becoming more essential. Based on the open literature, it can be concluded that there is a lack on the electrochemical dissolution studies of gold dealing with the electrochemical methods. In this regard, a critical literature review on the electrochemical dissolution and passivation of gold has been submitted to Hydrometallurgy

Journal (Chapter 2). This review paper examines the evaluation of the electrochemical methods used in gold dissolution studies from past to present, the treatment of complex gold ores, the development of a better understanding for the concept of passivation, and commonly used terms in gold dissolution studies were considered. Several new contributions, as following, have been proposed in this project. [Fig. 1.2](#) demonstrates the strategy adapted in this Ph.D. thesis.

During cyanidation, gold dissolution may slowdown in some conditions, and passivation of gold surface is considered one of the potential reasons for that. Prior to dealing with complex and oxidised gold ores, it is critical to revisit the pure gold studies to have a better understanding on the electrochemical behaviour of gold in cyanide solutions. In this respect, the first part of this Ph.D. thesis focuses on the dissolution and passivation characteristics of gold in pure systems. In pure gold study, dissolution behaviour of gold is examined as function of leaching parameters using potentiodynamic polarisation method. Further, three anodic potentials are imposed to investigate the passivation behaviour of gold using potentiostatic polarisation method. The results have shown that when gold is under passive conditions, increasing cyanide concentration and pH results in decreasing the current density, which suggest the partial passivation of gold surface. Surface characterisation at the offset of each test have identified the corrosion products on the surface of gold that are responsible for this passive behaviour.

Following the pure gold study, the electrochemical behaviour of roasted gold ore in cyanide solutions have been investigated. In this context, electrochemical interactions between gold and iron oxides of roasted gold ore are examined in galvanic corrosion using Zero-Resistance Ammeter (ZRA) mode. The results have shown that the galvanic current decreases in presence of magnetite whereas it increases in presence of hematite and maghemite, relatively. This suggest that hematite promotes the dissolution rate of gold, and magnetite slows down the rate.

For a better understanding, in the following part, the influence of iron oxides of roasted gold ore on the dissolution rate of gold is examined using potentiodynamic polarization

tests, and it was compared to that obtained in galvanic corrosion tests. The results have also showed that magnetite has a retarding effect on the dissolution rate of gold, while hematite and maghemite have positive effects. This highlights that galvanic corrosion and potentiodynamic polarization methods gave similar results. The negative effect of magnetite has also been confirmed by XPS and SEM-EDS studies.

Finally, electrochemical results have been compared to that obtained in conventional cyanidation to understand the dissolution behaviour of gold from roasted ore in industrial practice. It has been shown that considering only cathodic Tafel slope by extrapolating to open circuit potential represents better the practice leach rates of gold. The results have indicated that the dissolution rate of gold increases in the presence of hematite, and maghemite, and the rate decreases in the presence of magnetite. Generally, it can be deduced that the combination of the corrosion products and adsorbed layers could be responsible for the slowdown in gold dissolution from roasted ore, to some extent, but it is not a perfect type of passivation.








Chapter 2 	Critical Review of Electrochemical Dissolution of Gold
	<ul style="list-style-type: none"> ☑ The importance of treatment of oxidised gold ore ☑ Passivation phenomenon of gold is still in doubt ☑ Electrochemical methods for gold dissolution from past to present
Chapter 3 	Electrochemical Behaviour of Pure Gold in Cyanide Solutions
	<ul style="list-style-type: none"> ☑ Active and passive behaviours of gold in cyanide solutions ☑ Potentiostatic studies at three anodic potentials ☑ Application of some recent electrochemical methods
Chapter 4 	A study of electrochemical interactions between gold and its associated oxide minerals
	<ul style="list-style-type: none"> ☑ Galvanic corrosion to examine the influence of iron oxide minerals and soluble ions in separate containers ☑ Either in the presence and absence of slurry
Chapter 5 	Electrochemical dissolution of roasted gold ore in cyanide solutions
	<ul style="list-style-type: none"> ☑ Electrochemical behaviour of RGO as function of leaching parameters for optimal conditions
Chapter 6 	A study of the electrochemical dissolution and passivation phenomenon of roasted gold ore in cyanide solutions
	<ul style="list-style-type: none"> ☑ “Combined anode electrodes” in separate containers ☑ Influence of different iron oxides and RGO as slurry on gold dissolution ☑ MagHem-ES electrode for concurrent effect of iron oxides
Chapter 7 	Influence of Iron Oxide Slurries on the Dissolution of Gold Electrode
	<ul style="list-style-type: none"> ☑ Cathodic Tafel slope extrapolating to OCP for leach rate estimation ☑ Magnetic separation and electrochemical behaviour of leach tailings
Chapter 8 	Conclusions and Recommendations
	<ul style="list-style-type: none"> ☑ Influence of different iron oxides on gold dissolution is examined ☑ Roasted gold ore dissolution is evaluated ☑ Passivation behaviour of gold in presence of iron oxides is concluded

Fig. 1.2 A representative illustration of the methodology and approach adapted in this thesis

Chapter 2

Critical Review of Electrochemical Dissolution of Gold

A review on electrochemical dissolution and passivation of gold during cyanidation in presence of sulphides and oxides

Ahmet Deniz Bas^{a*}, Edward Ghali^a, Yeonuk Choi^b

^aDepartment of Mining, Metallurgical and Materials Engineering, Laval University, Quebec, Canada, G1V 0A6

^bBarrick Gold Corporation, Suite 3700, 161 Bay Street P.O. Box 212, Toronto, Ontario, Canada, M5J 2S1

*Corresponding author: 4186568657, Fax: 4186565343; (ahmet-deniz.bas.1@ulaval.ca)

Revised version has been submitted to Hydrometallurgy Journal

Résumé

Avec l'épuisement rapide des minerais d'or libre, des minerais d'or sulfurés sont souvent oxydés avant la cyanuration à cause de caractère réfractaire. Cela se traduit par l'augmentation du traitement des minerais d'or oxydé. Ainsi, l'évaluation de la dissolution électrochimique des minerais d'or plus complexes et oxydés deviennent de plus important pour l'industrie minière et de la R&D. Dans cette étude, les réalisations passées et les développements récents en matière des méthodes électrochimiques utilisées dans la dissolution d'or et les études de la passivation d'or pur, sulfurés, et les minerais oxydés d'or sont présentés.

Aux potentiels proches du potentiel de circuit ouvert (PCO) comme dans la pratique, le ralentissement la vitesse de la dissolution d'or pourrait être à cause de la passivation, soit par des couches adsorbées ou des produits de surface, ou des combinaisons de ceux-ci. Différents termes utilisés dans les études de dissolution d'or tels que passivation, inhibition, effet retardateur, et ralentissement ont été discutées. Les développements dans les approches électrochimiques, tels que deux cellules séparés, ont été résumés. Des procédés électrochimiques, ainsi que des techniques récentes, telles que la mesure du bruit électrochimique avec sa détection in situ de la vitesse de corrosion, et la technique du balayage de l'électrode de référence sont évalués.

Dans la plupart des études antérieures de polarisation, la réaction anodique a été étudiée en absence d'oxygène, tandis que la réaction cathodique en absence de cyanure, de façon séparée, et la dissolution a été considérée comme étant l'intersection des deux courbes. Cependant, certaines découvertes récentes indiquent que cela ne représente pas la vitesse de dissolution de l'or réel dans la pratique. En outre, la direction de balayage dans des essais de polarisation cathodique, soit PCO vers les potentiels cathodiques ou le potentiel cathodique vers le PCO, est également signalé.

Abstract

With the rapid depletion of free-milling types of gold ores, sulphidic gold ores are often oxidised prior to cyanidation due to the refractoriness. This results in the increase in the processing of oxidised gold ores. Thus, evaluation of the electrochemical dissolution of more complex and oxidised gold ores become ever important for the mining industry and for R&D. In this study, past achievements and recent developments in terms of electrochemical methods used in gold dissolution and passivation studies of pure gold, sulphidic, and oxidised gold ores are presented.

At potentials close to open circuit potential (OCP) as in practice, slowdown in the dissolution rate of gold could be due to passivation by either adsorbed layers or surface products, or combinations thereof. Different terms such as passivation, inhibition, retarding effect, and slowdown used in gold dissolution studies have been discussed. The developments in electrochemical approaches, such as two separate containers, have been summarized. Conventional electrochemical as well as recent methods, such as electrochemical noise measurement with its in-situ detection of corrosion rate, and scanning reference electrode technique are evaluated.

In the majority of the previous polarization studies, anodic reaction was examined in absence of oxygen whereas cathodic reaction in absence of cyanide, separately, and the dissolution was considered as the intersection of both curves. However, some recent findings report that this does not represent the actual gold dissolution rate as in practice. Additionally, the direction of scanning in cathodic polarization tests, either OCP to cathodic potentials or cathodic potential to OCP, is also reported.

Keywords: Gold, Electrochemical dissolution, Inhibition, Passivation, Oxidised and Roasted Gold Ores

2.1 Leaching and Types of Gold Ores

Gold, from ancient times to date, has been valued by humans due to its lustrous colour and its resistance to tarnishing, and has always been considered as the metal of perfection (Habashi, 2016). From the beginning, the processing of gold has been done using different chemicals (aqua regia, halides, ferric chloride, thiourea, thiosulphate etc.), and techniques, such as gold panning, amalgamation, chlorination, cyanidation, and refining of gold (Aylmore, 2016). Among the others, cyanide, with its competency to form a strong complex with gold, is the most preferable reagent for the leaching of gold from its ores. Cyanide has a proven track record of more than 125 years of being used by far the most suitable and effective reagent for recovering of gold (Anderson, 2016; Akcil, 2014). It is also important to mention that due to the environmental issues, high gold prices, and increase in the sharing of more complex gold ores, the application of alternative lixivants to cyanide has extensively been taken into consideration. Recently, Barrick Gold Corporation has announced the commercialisation of a thiosulphate-leaching plant at their Goldstrike operation (Choi, 2015). However, still ~ 85% of gold production worldwide is done using sodium cyanide, and it is more than 90% in U.S. (Cardarelli, 2008; Franks, 2015).

In general, gold ores are classified into two groups as free-milling and refractory type of gold ores by means of metallurgical definition. Free-milling gold ores, which are amenable to direct cyanidation (gold extraction \geq 85-90%) without any need of chemical pre-treatment, have been treated and consumed too much in the past (Zhou and Fleming, 2007). On the other hand, refractory types of gold ores (gold extraction \leq ~ 85-90%) often require some chemical and/or physical pre-treatment methods such as roasting (Dunne et al., 2013), bio-oxidation (BiOx) (Ciftci and Akcil, 2010), pressure-oxidation (POX) (Baron et al., 2016), ultra-fine grinding (UFG) (Celep et al., 2015) prior to cyanidation (Fig. 2.1), and also alkaline sulphide leach process (Anderson et al., 2005; Celep et al., 2011). Refractoriness is a term generally used to express the reason(s) for low or poor gold extractions (La Brooy et al., 1994). In recent years, there has been an increasing trend on the treatment of refractory gold ores due to the rapid depletion of free-milling types of gold ores (Adams, 2016).

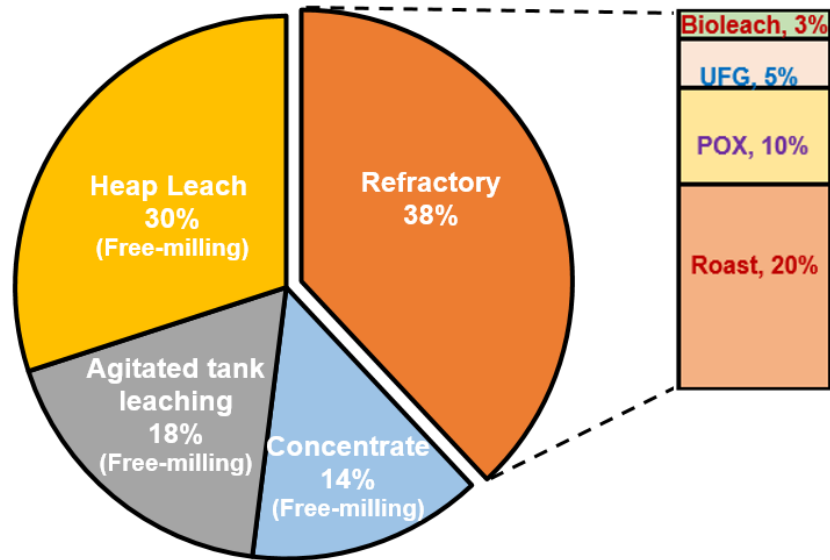
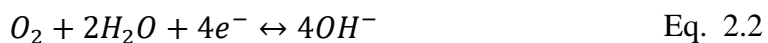
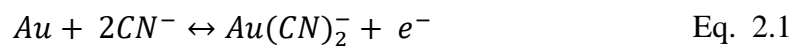
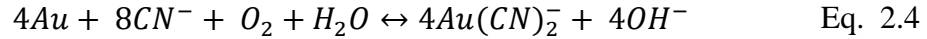
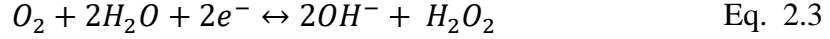


Fig. 2.1 Gold processing routes of the top 20 global gold producers in 2011 (Adams, 2016).

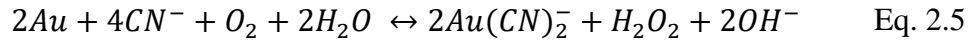
2.2 Electrochemical Dissolution of Gold

The commercial application of the cyanidation process was first applied by MacArthur in 1887 and about 60 years after the discovery of the process, it has been understood that the gold dissolution is an electrochemical corrosion process (Habashi, 2009). Cyanidation occurs as a result of the two redox half reactions; the oxidation of gold (Eq. 2.1), to be a single electron reaction, and the reduction of oxygen (Eq. 2.2) at alkaline pH. The mechanism of the cathodic reaction, i.e. the reduction of oxygen, has long been controversial (Marsden and House, 2006). In the potential range of the gold dissolution, the direct reduction of oxygen to hydroxyl ions does not usually take place. The reduction of oxygen has been found to follow a pathway of sequential two-electron transfer reactions involving the formation of hydrogen peroxide (Eq. 2.3) as an intermediate product (Lorösch, 2001; Evans and Lingane, 1963). The overall reaction will be described by the Elsner's (1846) equation (Eq. 2.4), which is stoichiometrically correct but does not completely describe the cathodic reactions associated with the dissolution.





Bodländer (1896) suggested the formation of hydrogen peroxide with an incomplete reduction of oxygen to hydroxide for the dissolution reaction of gold (Eq. 2.5). Direct reduction of hydrogen peroxide (Eq. 2.6) has been reported only a very limited extent (Kameda, 1949; Zurilla and Yeager, 1969). More details about the role of hydrogen peroxide in gold dissolution can be found in the literature, e.g. in the collection work of Habashi (2009). Hydrogen peroxide decomposes to form oxygen (Eq. 2.7), particularly in slurries. Thus, from a stoichiometric view, the overall dissolution reaction for gold is believed to be the Elsner's equation. The decomposition of hydrogen peroxide to elemental oxygen (Eq. 2.7) possibly takes place at elevated temperatures, and in the presence of incompatible chemical, since it is relatively unstable (Feldmann and Breuer, 2015). Oxygen was found to dissolve gold and silver much faster, i.e. 6-9 and 12 times, respectively, than that of hydrogen peroxide (Boonstra, 1943; Lund, 1951; Habashi, 1967).



2.3 Passivation Phenomenon and Inhibition of Gold Dissolution

In general, there are two common definitions for passivation, like the first one says that metals, which are passive, are covered by a chemisorbed film, e.g. of oxygen, hence this layer displaces the H₂O molecules and slows down the rate of anodic dissolution involving hydration of metal ions. The second approach considers that the passive film is always a diffusion-barrier layer of the reaction products, e.g. oxides, therefore corrosion rate decreases (Uhlig, 1963). Such phenomenon was first observed by M. Faraday in 1835 (Shreir et al., 1994). Crundwell (2015) identifies passivation, in terms of corrosion of metals, as the formation of a passive layer composed of metal oxides that lower the rate of dissolution by several orders of magnitude. There are some important terms in corrosion-

passivation studies such as the corrosion potential E_{corr} , the corrosion current density i_{corr} , the critical potential for passivation E_{cp} , the critical current density for passivation i_{cp} , the breakdown potential E_{b} , and the breakdown current density i_{b} (the highest passive current density just before or at E_{b}) (Uhlig, 1963; Fontana and Greene, 1978).

In the case of gold, the passivation phenomenon has been known since 1907 and Beyers (1936) quoted "Jacobson studied the anodic dissolution of gold in alkaline cyanide solution and established that gold became passive under certain conditions in commercial cyanide solutions. He assumed that the passivity is due to the formation of a film of comparatively insoluble sodium aurocyanide on the anodic gold" (Filmer, 1982). The decrease in current density indicates that the dissolution of gold has been partially blocked, suggesting the partial passivation (Kiss, 1988). Filmer (1982) stated that "All the researchers in gold leaching field have shown that oxidation initially follows normal Tafel behaviour, but passivation occurs as the potential is shifted anodically. The anodic current achieved prior to passivation is dependent on the cyanide concentration and on the concentration of the impurities in solution". For instance; this shift in the dissolution potential of gold towards anodic potentials was reported to be up to 150 mV in the presence of pyrite slurry (Lorenzen and van Deventer, 1992a). It was proposed that the adsorption of hydroxide ions (Kirk et al., 1980) or some form of adsorbed AuCN (Nicol, 1980) on the surface of pure gold are responsible for the passivation of gold. The polymeric nature of the AuCN_{ads} to form ...-Au-CN-Au-CN-.... chain may be responsible for the retard to further dissolution of gold (Sandenbergh and Miller, 2001). Tshilombo and Sandenbergh (2001) stated that if passivation is due to the formation of a polymeric layer of AuCN that results from the lack of enough cyanide, such that insoluble AuCN rather than the much more soluble Au(CN)₂⁻ is formed, indicates that peak current is dependent on the cyanide concentration. The nature of anodic peak(s) and the possible reasons of passivation is still a controversial issue. Moreover, two recent papers (Holmes and Crundwell, 2013; Crundwell, 2013) discussing the passive phenomenon of gold have been published. Crundwell (2013) claimed that each point on the surface is considered as both anodic site and cathodic site and concluded that there is no separation of anodic and cathodic sites on mineral surface. Habashi and Bas (2014) pointed out that certain experimental results demonstrated the existence of anodic

and cathodic zones during the dissolution of minerals. These studies show that examining the anodic behaviour of gold still receives much attention.

Passivation is a commonly used term to explain a phenomenon in many fields, but its meaning could potentially create a confusion according to the used area. The meaning of passivation differs from one to other; for example, it could express different meanings by hydrometallurgists and electrochemists. Sometimes, any reduction observed in gold leaching has been easily attributed to passivation without a detailed explanation, which could show the different/indecisive use of this term. In addition to passivation, there are other terms used to express the reduction in gold dissolution (rate) such as inhibition (Kasaini et al., 2008; Van Den Berg and Petersen, 2000; Alonso-Gómez and Lapidus, 2009; Luna and Lapidus, 2000), retarding effect (Gupta and Mukherjee, 1990; Jeffrey et al., 2008), and slowdown (Yannopoulos, 1991; Yang et al., 2010a). Inhibition is mainly defined as a chemical substance which, when added in small concentrations to an environment, minimises or prevents corrosion (Papavinasam, 2011; Riggs, 1973).

2.4 Electrochemical Methods Used in Gold Dissolution Studies

It has been known that gold cyanidation is an electrochemical reaction (Thompson, 1947), so the process can readily be studied using electrochemical techniques. Hence, electrochemical characterisation of gold could potentially provide significant information such as corrosion/dissolution current and potential. With the aid of polarization curves, the active and passive behaviours of gold specimen could also be obtained.

In complementary to the conventional electrochemical methods, such as cyclic voltammetry (CV), linear polarization (LP), galvanostatic, potentiostatic, and potentiodynamic polarization, and more recent electrochemical techniques such as electrochemical noise measurement (ENM), and scanning reference electrode techniques (SRET) have also been employed in gold dissolution studies (Table 2.1). The summary of the electrochemical methods used in gold dissolution studies as function of parameters such as cyanide solutions, pH, and agitation is given in Table 2.1.

Table 2.1 A brief summary of the electrochemical methods used for gold cyanidation (continue on the next page).

Reference	CN concentration (M)	pH	Agitation (rpm)	Method
Mills, 1951	0.38 M KCN	alkaline	400-1200	Anodic and cathodic polarization
Kudryk and Kellogg, 1954	7.67×10^{-4} - 10^{-2} M KCN	10.5-11	300	Potentiodynamic
Cathro, 1963; Cathro and Koch, 1964a,b	0.008, 0.023, 0.038, 0.077 M KCN N ₂ bubbling	11.2, 12, 12.8	600	Potentiodynamic, Potentiostatic, Galvanostatic
Mrkusic and Paynter, 1970	0.076 M KCN	alkaline	400	Potentiodynamic Potentiostatic
Kirk et al., 1978	0.05, 0.1, 0.2 KCN (+ 0.1 M KOH) N ₂ bubbling	alkaline	with and without	Potentiodynamic
Pan and Wan, 1979	0.2, 0.5, 1 KCN N ₂ bubbling	5, 8.1, 12.8	<i>n.m.</i>	Potentiodynamic
Kirk and Foulkes, 1980	0.1 - 0.2 KCN	alkaline	with and without	Potentiodynamic, Potentiostatic
Thurgood et al., 1981	0.1 M KCN	alkaline	with and without	Potentiodynamic, Potentiostatic
Filmer, 1982	0.2 M NaCN	12.4	500	Potentiodynamic
Dorin and Woods, 1991	0.02 M NaCN	10	4 s ⁻¹	Linear polarization
van Deventer et al., 1990	0.003 M KCN	10.3	100	Galvanic corrosion in one and two cells
Lorenzen and van Deventer, 1992a	0.003 M KCN	10.2	100	Galvanic corrosion
Guan and Han, 1994	0.001, 0.002, 0.005, 0.01, 0.02 M NaCN	10.5, 11, 12, 12.7	450	Potentiodynamic
Mughogho and Crundwell, 1996	0.003 M KCN	10-13	1000	Cyclic voltammetry
Guzman et al., 1999	0.01, 0.02 M NaCN	10-12.8	400	Potentiodynamic
Tshilombo, 2000; Tshilombo and Sandenbergh, 2001	0.005, 0.015, 0.025 NaCN	11	225, 450, 900	Potentiodynamic
Lin and Chen, 2001	0.1, 0.2 NaCN	10.56	500	CV
Jeffrey and Ritchie, 2001	0.02 NaCN	10	300	Potentiodynamic
Reyez-Cruz et. al., 2002	0.5 NaCN	10	<i>n.m.</i>	CV

Wadsworth and Zhu, 2003	0.01 M NaCN	10.5	300	Potentiodynamic Potentiostatic, CV
Cerovic et al., 2005	0.02 M CN ⁻	11	n.m.	Potentiodynamic
May et al., 2005	0.006 M NaCN	11	magnetic agitation	Potentiodynamic
Aghamirian and Yen, 2005	0.05, 0.025, 0.01, 0.005 M NaCN	10.5	n.m.	Potentiodynamic Galvanodynamic, Galvanic corrosion (ZRA)
Dai and Jeffrey, 2006	5 mM NaCN	alkaline	300	Linear sweep voltammetry
Tan et al., 2006	0.0037, 0.0075, 0.015 KCN	10.5, 11.5	300	Potentiodynamic
Qian et al., 2010	0.005, 0.002, 0.01, 0.02, 0.05, 0.1 M NaCN	11	400	Potentiodynamic
Azizi et al., 2010	10 mM CN	11	500	Linear Polarization, ZRA
Azizi et al., 2011, 2012a and 2012b	30 mM NaCN	11	500	Packed-bed electrochemical reactor, ZRA
Dai and Breuer, 2013	15 mM NaCN	10.6	300	Linear sweep voltammetry
Bas et al., 2015a, 2015b, 2015c, 2015d, 2016a, 2016b	0.01-0.04 M NaCN	10.5	100-400	Potentiodynamic, Potentiostatic, ENM, LP, SRET, ZRA, CV(no agitation)

(not mentioned: n.m.)

2.4.1 Potentiodynamic polarization

Potentiodynamic polarization is one of the most preferred methods used to determine the active/passive characteristics of a given metal-solution system, corrosion rate (current density), and Tafel curves (Fig. 2.2). The polarization diagram for a passivable system with the anodic and cathodic branches is shown in Fig. 2.3. For the anodic curve, potential scan typically starts at E_{corr} (the open circuit potential) and scanning in a positive direction, and usually to a potential positive enough to oxidise the test solution. The scan rate is typically 0.1 to 5 mV/s and depends on the system. The most reliable data is generally acquired at slow scan rates (Thompson and Syrett, 1992).

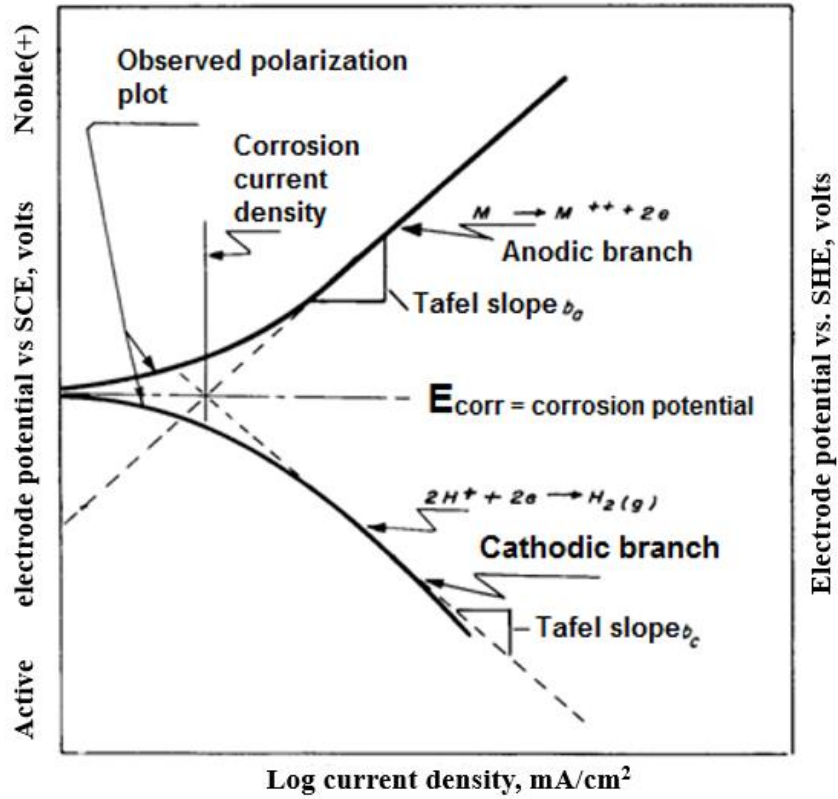


Fig. 2.2 Cathodic and anodic Tafel polarization diagram (ASTM G3-89, 2006).

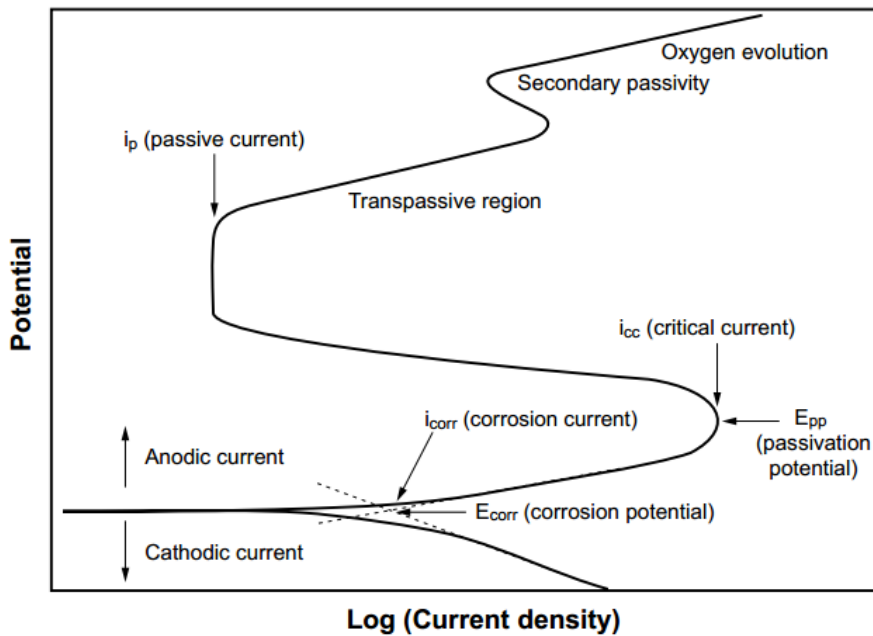


Fig. 2.3 Hypothetical polarization diagram for a passivable system with anodic and cathodic branches (ASTM G3-89, 2006).

Kudryk and Kellogg (1954) examined the anodic and cathodic dissolution of gold, separately, and calculated the rate of gold dissolution as the intersection of anodic and cathodic Tafel slopes. However, they did not observe any passivation, i.e. the dissolution was controlled by the diffusion of cyanide ions, whereas Mills (1951), Cathro (1963), and Cathro and Koch (1964a) observed passivation, i.e. sharp decrease in current density for gold dissolution. Nicol (1980) compared the anodic dissolution profiles of gold (Fig. 2.4, and Table 2.2).

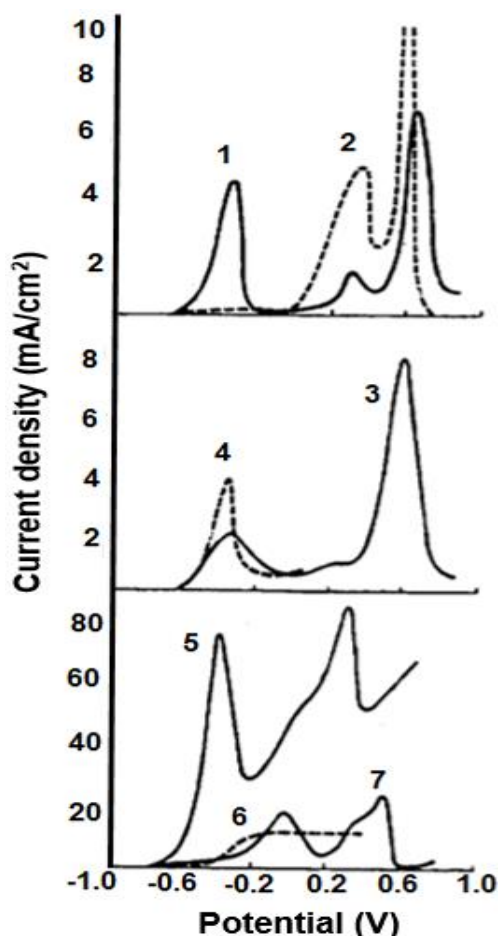


Table 2.2 Gold anodic dissolution profiles at different conditions (Nicol, 1980).

No	Reference	[CN ⁻] M	Condition
1	Cathro and Koch, 1964a	0.077	pH 12
2	Kirk et al., 1978	0.1	0.1 M OH ⁻
3	Pan and Wan, 1979	0.2	pH 12.8
4	Cathro, 1963	0.04	pH 12
5	Eisenmann, 1978	0.5	55 °C
6	Kudryk and Kellogg, 1954	0.1	pH 11
7	Mac Arthur, 1972	0.2	0.2 M OH ⁻ , 61 °C

Fig. 2.4 Comparison of the gold anodic dissolution profiles (Nicol, 1980).

As seen in Fig. 2.4, there is a variation in the potential range for the peaks and peak current densities. In general, three peaks leading to passivation were observed at -400, 300, and 600 mV/SHE. It should be noted that the main interest is on the first peak since gold oxidation occurs at potentials lower than 0 mV. Kirk et al. (1978) employed

potentiodynamic polarization tests to examine the anodic dissolution of gold in the potential range from -0.9 V to 0.4 V/SCE (standard calomel electrode) with a scan rate of 1 mV/s, and observed 3 peaks leading to passivation, as in their following works, [Kirk et al. \(1980\)](#), [Kirk and Foulkes \(1980\)](#), and [Thurgood et al. \(1981\)](#). [Pan and Wan \(1979\)](#) performed only anodic polarization tests scanning from -1.0 V to 1.0 V/SCE at a high speed of 50 mV/s scan rate, and observed four peaks that are responsible for passivation of gold.

The influence of additives such as lead, thallium, silver, clay and carbon, mercury, on the potentiodynamic polarization of gold was tested ([Filmer, 1982](#); [Tshilombo and Sandenbergh, 2001](#); [Qian et al., 2010](#)). For instance, [May et al. \(2005\)](#) reported that if the concentration of lead ions was equal to or greater than the sulphide ions, potential shifted to more negative potential (a potential drop) with a scan rate of 1 mV/s. [Bas et al. \(2015a, 2015b\)](#) examined the influence of iron oxide minerals associated with roasted gold ore on gold dissolution by using potentiodynamic polarization method as function of leaching parameters. Then, [Bas et al. \(2015c\)](#) proposed a new approach, named “Combined Anode Electrode Polarization”, where gold and iron oxide minerals were electrically connected to each other either in one or two separate containers.

One of the most important issues in electrochemical polarization tests is the direction of scanning in polarization tests. Most of the electrochemical experiments, in different fields, consist of a complete polarization curve, starting from a cathodic potential (more negative) to a more positive (anodic) potential ([Figs. 2.2 and 2.3](#)). However, in case of gold, according to the mixed potential theory, gold anodic (in absence of oxygen) and cathodic (in absence of cyanide) reactions/polarization curves have separately been studied/obtained by many research groups ([Kudryk and Kellogg, 1954](#); [Cerovic et al., 2005](#)). This approach, e.g. anodic curve in the absence of oxygen is more theoretical since it does not correspond to that in practice. Therefore, the direction of scanning especially in cathodic polarization is an important issue. So, the presentation of potential range of scanning with direction is highly recommended to be more precise. A comparison of scanning potential range for anodic and cathodic curves from some selected papers is demonstrated in [Table 2.3](#). As seen in [Table 2.3](#), the range of scanning potential varies in the open literature. It can be

deduced that in the case of cathodic polarization, scanning was initiated from the potential region of anodic curve. Similarly, anodic polarization was performed including the potential region of cathodic curve at a scan rate of 1 mV/s (Guan and Han, 1994; Guzman et al., 1999; Cerovic et al., 2005; Tan et al., 2006). May et al. (2005) considered the complete polarization curve starting from cathodic potential (-200 mV vs. OCP) to anodic, i.e. more positive potential in the same electrolyte at a scan rate of either 0.1 or 1 mV/s. Bas et al. (2015b) compared the cathodic polarization of gold in the presence of cyanide saturated with atmospheric oxygen scanning from open circuit potential (OCP) to more cathodic potential and scanning from cathodic potential to OCP at a scan rate of 0.166 mV/s. They obtained a clear difference on the shape of cathodic curve based on the direction of scanning and concluded that scanning from E_{corr} to more cathodic potentials provides more representative Tafel slopes and accurate results while scanning in the reverse direction is not suitable for gold leaching estimation.

Table 2.3 Comparison of the polarization potential range from some selected papers.

Reference	Cathodic polarization	Anodic polarization
Guan and Han (1994)	0 to -1 V/SCE	-1 to +0.6 V/SCE
Guzman et al. (1999)	0 to -1 V/Ag,AgCl	-0.8 to + 0.8 V/Ag, AgCl
Cerovic et al. (2005)	0 to -0.8 V/Ag,AgCl	-0.8 to 0 V/Ag,AgCl
Tan et al. (2006)	+0.2 to -1 V/Ag,AgCl	-0.8 to 0.8 V/Ag,AgCl
May et al. (2005)	Complete polarization from -0.55 to 0.15 V/SHE	
Bas et al. (2015b)	OCP to -300 mV more cathodic	-0.8 to 1.2 V/SHE

Linear Polarization (LP) (Linear Sweep Voltammetry, LSV) is also a common method used to obtain anodic and cathodic polarization curves. In LP, a fixed potential range within only the forward scan is applied unlike the cyclic voltammetry, no backward scan is done. This technique is specially dedicated to RDE (Rotating Disk Electrode) or RRDE (Rotating Ring Disk Electrode) investigations which allow user to carry out steady - state measurements. This leads to the determination of redox potential and kinetic parameters such as corrosion current and polarization resistance (Thompson and Payer, 1998). LP allows to obtain polarization resistance by scanning through a potential range ± 25 mV with respect to

corrosion potential (E_{corr}) (Fig. 2.2). The slope of anodic or cathodic curves is denoted as the resistance to polarization, R_p , and this value is used to calculate the I_{corr} utilising the well-known Stern-Geary equation (Stern and Geary, 1957). Dai and Jeffrey (2006) performed linear sweep voltammetry experiments to examine the influence of sulphide minerals on the dissolution rate of Au (95%)-Ag (5%) alloy electrode using rotating electrochemical quartz crystal microbalance (REQCM) with a scan rate of 1 mV/s. Azizi et al. (2010) also performed linear polarization tests using Au (96%)-Ag (4%) alloy RDE to test the influence of sulphidic mineral electrodes on gold dissolution either in one or two electrochemical cells with a scan rate of 0.5 mV/s. Dai and Breuer (2013) examined the dissolution rate of gold using pure gold and gold-silver alloy electrodes and compared to that of electrochemical corrosion rates with a scan rate of 1 mV/s.

2.4.2 Cyclic Voltammetry (CV)

CV is one of the most commonly used electro-analytical techniques, with its easy and fast ability to characterise an electrochemical reaction system, but it is not usually preferred for quantitative analysis. The determination of reversible or irreversible behaviour of a redox couple, the number of electrons transferred in an oxidation or reduction, rate constant, and reaction mechanism can be obtained by CV (Kelly et al., 2002). It is generally recommended that CV consists of cycling the potential of an electrode, which is immersed in an unstirred solution, and measuring the resulting current (Kissinger and Heineman, 1983). Reyes-Cruz et al. (2002) studied electrochemical deposition of gold and silver by cyclic voltammetry with a scan rate of 25 mV/s with the potential range from -2.0 to 0 V/SCE, and agitation speed was not mentioned. Bas et al. (2015d) performed CV in the absence of agitation in 0.04 M NaCN electrolyte at pH 10.5 at a scan rate of 10 mV/s. There are some studies in which CV was considered at high agitation rates. For instance, Mughogho and Crundwell (1996) tested electrochemical behaviour of gold rotating disc electrode at 1000 rpm in dilute cyanide solution (~ 0.003 M KCN) with at least five cycles and found that the rate of anodic reaction was enhanced with increasing pH in the region of the first peak, but not for the second and third peaks. Lin and Chen (2001) examined the influence of cyanide concentration and pH on gold dissolution by comparing cyclic voltammetry results scanning from -1.0 to 1.2 V/SCE with a scan rate of 10 mV/s at 500

rpm agitation. They reported that the three anodic peaks were found to be cyanide related whereas the cathodic peak was hydroxide related. These findings have revealed that three peaks, as in potentiodynamic polarization, were observed by CV either in absence or presence of agitation leading to the passivation of gold surface.

2.4.3 Potentiostatic and Galvanostatic Polarization Methods

Potentiostatic polarization is a method that applies a constant potential to the metal-solution interface and measures its electrochemical behaviour as a function of time. On the other hand, galvanostatic polarization is an alternative to potentiostatic polarization. In galvanostatic polarization measurements, the current between working and counter electrodes is controlled, and the potential between working and reference electrodes is automatically recorded to the value required to maintain the current. Potentiostatic experiments can be used to determine diffusion coefficients of dissolved materials in a solution, to measure passivation or re-passivation potentials and rates and to evaluate anodic and cathodic protection techniques (Thompson and Payer, 1998). Cathro and Koch (1964a) observed three current maxima by potentiostatic polarization at -0.6, +0.1, and +0.4 V/SCE, where they proposed that the first and last are pH dependent, and that at +0.1 V/SCE is not. They also performed galvanostatic polarization tests, in the potential range -0.8 to -0.6 V/SCE to obtain the Tafel slopes. Kirk et al. (1978), and Kirk and Foulkes (1980) reported that the peaks found in potentiostatic polarization is the result of a single over-all dissolution reaction with different rate-controlling steps. In the study of Wadsworth and Zhu (2003), potentiostatic experiments at open circuit potential were carried out as function of silver concentration, and found that the curves showed a similar behaviour as function of silver concentration that is an initial increase in current density followed by a decay and then a region of constant current. In complimentary to the previous works, Bas et al. (2015a) investigated the behaviour of gold dissolution by potentiostatic polarization applying the passive potentials obtained in potentiodynamic polarization tests. They concluded that when gold is under passive conditions, increasing cyanide concentration, and potential has led to a decrease in current density, suggesting the increase in the thickness of passive film on gold.

2.4.4 Galvanic Corrosion by Zero Resistance Ammeter

Zero resistance ammeter (ZRA) mode is used to measure the galvanic current flowing between two electrodes, working electrode 1 and working electrode 2, which acts as if they were coupled by a zero resistance wire and to monitor the potential of the galvanic couple. A zero resistance ammeter (ZRA) does not apply a signal, but passively measures both the current and voltage as a response ([Gamry Potentiostat Manual, 2012](#)). ZRA mode is particularly useful in studying galvanic corrosion or electrochemical noise.

[van Deventer and Lorenzen \(1987\)](#) proposed a new approach in which gold and mineral disc electrodes were in direct contact to each other and were placed either in the same or in separate containers. This approach was also considered in their following studies, e.g. [van Deventer et al., \(1990\)](#), and [Lorenzen and van Deventer \(1992a\)](#) for a better insight to understand the dominating effect in between galvanic interactions and passivation phenomenon. [Aghamirian and Yen \(2005\)](#) performed galvanic corrosion tests in one container and found that pyrite and pyrrotite showed positive effect on gold dissolution, whereas [Lorenzen and van Deventer \(1992b\)](#) reported the negative effect of pyrite. [Azizi et al. \(2011, 2012a, 2012b\)](#) investigated galvanic interactions in ZRA mode, between gold and sulphidic gold ores/minerals using packed bed electrochemical reactor (PBER) using a gold-silver alloy (96%-4%) electrode either in one or two electrochemical cells during 3 hours. They also examined multi effects of sulphide minerals on gold dissolution. [Bas et al. \(2015d\)](#) examined the influence of galvanic interactions between gold and iron oxide minerals (magnetite, hematite, maghemite) associated with roasted gold ore as function of agitation rate. Also, [Bas et al. \(2016a\)](#) demonstrated the influence of slurry of roasted gold ore on the galvanic corrosion between gold and iron oxide minerals by testing either in one or two separate containers.

2.4.5 Electrochemical Noise Measurement (ENM)

The term "electrochemical noise measurement (ENM)" was employed to describe the spontaneous fluctuations of potential and current as a function of time ([Eden, 2011](#)). [Ghali \(2010\)](#) underlined that ENM can be used to monitor all forms of corrosion and reported that it is sensitive to localized corrosion such as pitting and crevice corrosion and even

metastable pitting. The instantaneous response to the change of surface conditions enables this method to be a powerful online corrosion-monitoring tool (Cottis, 2001). In galvanic corrosion experiments, the metals are dissimilar; whereas, in ENM the metals are the same (Princeton Applied Research, 2014).

In general, the amplitude of ENM fluctuations can be correlated with the intensity of the corrosion process, while the fluctuation shape can be due to the type of the corrosion process (Aballe et al., 1999). The main advantage of this technique is the in-situ measurement of corrosion rate, low cost of the equipment consisting mainly of a zero resistance ammeter (ZRA) and digital voltmeter as well as the ease of data collection (Cottis and Turgoose, 1999). The analysis of electrochemical noise data can be performed in both time and frequency domains. In the time domain, the most interesting parameter of the statistical analysis is the noise resistance (R_n), defined as the ratio of a standard deviation of the potential noise to that of current noise which can be associated to the polarization resistance (R_p). The ratio $1/R_n$ is proportional to the corrosion rate. Noise data are transformed into the frequency domain using Fast Fourier Transform (FFT) algorithm and presented as power spectral density (PSD), calculated in a frequency domain (Loto, 2012). Although the majority of ENM studies have been carried out in corrosion studies, there is a recent attempt using ENM in leaching studies. Bevilaqua et al. (2006) tested the use of ENM in the bioleaching of bornite (Cu_5FeS_4) in the absence and presence of *A. ferrooxidans* LR strain bacteria, since it is a non-destructive method. They correlated the potential and current variations with the corrosion process, and found that bacterial activity showed an accelerated corrosion process. Recently, Bas et al. (2015a, 2015b) compared the corrosion rates of gold and roasted gold ore electrodes during 16 hours of ENM tests at free corrosion mode. This method could potentially be an alternative in gold leaching studies for the characterization of surface products that could lead to surface passivation. As seen, there is a paucity of in-situ ENM of gold leaching studies. Additionally, ENM is known as a promising tool with convenience for in-situ applications (Tan et al., 1996).

2.4.6 Scanning Reference Electrode Technique (SRET)

SRET in-situ provides significant information on anodic and cathodic potentials of a specimen as a function of time in the free corrosion mode (Zhang et al., 2006). It is also possible to analyse the active and passive behaviours of gold with the 3D image facility. Negative potential differences correspond to anodic reactions whereas positive potential differences correspond to cathodic reactions on the surface of the specimen. The results are reproducible up to 95% of accuracy (Zlatev et al., 2011). It is also possible to obtain the most intense anodic potential characterizing the more intense localized corrosion of each map and the most intense cathodic potential. So, the curve of the local quasi electromotive force (QEMF) (potential difference between the most active cathode and the most active anode on the surface of specimen) with time for each specimen *e.g.* gold, can be plotted. It is proved that the results of QEMF give the same trend as that of electrochemical polarization (Oltra et al., 2007).

Till now, SRET has not received much attention on gold cyanidation studies. Bas et al. (2015b) performed SRET experiments for gold and roasted gold ore electrodes at free corrosion mode. The SRET results were in line with the ENM findings showing the corrosion behaviour of roasted gold ore (RGO) electrode if compared to that of pure gold electrode. The reproducibility of the QEMF values for Au and RGO electrodes were found to be $\pm 10\%$ and 12% , respectively. A block diagram showing these components and the general layout of a SVP100 SRET system can be seen in Bas et al. (2015b)'s study. These results have indicated that SRET in-situ corrosion measurements without any imposed potential, which is very close to practice, provide significant information on the corrosion behaviour of gold and show the existence and polarization of anodic and cathodic sites during the leaching of gold.

2.4.7 Electrochemical Impedance Spectroscopy (EIS)

Electrochemical Impedance Spectroscopy (EIS) has been widely used to characterise electrode processes, to determine the double-layer capacitance, and to aid in understanding the kinetics of electrochemical systems. The principle of EIS is to measure the true resistance usually at a fixed potential during a frequency scan to assess the mechanisms

that regulate the electrochemical kinetics (Yang et al., 2010a). EIS measurements offer two major advantages over the more convenient voltammetry methods. Firstly, information regarding the kinetics of surface electrochemical reactions may be obtained in situ with a minimum of surface modification, since the applied potential perturbation is usually small. Secondly, EIS allows in-situ detection of the formation of surface layers on the electrode as changes in electrode capacitance (Wet et al., 1997). The results of EIS studies may be presented in a complex-plane plot, also known as a Nyquist plot, in which the imaginary and real impedances are plotted as a function of frequency.

EIS has been considered to study the oxidation of gold in cyanide solutions (Rogozhnikov and Bek, 1987). They reported that the adsorption of hydroxide ions is inhibited in the presence of cyanide ions. Some researchers have considered EIS to examine the influence of cyanide on pyrite flotation in presence of xanthate using a pyrite crystal as working electrode (Wet et al., 1997; Guo et al., 2015). Up to now, the use of EIS in cyanide solutions has received relatively less attention than that in thiourea, thiocyanate, and thiosulphate solutions (Yang et al., 2010a, 2010b, 2010c; Choudhary et al., 2016).

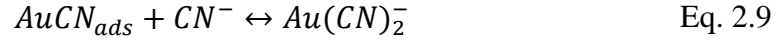
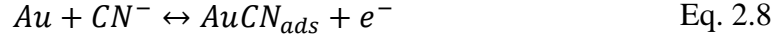
2.5 Electrochemical Studies of Gold Cyanidation

It is worth noting that passivation of gold dissolution could be due to adsorbed species, corrosion products (precipitates), and/or combinations thereof. In the following sections (2.5.1, 2.5.2, and 2.5.3), a summary of corrosion rate estimation, passivation, inhibition, and kinetics of gold dissolution have been given for pure gold samples (section 2.5.1), sulphidic gold ores (section 2.5.2), and oxidised gold ores (section 2.5.3) by means of electrochemical dissolution studies.

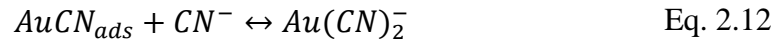
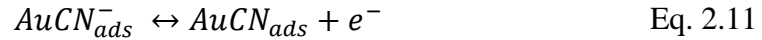
2.5.1 Pure Gold Studies

Generally, it has been accepted that 3 peaks are formed on the surface of gold by potentiodynamic polarization and/or CV which lead to passivation (Kudryk and Kellogg, 1954; Cathro and Koch, 1964a, 1964b; Kirk et al., 1978; Bek et al., 2001; Guzman et al., 1999). For the first peak region, Cathro and Koch (1964a) proposed the following reactions

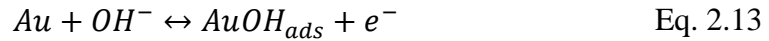
scheme (Eqs. 2.8 and 2.9). Eq. 2.8 and Eq. 2.9 were considered as the rate-determining step by Cathro and Koch (1964a) and MacArthur (1972), respectively.



Kirk et al. (1978, 1980) suggested the following reaction scheme Eqs. (2.10-12), and Eq. 2.11 was assumed to be the rate-determining step. Further, the existence of $AuCN_{ads}$ has been proved by Sawaguchi et al. (1995) using scanning tunneling microscopy (STM).



Guan and Han (1994) and Pan and Wan (1979) mentioned that the adsorption of hydroxyl ions on the surface of gold was the contributing cause of passivation (Eq. 2.13) according to the following equation:



Nicol et al. (1987) reported that based on many experiments measuring current as function of cyanide concentration at the active portion of the peak, the dissolution of gold occurs as shown in Eqs. 2.10-12. Therefore, it has been suggested that passivation is associated with an adsorbed layer of $AuCN$. Puddephatt (1978) proposed that solid, polymeric $AuCN$ forms a passive film on the surface of the gold particle which consists of linear chains of $-Au-CN-Au-CN-$ where the cyanide ion functions as a bidentate ligand. Nicol (1980) also suggested that the surface is covered by a film of $AuCN$ (rather than an adsorbed layer), which can be $(AuCN)_x$. It has been suggested that during the dissolution process, such a compound could form in two dimensions to block the gold surface (Jeffrey and Ritchie, 2001).

It is generally accepted that the region of the first peak is of great importance for researchers since the potential does not exceed zero during the cyanidation of gold (Nicol et al., 1987). The current density of the first peak (-0.3 V vs. SHE) shows large variations depending on the range of CN concentrations, pH, and measurement techniques (Table 2.4). When the first oxidation peak becomes passive, its current density sharply decreases down to ca. 0 mA/cm² then shows a flat region till the surface starts to become active again. In most of the works, this flat region shows a potential range of around 650 mV. Generally, current density of the first peak is lower than the other two successive peaks (Nicol, 1980; Bek et al., 1997). Additionally, the current densities of the three peaks showed certain differences as function of the experimental procedure, such as measurement techniques, agitation, cyanide concentration, pH, type of electrodes (Jeffrey, 1997; Guan and Han, 1994).

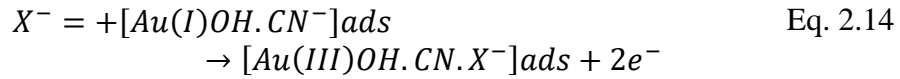
Table 2.4 Comparison of the peak current densities.

Reference	Peak current density (mA/cm ²)			[CN ⁻] M
	Peak 1	Peak 2	Peak 3	
Cathro and Koch (1964a)	1.2	1.5	4	0.038
Kirk et al. (1978)	0.096	5	11	0.05
Pan and Wan (1979)	~2	~1	~7	0.2
Guan and Han (1994)	~2.4	~2.5	~1.8	0.01
Guzman et al. (1999)	~1.5	~4.2	~2	0.01

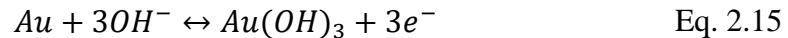
Nicol (1980) mentioned that the first peak may not be observed if the potential scan is applied immediately after gold placing into the solution while it was observed if the electrode allowed standing at open circuit around for 30 minutes at high rotation speeds. Mughogho and Crundwell (1996) suggested that the gold dissolution reaction has different mechanism in high cyanide concentration than that in low concentrations of cyanide. At low cyanide concentrations (< 0.04 M), the first peak current density was found to be very lower if compared to that of the other two peaks.

At about 0.3 V vs. SHE potential range which corresponds to the second peak region, Cathro and Koch (1964a) proposed the conversion of Au^I(OHCN)_x to the Au(III) basic cyanide film, where X is any anion except OH⁻ (Eq. 2.14). However, Kirk et al. (1978)

proposed the same reaction sequence for the second peak region that is due to the formation of gold(I) hydroxide (Eq. 2.13). Furthermore, Nicol et al. (1987) attributed the second peak to the complexation reaction between free cyanide and the adsorbed intermediate $AuCN_{ads}$ species (Eq. 2.12). The second peak current density changes as function of cyanide concentration, e.g. 7.37 mA/cm^2 was obtained in 0.1 M NaCN while it was only 0.22 mA/cm^2 in 0.005 M NaCN (Bas et al., 2015a). As a comparison, peak current densities were observed around 4.94, 6.52, and 3.24 mA/cm^2 (in 0.2 M NaCN) for the consecutive three peaks (Bas et al., 2015a), while Kirk et al (1978) observed $\sim 0.3, 10, \text{ and } 40 \text{ mA/cm}^2$, respectively, for the same cyanide concentration (0.2 M).



The final peak at 0.6 to 0.7 V/SHE is thought to be due to the formation of a Au(III) oxide (Au_2O_3) layer which passivates the gold surface. However, such passivation is unlikely to be a problem in practice because of the highly positive potentials required for this to occur (Finkelstein, 1972; Nicol, 1980). For the third peak region, no reaction scheme was proposed by Kirk et al. (1978). MacArthur (1972) stated that it is quite difficult to explain peak formations due to the complexity of reactions. It was generally agreed either direct oxidation of an adsorbed intermediate, or oxidation to gold (III) (Eq. 2.15), could cause passivation (Guan and Han, 1994).



In pure gold experiments, some additives were tested to alleviate the passive behaviour. Bek et al. (1997) concluded that gold is passive in pure solutions at low overpotentials and the presence of trace elements can accumulate at the gold surface and remove the passivation, thus allowing the gold to dissolve. It was found that lead, thallium, bismuth, and mercury could enhance the recovery of gold if used at desired concentrations, while sulphide ions retard (Beyers, 1936; Fink and Putnam, 1950; Hedley and Tabachnick, 1968; Lorenzen and van Deventer, 1992a; Weichselbaum et al., 1989; Jin et al. 1998; Deschênes et al., 2000; Jeffrey and Ritchie, 2000a, b). Chimenos et al. (1997) noted a remarkable

increase in gold dissolution rate in the presence of thallium (I) salt during cyanidation. The positive role of lead, the formation of the adsorbed species, and formation of the oxide layer leading to passivation have been detected on the gold surface via surface-enhanced raman scattering (SERS) spectroscopy (Jeffrey et al., 2005).

2.5.2 Sulphidic Gold Ore Studies

Gold is often associated with conductive/semiconductive minerals such as pyrite, pyrrhotite, arsenopyrite, chalcopyrite, galena, and also with oxide and gangue minerals such as hematite and magnetite (Marsden and House, 2006). Many researchers have suggested that the passivation of gold by the formation of films on the gold surface is a laboratory curiosity. In practical aspects, gold dissolution may slow down, and in that case, galvanic interactions and passivation by corrosion products are considered as important electrochemical factors (Lorenzen and van Deventer, 1992a; Azizi et al., 2011). Additionally, reversible electrode potential of the process, the exchange current density, the relative areas, the distribution of gold and conductive minerals involved, and the conductivity of the solution are the key factors affecting the galvanic interactions (Tshilombo, 2000).

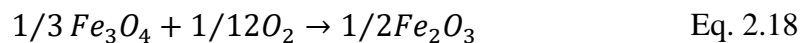
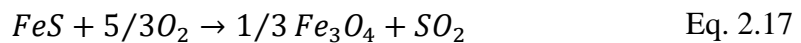
Early studies were mainly focused on the influence of dissolved minerals on the rate of gold dissolution (Fink and Putnam, 1950; Mrkusic and Paynter, 1970). For a better insight, van Deventer and Lorenzen (1987) proposed a new approach to understand and/or differentiate the dominating effect on gold dissolution between galvanic interactions and dissolved species (passivation phenomenon). In this manner, both the gold and metal or mineral electrodes were in direct contact with each other, as the working electrode, either in the same or in separate containers. If only the galvanic interaction was being investigated, the electrodes were placed in separate containers whereas the electrodes were placed in the same container if the combined effects of galvanic interaction and dissolved species were being investigated. van Deventer et al. (1990), and Lorenzen and van Deventer (1992b) considered this approach, and discussed mainly the conventional leaching results and the shift to more anodic potentials in the dissolution potential.

It is assumed that the gold dissolution rate may be influenced either in a positive or negative way by galvanic interactions. In other words, galvanic interactions could promote the dissolution rate of gold when the open circuit potential of gold is lesser than that of sulphides, or it can adversely affect the anodic dissolution of gold when sulphide mineral acquires anodic potential prompting on gold surface rather than the gold dissolution (Aghamirian and Yen, 2005). Potentiodynamic polarization, and galvanic coupling tests only in one container revealing the combined effects of galvanic interactions and passivation phenomenon were studied by Aghamirian and Yen (2005). Paul (1984) and Lorenzen and van Deventer (1992a) reported that the gold dissolution substantially decreases within the presence of pyrite and pyrrhotite, whereas Aghamirian and Yen (2005), and Dai and Jeffrey (2006) found positive effect on gold dissolution for these minerals. Aghamirian (1997) studied the influence of sulphide ions on gold dissolution in an oxygen enriched solution containing 47 ppm sulphide ions. Gold dissolution was found to increase from 0.085 to 0.17 mg/cm²/h with increasing O₂ concentration from 8 ppm to 32 ppm. However, the gold dissolution rate was still much lower than the standard rate, indicating that the passivation of the gold surface in oxygen enriched solution could still proceed (Aghamirian, 1997). Cruz et al. (2005) employed voltammetric studies before and after leaching using different pyrite bearing concentrates, such as sphalerite, galena, and acantithe (Ag₂S) to understand the activity of each sulphide minerals on gold. Wierse et al. (1978) reported that the elemental sulphur formed during gold dissolution could cover the exposed gold surface and prevent the further oxidation. Dai and Jeffrey (2006) discussed, individually, the anodic and cathodic behaviours between gold and sulphide minerals using a Au-Ag (5%) alloy electrode by employing linear sweeps. Azizi et al. (2010) performed the electrochemical dissolution of gold using Au/Ag (96%/4%) and mineral discs in the presence of sulphide minerals where four types of industrial ores were used either in one or two electrochemical cells. They examined the anodic and cathodic voltammograms, galvanic corrosion, and tested the electrochemical pre-oxidation treatment of the mineral electrodes. They reported that gold dissolution is controlled by positive galvanic interactions rather than by passivation in one electrochemical cell, whereas it is controlled mainly by positive galvanic effects in two electrochemical cells as a result of high galvanic currents. Azizi et al. (2011, 2012a, 2012b) used a bed reactor to examine the influence of

sulphide minerals on gold dissolution in one and two separate cells. They examined passivation and galvanic interactions during gold leaching in presence of industrial sulphide minerals and developed a Packed-Bed Electrochemical Reactor (PBER). PBER was used to decouple and quantify the individual contributions of passivation phenomena and galvanic interactions on gold and silver leaching rates. The highest gold extraction was achieved within the pyrite layer while the lowest was within the silica layer. It was found that the galvanic interactions due to pyrite, chalcopyrite and an industrial sulphidic ore were so positive that they largely outweighed the negative impact of precious metals passivation.

2.5.3 Oxidised Gold Ores Studies

In recent years, there has been an increasing trend for the treatment of refractory gold ores which often requires oxidation, such as roasting, as a pre-treatment process prior to cyanidation (Adams, 2016; Zhou and Fleming, 2007). Via oxidizing/roasting, pyrite (the most common gold carrier sulphide phase) is resulted in having predominantly hematite, magnetite (Eqs. 2.16-18) and maghemite (Stephens et al., 1990). Paktunc et al. (2006) reported that maghemite associated with gold is problematic for cyanidation as a result of its non-porosity. It has been reported that iron oxides, which are often found to be detrimental in cyanidation (Filmer, 1982; Lorenzen and van Deventer, 1992a, b), can contain appreciable amounts of gold (30 ppb to 260 ppm) (Paktunc et al., 2006). In order to understand the influence of iron oxide minerals on gold dissolution kinetics, different approaches or pre-treatment methods have been considered in the literature to treat these minerals, such as magnetic separation, and diagnostic leach procedures (Lorenzen and van Deventer, 1993; Douglas and Semenyina, 2013). However, electrochemical studies of oxidised gold ores have received less attention.



Magnetite is known to be $\sim 10^6$ times better conductor than hematite and maghemite (Barroso-Bogeat et al., 2014). Hence, the solubility of magnetite in cyanide solutions is expected to be relatively higher as compared to hematite.

It is well known that oxygen is essential for the dissolution of gold. Then, if the associated mineral with gold is electrically conductive, e.g., magnetite, oxygen reduction can take place over the entire surface of the mineral electrode, leading to an increase in the magnitude of the cathodic current (Filmer, 1982). As a result, the open circuit potential of gold is shifted to more noble or less active potentials, suggesting the (partial) passivation of the gold's surface. In this case, the rate of gold leaching tends to slow down. Mrkusic and Paynter (1970) reported that the anodic curve obtained in the presence of magnetite shows that the current is lower at all potentials than that in the absence of magnetite, and that the range of potentials, in which passive behaviour was observed was extended. These results would be compatible with the hypothesis that gold surface becomes partially covered by some form of film in the presence of magnetite. Thus, such a film would be expected to be of some iron compound. In the presence of magnetite, it is not clear which way the dissolution potential would move, if at all. They found that it can be expected that the rate of gold dissolution could be controlled by the rate of anodic or cathodic reaction, and not by diffusion. Hence, the role of agitation is expected to have relatively little effect. Mrkusic and Paynter (1970) found that when cyanidation is performed in the presence of magnetite, and the oxygen partial pressure is increased, it is possible that passive behaviour could be encountered at high dissolution potentials. They, however, did not demonstrate potentiostatic curves in presence of hematite since the hematite used was a very fine powder that tended to adhere to the electrode. They noted that this tendency would invalidate the results.

Alternately, in the case of hematite, which is a lesser conductor than magnetite, it can be expected that the reduction of oxygen takes place mainly at the surface of gold, so the rate would not be expected to decrease in these conditions (Filmer, 1982). As a result, the open circuit potential of gold is shifted to more active potentials, suggesting the increase in leach kinetics in the case of hematite, and maghemite as well. Filmer (1982) examined the

passivation of gold using partially oxidised, and almost complete oxidised calcine. It was found that the dissolution of gold in contact with magnetite, pyrite, and pyrrhotite could be expected to passivate as a result of the enhanced magnitude of the cathodic current. However, in the case of completely oxidised calcine representing hematite, gold dissolution would not be expected to decrease. [Paktunc et al. \(2006\)](#) examined such a roasted gold ore and concluded that calcines should dominantly be hematite containing more magnetite as an intermediate product and that the presence of maghemite should be avoided.

Recently, [Bas et al. \(2015a, 2015b\)](#) investigated the electrochemical dissolution behaviour of roasted gold ore. The influence of iron oxide minerals associated with roasted gold ore, individually (hematite, magnetite, and maghemite), on gold dissolution was examined. [Bas et al. \(2015c\)](#) studied Combined Anode Electrodes polarization (CAP), as a new approach, where gold and iron oxide mineral electrodes were electrically connected to each other to have one anode, with imposed potentials as function of leaching parameters where platinum was used the counter electrode. [Bas et al. \(2015d, 2016a\)](#) performed galvanic corrosion studies between gold and iron oxide minerals at Zero Resistance Ammeter (ZRA) mode as function of agitation. Galvanic interactions and passivation phenomena without imposed potentials either in the absence or in the presence of slurry at Zero Resistance Ammeter (ZRA) mode were discussed. To identify the dominating effect in between galvanic interactions and passivation phenomena on gold dissolution, CAP and ZRA tests have been performed either in one or two separate containers in the absence or presence of slurry of roasted gold ore. ([Bas et al., 2015c, 2015d, 2016a](#)). Since magnetite and hematite are the major iron oxides in roasted gold ore sample, a new electrode named “MagHem-ES” is developed to examine the concurrent effects of these minerals on the dissolution of gold ([Bas et al., 2015c](#)). The dissolution rate of gold by Tafel curves, and Stern-Geary methods have been compared to that in practical cyanidation. It was found that the dissolution rate of gold by considering only cathodic Tafel slope could better represent the practical cyanidation results ([Bas et al., 2015b, 2015c, 2016b](#)). Anodic curve was found to be misleading for the gold leach rate estimation due to passivation. The presence of slurry of roasted gold ore resulted in lower current densities (gold corrosion rates) ([Bas et al., 2015c](#)). Hematite was found to promote gold dissolution whereas magnetite retarded,

which has been confirmed by surface analysis (Bas et al., 2015d, 2016b). Bas et al. (2016b) found that the gold dissolution was retarded by 40% in the presence of magnetite slurry, whereas increased by 25% and 10% in the presence of hematite, and maghemite, respectively. They confirmed the negative influence of magnetite by SEM-EDS and XRD results. Following the leaching tests, the residue collected and it was subjected to magnetic separation tests (Bas et al., 2016b). Electrochemical characterization of magnetic part, non-magnetic part, synthetic maghemite, and roasted gold ore samples were performed. It was found that roasted gold ore, magnetic tailings, and synthetic maghemite electrodes exhibited a cathodic peak, suggesting the reduction of ferric to ferrous cyanide, which could be responsible for the slowdown of the gold leach kinetics, whereas magnetic concentrate did not. Furthermore, when oxygen was bubbled, this peak disappeared in the case of roasted gold ore and synthetic maghemite, though magnetic tailings still exhibited the peak (Bas et al., 2016b).

2.6 Interpretation of Electrochemical Findings

2.6.1 Practical Implications

In recent years, the treatment of low-grade ores, the shift from surface mining to underground mining, the increasing complexity of treatment, and the concern for environmental constraints are the main developments in the cyanidation of gold. The application of ultra-fine grinding technology to liberate gold finely disseminated in sulphides for subsequent leaching, optimization of reagent addition (e.g., cyanide and oxygen) are the subjects of research. In the late 1980s, online cyanide analyzers were introduced however, progress was slow. Additional testing was made to make the analyzer more reliable and effective and to have more accurate titration results. Online dissolved oxygen (DO) sensors were integrated in the late 1980s simultaneously with oxygen addition and various injection devices (Deschênes, 2016).

In practice, the rate of gold dissolution depends on several factors such as particle size, degree of liberation, alkalinity of the solution, cyanide concentration, aeration, agitation speed, gold and silver content, impurity content and surface coatings constituents. In this

regard, a comparison of the dissolution rates of gold by different research groups is given in [Table 2.5](#).

It is seen that the gold dissolution rates from real ores are relatively lower than that of pure gold samples which indicates the negative influence of sulphides, and oxides. The dissolution of gold may be reduced/slowed down in some conditions, and in that case passivation and galvanic interactions phenomena are considered as potentially significant electrochemical factors ([Lorenzen and van Deventer, 1992](#); [Mrkusic and Paynter, 1970](#)).

Table 2.5 Comparison of dissolution rates of gold from some selected papers.

Reference	Dissolution rate of Au (mol m ⁻² s ⁻¹)	Gold sample
Cathro and Koch (1964a)	5.52 x 10 ⁻⁵	Pure gold
Lorenzen and van Deventer (1992a)	6.27 x 10 ⁻⁶	Pure gold
Aghamirian and Yen (2005)	8.50 x 10 ⁻⁶	Pure gold
Dai and Jeffrey (2006)	5.6 x 10 ⁻⁵	Pure gold
Azizi et al. (2010)	6.6 x 10 ⁻⁶	Sulphidic gold ore
Bas et al. (2015b)	5.3 x 10 ⁻⁸	Oxidised gold ore

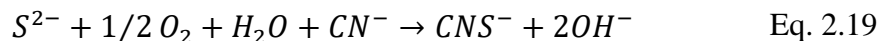
In general, when gold is electrically connected with a mineral/ore electrode, higher dissolution rate of gold could be expected due to the increase in surface area and electrochemical interactions ([Aghamirian and Yen, 2005](#)). Different surface areas of gold (a general range between 0.25 and 3.8 cm²) and mineral (typically between 2.7 and 6.2 and up to 900 cm²) electrodes have been considered ([Lorenzen and van Deventer, 1992a](#); [Aghamirian and Yen, 2005](#); [Azizi et al., 2011](#)). To note that, it is difficult to mimic the practical conditions in laboratory studies concerning the surface areas due to the low quantity of gold in its ores, but the chosen ratio in surface areas of electrodes is considerably suitable to see the main tendencies and influences of minerals on gold dissolution ([Bas et al., 2015b](#)).

In cyanide solutions, the rate of gold dissolution is normally controlled by mass transport with an activation energy of 8-20 kJ/mol ([Habashi, 1967](#)). The formation of precipitates on gold surface is very important affecting the shape of the leaching kinetics plot. Kinetics of gold reactions are very essential because most cyanidation plants operate at maximum

throughput (Deschênes, 2016). Faster gold dissolution kinetics favours high ore throughput, reduced cyanide consumption, and low impurity content (Kondos et al., 1995). The presence of metals/minerals such as silver, iron, arsenic, calcium, and magnesium, which are associated with gold, are important phases that could influence the leach rate of gold (Marsden and House, 2006). During cyanidation, not only the individual effects of these metals are important, but also multi-effects of these minerals, i.e. interactions between many phases, should be taken into consideration (Aghamirian and Yen, 2005; Azizi et al., 2012b). Deschênes (2016) pointed out that the use of an online cyanide analyzer, oxygen enrichment of the pulp, and the addition of lead nitrate have proved to be very efficient in reducing cyanide consumption. It has been reported that some ions (silver, lead) in the solution could act as removing the passivation of gold surface and promote gold dissolution whereas some others (pyrite, copper) slow down the kinetics (Lorenzen and van Deventer, 1992a; Deschênes et al., 2000). It has been reported that the consumption of lead nitrate could be decreased up to 55 % with an increase in the oxygen concentration (Deschênes and Wallingford, 1995). If the gold dissolution kinetics was reduced due to the passivation, the introduction of an additional cathodic reaction, such as the reduction of lead, could shift the dissolution potential to more positive values, suggesting the passivation of gold rather than dissolution (Tshilombo and Sandenbergh, 2001). In cyanide solutions, pH at high levels could show a negative influence on the concentration of free lead ions and also it would decrease the magnitude of the anodic peak (Mussatti et al., 1997). Lin and Chen (2001), and Guzman et al. (1999) reported that the passivation reaction enhances at high alkalinity, hence a faster passivation reaction occurs at a high pH. During cyanidation, increasing the oxygen concentration is beneficial where dissolution is controlled by the dissolved oxygen concentration (Jara and Bustos, 1992). Conventional cyanidation is usually performed at a pH higher than 10 and an O₂ concentration greater than 6 ppm. If the concentration of DO drops below 4 ppm, the rate of gold dissolution is greatly reduced. On the other hand, the rate of gold dissolution will increase markedly as the concentration of DO rises above 10 ppm. An oxygen-enriched operation is one that is conducted at 12-18 ppm O₂ by sparging oxygen into the slurry. It is important to underline that in cyanidation plants, oxygen is not only used to optimize plant throughput but also to enhance gold extraction (Deschênes, 2016). Pure oxygen was first

used to improve the cyanidation process by Air Products in South Africa in the 1980s (Stephens, 1988). This practice was introduced in Canadian plants at about the same time (McMullen and Thompson, 1989; Deschênes, 2016). In the leach solutions, dissolved oxygen concentration tends to decrease and the diffusion of reactants through the Nernst layer becomes much faster by increasing the temperature (Aghamirian, 1997). However, in plants most of the time the increase of the temperature creates a problem such as the increase in the decomposition and consumption of cyanide (Habashi, 1967). In hot climates, the leaching of gold takes place outside while it is normally carried out inside in colder climates to minimise the effect of the temperature. Accordingly, leach tanks are mostly located in buildings to minimise the retarding effect of colder weather (Deschênes, 2016).

Tshilombo and Sandenbergh (2001) stated that the peak current is an indication of the rate of reaction required to cause the passivation of gold surface. If passivation is due to the lack of cyanide, such that insoluble AuCN forms, it is not surprising that the peak current density is dependent on the cyanide concentration. Once gold becomes passive, it is a slow process to make it again active especially at the more positive potentials since the passive layer on the gold surface would presumably be thicker. To make the gold active, the formed polymeric AuCN could be disrupted (Nicol, 1980), or the presence of some minerals/metals could promote the dissolution of gold via galvanic interactions (Lorenzen and van Deventer, 1992b; Chimenos et al., 1997). Generally, high dissolved oxygen levels are considered to overcome the passivation of gold that typically occurs due to the release of sulphide ions from pyrite concentrates. Sulphide ions released from sulphidic minerals may react with oxygen and cyanide to form thiocyanate ion (Eq. 2.19) (Osseo-Asare et al., 1984). Gold-sulphur compounds such as Au₂S, Au₂S₃, AuS₂O₃⁻ and AuS⁻ have been reported as responsible for reduction in the gold dissolution (Osseo-Asare et al., 1984).

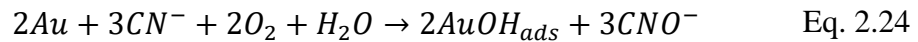
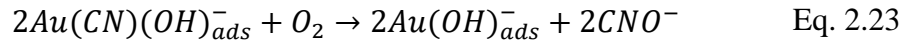
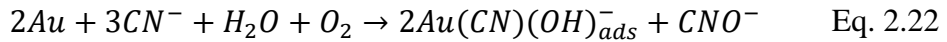
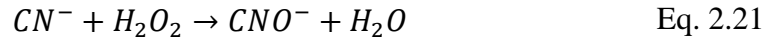
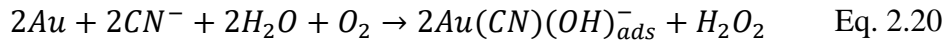


Electrochemical dissolution rates of gold have been reported in the literature using different kinetic approaches, such as mixed-potential (Tafel curves), Evan's diagrams, galvanic

corrosion, cathodic curve only, Stern-Geary method, mass transport, and etc. (Nicol et al., 1987; Choi et al., 1991; Dorin and Woods, 1991; Li et al., 1992; Lorenzen and van Deventer, 1992a; Guan and Han, 1994; Sun et al., 1996; McCarthy et al., 1998; Crundwell and Godorr, 1997; Jeffrey and Ritchie, 2001; Xue and Osseo-Asare, 2001; Wadsworth, 2000; Dai and Breuer, 2013; Bas et al., 2015b). In these works, gold foils and rotating gold discs with constant surface areas have been used to determine the leach rates assuming that the surface roughness does not change during the test-work (Senenayake, 2008). It is worthy to note that due to the difficulty in Tafel extrapolation, two recommended rules as follows should be carefully considered: i) the extrapolation should start at least 50-100 mV away from E_{corr} , and (ii) at least one of the branches of the polarization curve (cathodic or anodic) should exhibit Tafel over at least one decade of current density (Kelly et al., 2002). In mixed (dissolution) potential theory, it has been suggested that, each half reaction can be examined independently; for example, gold dissolution is studied in the absence of oxygen. In order to estimate the dissolution/corrosion rate of gold, the intersection point of anodic and cathodic curves was considered (Kudryk and Kellogg, 1954; Cerovic et al., 2005). However, Dai and Breuer (2013) have reported that the actual leaching point of pure gold does not match to the intersection of Tafel curves, suggesting that the leaching of gold takes place at higher rate than that of Tafel curves. They concluded that intersection point could be misleading for the estimation of the corrosion rate of gold, since the influence of cyanide is not included in the cathodic curve whereas the influence of oxygen is not included in the anodic curve. Recently, Bas et al. (2015b, 2015c, 2016b) have considered cathodic Tafel slope only by extrapolating from open circuit potential in presence of atmospheric oxygen, since there may be passive behaviour in anodic curve, and that was compared to the conventional cyanide leaching results. It was found that considering cathodic Tafel slope only better represents the leach rate of gold as in practice (Bas et al., 2016b). The findings have indicated that cathodic slope provides significant information, and has the major controlling effect on the electrochemical behaviour of tested specimen, in this case gold (Bas et al., 2015c, 2016b).

2.6.2 The Mechanism of Dissolution Slowdown During Cyanidation

The dissolution rate of gold can be very low and this could be due to passivation by the formation of a highly insoluble aurocyanide polymer on the surface or to an adsorbed hydroxide as suggested by Kirk et al. (1980). Wadsworth and Zhou (2003) explains the anodic oxidation model for gold in the following three steps: i) steady-state formation of a passivate action of AuCN at the metal-film interface; ii) diffusion of gold ion through the film, and iii) dissolution of AuCN at the film-solution interface. It is believed that the surface of gold during cyanidation is blocked/covered by a film of AuCN at low overpotentials which leads to poor gold extractions in cyanidation (Catro and Koch, 1964a; Nicol et al., 1987; Zheng et al., 1995; Jeffrey, 1997). Hydroxides are also known to be responsible for the passivation of gold which could be due to the following reactions (Eqs. 2.20-24) (Senanayake, 2008).



As seen in Fig. 2.5, the current increases continuously as the potential shifts from -0.8 V to -0.4 V vs SCE, above this potential the current, i.e. the rate of dissolution becomes plateau, being limited by the rate of diffusion of cyanide to the electrode. Also, anodic curve covers a wide range of cyanide concentrations, which represent as in cyanidation plants, preferably 20 - 2000 ppm CN^- (corresponding to 0.005 - 0.5 % KCN) (Fig. 2.5) (Lörosch, 2001).

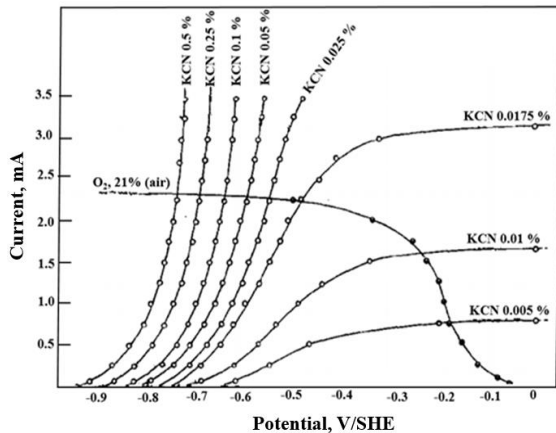


Fig. 2.5 Anodic (as function of cyanide concentration) and cathodic curves for gold dissolution (adapted from Kudryk and Kellogg, 1954).

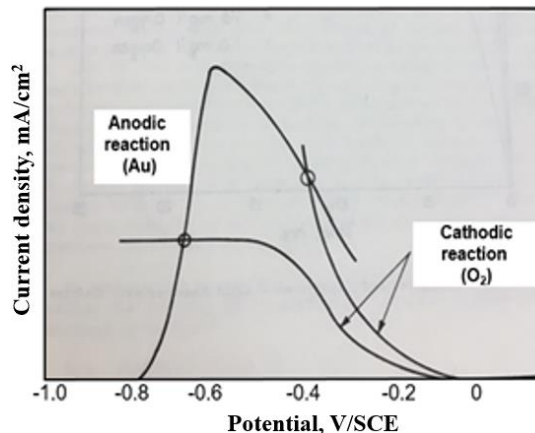


Fig. 2.6 Polarization curves showing anodic passivation of the anodic reaction from the work of Mills (1951), retrieved and adapted from Cathro and Walkley (1961).

Mills (1951) however, obtained somewhat different results (Fig. 2.6). It is also in line with the results of Kudryk and Kellogg (1954) up to -0.5 V vs SCE, but as the potential becomes more positive the current suddenly decreases suggesting that the gold becomes passive. Gilroy and Conway (1965) reported that in electrochemistry, the diffusion limitation will tend to lead, under most conditions, only to a constant limiting current with increasing potential whereas a true passivation under potential control is associated with a region of decreasing current. Kolotyркиn (1958) has considered the initiation of passivation as being associated with the appearance of a monolayer or less of an inhibiting species. Hackerman (1959) reported that in case of steel electrodes in most cases, the inhibiting species were found to be a “surface” or “adsorbed” oxide, e.g. MOH or MO generated from aqueous solution.

Mrkusic and Paynter (1970) used pure gold discs and reported that the dissolution of gold in cyanide solution was inhibited by the presence of iron sulphide minerals, and their oxidation products by the formation of strongly adherent films of some yet unknown species on the surface of the gold. MacArthur (1972) concluded that the oxidation of gold proceeds through a surface intermediate, (probably $[\text{AuCN}]_{\text{ads}}$) and that the oxidation of gold in the region -0.6 to -0.2 V is limited by the dissolution of the surface intermediate.

When the surface is completely covered, the rate of reaction is controlled by the rate of chemical dissolution of the intermediate.

Table 2.6 Gold deportment results of carbon-in-leach tailings and the techniques used to analyse forms of gold (Total assayed gold = 3.4 g/L) (Dimov and Hart, 2014).

Technique	Au assayed	Form of Gold
Assayed	1.1%	Soluble gold
D-SIMS	24.7%	Sub-microscopic gold in hematite
D-SIMS	17.4%	Sub-microscopic gold in unoxidized pyrite
TOF-SIMS	46.5%	Surface gold preg-robbed on c-matter
Assayed	4.4%	Gold enclosed in rock

It can be stated that some of the previous studies suggested the passivation of gold, and that was not frequently accompanied with thorough surface studies. It is believed that surface characterization is very critical and necessary for a better understanding of the passivation phenomenon of gold. The formation of AuCN_{ads} layer on the surface of gold has been confirmed by employing electrochemical scanning tunnelling microscopy (STM) (Sawaguchi et al., 1995; McCarley and Bard, 1992). Further, X-ray photoelectron spectroscopy (XPS) and X-ray absorption near-edge structure spectroscopy (XANES) techniques have been used to determine the chemical state of gold associated with arsenopyrite and pyrite (Cabri et al., 2000; Simon et al., 1999). Deschênes et al. (2012) examined leaching of gold in the presence of copper sulphide minerals. They reported that XPS analysis of the djurleite (a copper sulphide mineral) showed that lead nitrate favored the formation of $\text{Cu}(\text{OH})_2$ and the precipitation of lead oxide and hydroxide. The formation of these compounds were found to reduce the passivation of gold. XPS was also used to confirm the gold species adsorbed by activated carbon (Dimov et al., 2003). Other specific techniques used in gold studies are dynamic-secondary ion mass spectroscopy (D-SIMS) and time of flight-secondary ion mass spectroscopy (TOF-SIMS). D-SIMS is used to analyse the sub-microscopic gold that is associated with iron oxides and pyrite, whereas TOF-SIMS is a suitable technique used to analyse the deportment of gold associated with carbonaceous matter (c-matter). Table 2.6 shows an example of the use of different

techniques to characterize the gold in carbon-in-leach residue samples (Dimov and Hart, 2014). Recently, gold ores are becoming more complex, and passive layer on the surface is often difficult to observe. Therefore, sensitive techniques/equipments with specific features would likely be required for future studies to characterize the surface species on gold.

It has been deduced that passivation is an anodic phenomenon and it is always accompanied by a natural potential which is more positive than -0.6 V/SCE (Mills, 1951; Cathro, 1964a; Lorenzen, 1992). Accordingly, the reduction potential of oxygen in alkaline cyanide solutions is in the region of -0.3 to -0.4 V/SCE. Then, it could be asked if oxygen is the most suitable oxidizing agent for the reduction. It would appear that a thermodynamically weaker oxidant than oxygen should have advantages in being less likely to initiate passivation and less likely to oxidise cyanide (Lorenzen, 1992). It can be concluded that film formation and passivation are not merely a laboratory curiosity, but also can reduce the efficiency in industrial practice. The formation of a film on the surface of the gold owing to diffusion of species from other partially soluble minerals also decreased the leaching rate. Finkelstein (1972) suggested that the efficiency of industrial cyanidation can be reduced by passivation, but it is not known whether all ores and operations are affected, nor whether the degree of passivation has major influence on operating efficiencies.

The effect of the addition agents in reducing corrosion is called inhibition (Scully, 1966). Passivation, in electrochemical studies, is mainly related to the oxidation of metals and resulting the formation of layers on the surface which is responsible for the reduction in dissolution by several orders of magnitude, as illustrated in case of iron in stainless steel in Fig. 2.7. The $\text{Fe}^{3+}/\text{Fe}^{2+}$ reaction can promote inhibition through passivity. At low concentration and at active potential values, the introduction of reduction as an additional cathodic reaction increases the dissolution rate, but if the cathodic current density is increased beyond the critical current density of the anode reaction then the metal becomes passivated (Scully, 1966). This type of inhibition that induces passivity in presence of the ferric/ferrous ion reduction is somewhat different from inhibition by chromates and nitrites, since the latter lose oxygen as part of the reduction process (Scully, 1966). Accordingly,

Choundhary et al. (2015), and Crundwell (2015) considered the electrochemical behaviour of stainless steel to discuss passivation as a comparison to gold and copper dissolution.

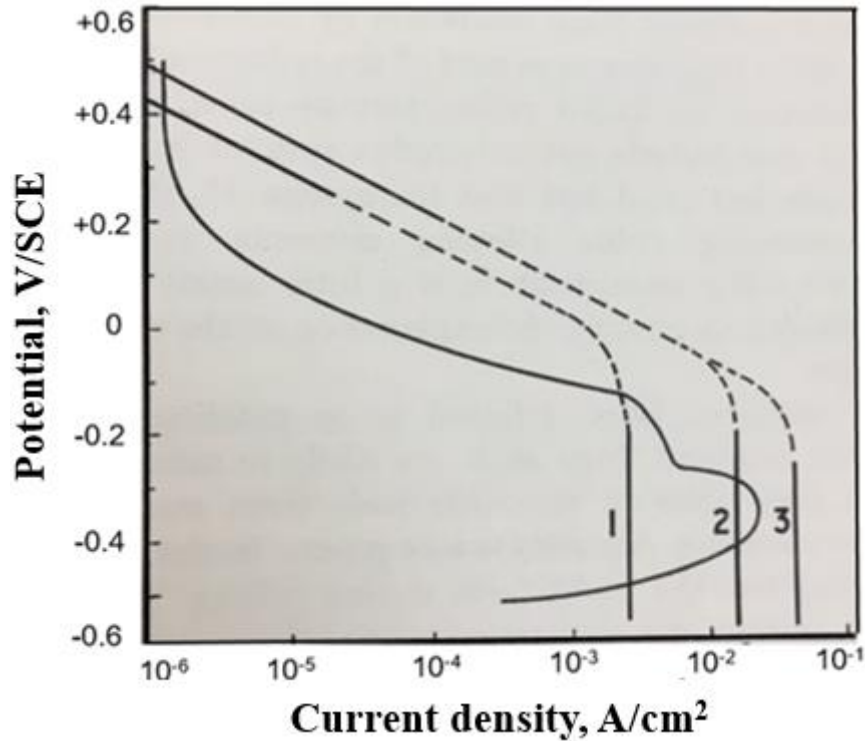


Fig. 2.7 Superposition of reduction curves for ferric ion and of the anodic polarization curve of Type 410 stainless steel in M H₂SO₄. Curve (1) 0.01 M Fe³⁺ at 55 cm/sec, (2) 0.066 M Fe³⁺ at 55 cm/sec, and (3) 0.066 M Fe³⁺ at 100 cm/sec. In case (3) the limiting diffusion current density for the ferric ion is greater than the critical current density for the steel and the ferric ion therefore passivates the steel (adapted from Scully, 1966).

During electrochemical measurements, anodic polarization has been frequently carried out in an electrolyte containing cyanide in absence of oxygen, whereas the cathodic polarization has been considered in presence of oxygen and absence of cyanide. However, to mimic the practical cyanidation process, it is strongly recommended to consider anodic and cathodic polarization in presence of cyanide and atmospheric oxygen. Additionally, the change in the exposed anodic and cathodic areas could not be controlled, however SRET in-situ could monitor the potential variations of micro-sites.

Chapter 3

Electrochemical Behaviour of Pure Gold in Cyanide Solutions

Active and Passive Behaviours of Gold in Cyanide Solutions

Ahmet Deniz Bas^{a*}, Fariba Safizadeh^a, Wei Zhang^a, Edward Ghali^a, Yeonuk Choi^b

^aDepartment of Mining, Metallurgical and Materials Engineering, Laval University, Quebec, Canada, G1V 0A6

^bBarrick Gold Corporation, Suite 3700, 161 Bay Street P.O.Box 212, Toronto, Ontario, Canada, M5J 2S1

*Corresponding author: 4186568657, Fax: 4186565343; (ahmet-deniz.bas.1@ulaval.ca)

Published in: *Trans. Nonferrous Met. Soc. China*, Elsevier, 25, 10, 3442-3453

DOI: [10.1016/S1003-6326\(15\)63981-4](https://doi.org/10.1016/S1003-6326(15)63981-4)

Résumé

Les comportements actifs et passifs pour des électrodes d'or pur (Au) et de minerai d'or grillé (RGO) ont été étudiées à 25 °C dans les milieux de cyanure agité de-aéré. Voltamétrie cyclique et polarisation potentiodynamique avec une agitation à 100 tours par minute dans une solution de NaCN 0,04 M montrent différentes positions des crêtes et des densités de courant. Les tests potentiodynamiques ont illustré que les densités de courant de crête grandement accrues avec l'augmentation de la concentration de cyanure. L'augmentation du pH de 10 à 11, a entraîné environ 35 fois plus faible densité de courant, alors qu'elle a augmenté de ~ 32 fois en diminuant l'agitation 100-60 tours par minute. En présence d'oxygène, Au et RGO électrodes ont présenté des caractéristiques différentes des positions des pics et des vitesses de la corrosion. Les études potentiostatiques ont montré que le potentiel a augmenté de 1 à 1,4 V à pH 11 et a entraîné une diminution de 80% tout en augmentant le pH de 10 à 11 à 1 V a donné une diminution de 1,7 fois la densité de courant, peut-être due à une couche passive plus efficace. Après la polarisation, les mesures de bruit électrochimique (ENM) pendant les périodes de désintégration ont montré que Au a donné lieu à des états plus passifs à hauts potentiels, montrant la corrosion par piqûres. Les résultats ont montré que cette ENM technique pourrait être un outil prometteur pour une meilleure compréhension de la lixiviation de l'or. Des études de XPS ont prouvé la présence d'oxydes passifs.

Abstract

Active and passive behaviours of pure gold (Au) and roasted gold ore (RGO) electrodes were investigated at 25°C in de-aerated agitated cyanide media. Cyclic voltammetry and potentiodynamic polarization with agitation at 100 rpm in 0.04 M NaCN solution showed different peak positions and current densities. Potentiodynamic tests illustrated that peak current densities greatly increased with increasing cyanide concentration. Increasing pH from 10 to 11, resulted in ~ 35 times lower current density, while it was increased ~ 32 times by decreasing agitation from 100 to 60 rpm. In the presence of oxygen, Au and RGO electrodes showed different characteristics of peak positions and corrosion rates. Potentiostatic studies showed that increasing potential from 1 to 1.4 V at pH 11 resulted in an 80% decrease while increasing pH from 10 to 11 at 1 V gave a 1.7-fold decrease in current density, possibly due to more effective passive layer. Following polarisation, Electrochemical Noise Measurements (ENM) during decay periods showed that Au has resulted in more passive states at high potentials, showing pitting corrosion. ENM results showed that this technique could be a promising tool for a better understanding of gold leaching. XPS studies proved the presence of passive oxides.

Keywords: pure gold, roasted gold ore, cyanide, passivation, electrochemical noise, XPS

3.1 Introduction

Due to rapid depletion of free-milling gold ores, refractory gold ore processing has become ever important (Marsden and House, 2006). In practice, refractoriness of the ore leads to low gold extractions and high cyanide consumptions (Muir, 2011; Lorenzen and van Deventer, 1992a). In gold ore processing, passivation of the gold surface and/or diffusion control are the practically faced problems. During cyanidation process and in certain conditions, gold surface is protected by a surface film, which causes poor gold extractions. There are several electrochemical measurement techniques to evaluate the anodic behaviour of gold.

Passivation phenomenon of gold surface can be considered as one of the challenges in practical cyanidation, and so a better understanding of this phenomenon is quite important. Two recently published papers (Holmes and Crundwell, 2013; Crundwell, 2013) considered the passive phenomenon of metals including gold during dissolution. Holmes and Crundwell (2013) used pyrite sample and mentioned that polysulphides do not cause passivation. Crundwell (2013) claimed that each point on the surface is considered as both anodic site and cathodic site and concluded that there is no separation of anodic and cathodic sites on the surface of mineral. Habashi (1966) and Habashi and Bas (2014) pointed out that certain experimental results demonstrated the existence of anodic and cathodic zones during the dissolution of minerals. Moreover, Azizi et al. (2013) examined the passive behaviour of gold ore and concluded that all minerals directly affected the leaching of gold and pre-oxidation may be an effective option for gold dissolution. These studies show that active and passive behaviours of gold still receive high attention and need to be examined.

In the case of gold, to date, some electrochemical techniques were conducted to monitor the anodic behaviour of gold. Cyclic voltammetry (CV) (Lin and Chen, 2001; Mughogho and Crunwell, 1996) and potentiodynamic techniques (Guzman et al., 1999; Kirk et al., 1980; Pan and Wan, 1979) were used by some research groups for observation of interfacial reactions. Lin and Chen (2001) used relatively high cyanide concentration (0.2 M) as compared to leaching practice when using cyclic voltammetry testing with rotating disk

electrode at 500 rpm in oxygen-free electrolyte. Three oxidation and one reduction peaks were observed. [Mughogho and Crundwell \(1996\)](#) employed cyclic voltammetry of rotating disk gold electrode at 1000 rpm at 100 mV/s scan rate using dilute cyanide solution (0.003 M). Three oxidation peaks, one reduction and one small oxidation peak in the return sweep were obtained with relatively lower current densities in this rarely used dilute solution in practice. In the previous potentiodynamic studies, the effects of cyanide concentration and pH were tested and found that in most cases gold had three oxidation peaks and certain intermediate reactions were advanced ([Guan and Han, 1994](#); [Kirk et al., 1978](#)). [Mac Arthur \(1972\)](#) mentioned the complexity of the reaction and emphasised the difficulty to obtain a precise result. It was suggested that gold oxides and cyanide films were responsible for the passivation of gold surface ([Kirk and Foulkes, 1980](#); [Guan and Han, 1994](#)). Electrochemical Noise Measurements (ENM) ([Eden, 2011](#)) is referred as a random fluctuation of current and/or potentials that have received widely attention to study the electrochemical systems. The instantaneous response to change of surface conditions enables this method to be an online-monitoring tool. Although ENM technique was being considered for stainless steel ([Klapper et al., 2013](#)), copper ([Safizadeh and Ghali, 2013](#)), zinc ([Zhang et al., 2005](#)), aluminium ([Curioni et al., 2013](#)) and other metals, there is a paucity of in-situ ENM studies on gold.

In this study, cyclic voltammetry and the effect of cyanide concentration and pH on the anodic behaviour of pure gold (Au) and roasted gold ore (RGO) electrodes were tested in cyanide solutions using potentiodynamic and potentiostatic techniques in presence of moderate agitation to simulate the practical conditions. In potentiostatic tests, as complimentary to the previous studies, the influence of imposed two anodic potentials, representing the passive region, in different electrolytes on the anodic behaviour of gold and gold ore was examined. It is worth noting that, the majority of gold ore studies were conducted using sulphidic gold ores ([Aghamirian and Yen, 2005](#); [Azizi et al. 2010, 2011, 2012](#)). In this paper, oxidised gold ore which was predominantly consisted of iron oxides were used. Electrochemical Noise Measurements (ENM) technique was also applied to monitor the anodic behaviour of gold during decay periods after anodic polarization. This

could give an insight for better understanding of the anodic behaviour of gold in cyanide solutions. Surface film identification of gold was carried out in parallel by XPS.

3.2 Experimental Conditions

3.2.1 Ore Sample and Roasted Gold Ore Electrode Preparation

The gold ore sample was obtained from Barrick Gold Corp. This was the calcine after roasting of refractory gold ore. The sample (which was already reduced in size 80% passing $-75\ \mu\text{m}$ (d_{80})) was riffled as portions prior to use in experiments. Mineralogical analysis of the sample indicates that the ore sample consists predominantly of hematite, magnetite and maghemite. Presence of maghemite content renders the ore refractory in character due to difficulties in cyanidation (Paktunc et al., 2006).

Roasted gold ore (RGO) with an exposed surface area of $4.9\ \text{cm}^2$ was used as compared to $1\ \text{cm}^2$ of pure gold electrode (Au). The difference in surface areas of electrodes is somewhat reflecting the practice. Gold ore was mixed with graphite powder (to increase conductivity) 3:1 and with around 0.5 g of silicone oil, for binding, till a paste was obtained. Then, it was mechanically pressed at 20 tons to have uniform sample surface. After that, roasted gold ore electrode was kept under nitrogen over a night. Then, connected with an insulated copper wire, cast in acrylic resin and conductivity of the electrode was also checked.

3.2.2 Cyclic Voltammetry, Potentiodynamic, and Potentiostatic Tests Procedures

$1\ \text{cm}^2$ of gold foil (99.9% purity from Sigma Aldrich) was used as a working electrode. Platinum as a counter electrode and Ag/AgCl/KCl saturated as reference electrode were used. Gold electrodes were first washed and polished with fine (MicroCut® 100 Grit Soft) polishing paper and then rinsed in distilled water. Electrodes were then introduced to aqua-regia for 10 seconds to clean the surface, washed with distilled water and ethanol and finally rinsed with distilled water again, for reproducibility. NaCN ($\geq 98\%$ purity) was obtained from Thermo Fisher Scientific Company. Cyclic voltammetry of pure gold electrode without agitation was carried out in 0.04 M NaCN solution at pH 10.5. Electrolyte of 1 L solution was first bubbled with argon and magnetically agitated at 250 rpm for 50 minutes to eliminate the oxygen. Then, three typical electrodes system was placed into the

solution with slight argon bubbling on the surface of the electrolyte. CV studies were conducted in duplicates between -1 V to 1.2 V and the first two cycles were reported. The scan rate was controlled at 10 mV/s. In potentiodynamic and potentiostatic tests, argon was profoundly bubbled over the test period. Electrolyte medium (1L) was prepared using distilled water and pH was adjusted by adding 1 M NaOH. Electrolyte was magnetically agitated (moderate agitation) (4 cm long and 1 cm diameter) during the test (100 rpm). In this study, EC-Lab software from (Biologic, France) was used to monitor and interpret the obtained results. The preparation procedure for EN studies includes 3 steps. First step was the application of potentiostatic cathodic potential at -0.8 V for reducing any oxidised material for 30 min. Second step was the potentiodynamic test applied with a scanning rate of 0.166 mV/s for the range from -0.8 V to the desired two anodic potentials of 1 or 1.4 V, respectively. This was followed immediately by potentiostatic studies at three different potentials to monitor the changes in current for 2 hours as the last step. All tests were performed in duplicates and all potentials were reported with respect to the Standard Hydrogen Electrode (SHE).

3.2.3 Electrochemical Noise (EN) Measurement Test Procedure

Prior to electrochemical noise measurement (ENM) tests, two working gold electrodes were prepared separately following the three steps, mentioned at section 3.2.2. Electrochemical noise measurements were conducted in employing a set-up using zero resistance amperometer (ZRA) mode. In this mode, the electrochemical noise could be measured between two nominally identical working electrodes as the galvanic coupling kept at the same potential. The samples were immersed in the solution where the system was allowed to stand at open circuit for 5 min. Then, the potential and current fluctuations were simultaneously recorded during 16 hours at a scan rate of $f_s=10$ Hz giving 1024 data points per block. All potentials were measured via Ag, AgCl/KCl saturated reference electrode (0.202 V), and reported with respect to Standard Hydrogen Electrode (SHE).

The ENM tests were carried out without agitation in the absence of oxygen (argon bubbling). A Gamry[®] PC4/300 potentiostat was used to log current and potential variations in time. The analyses were performed using a GAMRY[®] PC4 750/ESA400 software and

analyser v. 2.35. The DC drift was removed before all analyses to eliminate the trend. At least, two series of test were performed for each tested sample.

3.2.4 Procedure of Surface Characterization Test

Surface characterization studies were carried out using X-ray photoelectron spectroscopy (XPS). XPS results were collected using an AXIS-ULTRA instrument by Kratos (UK). The X-ray source is a monochromatic Al source operated at 300 watts. Analyser runs in the constant pass energy mode. Survey scan is recorded with pass energy of 160 eV and a step size of 1 eV. In order to have a precise knowledge of the binding energy scale just before the analysis of the sample, a gold foil surface has been cleaned in situ by sputtering with argon ion beam (10 μ A and 2 keV) for about 20 minutes. The $Af4f_{7/2}$ line was then recorded at high resolution. As expected, the Au peak, fitted to having a binding energy (BE) of exactly 83.95 eV. Thus the instrument is in good shape and ready for analysis of gold surface (Adnot, 2013).

3.3 Results and Discussion

3.3.1 CV without Agitation and Potentiodynamic Tests

Peak determination of pure gold surface was carried out by CV. Fig. 3.1 demonstrates the cyclic voltammetry results in 0.04 M NaCN, pH 10.5 electrolyte in the first two cycles. pH and cyanide concentration were chosen based on industrial practice of gold leaching. Three oxidation and one reduction peaks were observed. In Fig. 3.1, peaks A and B could correspond mainly to $AuOH_{ads}$, while peak C is related to $Au(OH)_3$, and more detailed explanations are given in the following potentiodynamic results. Hydrogen evolution reaction (Eq. 3.1) takes place as shown in region F, and this could also correspond to the reduction reaction assisted with the dissolved atmospheric oxygen in the electrolyte. The increased current above potential of 1.5 V indicates the oxygen evolution reaction (Eq. 3.2) and also potentially the presence of the reaction of cyanide oxidation to cyanate (Eq. 3.3) which is shown as peak D. It can be deduced that while oxidation peaks are cyanide related, the reduction peak (peak E) is related to OH^- as has been previously suggested (Lin and Chen, 2001).

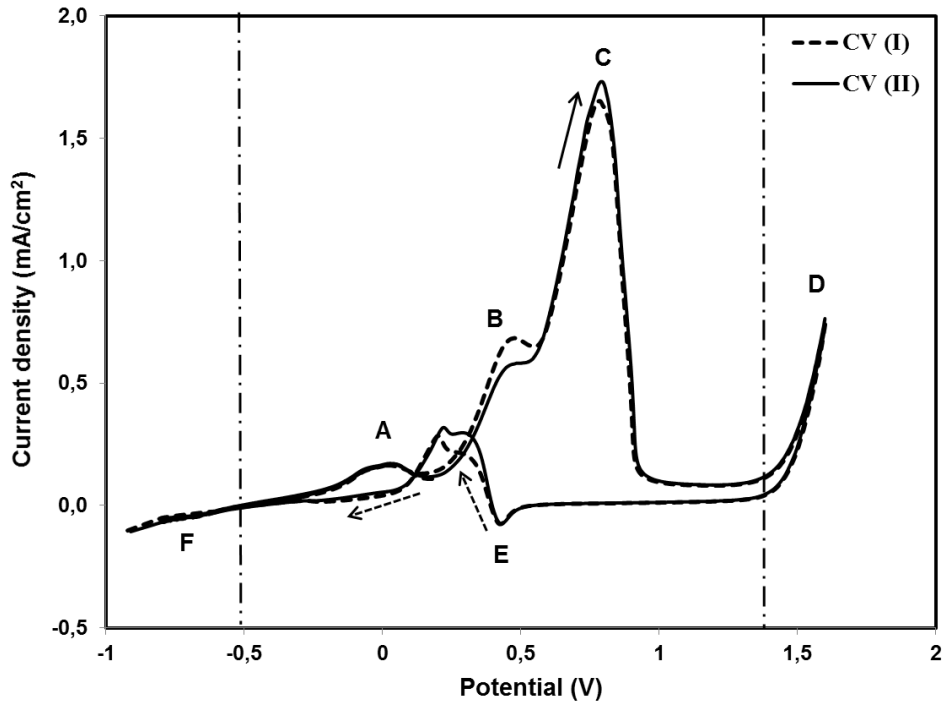
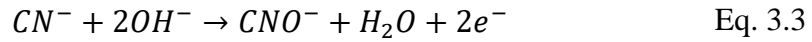
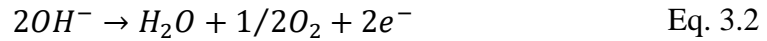
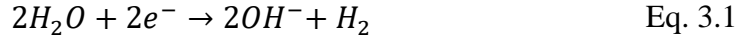


Fig. 3.1 Cyclic voltammetry of pure gold electrode (Au, 1 cm²) in the first two cycles (CV I and II) without agitation (dotted arrow indicates the return) in 0.04 M NaCN solution in oxygen-free conditions at pH 10.5.

Fig. 3.2 shows the effect of cyanide concentration (0.005-0.2 M) on the anodic behaviour of gold electrodes using potentiodynamic test. The potentiodynamic findings with moderate agitation and scanning rate in cyanide solutions showed that an increase in cyanide concentration leads to an increase in current density up to 0.1 M then showed a slight decrease (0.2 M) although the relative magnitudes of the peak current densities were somewhat different.

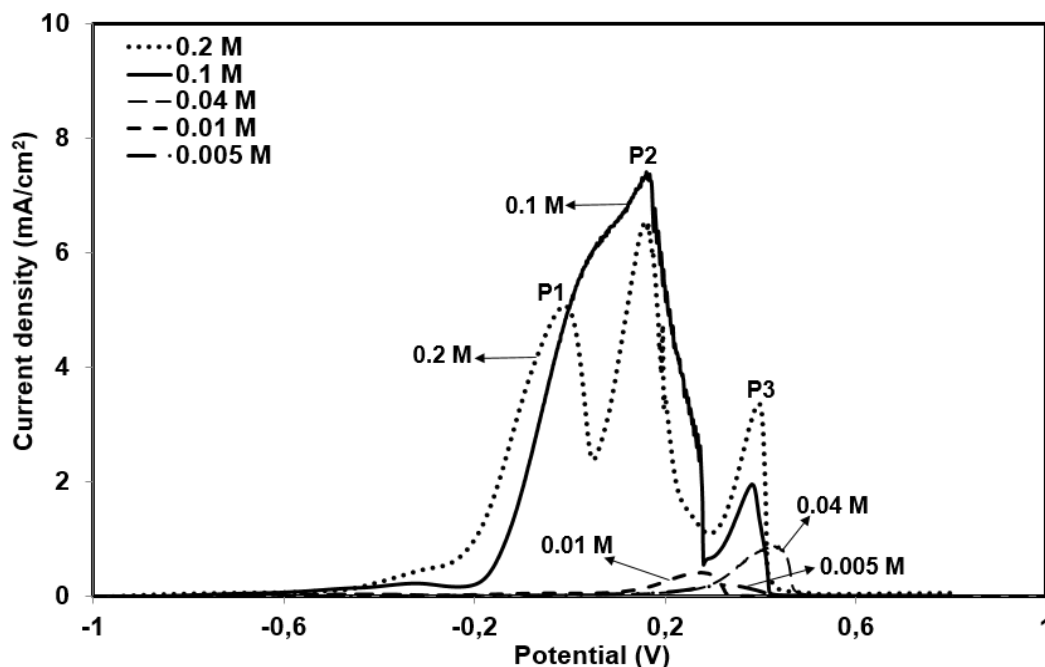
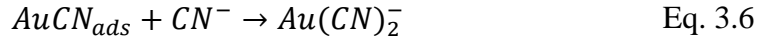
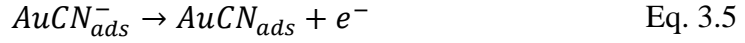


Fig. 3.2 Effect of NaCN concentration on anodic potentiodynamic behaviour of gold electrode (Au, 1 cm²) (NaCN: 0.005 - 0.2 M, pH 10.5, T: 25°C, scan rate: 0.166 mV/s and argon bubbling).

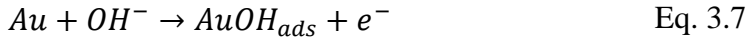
Peak current density (*e.g.* second peak) was measured around 7.37 mA at 0.1 M while it reached only 0.22 mA at 0.005 M. For instance, peak current densities were observed around 4.94, 6.52 and 3.24 mA (at 0.2 M) for the consecutive three peaks, while Kirk et al. (1978) observed almost 0.3, 10, 40 mA, respectively, at the same concentration of cyanide (0.2 M). The first peak generally gave very low current density and sometimes was not observed. These results confirmed the presence of three peaks and differences in peak current densities could be linked to some experimental parameters, such as magnitude of agitation and scan rate.

In the tested range, 3 peaks P1, P2 and P3 (Fig. 3.2) of passivation were identified, corresponding very possibly to peaks A, B and C in non-agitated solutions for CV studies (Fig. 3.1). The first peak was occurred at around -0.2 V, second peak was 0.15 V and third peak at 0.45 V vs. SHE. The reaction in each of these peaks has been observed to be a one

electron transfer process (Kirk and Foulkes, 1980) following the reaction sequence (Eqs. 3.4-6):



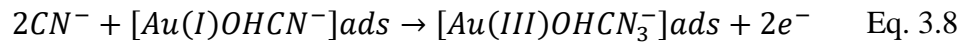
For the first peak region, the second step (Eq. 3.3) was suggested to be the rate-determining step. When the gold surface was covered by $AuCN_{ads}^{-}$ film, the rate of dissolution of gold was controlled by the rate of chemical dissolution of this intermediate. However, Pan and Wan (1979) mentioned that the adsorption of hydroxyl ions on the surface of gold was the contributing cause of passivation (Eq. 3.7) according to the following equation:



At concentrations tested in this study (0.005-0.2 M NaCN), lower current density was observed for the first peak (P1) if compared to other two peaks (P2 and P3) for all concentrations. Generally, first peak current density is smaller than the other two successive peaks (Nicol, 1980; Bek et al., 1997). High cyanide concentration leads to higher peak densities of Au^{+} as it corresponds to the formation of first peak. Therefore, Au^{+} promotes passivation in this passive region. This approach could be ascribed for the second and third peaks due to the accumulation of Au^{+} and Au^{3+} ions, respectively.

The current density of the first peak (-0.2 V vs. SHE) shows large variations depending on the range of CN concentrations, pH tested and measurement techniques. Different concentrations of cyanide were investigated by several research groups such (0.2-1 M KCN) (Pan and Wan, 1979), (0.001-0.02 M KCN) (Guan and Han, 1994), (0.05-0.2 M KCN) (Kirk et al. 1978), (0.2 M) (MacArthur, 1972), (0.008-0.077 M KCN) (Nicol, 1980). Mughogho and Crundwell (1996) suggested that gold dissolution reaction has different mechanism in high cyanide concentration than that in low concentration. At low cyanide concentrations (< 0.04 M), first peak current density was found to be very small if

compared to that of the other two peaks. Nicol (1980) concluded that the first peak was not observed if the potential scan was applied immediately after gold placing into the solution while it was observed if the electrode allowed standing at open circuit for 30 minutes at high rotation speeds. At about 0.35 V vs. SHE potential range which corresponds to second peak region, Cathro and Koch (1964a) proposed the conversion of Au(I) to Au(III) basic cyanide film (Eq. 3.8). However, Kirk et al. (1978) carried out many studies and suggested the same reaction sequence (Eqs. 3.4-6) for the second peak region and the second peak could be attributed to the formation of gold (I) hydroxide (Eq. 3.7).



For the third peak region, Kirk et al. (1978) suggested that the same reaction sequence as for the first and second peaks, but the last step was determined to be the rate-determining step. However, Mac Arthur (1972) stated that it is quite difficult to explain peaks formations due to the complexity of reactions. It was generally agreed either direct oxidation of an adsorbed intermediate, or oxidation to gold (III) (Eq. 3.9), could cause passivation (Senanayake, 2008).

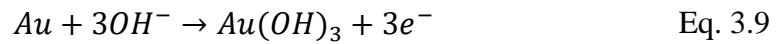


Fig. 3.3 shows the comparison of potentiodynamic and cyclic voltammetry (CV) of pure gold electrode in 0.04 M NaCN electrolyte, as example. Gold oxidation starts around -0.65 V/SHE and three oxidation peaks were observed at around -0.1, 0.5 and 0.7 V with CV. A reduction peak around 0.4 V and small anodic peak were seen at ~ 0.25V. Oxidation peak current densities were found to be 0.2, 0.5 and 1.8 mA in 0.04 M NaCN solution, respectively. Mughogho and Crundwell (1996) tested electrochemical behaviour of gold rotating disc electrode (1000 rpm) in dilute cyanide solution (~ 0.003 M) and reported also three anodic oxidation peaks with small current densities (0.05, 0.15, 0.2 mA), one reduction peak and one small anodic peak in the turn sweep, as well. Potential and current density shift between potentiodynamic and cyclic voltammetry are probably due to the influence of agitation. It is worth mentioning that peak current densities in this study at

high cyanide concentration (0.04 M) without agitation were significantly increased (3 to 9 times) if compared to the work of [Mughogho and Crundwell \(1996\)](#) at lower cyanide concentration (~ 0.003 M). Anodic current densities in 0.04 M NaCN electrolyte by potentiodynamic test were found to be ~ 0.1 , and 0.8 mA/cm^2 , respectively. Then, it is important to note that, agitation plays an important role on the anodic dissolution of gold (100 rpm in potentiodynamic as compared to static solution in CV).

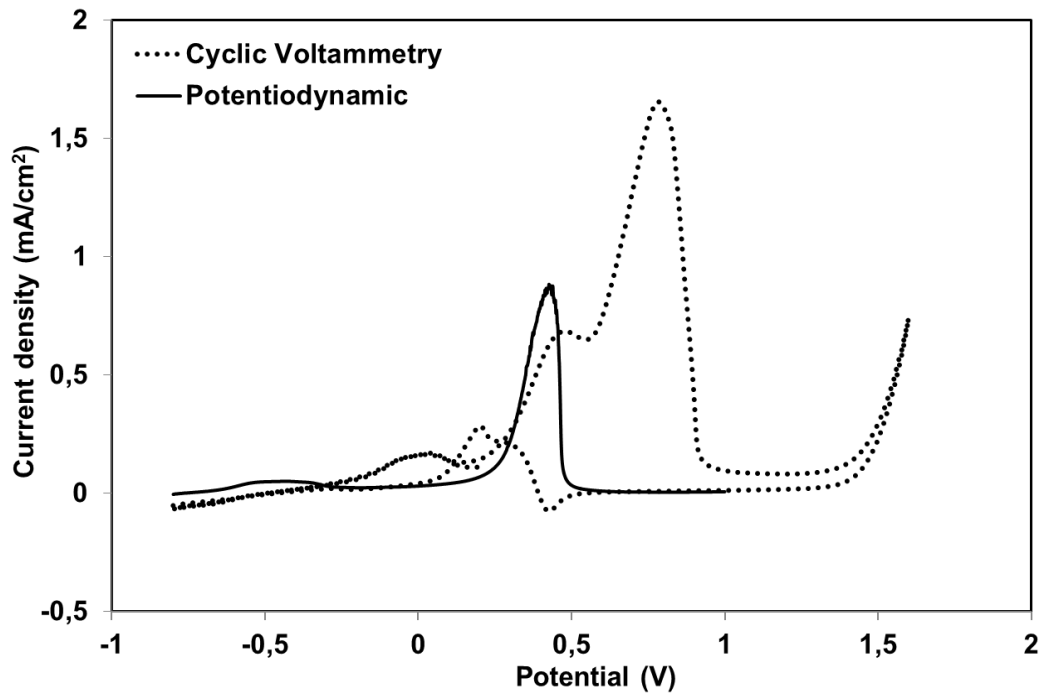


Fig. 3.3 Potentiodynamic and cyclic voltammetry test of pure gold electrode (Au, 1 cm^2) at 100 rpm agitation in 0.04 M NaCN solution in oxygen-free conditions at pH 10.5.

Since oxygen is essential for industrial cyanidation practice then, it is quite important to examine the effect of oxygen on pure gold electrode polarization. [Fig. 3.4](#) represents the influence of oxygen in anodic polarization test of pure gold electrode (Au) at 0.04 M NaCN electrolyte. In the absence of oxygen, with argon bubbling, two peaks leading to passivations were obtained at -0.5 V (very slight), and 0.4 V/SHE, respectively. On the other hand, in the presence of oxygen, one passive peak was observed at around 0.65 V/SHE. Higher current densities were obtained in argon bubbling (in absence of oxygen),

while 1.5 times lower current density with respect to the second peak was obtained in presence of oxygen. These results indicate the significant role of oxygen in gold dissolution processes. Additionally, polarization of roasted gold ore (RGO) electrode was also tested for comparison (Fig. 3.4). It is clearly seen that dissolution started later for RGO in presence of oxygen if compared to Au. This could be linked to the less soluble characteristics of iron oxides (Marsden and House, 2006). Au electrode showed higher current density at 0.7 V/SHE if compared to RGO. At the same potential, current density of Au was then reduced due to the formation of surface products, probably $\text{Au}(\text{OH})_3$. Current density of RGO was linearly increased to 0.6 mA/cm^2 till about $\sim 0.75 \text{ V}$ and slight passive peak was observed. Then, current density continued to increase up to 1.2 mA/cm^2 . The results were reproducible to within 5, 7, and 10% for Au electrode without oxygen, with oxygen and for RGO with oxygen, respectively.

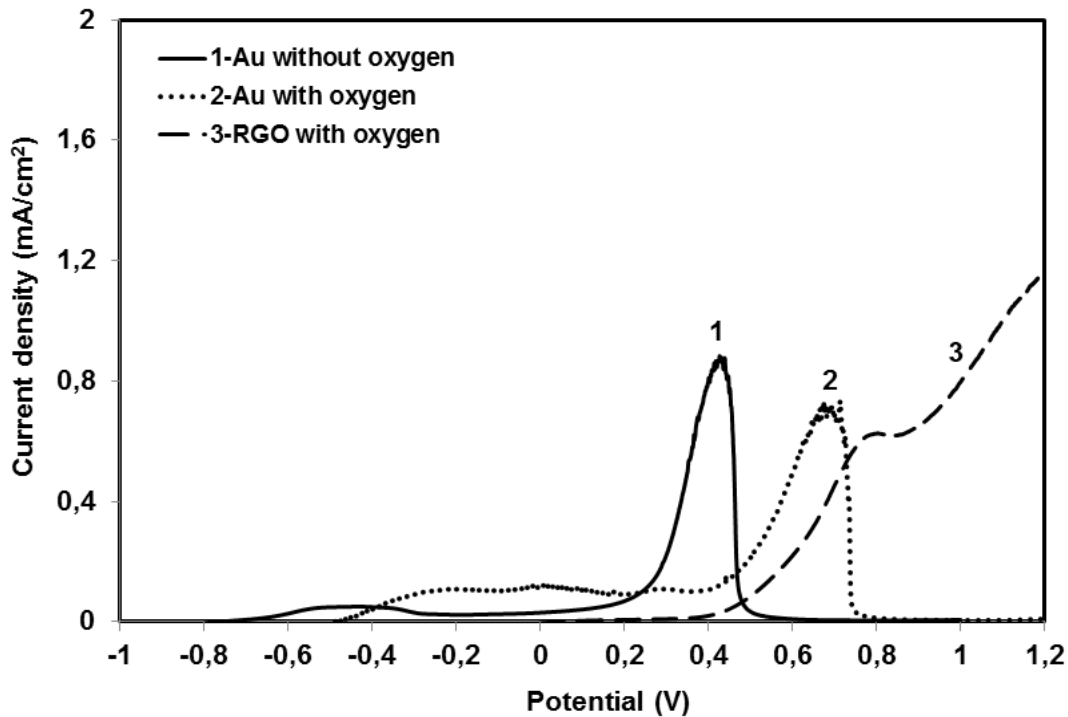


Fig. 3.4 Influence of oxygen on anodic potentiodynamic behaviour of pure gold (Au, 1 cm^2) and compared to roasted gold ore electrode (RGO, 4.9 cm^2) in solution with atmospheric oxygen, 100 rpm agitation in 0.04 M NaCN solution (pH 10.5), T: 25°C , scan rate: 0.166 mV/s).

3.3.2 Effect of pH on Anodic Behaviour of Gold

Fig. 3.5 demonstrates the effect of pH (10-12) on the anodic behaviour of gold foil electrode in 0.04M NaCN solution at 100 rpm agitation. It was found that peak current densities decreased with increasing pH. The second peak current density was greatly increased (~ 40 times) at pH 10 if compared to other two pH values. Barsky et al. (1934) experimentally proved that gold dissolution was decreased above pH 11 using gold discs (Fleming, 1999). At higher pH values (> 10), first peak current density was found to be very small (~ 0.05 mA/cm²). It is worth noting that passivation increases at high pH values due to the accumulation of hydroxyl ions on the surface (Habashi, 2009; Tshilombo, 2000). These findings have revealed that peaks 1 (p₁) and 2 (p₂) were formed due to the formation of gold (I) hydroxide while the third peak (p₃) was formed by gold (III) hydroxide.

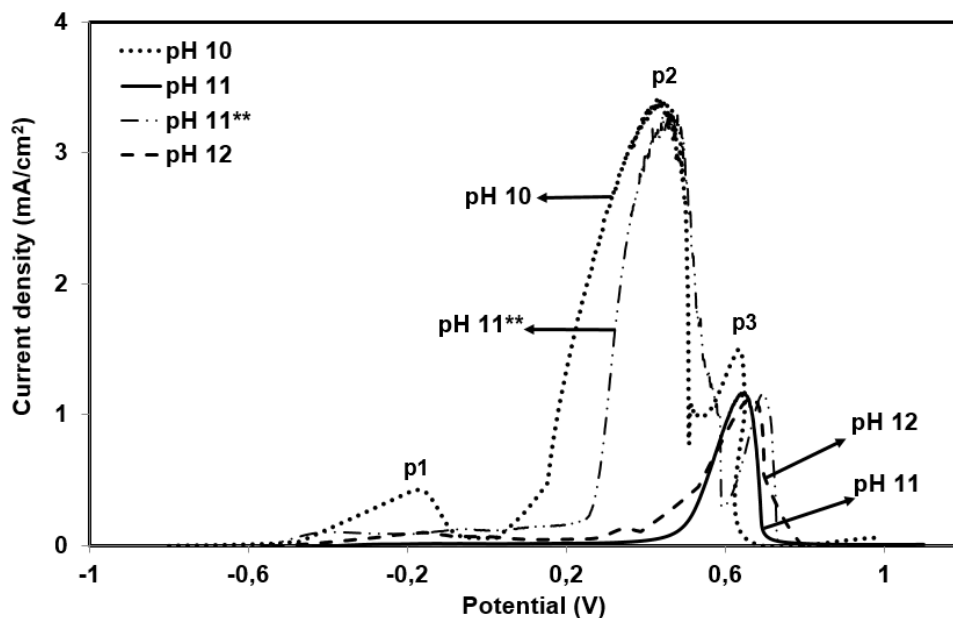


Fig. 3.5 Effect of pH on the anodic potentiodynamic behaviour of gold electrode (Au 1 cm²) in 0.04 M NaCN solution at 100 rpm agitation (pH: 10-12), T: 25°C, scan rate: 0.166 mV/s (** 60 rpm agitation).

Additionally, low level of agitation (60 rpm) was tested at pH 11, since agitation is a quite important parameter for the electrochemical dissolution of gold. It was found that decreasing agitation from 100 to 60 rpm has resulted in a great increase in the second peak

current density which was very close for that of pH 10. The third peak at 60 rpm agitation gave almost the same current density if compared to the 100 rpm agitation. These results clearly show that agitation is of prime importance for the leaching of gold (Nicol, 1980; Cathro and Koch, 1964a; Habashi, 2009). All these tests were performed at least in triplicates and relative standard deviation (RSD) was found to be 8%.

Fig. 3.6 illustrates the effect of pH on the corrosion rates of RGO in duplicates (calculated based on i_{corr} (ASTM G 102-89, 2006)). RGO electrode at pH 10 had the highest corrosion rate (i_{corr}) of $0.24 \text{ mg.cm}^{-2}.\text{h}^{-1}$ (± 0.02) while that at pH 10.5 and 11.5 showed $0.19 \text{ mg.cm}^{-2}.\text{h}^{-1}$ (± 0.01) and $0.109 \text{ mg.cm}^{-2}.\text{h}^{-1}$ (± 0.04), respectively. It is clearly seen that corrosion rate at pH 10 was found to be ~ 2 times higher than that of pH 11.5. The decreasing trend in corrosion rate of RGO at higher pH values could be linked to the hydroxylation reactions. These findings suggest that pH 10-10.5 has more significant effect on the dissolution process. In gold cyanidation practice, pH is often maintained around 10.5 depending on the type of gold ore and the presence of minerals.

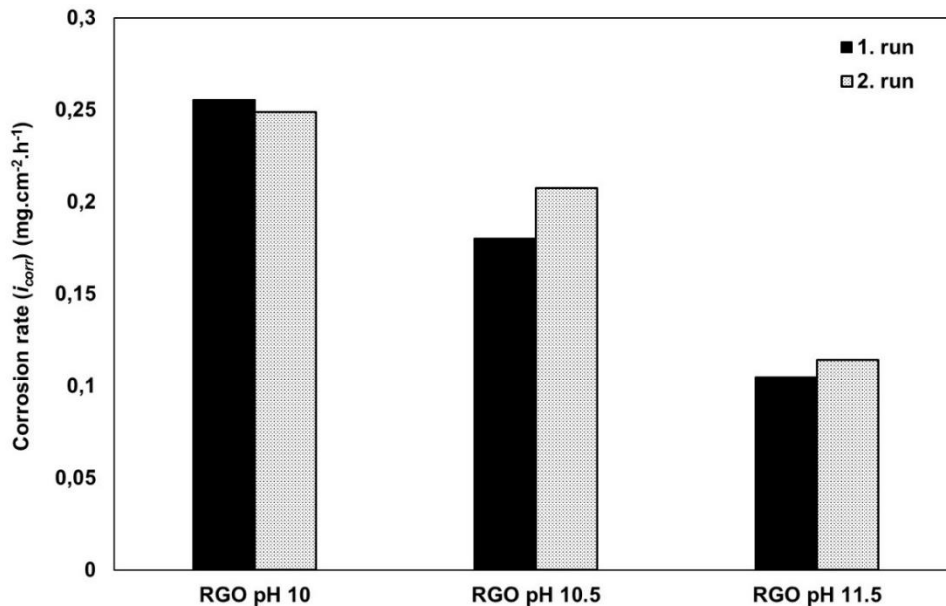


Fig. 3.6 Corrosion (dissolution) rates (i_{corr}) of RGO (4.9 cm^2) after 0.166 mV/s scan rate at different pH values (10.5-11.5) in 0.04 M NaCN electrolyte at 100 rpm agitation in duplicates (1. run and 2. run).

3.3.3 Potentiostatic Tests at Different Anodic Potentials

After potentiodynamic tests, 2 different potentials (1 V and 1.4 V vs. SHE) were chosen in the passive region to evaluate the behaviour of gold electrodes. It is important to monitor current changes when the gold is under passive conditions and also it provides additional data on the duration of passivity. These shown results were reproducible to within 6%. Fig. 3.7 illustrates the effect of potential (1 and 1.4 V) on current changes in passive region as function of cyanide concentration (0.04 and 0.1 M) and pH (10-11).

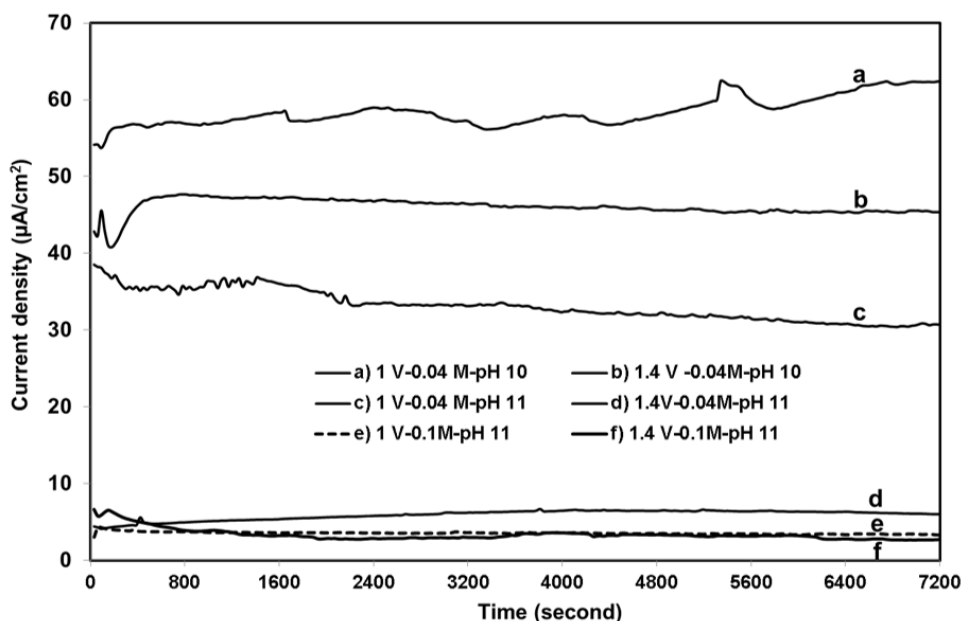


Fig. 3.7 Effect of potential (1 and 1.4 V) on current changes in different cyanide concentrations (0.04 and 0.1 M) using potentiostatic test (pH 10-11, T: 25°C, scan rate: 0.166 mV/s, Argon bubbling) (a: pH 10 at 1 V 0.04M NaCN; b: pH 10 at 1.4 V 0.04M NaCN; c: pH 11 at 1 V 0.04M NaCN; d: pH 11 at 1.4 V 0.04M NaCN; e: pH 11 at 1 V in 0.1M NaCN; f: pH 11 at 1.4 V in 0.1M NaCN).

It was found that at 0.04 M NaCN solution at pH 11, current density decreased (~ 80%) with increasing potentials in the two tested cyanide concentrations, *e.g.* 35 μA at 1 V, *c.f.* 6 μA at 1.4 V. It should be mentioned that decreasing pH level from 11 to 10 resulted in 1.7-fold increase in current density at 1 V in 0.04 M solution medium (Fig. 3.5). This could be linked with stabilising of passivity at pH 11 that promotes generation of AuCN basic

films on the surface (Nicol, 1980; Jeffrey and Ritchie, 2001). However, the effects of cyanide concentration, pH, and potential on the evaluation of current density as function of time indicated that it is not stable and efficient type of passivation.

It was found that at 1.4 V passive potential, increase in NaCN concentration from 0.04 M to 0.1 M has led to a decrease in current density with also a similar trend for other potential. This decrease could be attributed to the hypothesis that high NaCN concentration favours passive state according to formation of basic cyanide films that leads to sharp decrease in current (Kirk et al., 1978; Bek et al., 1997). In this situation, diffusion control could not be an important contributing factor since moderate agitation was applied. Current density has a decreasing trend with increasing potential from 1 V to 1.4 V. Such that, in the passive region increase in potential from 1 to 1.4 V (0.1 M) resulted in 10% decrease in current density. Furthermore, increase in NaCN concentration from 0.04 M to 0.1 M at 1 V has led to about a 62% decrease in current density in the passive region. Qian et al. (2010) mentioned that peak current density drops with the increase in cyanide concentration. This could be also due to the passivation, since at first the surface reaches a passive region, and then passivation could become more stable by time and increases in anodic potential.

3.3.4 Electrochemical Noise Measurements (ENM)

Open Circuit Potentials

The corrosion potential and current noise recorded for three concentrations of NaCN (0.01, 0.04 and 0.1 M) during anodic polarisation were presented in Figs. 3.8a and b, respectively. The potential evolution (Fig. 3.8a) changes significantly from concentration 0.01 to two other concentrations of 0.04 and 0.1 M. The anodic potential values change around -0.4 V for 0.1 M while it decreases around -0.55 to -0.6 V for two higher concentrations. The current density variations in function of time show higher current densities for the two higher concentrations indicating easier dissolution (Fig. 3.8b). The current density values were varied from about 2×10^{-4} mA cm⁻² for two higher concentrations to about 1.7×10^{-4} mA cm⁻² for lower concentration (0.01 M). It can be deduced that the gold dissolution is realized more efficiently at these higher concentrations of CN⁻ solutions of 0.04 and 0.1 M than that of 0.01 M.

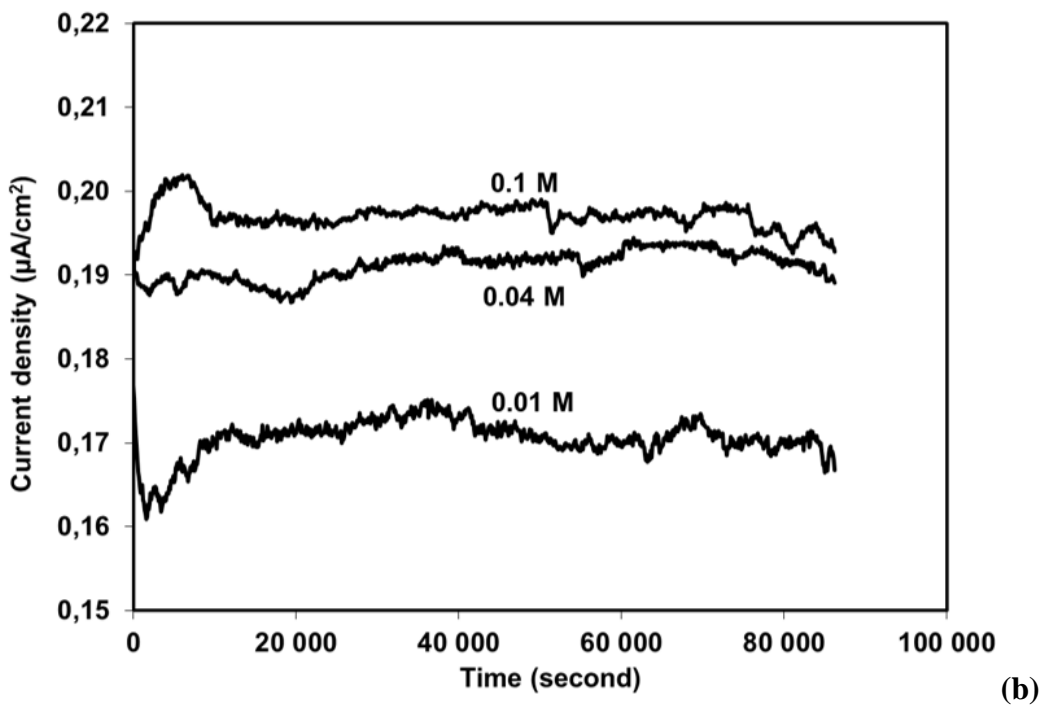
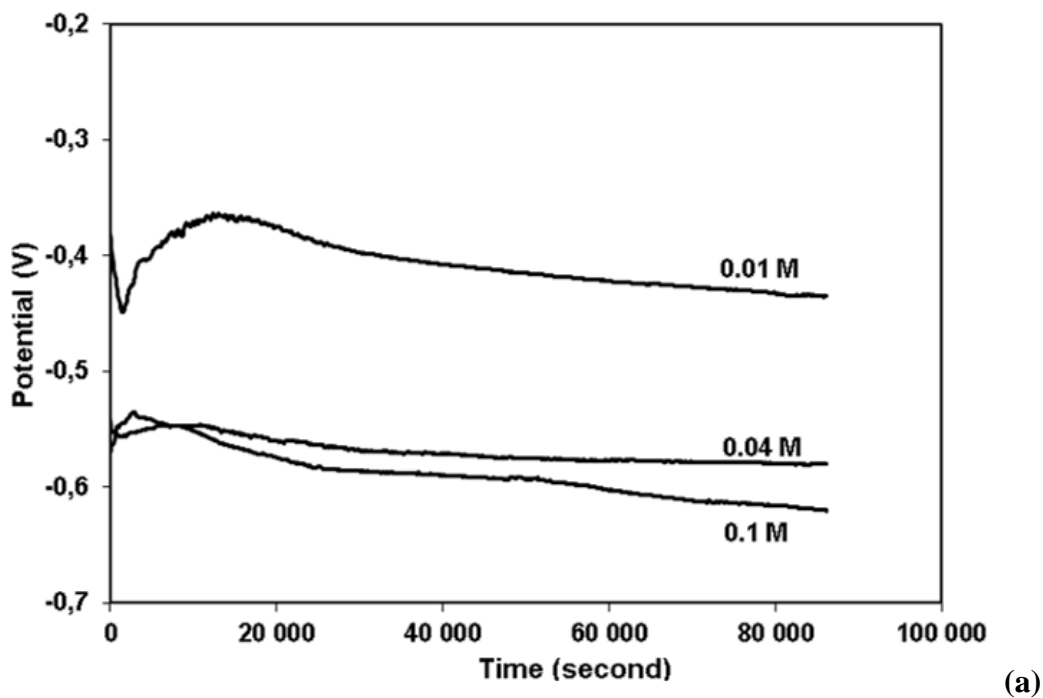


Fig. 3.8 Potential (a) and current (b) noise recorded during 24 h immersion of gold electrode in three concentrations of NaCN (0.01, 0.04 and 0.1 M) at pH 10.5.

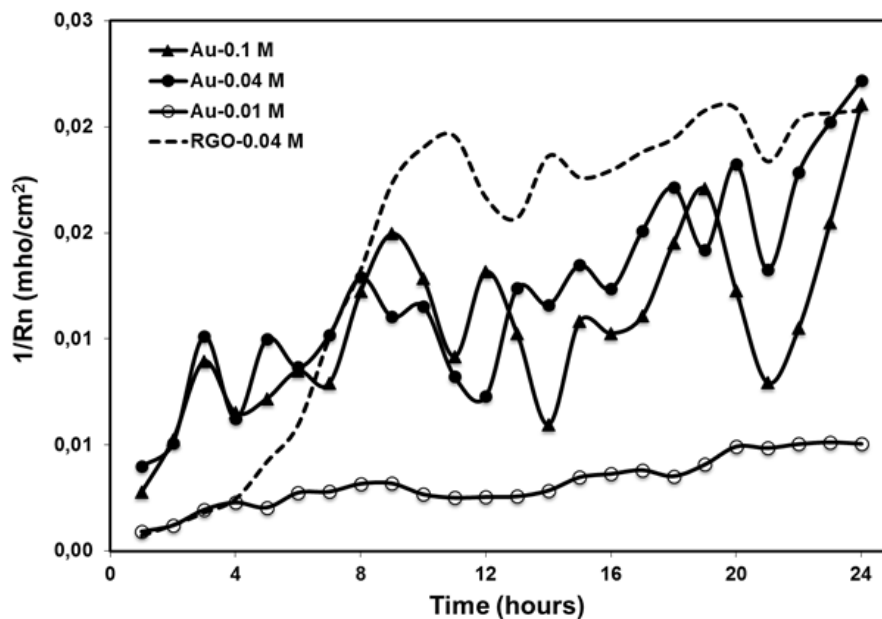


Fig. 3.9 Instantaneous measured $1/R_n$ for gold ($\text{Au } 1 \text{ cm}^2$) immersed in three concentrations of NaCN (0.01, 0.04 and 0.1 M) and roasted gold ore (RGO 4.9 cm^2) for comparison in 0.04 M NaCN at pH 10.5.

One of the most popular statistical parameters of ENM analyses in the time domain is the noise resistance (R_n). The noise resistance is defined as the ratio of the standard deviation of the potential noise to that of the current noise that can be associated to the polarization resistance (R_p). The ratio $1/R_n$ (admittance) is referred to the corrosion rate (Loto, 2012). The ENM data values of $1/R_n$ for each specimen were measured during immersion period. The mean of measurements for two series of each experiment was presented in Fig. 3.9. It can be observed that in general the corrosion rate increases in function of time for all examined concentrations of sodium cyanide. However, the corrosion rate increases more quickly with time for the higher concentrations (0.1 M and 0.04 M) than that of lower concentration of NaCN (0.01 M). Furthermore, the rate of corrosion for two concentrations of 0.1 and 0.04 M are very similar. Results of ENM analyses are consistent with the results obtained by other researchers employing direct cyanide leaching tests (Tshilombo, 2000) indicating that the rate of gold dissolution increases with increasing cyanide concentration until a maximum. Passing the maximum, in contrary, it can be observed a slight retarding effect on gold dissolution procedure leading to slight corrosion rate. According to Fig. 3.9,

the corrosion rate decreases slightly for the sodium cyanide solution of 0.1 M as compared to that of 0.04 M. This indicates also the presence of different phenomena such as limited current diffusion control of cyanide ions even at free corrosion potentials, and there should be certain increase in the formation of adsorbed or precipitated passive compounds as function of the cyanide ion concentration on the electrode surface.

Since gold is always found as alloys in the nature, then roasted gold ore (RGO) was used as an electrode, to compare the corrosion rate with pure gold (Au) electrode. In this case, the middle concentration (0.04 M) between three different concentrations was chosen since this one is often selected in practical cyanidation. The results demonstrated that the corrosion rate of RGO increases rapidly till about 11.5 h. However, after this period, the dissolution rate becomes almost flat around an average value of ~ 0.02 (mho/cm²) till 24 hours. This slowdown trend in the corrosion rate of RGO as function of time could be linked to the release of detrimental ions from roasted gold ore and the diffusion control due to the consumption of cyanide ions by these species. At the end of the test, RGO and Au electrodes had very close corrosion rates at 0.04-0.1 M.

Potential Decay after Polarisation

The potential and current evolutions of gold specimens, polarized at anodic potentials during 2 h, were recorded during 16 h decay. Fig. 3.10a and b illustrates the variations of voltage and current density, respectively. According to this figure, more anodic potential and higher current density can be found for the passivated specimen at 1 V indicating easier dissolution. Furthermore, it can be observed that the potential of gold specimens polarized potentiostatically at 1 V (Fig. 3.10a), is about -0.55 V such as the specimen without previous polarization in Fig. 3.8a (0.04 M). It could be deduced that the passive film formed during potentiostatic polarization at 1 V is not enough stable and resistant hence it dissolves quickly after immersion in 0.04 M NaCN. Although, the layer of gold oxides (I and III) that have been formed during potentiostatic conditions at 1.4 V, seems to be more efficient and resistant to corrosion as compared to that of 1 V, the reduction of potential towards more active potentials (-0.55 V) (Fig. 3.10a) was observed confirming the dissolution of this passive film.

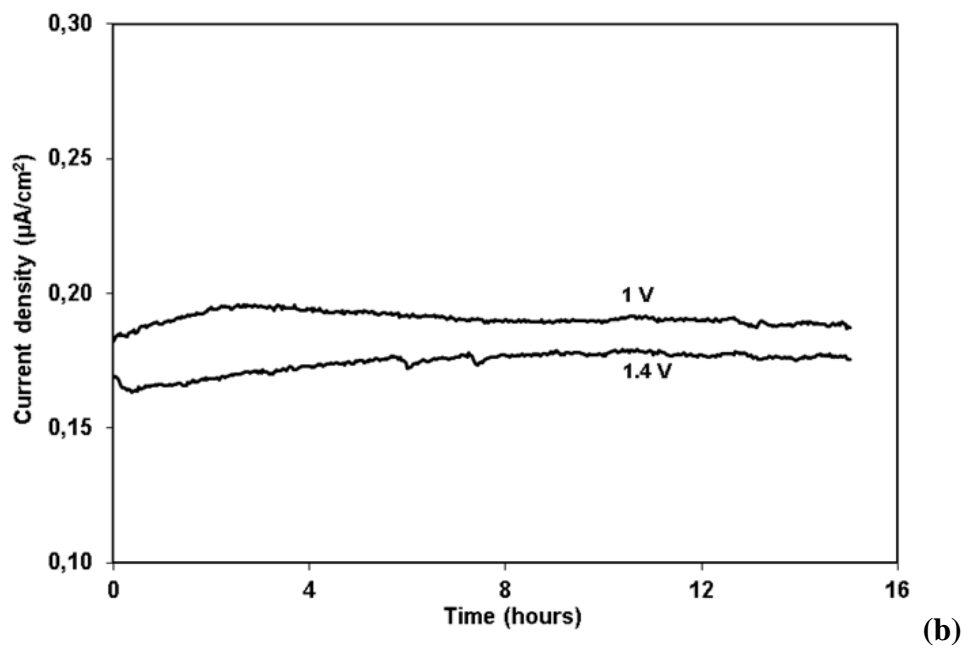
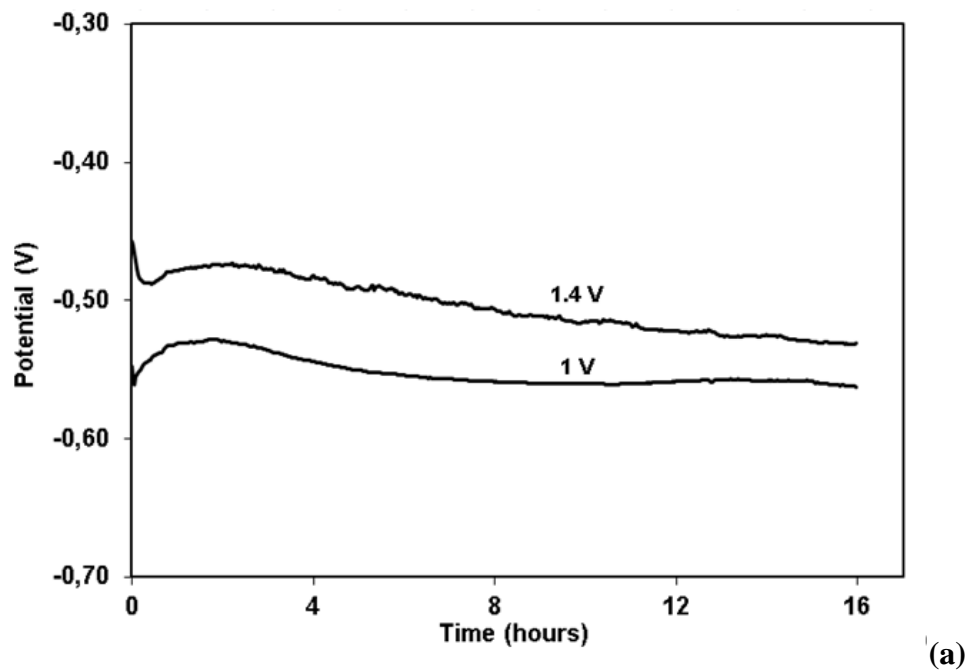


Fig. 3.10 Recorded potential noise (a) and current noise (b) decay in time for two polarized gold electrodes under potentiostatic conditions at 1 and 1.4 V during 16 h immersion in NaCN solution (0.04 M).

The potential and current noise for a sampling data point of 20 seconds of 1 h and 16 h during decay was monitored and only that of 16 h was illustrated in Fig. 3.11a-c. This figure presents the potential and current comparison for three potentiostatically polarized gold specimens at 0.3 V as an active and passive potentials of 1 V and 1.4 V/SHE. Fig. 3.11a shows the potential and current noise for pure gold electrode (Au) that was previously polarized at active potential 0.3 V/SHE for 2 h. The amplitude of potential noise changed about $\pm 60 \mu\text{V}$ in the two selected zones (1 and 16 h). On the other hand, polarized at two passive potentials were considered for comparison to the active potential. Fig. 3.11b illustrates the potential and current noise signature of the polarized gold electrode at 1 V. It was observed that the amplitude of potential noise for this electrode changes between $\pm 30 \mu\text{V}$ in the two selected zones (1h and 16h) while for the polarized specimen at 1.4, the fluctuation change was between $\pm 15 \mu\text{V}$ (Fig. 3.11c). It can be deduced that ~ 2 -4 times larger fluctuations in potential were obtained with a specimen that was previously polarized at active potential (0.3 V) if compared to the passive potentials. The larger fluctuations could be attributed to easier dissolution of the specimen and its oxides. Moreover, similar characteristics for the potential and current transients were obtained at 1 and 16h (Fig. 3.11b) for the polarized gold electrode at 1 V. In general, the amplitude of EN fluctuations can be correlated to the intensity of the corrosion process, while the fluctuation shape can be due to the type of the corrosion process (Aballe et al., 2001; Jiang et al., 2012). The patterns of potential and current noise recorded for the gold specimen polarized at 0.3 V (Fig. 3.11a) showed sharp fluctuations for both potential and current during all period of immersion. The pattern presented in Fig. 3.11b shows the oscillations toward less negative potential directions followed by no abrupt recovery that have similar form generally. This form of oscillations could be attributed mainly to the stable pitting corrosion form (Lafont et al., 2010a). The fluctuations that were obtained under polarization of the gold electrode at 1.4 V could be attributed to the instability of the passive film, the film breakdown and re-passivation processes associated with metastable pitting (Amira et al., 2007). It should be noted that the amplitude of the current fluctuations reduced from $\pm 15 \mu\text{V}$ (measured after 1 h) to about $\pm 5 \mu\text{V}$ after 16 h of immersion for this electrode (Fig. 3.11c). These variations could be indicative of formation of a passive film (gold hydroxide formation) due to Eqs. 3.7 and 9 on the electrode surface.

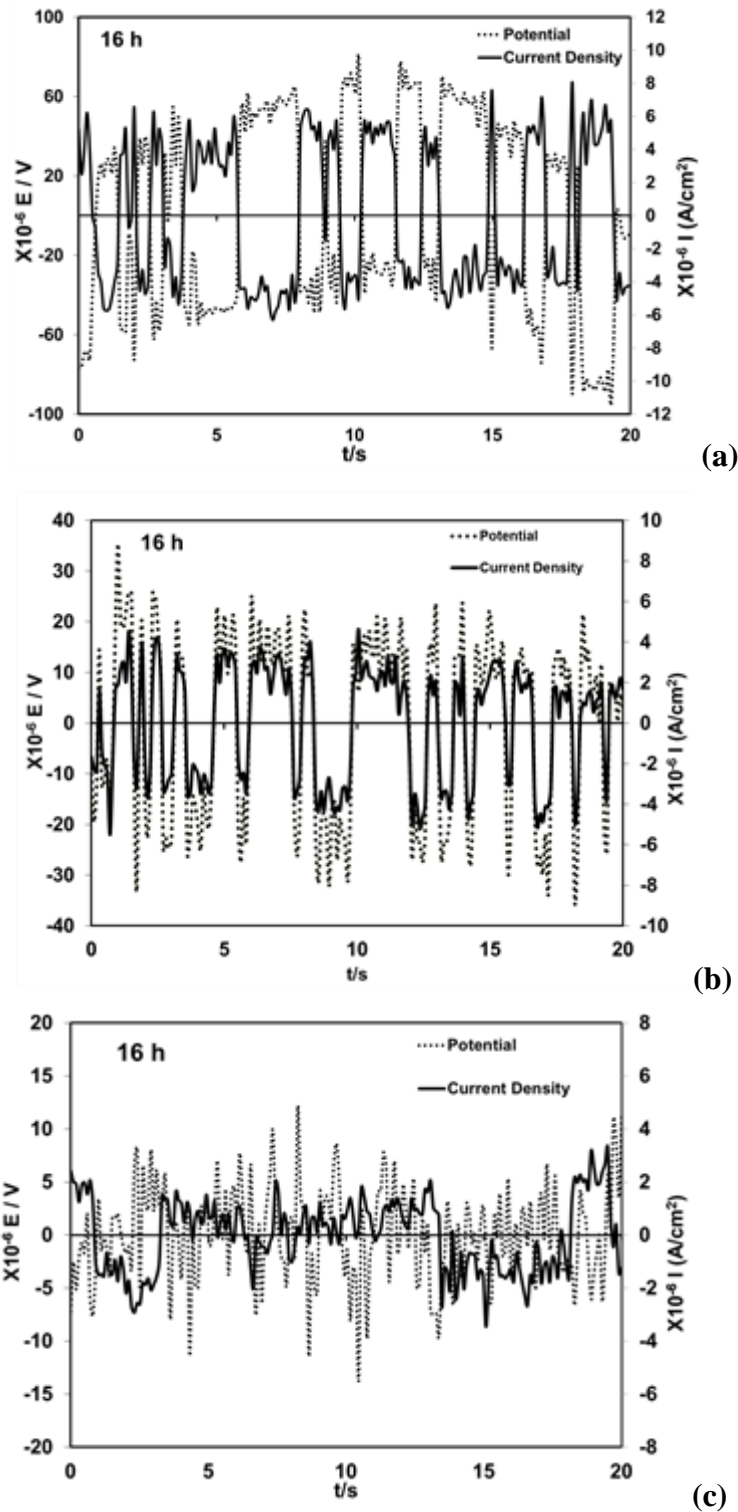


Fig. 3.11 Potential noise (...) and current noise (—) for two polarized gold electrodes under potentiostatic conditions applying one active potential (a) 0.3 V and two passive potentials (b) 1 V and (c) 1.4 V immersed in NaCN solution (0.04 M) after 16h.

3.3.5 Surface Characterization

Chemical characterization of gold surface was performed to provide an insight into the surface reaction processes. XPS study was carried out after 30 minutes cathodic cleaning at -0.8 V, followed by potentiodynamic test at 0.166 mV/s between -0.8 V and 1 V and finally 2 h potentiostatic test at 1 V in a 0.1 M NaCN solution at 25°C with argon bubbling and magnetically stirred at 100 rpm. XPS studies showed the presence of Au⁺ and Au³⁺ oxides on the surface of gold electrode (Fig. 3.12). It is believed that oxides promote the passivation of gold surface (Kirk et al., 1980; Nicol, 1980). Due to rapid reactions during leaching, detecting of oxides is highly sensitive. Although the presence of oxides could be identified according to two very slight peaks, a standard conventional peak as observed in sulphuric acid medium, indicative of stable passive film was not observed. This could be mainly attributed to the examined cyanide concentration (0.1 M). This finding highlights that passivation is more likely to be caused of corrosion products than real passivation. XPS studies on gold surface confirm that there is a kind of partial passivation due to corrosion products.

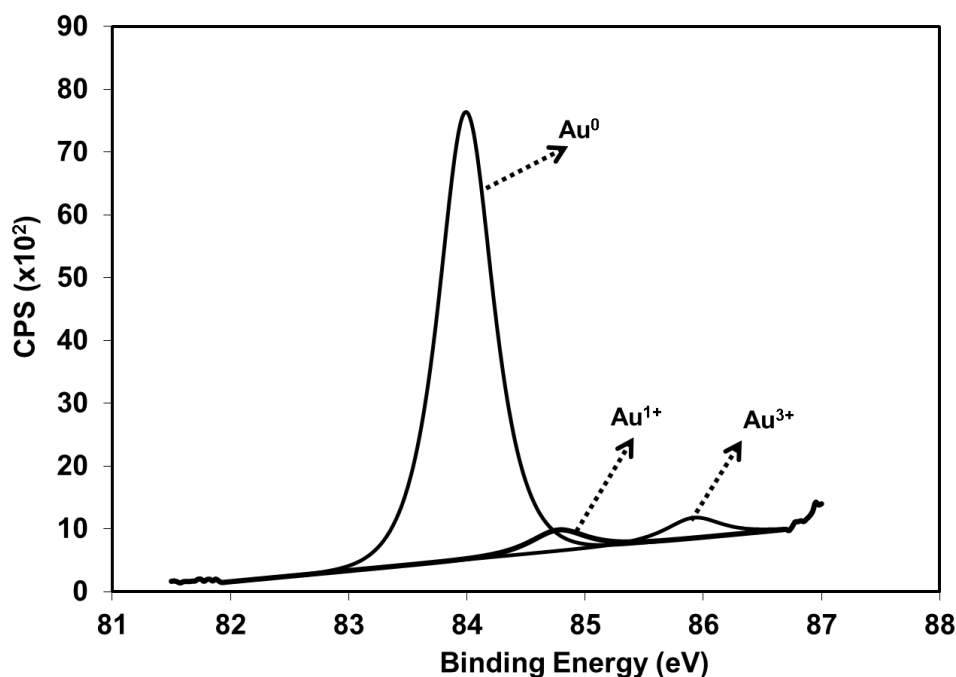


Fig. 3.12 X-ray photoelectron Spectroscopy (XPS) surface analysis for gold electrode after 2 h potentiostatic in 0.1 M NaCN at 25°C, argon bubbling and magnetically stirring at 100 rpm.

3.4 Conclusions

1. The leaching rate of gold increases with an increase in cyanide concentration until 0.1 M, and then slows down at 0.2 M. In addition, a shift in pH values from 12 to 10 increases the rate of gold leaching. Differences in peak positions and current densities in cyclic voltammetry (without agitation) and potentiodynamic polarization (at 100 rpm agitation) are indicative of prime importance of agitation on the passivation of gold surface.
2. In the absence of oxygen, pure gold electrode showed two passive peaks while one passive peak was observed in the presence of oxygen. On the other hand, roasted gold ore electrode gave only a slight passive peak in the presence of oxygen if compared to that of pure gold.
3. Potentiostatic studies showed that increase in cyanide concentration and potentials (1 V to 1.4 V) in the passive region has led to a decrease in current density up to 80% while increasing pH from 10 to 11 resulted in 1.7-fold decrease in current density at 1 V in 0.04 M NaCN solution. These findings have revealed that when gold was in the passive region, increasing cyanide concentration, pH, and potentials adversely affect the gold, leading to more passive behaviour.
4. According to electrochemical noise measurements (ENM) analysis, without previous polarization, ~ 3 times higher corrosion rate was obtained for more concentrated NaCN solutions (0.1 M and 0.04 M) than that of the lower one (0.01 M) at open circuit potential. Pure gold electrode showed an increasing trend of corrosion rate while roasted gold ore electrode was found to have a plateau after the initial 11.5 h till the end of test (24 h). This was consistent with the obtained higher current density for pure gold electrode when compared to roasted gold ore electrode during decay periods.
5. ENM gives in-situ current, potential and corrosion rate as function of time and stable pitting type of localised corrosion form was observed during potential decay after potentiostatic polarization. Instability of the passive film, the film breakdown and re-passivation processes were associated with metastable pitting. Based on the findings in this

study, it could be suggested that electrochemical noise measurement (ENM), as a more recent electrochemical technique, can be suitably used for further gold leaching studies.

6. The formed gold oxide films (I and III) during potentiostatic conditions (at 1.4 V) have been determined by XPS studies and were found to be more efficient and resistant to corrosion as compared to that of 1 V. These detected gold oxides are the main factors contributing to the passivation of gold surface.

3.5 Acknowledgements

The authors would like to express their sincere thanks and appreciations to Natural Sciences and Engineering Research Council of Canada, Barrick Gold Corporation, Hydro-Quebec, Glencore–Zinc electrolytic of Canada for their financial support through R&D NSERC Program and to Dr. Alain Adnot (Laval University) for the help during XPS analysis and to Majid Heidari for the participation in XPS studies.

Chapter 4

Galvanic Interactions Between Gold and Iron Oxide Electrodes in Cyanide Solutions

A Study of Electrochemical Interactions between Gold and Its Associated Oxide Minerals

Ahmet Deniz Bas^{a*}, Edward Ghali^a, Yeonuk Choi^b

^aDepartment of Mining, Metallurgical and Materials Engineering, Laval University, Quebec, Canada, G1V 0A6

^bBarrick Gold Corporation, Suite 3700, 161 Bay Street P.O.Box 212, Toronto, Ontario, Canada, M5J 2S1

*Corresponding author: 4186568657, Fax: 4186565343; (ahmet-deniz.bas.1@ulaval.ca)

Published in 54th Annual Conference of Metallurgists (COM 2015), The Metallurgy and Materials Society of CIM, The LUCY ROSATO Memorial Symposium, Toronto, Canada, August 23-26, paper no 8897.

Résumé

Il y a un manque d'études électrochimiques de minerais d'or oxydés puisque la majorité des études antérieures ont été réalisées avec des minerais d'or sulfurés. Dans cette étude, l'influence de l'agitation et des minéraux d'oxyde de fer, comme la magnétite, l'hématite et la maghémite sur la lixiviation de l'or a été étudiée au moyen de phénomènes galvaniques et de passivation. Les études de voltamétrie cyclique de minerai d'or grillé (RGO) dans un électrolyte désaéré ont montré une oxydation et une réaction de réduction, tandis que trois pics d'oxydation et un pic de réduction ont été observés avec une électrode en or. Les résultats de couplage galvaniques par résistance zéro ampéromètre (ZRA mode) ont indiqué que la magnétite a montré un effet négatif sur la dissolution d'or tandis que la maghémite et l'hématite ont montré un effet positif, relativement, en raison de vitesses de corrosion galvanique plus élevées. En général, la dissolution d'or a été trouvée d'augmenter pendant les premières 15 minutes. L'augmentation de la vitesse d'agitation 100-400 tours par minute a donné lieu à de vitesses plus élevées de corrosion galvanique pour les électrodes de RGO, magnétite, maghémite, tandis que la vitesse de 250 tours par minute a été trouvée optimale pour électrode l'hématite. Des produits passifs tels que l'argent et de l'oxyde de fer ont été identifiés par les analyses de XPS et MEB-EDX, respectivement.

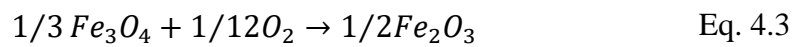
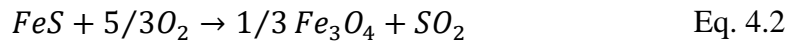
Abstract

There is a lack of electrochemical studies of oxidised gold ores since the majority of previous studies were conducted with sulphidic gold ores. In this study, the influence of agitation and iron oxide minerals, i.e. magnetite, hematite, and maghemite on gold leaching was investigated by means of galvanic and passivation phenomena. Cyclic voltammetry studies of Roasted Gold Ore (RGO) in de-aerated electrolyte have shown one oxidation and one reduction reaction while three oxidation peaks and one reduction peak were observed with gold electrode. Galvanic coupling results by Zero Resistance Ammeter (ZRA) mode indicated that magnetite showed a negative effect on gold dissolution while maghemite and hematite showed a positive effect, relatively, as a result of higher galvanic corrosion rates. Generally, gold dissolution was found to increase in the initial 15 minutes. Increasing agitation speed from 100 to 400 rpm resulted in higher galvanic corrosion rates for RGO, magnetite, and maghemite electrodes, while 250 rpm was found to be optimum for hematite electrode. Passive products such as silver and iron-oxide were identified by XPS and SEM-EDS analysis, respectively.

Keywords: Roasted gold ore, magnetite, hematite, maghemite, cyanide, passivation, galvanic corrosion, XPS, SEM-EDS

4.1 Introduction

Cyanide has a proven track record of more than 120 years of being used by far the most suitable and effective reagent for recovering of gold (Akci, 2014). In the present time, it is accepted worldwide that there is an increasing trend for the treatment of refractory gold ores which often requires oxidation as a pre-treatment process due to the rapid depletion in free-milling type of gold ores (Taylor, 2013; Zhou and Fleming, 2007). Pyrite, as the most common sulphide phase of the gold ore is converted predominantly to hematite, magnetite (Eqs. 4.1-3) and also maghemite (Stephens et al. 1990; Adams, 2005) by roasting/oxidizing. Iron oxides can contain appreciable amounts of gold (30 ppb to 260 ppm) (Adams, 2005). These types of iron oxides, as calcine products, are often found to be detrimental in cyanidation (Filmer, 1982; Lorenzen van Deventer, 1992a). Maghemite, with its non-porous property is problematic for gold dissolution (Marsden and House, 2006). Paktunc et al. (2006) examined such a roasted gold ore and indicated that gold is found with maghemite minerals that are impervious in character.



It has been known that when gold is in contact with conductive minerals, galvanic interactions can be important on gold dissolution (van Deventer et al., 1990). It was experimentally demonstrated that the different types of dissolved minerals may have either positive or negative effects on gold leaching (Jeffrey and Ritchie, 2001). Azizi et al. (2012a) reported the positive galvanic effect of galena-pyrite on gold dissolution, while negative effect was observed when galena was associated with minerals such as chalcopyrite, sphalerite and chalcocite. Dissolution of gold from a gold electrode in electrical contact with another electrode may be influenced by galvanic interactions, or passivation phenomena or their combinations (van Deventer and Lorenzen, 1987).

Actually, galvanic interactions and passivation phenomena between gold and sulfide minerals were examined in detail by many different research groups as function of leaching parameters such as cyanide concentration, pH, temperature, and added ions (van Deventer and Lorenzen, 1987; van Deventer et al., 1990; Lorenzen and van Deventer 1992a, 1992b; Aghamirian and Yen, 2005; Cruz et al., 2005; Dai and Jeffrey, 2006; Azizi et al., 2010; Azizi et al., 2011, 2012a, 2012b; Azizi et al., 2013). Although the influence of agitation speed has been studied in cyanide leaching (Ellis and Senanayake, 2004; Zhang et al., 2014), there is a lack of agitation in gold and mineral electrodes electrochemical studies. Generally, polarization and zero-resistance ammeter (ZRA) mode are being used for gold corrosion/leaching studies (Cruz et al., 2005; Azizi et al., 2011). On the other hand, there is paucity on gold and oxide minerals galvanic interaction studies.

In this study, cyclic voltammetry (CV) tests were performed to identify the corrosion peaks of different reactions on Au and Roasted Gold Ore (RGO) oxides. The influence of oxide ore and minerals on the galvanic corrosion of gold at different agitation speeds were examined by using zero resistance ammeter (ZRA) mode. Roasted gold ore (RGO), magnetite (Mag), maghemite (Mgh), and hematite (Hem) disc electrodes were used. Furthermore, a new disc electrode which consisted of equal quantities and surfaces of magnetite and hematite in one electrode (MagHem-ES) was developed to see the influence of the presence of these major two iron oxide minerals (in the ore) on gold dissolution, concurrently.

4.2 Experimental

4.2.1 Ore Sample

The gold ore sample was obtained from Barrick Gold Corp. This was the calcine after roasting of refractory gold ore. In roasted gold ore sample, gold is mainly associated with iron oxides (Fig. 4.1) such as magnetite, hematite and maghemite. The sample (which was already reduced in size 80% passing $-75 \mu\text{m}$ (d_{80})) was riffled as portions prior to use in experiments.

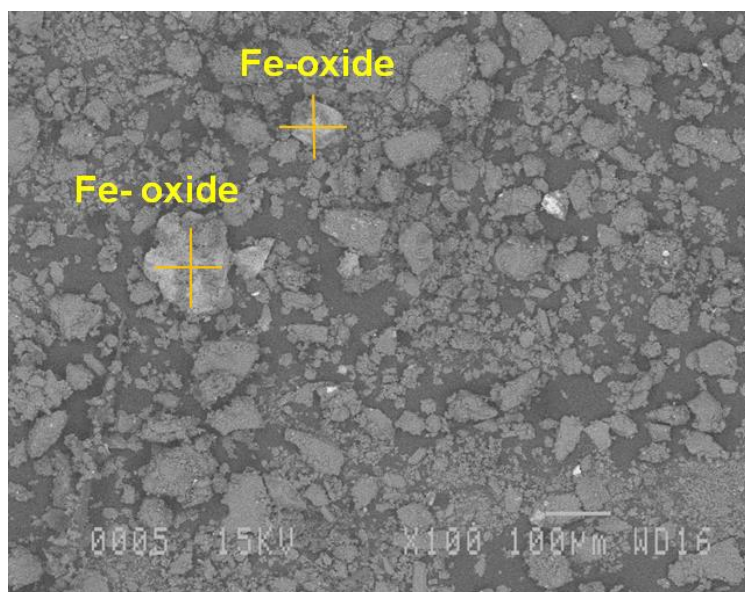


Fig. 4.1 Fe-oxides identified by SEM analysis from the received roasted gold ore sample.

4.2.2 Material and Preparation of Electrodes

NaCN ($\geq 98\%$ purity) was obtained from Thermo Fisher Scientific Company. Electrolyte medium (1L) was prepared using distilled water at 0.1 M NaCN concentration and pH was adjusted at 10.5 by adding 1 M NaOH. Electrolyte was magnetically agitated at different speeds of 100, 250, and 400 rpm (stir bar dimensions: 4 cm long and 1 cm diameter) during the test. 0.25 cm^2 of gold foil electrode (Au) (99.9% purity from Sigma Aldrich) was used as working electrode. Au was first polished with fine (MicroCut® 100 Grit Soft) polishing paper and then rinsed in distilled water. Then, it was introduced in aqua-regia for 10 seconds to clean the surface, washed with distilled water and ethanol and finally rinsed with distilled water again. This pre-treatment assured the reproducibility of the electrode surface area and state (Kirk and Foulkes, 1980).

Roasted gold ore (RGO), magnetite (Mag), maghemite (Mgh), hematite (Hem) and magnetite-hematite (MagHem-ES) disc electrodes with an exposed surface area of 4.9 cm^2 were prepared. Maghemite was prepared by heating magnetite in oven at $200 \text{ }^\circ\text{C}$ for 3 h, just giving a light brown color to be maghemite (Legodi and de Waal, 2007) and this was proved by XRD. Roasted gold ore, magnetite, maghemite, and hematite, separately, were mixed with graphite powder (to increase conductivity) 3:1 and with around 0.4 g of silicone

oil, for binding, till a paste was obtained. Next, it was mechanically pressed at 20 tons to have uniform sample surface. After that, roasted gold ore electrode was kept under nitrogen over a night. Finally, connected with an insulated copper wire, cast in acrylic resin and conductivity of the electrode was also checked. Since the quantity of gold is less than other minerals in gold ore (real practice), the difference in surface areas of electrodes compared to Au has been therefore selected.

4.2.3 Electrochemical Test Procedure

Cyclic voltammetry (CV) without agitation was carried out in 0.04 M NaCN solution at 10 mV/s scan rate. Solution was first bubbled with argon and magnetically agitated at 250 rpm for 50 min. to eliminate the oxygen. CV studies were conducted between -1 V to 1.6 V values and steady-state cycle was considered. Pure gold (Au, 0.25 cm²) and mineral disc electrodes (4.9 cm²) were used for galvanic corrosion tests. Au electrode was considered as the main electrode and its potential was measured against a Ag,AgCl/KCl_{sat} reference electrode at 0.01 M NaCN solution. Different combinations, e.g. Au+RGO or Au+Mag, electrically connected to each other in the same cell through a zero resistance ammeter (ZRA) was considered (Aghamirian and Yen, 2005; Azizi et al., 2011). Experiments were performed with saturated atmospheric oxygen.

4.3 Results

4.3.1 Peak Determination by Cyclic Voltammetry (CV)

Cyclic voltammetry (CV), one of the potentiodynamic technique has been used to study the redox processes, for obtaining stability of reaction products, the presence of intermediates, reaction, and electron transfer kinetics, and the reversibility of a reaction. CV of different electrodes in de-aerated 0.04 M NaCN solution is shown in Figure 2. It is seen that there were oxidation and reduction reactions taking place for Au, RGO and Hem disc electrodes. Au disc electrode showed three oxidation peaks at around -0.1, 0.5 and 0.7 V, a reduction peak around 0.4 V and small anodic peak were seen at ~ 0.25V with Au (Fig. 4.2a), while one oxidation peak (~ 0.5 V) and one reduction peak were observed for RGO (Fig. 4.2b) and Hem (Fig. 4.2d). These obtained peaks with Au electrode could be due to the formation of surface products that could passivate gold surface. In Fig. 4.2a,

peaks A and B could correspond mainly to AuOH_{ads} , while peak C is related to $\text{Au}(\text{OH})_3$. Hydrogen evolution reaction (Eq. 4.4) takes place as shown in region F. The increased current above potential of 1.5 V indicates the oxygen evolution (Eq. 4.5) reaction which is shown as peak D (Lin and Chen, 2001). One oxidation peak (~ 0.5 V) and one reduction peak (~ 0.3 V) were observed for RGO and it can be deduced that the oxidation and reduction reactions took place at close potentials. Current density of RGO has reached more than 3 mA/cm^2 (Fig. 4.2b). The difference in current densities of duplicates ($\pm 5\%$) could be due to the difference of the starting surface conditions of RGO. Contrary, no oxidation peak was obtained with magnetite disc electrode (Mag) (Fig. 4.2c) and this could be linked to its relative stability or to its cathodic galvanic effect.

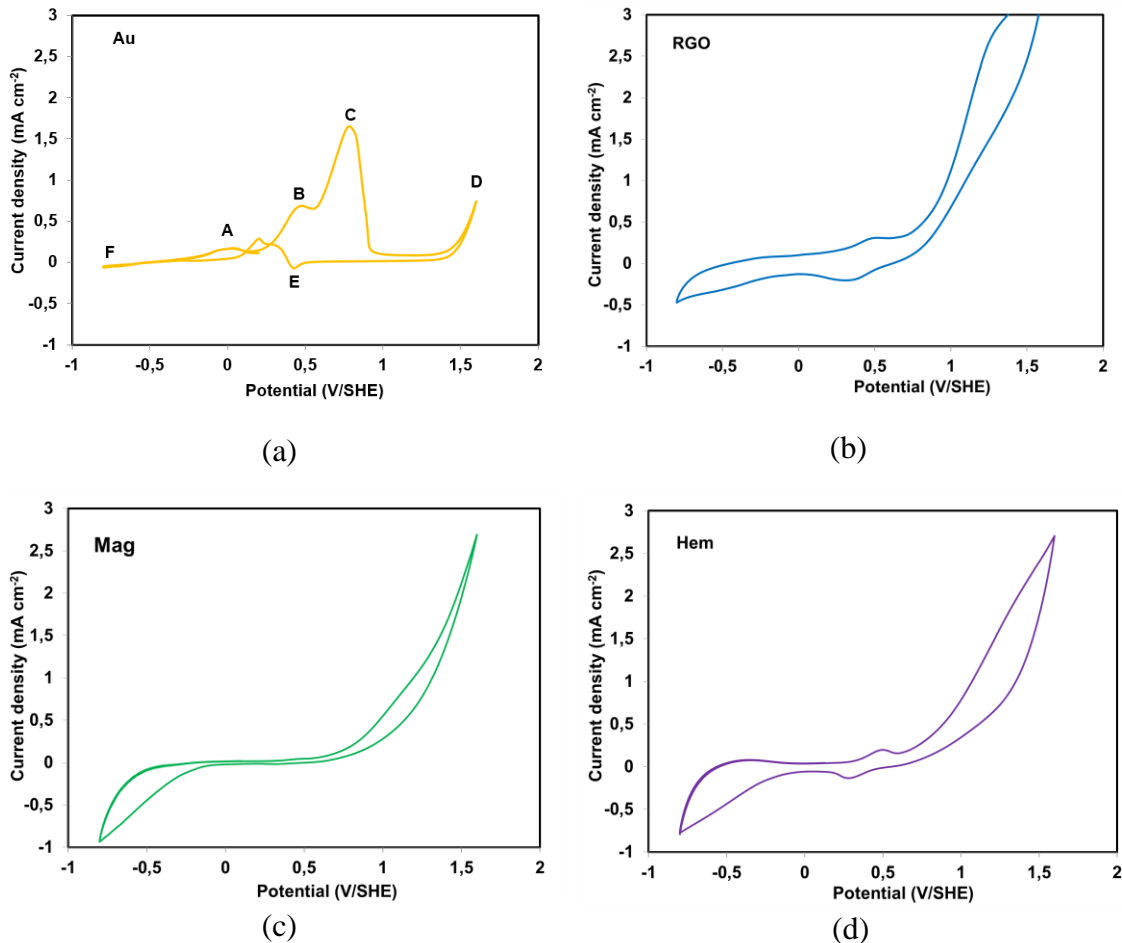
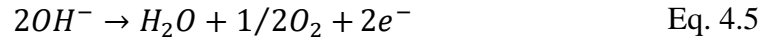
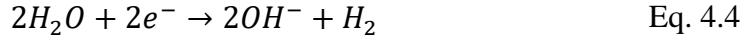


Fig. 4.2 Cyclic voltammetry (CV) of different electrodes; (a) Au (pure gold), (b) RGO (roasted gold ore), (c) Mag (magnetite), (d) Hem (hematite) disc electrodes in 0.04 M NaCN solution at pH 10.5 with scan rate of 10 mV/s, argon bubbling onto the surface of electrolyte at 25 °C.



Oxidation peak current densities of Au electrode were found to be 0.2, 0.5 and 1.8 mA/cm² in 0.04 M NaCN solution, respectively. [Mughogho and Crundwell \(1996\)](#) tested electrochemical behaviour of gold rotating disk electrode (1000 rpm) in dilute cyanide solution (~ 0.003 M) and reported also three anodic oxidation peaks with small current densities (0.05, 0.15, 0.2 mA), one reduction peak and one small anodic peak in the turn sweep, as well. Comparatively, in this study (0.04 M NaCN) without agitation, it is seen that peak current densities in higher cyanide concentration were found to be significantly higher (3 to 9 times). It can be concluded that Au electrode undergoes more passive behaviour if compared to RGO due to the formation of surface products/peaks ([Fig. 4.2](#)). [Han and Guan \(1995\)](#) tested the dissolution of gold from different gold alloys and noted that gold corrosion rate of alloys (Ag, Pb, Pt) was higher than that of gold due to the formation of passive film on the gold surface. [Jeffrey and Ritchie \(2001\)](#) reported that in practice due to the presence of many minerals, the ore passivation takes place less than that of gold. These results indicate that gold alone shows more passive behaviour than that of gold ore in cyanidation practice.

4.3.2 Galvanic Dissolution of Gold

Electrochemical Interactions between Au and RGO

Open circuit potentials of each electrode were measured prior to any electrochemical tests. It has been found that roasted gold ore (RGO) had the most positive potential (0.245 V), followed by hematite (0.235 V), and finally magnetite (Mag) (0.210) in 0.01 M NaCN solution after 2 h (at the end of test). These findings have indicated that corrosion potentials of electrodes have less active potentials than gold electrode (-0.55 V) suggesting that these mineral electrodes can act as cathode in a gold galvanic coupling. The passivation of gold surface, film formation, and galvanic interactions are important phenomena in the leaching of gold. In this case, roasted gold ore (RGO) disc electrode which has been prepared from roasted gold ore sample was used to couple with gold in galvanic corrosion tests in zero-

resistance ammeter (ZRA) mode. ZRA is the preferable tool for galvanic corrosion tests (Aghamirian and Yen, 2005; Azizi et al., 2011).

Fig. 4.3 shows the cathodic polarization profiles of electrodes by scanning from E_{corr} to -300 mV at pH 10.5 at 100 rpm agitation. Oxygen reduction takes place in cathodic area (Eq. 4.6) with a 605 mV standard potential at pH 10.5. The standard potential of other possible reactions in cathodic section are given vs. standard hydrogen electrode in Eqs. 4.7 and 8 (Aghamirian and Yen, 2005; Ahmed, 1978). Magnetite, hematite, and gold ore at high over-potentials are less active than gold. At low over-potentials, hematite was more active than magnetite. This can suggest that magnetite and hematite are good electrocatalysts for oxygen reduction.

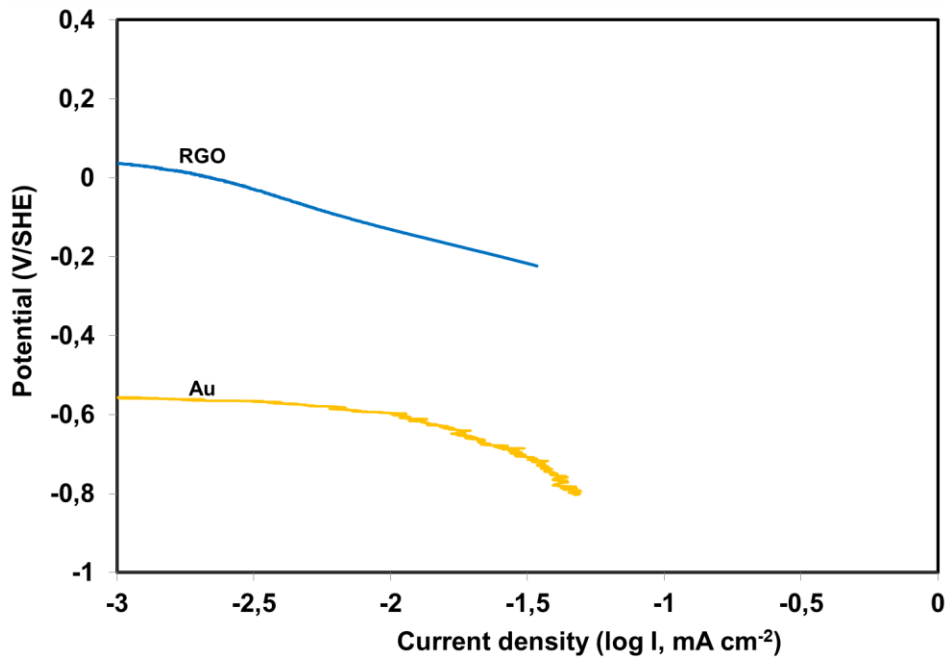
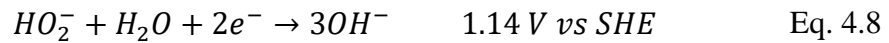
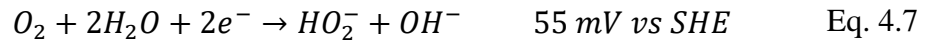
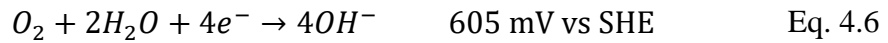


Fig. 4.3 Potentiodynamic cathodic polarization of gold (Au), and roasted gold ore (RGO) with scan rate of 0.166 mV/s at pH 10.5, 100-rpm agitation, atmospheric oxygen, 25 °C.

Fig. 4.4 illustrates the galvanic potential and current couples between gold (Au) and roasted gold ore (RGO) disc electrodes as function of agitation speed. As seen, corrosion potential decreased by 100 mV with increasing agitation speed from 100 to 400 rpm after 2 hours of test (Fig. 4.4a). Concurrent recording of galvanic currents showed that increasing agitation speed from 100 to 250 rpm resulted in giving close dissolution rates (145 μA). These obtained close corrosion rates could be linked to the insufficiency of agitation speed to provide the mass transfer of dissolved O_2 and CN^- ions to the surface of gold (Ellis and Senanayake, 2004). The other reason for that could be due to the consumption of oxygen and cyanide as a result of leaching of other minerals (silver, iron). However, dissolution rate was increased by 7% at 400 rpm (145 to 155 μA). This finding could be linked to the increased diffusion of oxygen by increasing agitation speed. Since oxygen reduction takes place on both electrode surfaces, then increasing agitation speed could enhance the positive galvanic interactions leading to dissolution of gold by increased oxygen-diffusion (Azizi et al., 2010).

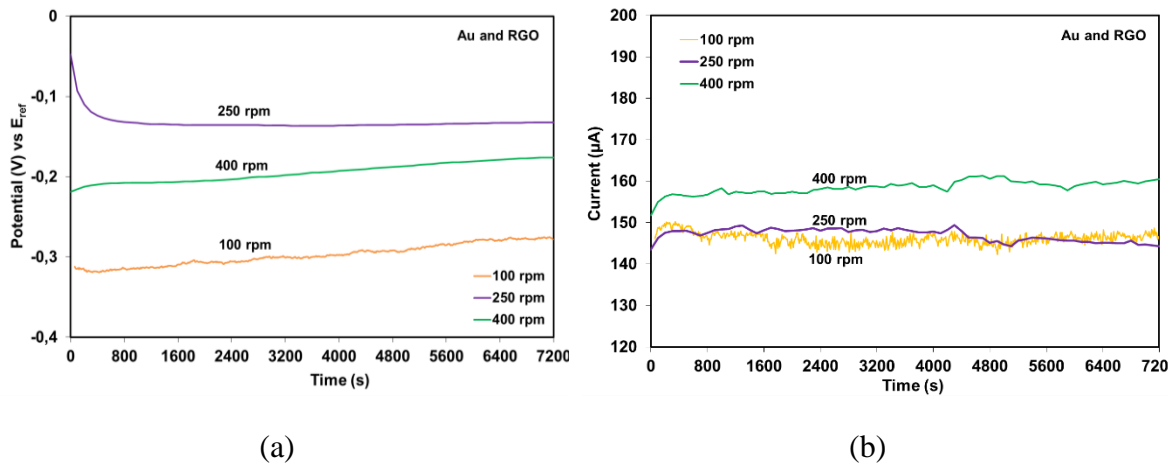


Fig. 4.4 The influence of agitation speed on the galvanic potential (a) and current (b) between gold (Au) and roasted gold ore (RGO) electrodes, pH 10.5, 25 °C, cyanide conc. 0.01 M, 25 °C, saturated atmospheric oxygen, Au electrode surface area 0.25 cm², RGO area 4.9 cm².

XPS study was carried out after Au was connected to RGO galvanic corrosion test in ZRA mode. A slight Ag peak was observed at 367.91 eV and presented in Fig. 4.5. In fact, low Ag concentration is quite difficult to detect when Au is present, however the presence of

Ag on the surface of gold was detected by XPS. The presence of Ag could be linked to the indication of the decrease in galvanic current that was presented in Fig. 4.5. Similarly, Ag coatings on Au surface was found by TOF-SIMS (time-of-flight secondary ion mass spectroscopy) and interpreted as the responsible for gold passivation (Surface Science Western, 2014). This finding highlights that passivation is more likely to be caused by the release of species and formation of compounds.

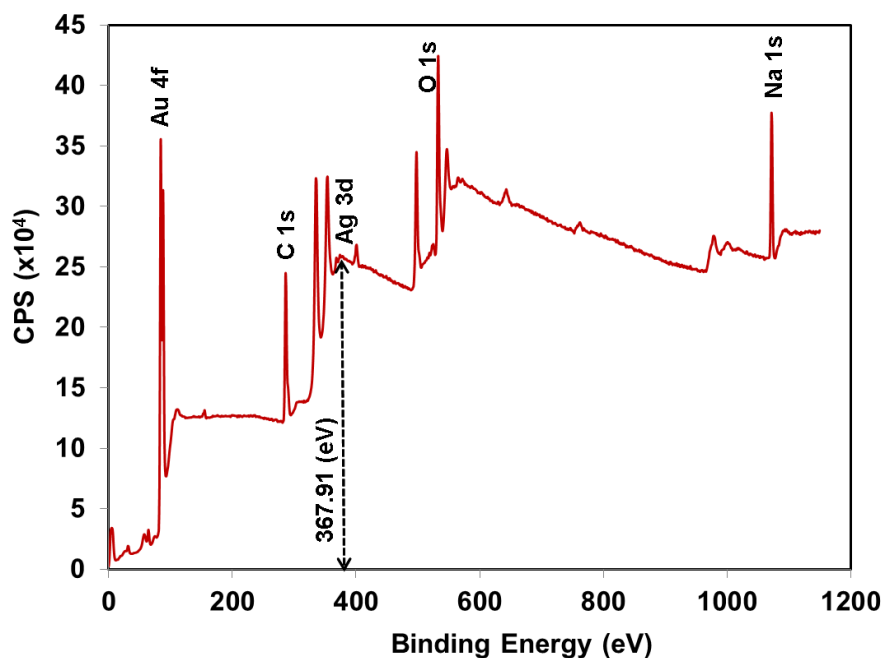


Fig. 4.5 XPS surface image showing the presence of Ag on the surface of Au electrode after galvanic coupled with Au and RGO.

Since the presence of magnetite has an important effect on gold leaching in practice, magnetite and roasted gold ore galvanic coupling was conducted. The galvanic current of magnetite and roasted gold ore electrodes showed an increasing trend and stabilized at 160 μ A (Fig. 4.6a). Roasted gold ore electrode leaching was promoted by RGO+Mag galvanic combination. A strong galvanic cell was formed with RGO acting as anode and magnetite as cathode. On the other hand, when roasted gold ore electrode (RGO) was coupled with hematite (Hem), galvanic current was step-wise decreased by 10 μ A suggesting that hematite showed negative effect on the leaching of roasted gold ore (Fig. 4.6b). The

different effects of magnetite and hematite on roasted gold ore leaching could be linked to the difference in solubility and conductivity of these minerals where magnetite is $\sim 10^6$ times more conductive than hematite (Greenwood and Earnshaw, 1997).

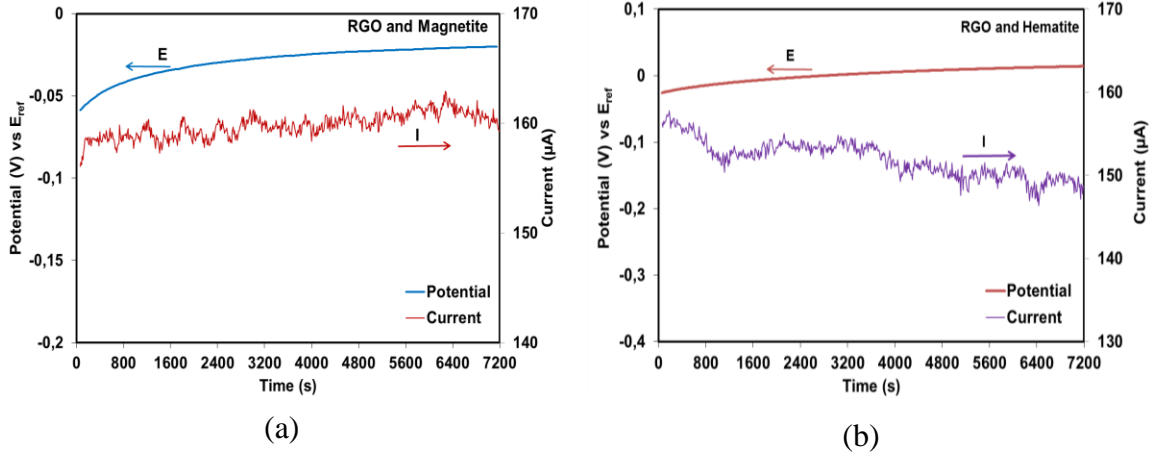


Fig. 4.6 Galvanic couple potential and ZRA vs. time at 100 rpm agitation, pH 10.5, 0.01 M cyanide conc., saturated atmospheric oxygen, 25 °C, (a) RGO (roasted gold ore electrode 4.9 cm²) and Mag (magnetite disc electrode 4.9 cm²); (b) RGO (roasted gold ore electrode 4.9 cm²) and Hem (hematite disc electrode 4.9 cm²).

Relative surface areas between two electrodes during galvanic interactions is another important parameter to be considered. Generally, corrosion rate of the anode would increase with an increase in cathodic electrode's surface area (Jones, 1992; Aghamirian and Yen 2005). Davis et al. (1986) stated that increasing the cathodic area, however, may also reduce the galvanic current if the cathodic curve intersects the anodic curve in an active-passive region. But then, the difference between free corrosion potentials of the cathode and anode (the emf of the cell) has an impact on the role of cathode to anode area ratio on the galvanic current. Aghamirian and Yen (2005) mentioned the importance of electrode surface alteration and adsorption of dissolved ions on the gold surface on galvanic current and gold leaching rate.

Galvanic Interaction between Gold and Magnetite

Magnetite, with its non-porous character, is less soluble in cyanide solutions (Habashi, 2009). Previously, it was observed that open circuit potential of magnetite is more active than gold suggesting that magnetite acts as cathode in galvanic coupling. Fig. 4.7a illustrates the galvanic potentials as function of agitation speed when gold electrode was galvanically coupled with magnetite disc electrode (Mag). Corrosion potential showed a 110 mV and 90 mV increase with increasing agitation speed from 100 to 250 and 400 rpm, respectively.

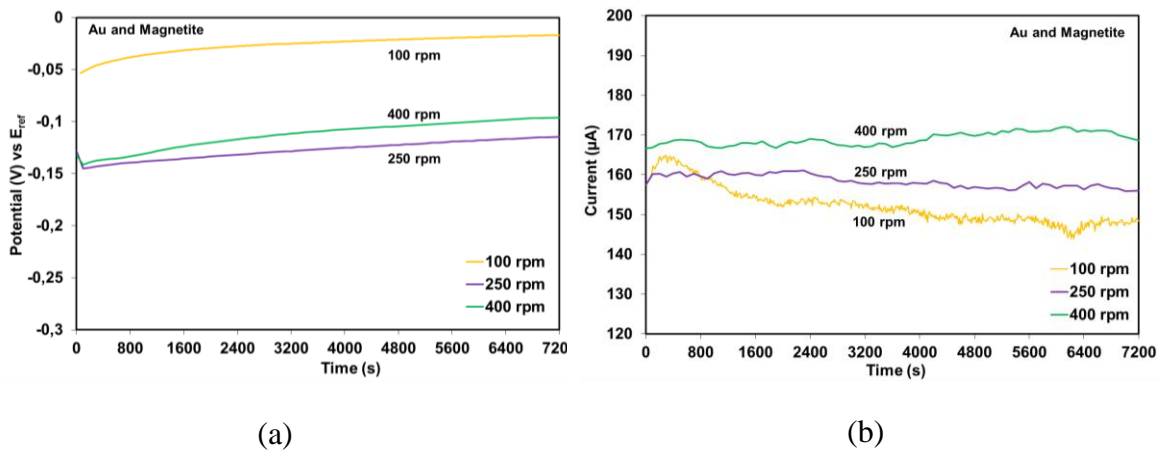


Fig. 4.7 The influence of agitation speed on the galvanic potential (a) and current (b) between gold (Au) and magnetite electrodes, pH 10.5, 25 °C, cyanide conc. 0.01 M, 25 °C, saturated atmospheric oxygen, Au electrode surface area 0.25 cm², Mag area 4.9 cm².

On the other hand, at 100 rpm agitation speed, galvanic current first increased and showed a certain decrease in the initial 15 min (Fig. 4.7b). Then, slowing slightly by 15 μA giving $\sim 148 \mu A$ at the end. This decreasing trend of galvanic current can be attributed to the release of soluble species (Azizi et al., 2010; Aghamirian and Yen, 2005) from magnetite that accumulate on gold surface suggesting the formation of passivating layer such as Fe(OH)₃ (Guo et al., 2005). Presence of iron hydroxide layer was suggested to diminish the oxygen reduction process (Aghamirian and Yen, 2005). This means that the decrease in cathodic current due to the oxidation of the most active species at the mineral surface could lead to a decrease in dissolution rate of gold (Azizi et al., 2010). Similarly, as stated

by [Filmer \(1982\)](#), gold in contact with magnetite could be expected to passivate due to the enhanced magnitude of cathodic current. However, increasing agitation speed from 100 to 400 rpm (145 to 165 μA) resulted in 12% increase in dissolution rate ([Fig. 4.7b](#)). This finding suggests that increasing agitation speed has led to a decrease in the of diffusion layer thickness ([Ellis and Senanayake, 2004](#)).

[Fig. 4.8a](#) illustrates SEM (scanning electron microscopy) image and [Fig. 4.8b](#) illustrates energy dispersive spectroscopy (EDS) of pure gold electrode after galvanic coupling test with Mag disc electrode. Black zone ([Fig. 4.8a](#)) was found to be composed of iron-oxide species ([Fig. 4.8b](#)) while the grey zone around the black zone was found to be Au-C compound that potentially could be insoluble Au-cyanide (i.e., N atom is not detectable at low concentrations by SEM-EDS). These findings have revealed that the species released from MagHem-ES electrode passivate the surface of gold electrode (Au).

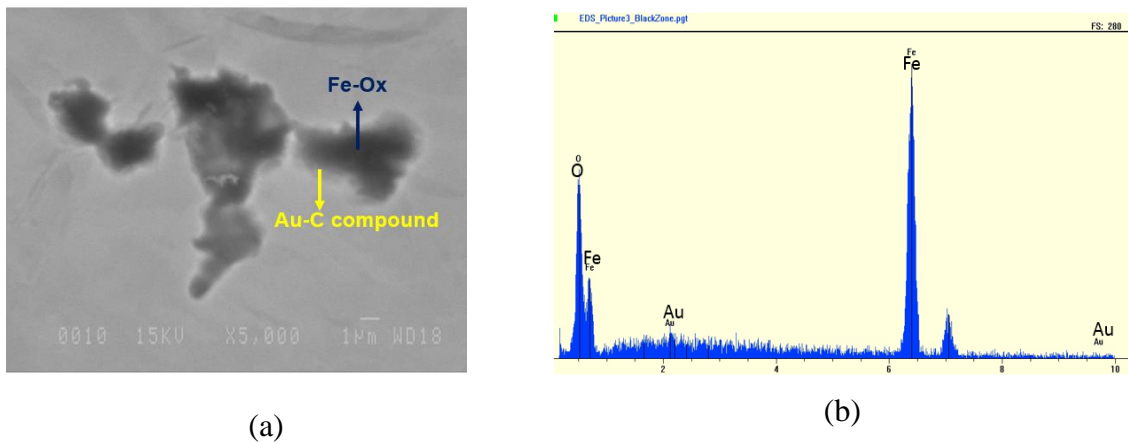


Fig. 4.8 SEM (a) and EDS (b) images of Au electrode surface after galvanic coupling with Mag disc electrode, pH 10.5 at 100-rpm, cyanide conc. 0.01 M, 25 °C, saturated atmospheric oxygen, Au electrode surface area 0.25 cm², Mag area 4.9 cm².

Galvanic Interaction between Gold and Maghemite

[De Faria et al. \(1997\)](#) reported that magnetite (Fe_3O_4) is oxidised to give maghemite ($\gamma\text{-Fe}_2\text{O}_3$) and hematite ($\alpha\text{-Fe}_2\text{O}_3$) by heating at 200 °C and 400 °C, respectively ([Eq. 4.9](#)). [Paktunc et al. \(2006\)](#) examined the distribution of gold in an ore sample after roasting of a refractory gold ore and found that gold is associated with magnetite, hematite, and as well

as maghemite minerals which is impervious in character and are responsible for low gold extractions. In this manner, the effect of maghemite on the leaching of gold was examined.

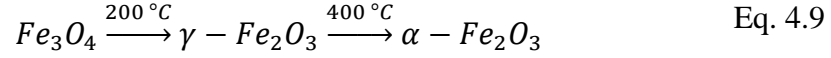


Fig. 4.9a illustrates the galvanic potentials when gold and maghemite (Mgh) electrodes were in galvanic coupling. It is seen that at 100 rpm agitation, corrosion potential sharply increased from -80 to -180 mV in the initial 7 minutes, then stabilized almost at the initial value (-80 mV). On the other hand, at the beginning of the test, at 100 rpm agitation speed galvanic current suddenly increased by 5% (215 to 225 μ A) that is indicative of the initial sharp decrease in galvanic potential (Fig. 4.9a). Then, it decreased to 170 μ A and was kept almost at that value through the test (Fig. 4.9b). However, at 250 rpm agitation speed, galvanic current gave almost the same value of 145 μ A through the test-work. It was observed that galvanic corrosion rate decreased by 15 % at higher agitation speed. This decrease can be linked to the increased leaching of maghemite electrode at higher agitation speed than 100 rpm. Due to the difficulty in distinguishing of magnetite and maghemite minerals with XRD, a new maghemite preparation procedure was also considered to see the effect of maghemite as function of time (5 hours) and temperature (250 $^\circ$ C) (D. Paktunc, personal communication, October 10, 2014). However, very close potential and current values were obtained if compared to the first prepared maghemite (at 200 $^\circ$ C for 3 hours).

Since iron oxides are the main phase in gold ore, a new electrode consisted of equal surface areas of magnetite and hematite (MagHem-ES) was developed. Fig. 4.10a shows that increasing agitation from 100 to 250 rpm has led to a decrease in corrosion potential by 85 mV. Concomitantly, at both agitation speeds, galvanic corrosion rate initially (in the first 10 min) increased and then stabilized. At the off-set of the test, a 7% increase in galvanic corrosion rates was obtained with increasing agitation speed from 10 to 250 rpm. It can be seen that at 100 rpm agitation, Au and MagHem-ES and Au and Magnetite couplings gave very close corrosion rates suggesting that the influence of magnetite is dominating over hematite where conductivity of magnetite is $\sim 10^6$ times higher than hematite (Greenwood and Earnshaw, 1997).

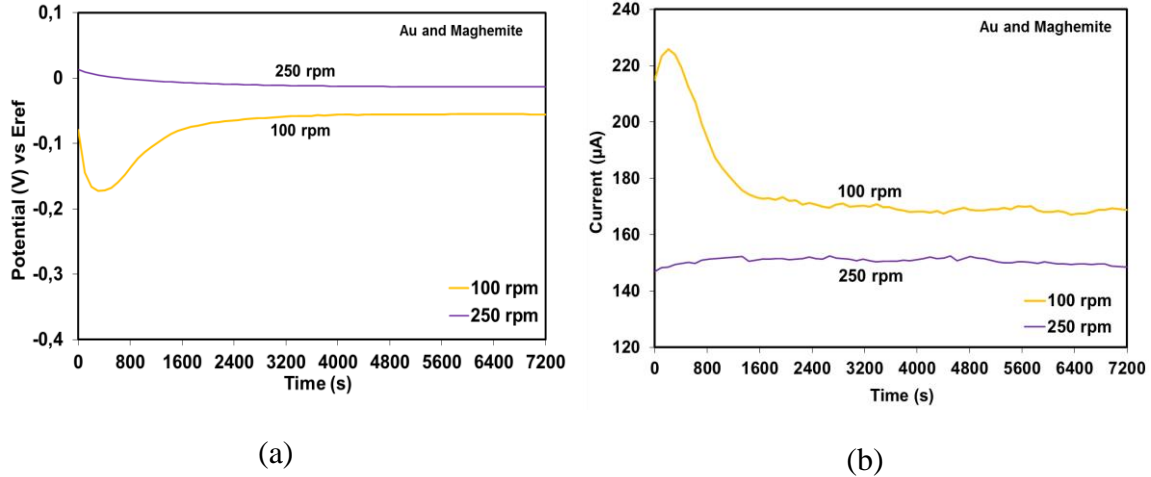


Fig. 4.9 The influence of agitation speed on the galvanic potential (a) and current (b) between gold (Au) and maghemite (Mgh) electrodes, pH 10.5, 25 °C, cyanide conc. 0.01 M, 25 °C, saturated atmospheric oxygen, Au electrode surface area 0.25 cm², Mgh area 4.9 cm².

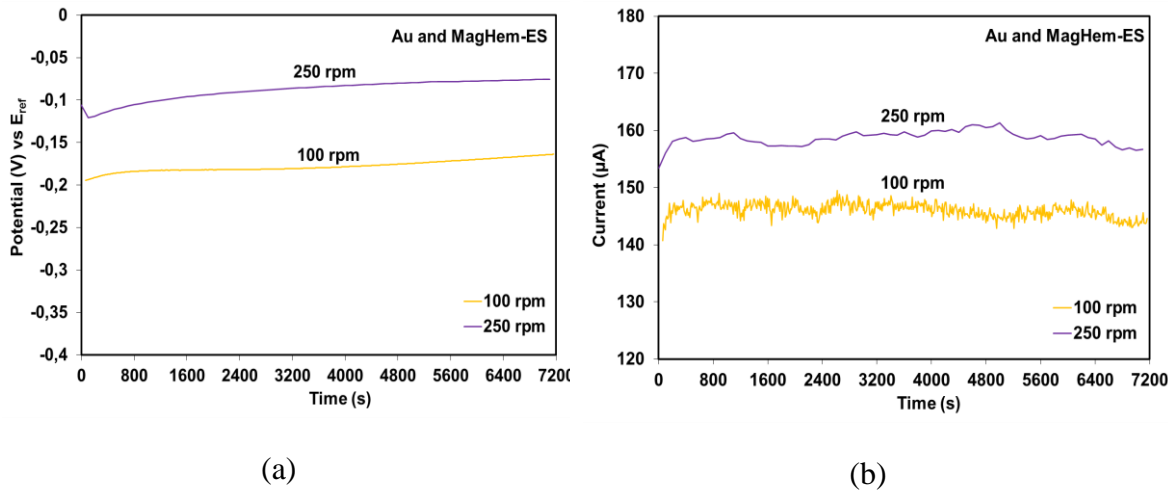


Fig. 4.10 The influence of agitation speed on the galvanic potential (a) and current (b) between gold (Au) and MagHem-ES electrodes, pH 10.5, cyanide conc. 0.01 M, 25 °C, saturated atmospheric oxygen, Au electrode surface area 0.25 cm², MagHem-ES area 4.9 cm².

Galvanic Interaction between Gold and Hematite

Lorenzen and van Deventer (1992a) mentioned that gold when in contact with conductive minerals such as hematite, galvanic interactions play important role on gold leaching. Corrosion potential decreased with increasing agitation speed from 100 to 250 rpm. However, at 400 rpm agitation speed, generally higher but a wavy trend was observed (Fig. 4.11a). On the other hand, at 100 rpm agitation galvanic current initially increased, then

became stable. It can be deduced that dissolution rate increased by 20% with increasing agitation from 100 to 250 rpm, and then showed a slight decrease (by 2%) at 400 rpm (Fig. 4.11b). This finding is an indication of the change on gold electrode surface. This could be explained by the fact that increasing agitation speed resulted in an increase in the leaching rate for diffusion controlled systems till it reaches to maximum level where the rate remains constant. At this level, the diffusion contribution is minimized and the rate of extraction was mainly controlled by chemical reactions. The release of soluble iron species could be responsible for the reduction in gold leaching rate which has been proved by SEM analysis (Fig. 4.8). van Deventer and Lorenzen (1987) observed an 8% decrease in dissolution rate of gold when it is connected with hematite.

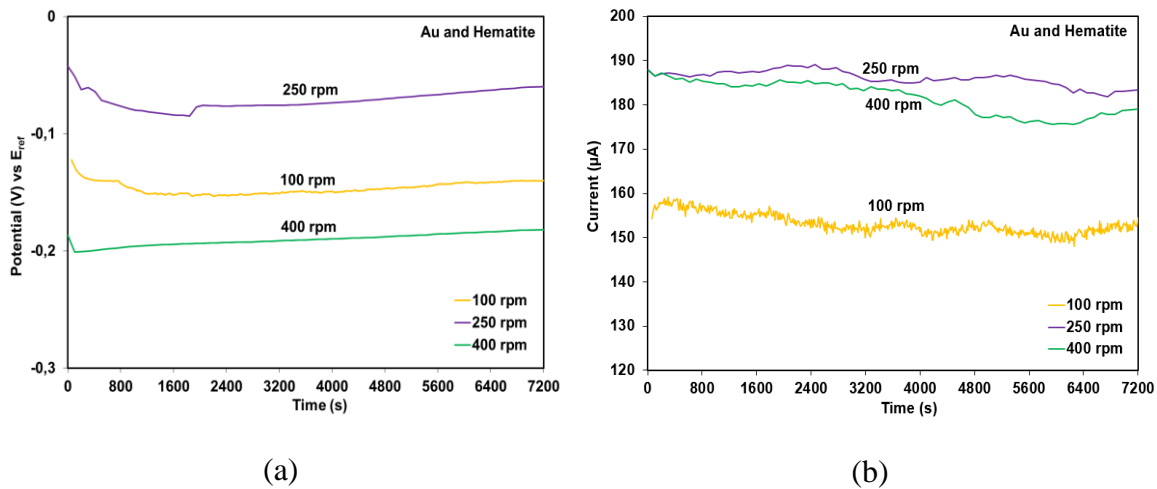


Fig. 4.11 The influence of agitation speed on the galvanic potential (a) and current (b) between gold (Au) and hematite (Hem) electrodes, pH 10.5, cyanide conc. 0.01 M, 25 °C, saturated atmospheric oxygen, Au electrode surface area 0.25 cm², Hem area 4.9 cm².

Among all minerals, higher galvanic corrosion rates were obtained when hematite was coupled with gold. Filmer (1982) mentioned the relative positive effect of hematite on gold leaching if compared to magnetite. It can be deduced that hematite can promote gold dissolution only in a certain case. Similarly, in potentiodynamic polarization tests when hematite was electrically connected to gold, it was found to eliminate the passive peaks, while magnetite with gold showed a certain passive behaviour (Bas et al., 2014). Then, it is worth noting that the influence of minerals on gold dissolution can vary depending on

the anodic and cathodic behaviours of gold and associated minerals. For instance, although pyrite was known to reduce the gold extraction when galvanically coupled with gold (Filmer, 1982; Lorenzen & van Deventer, 1992a), however Aghamirian and Yen (2005) observed the contrary results. Generally, in case of all minerals coupled with gold, it is seen that there is a certain different trend in the initial 15 minutes if compared to the rest of the test. Galvanic corrosion tests were performed at least three times to ensure the reproducibility of the results due to rapid reactions and surface changes. Galvanic potential results were reproducible within ± 12 mV, while galvanic currents were obtained within ± 3 μ A. The findings in this study have revealed that a more detailed study of galvanic interactions between gold and oxide mineral electrodes is highly required.

4.4 Conclusions

1. Cyclic voltammetry studies of RGO in de-aerated electrolyte showed one oxidation and one reduction reaction while three oxidation peaks and one reduction peak were observed with Au electrode.
2. Corrosion potentials of hematite, magnetite, maghemite, and roasted gold ore indicated that they can act as a cathode and could potentially or at least temporarily promote the dissolution of gold in galvanic coupling.
3. Increasing agitation speed (100 to 400 rpm) has led to an increase in galvanic corrosion rate of gold when coupled with roasted gold ore, magnetite, and maghemite disc electrodes. However, hematite showed a maximum increase in corrosion rate at 250 rpm as compared to that of 400 rpm.
4. Generally, in case of all tested minerals coupled with gold, it is seen that there is a certain different trend in the initial 15 minutes, then the corrosion rate decreased or became stable, relatively. This suggests that each oxide mineral has different effect on gold dissolution potentially due to the difference in conductivity and changes in the surface state.
5. In galvanic corrosion tests, the tested minerals showed a negative effect on gold leaching in decreasing order: magnetite, magnetite-hematite (MagHem-ES), roasted gold ore.

However, maghemite and hematite showed a positive effect, relatively. These results have revealed that formation of corrosion products, passivation, concentration of soluble ions, and diffusion control are responsible for the retarding or promoting effect on the leaching of gold. This could be also linked to the difference in conductivities of these electrodes.

6. XPS studies indicated the presence of silver on gold surface that could lead to partial passivation of the surface. Furthermore, Fe-oxides and Au-C compound (potentially insoluble Au-CN basic film) were demonstrated by SEM analysis.

4.5 Acknowledgements

Natural Sciences and Engineering Research Council of Canada, Barrick Gold Corporation, and Hydro-Quebec for their financial support through R&D NSERC Program are gratefully acknowledged. The authors would like to express their sincere thanks and appreciation to Dr. L. Gavril for the help during the test-work and to Laval University personnel to Mrs. V. Dodier for AAS analysis, to Dr. A. Adnot for XPS analysis and valuable contributions, to Mr. A. Ferland for SEM analysis, to Mr. J. Frenette for XRD analysis and to Mr. F. Kanku Kadiavi for the help during his internship period.

Chapter 5

Electrochemical Behaviour of Roasted Gold Ore During Cyanidation

Electrochemical Dissolution of Roasted Gold Ore in Cyanide Solutions

Ahmet Deniz Bas^{a*}, Liliana Gavril^a, Wei Zhang^a, Edward Ghali^a, Yeonuk Choi^b

^aDepartment of Mining, Metallurgical and Materials Engineering, Laval University, Quebec, Canada, G1V 0A6

^bBarrick Gold Corporation, Suite 3700, 161 Bay Street P.O.Box 212, Toronto, Ontario, Canada, M5J 2S1

*Corresponding author: 4186568657, Fax: 4186565343; (ahmet-deniz.bas.1@ulaval.ca)

Published in Hydrometallurgy, 156, 188-198. DOI: [10.1016/j.hydromet.2015.07.003](https://doi.org/10.1016/j.hydromet.2015.07.003)

Résumé

Dans les tests de corrosion libre, une électrode d'or pur (Au) a un comportement plus actif que celui de l'électrode de minerai d'or grillé (RGO). Les mesures de bruit électrochimique de l'électrode d'Or ont généralement montré une tendance à la hausse de la vitesse de corrosion, tandis que RGO a atteint un plateau après 10 h jusqu'à 24 h. La technique de balayage de l'électrode de référence au potentiel de circuit ouvert, a montré une force électromotrice quasi plus élevée pour Au que RGO. Les conditions de lixiviation optimales pour RGO se sont révélés être une concentration de 0,04 M NaCN, le pH 10 à 10,5, avec 250 tr/min comme vitesse d'agitation. On a constaté que dans les solutions de cyanure saturées avec l'oxygène atmosphérique, la pente cathodique de Tafel seulement ($3,30 \times 10^{-8} \pm 3,27\% \text{ mol m}^{-2} \text{ s}^{-1}$) fournit de vitesses de corrosion représentatifs de l'or pour RGO proche à celle de la cyanuration pratique ($3,07 \times 10^{-8} \pm 7,03\% \text{ mol m}^{-2} \text{ s}^{-1}$). Compte tenu des méthodes de la courbe anodique pour la pente de Tafel ou Stern-Geary ont été trompeuse en raison de la présence de différents constituants. La réaction cathodique sur quelques sites de la phase conductrice métallique est le contrôle de la vitesse de la réaction un balayage potentiodynamique de la courbe de polarisation cathodique devrait aller directement sans nettoyage cathodique du potentiel de corrosion versus pour les plus cathodiques pour les deux électrodes Au et RGO. L'analyse de MEB a indiqué la présence de Fe-oxyde, le contributeur principal de la passivation l'or.

Abstract

In free corrosion tests, pure gold (Au) electrode gave more active behaviour than that of roasted gold ore (RGO) electrode. Electrochemical noise measurements of Au electrode generally showed an increasing trend in corrosion rate, while RGO plateaued after initial 10 h until 24 h. Scanning reference electrode technique, at open circuit potential, showed higher quasi electromotive force for Au than RGO electrode. Optimal leaching conditions for RGO were found to be 0.04 M NaCN concentration, pH 10-10.5, and 250 rpm agitation speed. It was found that in cyanide solutions saturated with atmospheric oxygen, cathodic Tafel slope only ($3.30 \times 10^{-8} \pm 3.27\%$ mol m⁻² s⁻¹) provides representative corrosion rates of gold for RGO compared to practical cyanidation ($3.07 \times 10^{-8} \pm 7.03\%$ mol m⁻² s⁻¹). Considering the anodic curve for Tafel slope or Stern-Geary methods was found to be misleading due to the presence of different constituents. The cathodic reaction on few sites of metallic conductive phase is the rate controlling one. Potentiodynamic scanning of cathodic polarisation curve should go directly without cathodic cleaning from corrosion potential to more cathodic ones for both Au and RGO electrodes. SEM analysis indicated the presence of Fe-oxide products could be the main contributor to the passivation of the gold surface.

Keywords: Roasted gold ore, corrosion rate, passivation, cathodic Tafel, cyanidation

5.1 Introduction

During cyanidation, leaching of gold is reduced or retarded in some conditions. Since cyanidation is an electrochemical based process (Habashi, 2009), thus dissolution of gold can be readily studied by electrochemical techniques. Recently, Crundwell (2013) claimed that each point on the mineral surface is considered as both an anodic site and a cathodic site and concluded that there is no separation of anodic and cathodic sites on a mineral's surface. Habashi and Bas (2014) pointed out that certain experimental results demonstrated the existence of anodic and cathodic zones during the dissolution of minerals. These findings have revealed that electrochemical studies of gold still receive much attention.

Passivation of gold, diffusion control, and galvanic interactions are considered as important factors affecting the leaching of gold (Filmer, 1982; Azizi et al., 2011). Passivation of gold has been known since 1907 and gold becomes passive under certain conditions in commercial cyanide solution and assumed that the passivity is due to the formation of insoluble sodium aurocyanide film on the surface of gold (Cathro and Walkley, 1961). Mrkusic and Paynter (1970) identified the passivation as the film formation of dissolved species from calcine while Nicol (1980) reported that passivation of gold mainly depends on the presence of impurities in the solution. It was suggested that gold oxides and cyanide films are responsible for the passivation of the surface of gold (Kirk et al., 1978). The different types of dissolved minerals found in the ore may have positive and/or negative effect on the rate of gold dissolution (Jeffrey and Ritchie, 2001; Nicol, 1980). Although many studies have been carried out, there is still a doubt on gold passive phenomenon.

In the present time, it is well known worldwide that there is an increasing trend on the treatment of refractory ores (often requires oxidation prior to cyanidation) due to the rapid depletion in free-milling gold ores (Adams, 2016). Till now, almost all previous electrochemical studies of gold were conducted using only sulphidic gold ores (van Deventer and Lorenzen, 1987; van Deventer et al., 1990; Lorenzen and van Deventer, 1992a, 1992b; Aghamirian and Yen, 2005; Cruz et al., 2005; Dai and Jeffrey, 2006; Azizi et al., 2010, 2011, 2012a, 2012b, 2013). On the other hand, there is a paucity on electrochemical interaction studies between gold and its oxide minerals. At the same time,

the influence of agitation was not systematically considered in previous studies. Therefore, an increasing request of the gold mining industry for this issue is created. Furthermore, the corrosion (dissolution) rate of gold was considered from the intersections of anodic and cathodic Tafel slopes (Cerovic et al., 2005). However, Dai and Breuer (2013) showed that using only Evans' diagrams is misleading for gold dissolution estimation. These findings indicate that calculation of corrosion rate of gold is still an important issue.

Based on the above statements, the main objective of this study is to provide a detailed understanding of electrochemical behaviour and optimal leaching conditions (NaCN concentration, pH, and agitation speed) for roasted (oxidised) gold ore, as far as possible, by using conventional and more recent electrochemical techniques such as Electrochemical Noise Measurement (ENM) and Scanning Reference Electrode Technique (SRET). ENM is referred to as a random fluctuation of current and/or potentials that has received widely attention to study the electrochemical systems (Eden, 2011) and is used for monitoring active and passive behaviours, and type of corrosion of tested specimen (Lafront et al., 2010b; Safizadeh and Ghali, 2013). Although the majority of ENM studies have been carried out in corrosion studies, there is a recent attempt using ENM in leaching studies (Bevilaqua et al., 2006). This method could potentially be an alternative in gold leaching studies for the characterization of surface products that could lead to surface passivation. SRET was considered to contribute to the electrochemical dissolution of gold since SRET in-situ provides significant information on anodic and cathodic potentials of a specimen as a function of time in free corrosion mode (Zhang et al., 2006). It is also possible to analyse the active and passive behaviours of gold with the 3D image facility of SRET. Furthermore, electromotive force of the corrosion cell is calculated by the evaluation of SRET data. This study also investigates the corrosion rate of gold by cathodic Tafel slope, Stern-Geary method, and compared to that obtained by conventional cyanidation. Concurrently, providing an appropriate understanding on the passivation phenomenon of gold is also one of the objectives.

5.2 Experimental Conditions

5.2.1 Roasted Gold Ore Sample

The gold ore sample was obtained from Barrick Gold Corp. This was the calcine after roasting of refractory gold ore. The sample (which was already reduced in size 80% passing $-75\ \mu\text{m}$ (d_{80})) was riffled as portions prior to use in experiments.

Qualitative mineralogical analysis of the sample indicates that the ore sample consists predominantly of quartz, dolomite, calcite, gypsum, and iron oxides such as hematite, magnetite, and maghemite and with almost non sulphur content. Gold is mostly associated with iron oxides. Metal analysis of the ore sample by AAS for Au and Ag after hot aqua regia digestion has shown that gold and silver contents are ~ 8 and ~ 5 g/t, respectively.

5.2.2 Material and Preparation of Electrodes

NaCN ($\geq 98\%$ purity) was obtained from Thermo Fisher Scientific Company. Electrolyte medium (1L) was prepared using distilled water and pH was adjusted at 10.5 by adding 1 M NaOH. Electrolyte was magnetically agitated (4 cm long and 1 cm diameter) during the tests. Pure gold (Au), rotating disc (RDE), roasted gold ore (RGO) and its oxide electrodes magnetite (Mag), and hematite (Hem) disc electrodes were used as working electrode while platinum (Pt) as a counter electrode and Ag/AgCl/KCl_{sat} as reference electrode.

1 cm² of gold foil (99.9% purity from Sigma Aldrich), as pure gold electrode (Au), was first polished with fine (MicroCut® 100 Grit Soft) polishing paper and then rinsed in distilled water. Then, it was introduced in aqua-regia for 10 seconds to clean the surface, washed with distilled water and ethanol and finally rinsed with distilled water again, to assure the reproducibility. Rotating ring disc electrode (RDE), where disc electrode was connected to a rotator, with a surface area of 0.05 cm² gold was obtained from ALS Co., Ltd. (Japan) and was used in certain tests.

Roasted gold ore (RGO), magnetite (Mag), and hematite (Hem) disc electrodes with an exposed surface area of 4.9 cm² were prepared. In each case, roasted gold ore, magnetite, hematite was mixed with graphite powder (to increase the conductivity) 3:1 and with around 0.4 g of silicone oil, for binding, till a paste was obtained. Graphite powder, which

has a particle size of $<45\ \mu\text{m}$, and a 99% purity, was obtained from Sigma-Aldrich. The mixture was manually homogenized during 30 minutes, in general. Then, it was mechanically pressed at 20 tons to have uniform sample surface. After that, all disc electrodes were kept under nitrogen atmosphere over a night. The electrical contact was assured by an insulated copper wire, cast in acrylic resin. Although it is difficult to mimic the practical conditions in laboratory studies (for surface areas), due to the low quantity of gold in its ore, however, the chosen difference in surface areas of electrodes is considerably suitable to see the main tendencies and influences of minerals on gold dissolution.

5.2.3 Electrochemical Test Procedures

Open Circuit Potential (OCP)

In open circuit potential (OCP) or free corrosion potential tests, NaCN concentration was kept at 0.04 M and tests were carried out in 400 mL beakers. Dissolution potential of gold may be influenced either in a positive or negative way due to the presence of soluble ions in the solution. Therefore, to monitor the changes in open circuit (dissolution) potential of gold and roasted gold ore electrodes as function of soluble species, the addition of slurry into the solution was considered to mimic the real leaching conditions. When the tests were conducted in presence of roasted gold ore the solid ratio was adjusted at 35% wt/vol. All the tests were conducted for 24 h. In the case of RDE the electrode was monitored for the first hour. After that, RDE was taken off from the solution and kept under N_2 conditions for the next 22 h to prevent its corrosion. During this period the solution was continually magnetically agitated (100-rpm). After 22 h (23 h since the beginning of experiment), the RDE was again placed into the solution without any change in the potential for 1 h to complete 24 h in total.

Electrochemical Noise Measurement (ENM)

Prior to electrochemical noise measurement (ENM) tests, two working electrodes were prepared separately following the three steps: cathodic cleaning for 50 min. and potentiodynamic polarization (-0.8 to 1.2 V) and then potentiostatic measurement (at 1 V) for 2 h. The Electrochemical noise measurements were performed in employing a set-up using zero resistance ammeter (ZRA) mode in 0.04 M NaCN solution. In this mode, the

electrochemical noise could be measured between two nominally identical working electrodes as the galvanic coupling kept at the same potential. The samples were immersed in the solution where the system was allowed to stand at open circuit for 5 min. Then, the potential and current fluctuations were simultaneously recorded during 24 hours at a scan rate of $f_s=10$ Hz. This scan rate is generally preferred since it is quite enough to have a clear trend in noise data. If a more precise of noise data is requested, then a higher scan rate could be applied, however, the general trend will be same and this does not affect to the noise resistance, in overall. All potentials were measured vs. Ag, AgCl/KCl saturated reference electrode (0.199 V), and reported with respect to the Standard Hydrogen Electrode (SHE).

The ENM tests were carried out without agitation and exposed to atmospheric oxygen. A Gamry[®] PC4/ 300 potentiostat was used to log current and potential variations in time. The analyses were performed using a GAMRY[®] PC4 750/ESA400 software and analyser v. 2.35. The DC drift was removed before all analyses to eliminate the trend. At least, three series of tests were performed for each examined sample.

Scanning Reference Electrode Technique (SRET) Procedure

Au and roasted gold ore electrodes were mounted horizontally in the cell of SRET apparatus (EG&G Instruments-Model SVP100) for free corrosion potential measurement (Fig. 5.1). After ensuring that the surface of the specimen was parallel to the surface on the Perspex tripod and leveled, the probe was lowered to a distance of 100 μm above the sample surface, and then the cyanide solution was added. The basic configuration is to connect one input (+ve) to the vibrating probe and the other input (-ve) to a separate reference probe (carbon electrode in this case) placed in the solution local to the surface to be measured. After conditioning of the signal, a rectangular area (18.0 mm by 13.5 mm) was scanned, overlapping slightly the acrylic resin. The vibrating probe amplitude was adjusted at 45 μm , and the data collection was scanned at 32 points per scan line on X-axis and for a total of 24 lines on Y-axis. For each data point, 500 potential measurements were taken at a frequency of 81 Hz. Each SVP scan lasted approximately 19 min and 1 min of rest was allocated between each scan, all the experiments were conducted over a period of 16 hours. The overall SRET data were used to reproduce a three-dimensional image

mapping of the surface potential over the specimen. Referring to this 3-D image map, the down cones (\downarrow) correspond to anodic potentials (inside pits) and the up cones (\uparrow) represent the cathodic potentials (Zhang et al., 2006).

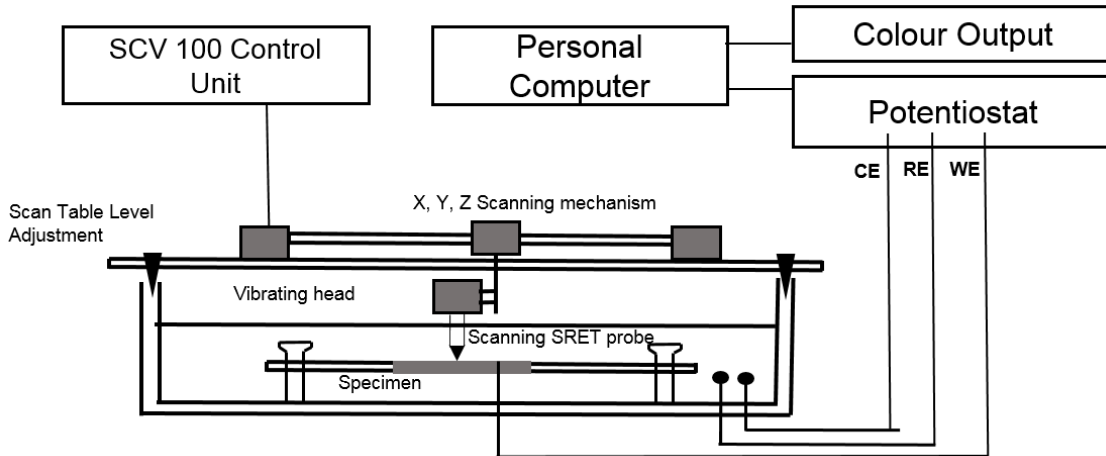


Fig. 5.1 Schematic illustration of Scanning Reference Electrode Technique (SRET) set-up (CE: counter electrode; RE: reference electrode; WE: working electrode).

Linear and Potentiodynamic Polarization

Corrosion current by cathodic Tafel polarization results were performed and compared to that of obtained from linear polarization by using Stern-Geary method. First, electrodes were allowed to stay at open circuit potential for 2 minutes before linear polarization tests for corrosion rates with a range of ± 25 mV with respect to corrosion potential (E_{corr}). Actually, different stabilization times (up to 30 minutes) were also considered, however the difference (only up to $\pm 5\%$) was found to be negligible. Then, cathodic polarization tests by scanning from E_{corr} to -300 mV were performed to calculate also the corrosion current (i_{corr}), considering cathodic Tafel slope only. Tests were performed generally in 0.04 M NaCN electrolyte at pH 10.5 at 100 rpm magnetic agitation (4 cm long and 1 cm diameter) at room temperature, saturated with atmospheric oxygen and 0.166 mV/s scan rate, considering polarization standards (ASTM Standard G 5-94, 2006). Each test was carried out at least in triplicates to assure the reproducibility. To simulate the practical

conditions, polarization tests with the same procedure was also carried out in the presence of slurry (35 % solid ratio).

5.2.4 Conventional Cyanide Leaching

Leach solutions were prepared using deionised-distilled water at the prescribed concentration of reagents (0.04 M NaCN). Leaching tests were conducted at 250 rpm agitation speed for 24 h in 0.48 L solutions into which roasted gold ore disc electrode (4.9 cm²) was placed. During the experiments, pH was maintained at 10.5 by the addition of 1 M NaOH. Solution was sampled at predetermined intervals and analysed by atomic absorption spectrophotometer (Atomic Absorption Spectroscopy, AAS - Perkin Elmer AAnalyst 800) to determine the gold leaching rate.

5.3 Results and Discussion

5.3.1 Dissolution Behaviour of Gold at Open Circuit Potentials (OCP)

OCP Studies of Disc Electrodes as function of Slurry

Open circuit potential also known as free corrosion potential is critical in electrochemical tests since open circuit potential (E_{corr}) provides significant information about the corrosion behaviour of each mineral or metal, also it is important for galvanic interactions. Preliminary tests have confirmed that 100 rpm agitation could be suitably used for open circuit potential tests at 25 °C. This is supported by the work of [Sheveleva and Kakovskii \(1979\)](#), who have shown that the dissolution rate of gold is controlled by diffusion (mass transfer) at agitation speeds below 100 rpm. However, in practice, the agitation speed is variable and generally lower than 100 rpm. It has been found that roasted gold ore (RGO) had the most positive potential (0.245 V), followed by hematite (0.235 V) and finally magnetite (Mag) (0.210) in 0.04 M NaCN solution after 2 h (at the end of test). These findings have indicated that corrosion potentials of electrodes have less active potentials than pure gold electrode (-0.404 V) suggesting that these mineral electrodes can act as cathode in a gold galvanic coupling. Additionally, effect of slurry on the corrosion potentials of especially roasted gold ore (RGO) and pure gold (Au) disc electrodes, as well

as rotating ring disc (RDE) and platinum (Pt) disc electrodes were tested for 24 h and the first 1 hour and the last 1 h (23-24h) were reported in [Table 5.1](#).

In the first hour of test work, RGO (roasted gold ore electrode) reached to 0.170 V corrosion potential in the absence of slurry and 0.190 V in the presence of slurry. At the end of 24 h, RGO electrode had the close corrosion potential in presence and/or absence of slurry which suggests that oxidation products on the surface is more stable and resistant to dissolution. Moreover, according to first 1 h and the last 1 h in presence and/or absence of slurry, RGO electrode showed more tendencies to passive behaviour when compared to Au and rotating disc electrodes (RDE). This could be linked to the presence of different mineral phases and formation of surface products on the surface of RGO disc electrode.

Table 5.1 Corrosion potentials of different electrodes in absence and in presence of gold ore slurry in 0.04 M NaCN solution, pH 10.5 at 25 °C.

Type of electrode	Absence of slurry E/V				Presence of slurry (35%) E/V			
	0h	1h	23h	24h	0h	1h	23h	24h
RGO	0.160	0.170	0.196	0.180	0.206	0.190	0.185	0.193
Au	-0.328	-0.404	-0.436	-0.404	-0.241	-0.248	-0.275	-0.343
RDE**	-0.436	-0.475	-0.436	-0.475	-0.273	-0.289	-0.286	-0.415
					-0.259*	-0.265*	-0.269*	-0.416*
Pt	0.178	0.170	0.148	0.142	0.167	0.165	0.134	0.167

* The duplicate values of the same test of RDE for instance; **Rotating gold disc electrode (RDE) was removed from the solution and was kept under nitrogen atmosphere for 22 h just after the end of the initial 1 h to prevent surface corrosion.

In the absence of slurry, Au (pure gold electrode) reached to -0.404 V corrosion potential in the first hour. The same value was recorded after 24 h. Contrary, after 24 h in the presence of slurry, an inhibition in corrosion potential (-0.343 V) was found for Au electrode due to the presence of dissolved ions. This is probably due to the effect of oxide products that were formed and accumulated on the surface of gold electrode. At the end of the experiment, it was also observed that the surface of gold electrode was covered with surface products and that can be attributed to the potential shift in the less active region.

In the absence of slurry (35%), in the first 1 h, corrosion potential of RDE was heading with a 40 mV potential change to more active region (-0.436 to -0.475V) and the same trend was also observed in the last hour (between 23 and 24 h). It is worth noting that RDE was removed from the solution and was kept under nitrogen atmosphere for 22 h to prevent corrosion (from the end of 1 h till the beginning of 23 h) and almost the same corrosion potential was obtained. As it is seen, there is somewhat difference (~ 70 mV) in the dissolution potentials of Au and RDE electrodes, where gold is present in both cases. This difference could be arisen since the surfaces of Au and RDE electrodes were subjected to different exposure times and preparation procedure which is mentioned in Section 5.2.3. Additionally, this could also be attributed to the efficiency of the two different agitation methods, and as a result the difference in quantity and the quality of surface products. However, in the first hour in presence of slurry, corrosion potential has been shifted about 20 mV (from -0.27 to -0.29 V) and 145 mV shift in active region (from -0.27 to -0.415 V) was observed for the last hour. This finding suggested that RDE undergoes more active behaviour. This could be attributed to the increase in the dissolution of gold.

In the absence of slurry, platinum (Pt) electrode had 0.142 V corrosion potential after 24 h while RGO electrode had 0.180V. This 35 mV difference suggested that more active behaviour for Pt surface compared to RGO. This could be attributed to the value of oxide-reduction reactions of cyanides on the noble platinum surface. Platinum electrode has also demonstrated more active behaviour in the absence of slurry after 24 h having the corrosion potential of 0.142 V compared to 0.170 V (in the first hour). In the presence of slurry, Pt electrode had almost similar corrosion potentials in the first hour and in the last 1 h, about 0.167 V that is almost the same as the initially obtained potential in absence of slurry. That means the slurry has no significant influence on the platinum surface. This result suggests that platinum electrode can be suitably used as a counter electrode in gold and mineral disc polarization studies.

Electrochemical Noise Measurements (ENM) of Au and RGO Electrodes

The corrosion potential and current noise were recorded for roasted gold ore disc electrode (RGO) and pure gold disc electrode (Au) in 0.04M NaCN solution during free corrosion.

The anodic potential value of RGO constantly increased from 0.24 to 0.252 V while potential for Au showed a slight decrease and became stable at about -0.55 V. The current density variations in function of time showed a slight increasing trend from 4×10^{-5} to 4.5×10^{-5} mA/cm² for RGO that suggested an increase in the dissolution of different minerals from RGO. However, current density for gold electrode was found to show almost the same trend through the test-work.

One of the important statistical parameters of ENM analyses in the time domain is the noise resistance (R_n). The noise resistance is defined as the ratio of the standard deviation of the potential noise to that of the current noise that can be associated to the polarization resistance (R_p). The ratio $1/R_n$ (admittance) is referred to the corrosion rate. The EN data values of $1/R_n$ for each specimen were measured during immersion period of 16 h. The mean of measurements for two series of mineral disc electrode and gold electrode were demonstrated in [Fig. 5.2](#). ENM in-situ provides a general trend in corrosion rates of electrodes. In case of Au, it is subjected only to gold metal, whereas it is the dissolution behaviour of roasted gold ore for RGO electrode. However, the curve of RGO could be considered as the dissolution of gold, mainly. It is clearly seen that Au generally showed an increasing trend in the corrosion rate of gold until the end of test (24 h), while RGO showed a decreasing trend after initial 10 h. RGO and Au had the same corrosion rate of 1.29×10^{-2} (mho/cm²) at 8 h. Then, the corrosion rate of RGO was found to be flat till the end of the test. This decrease in corrosion rate of RGO by the time could be linked to the presence of detrimental minerals mainly to gold dissolution. At the end of the test, two electrodes had very close corrosion rates. For active and passive regions of the surface, electrochemical noise measurement (ENM), as a novel tool, could be suitably used for corrosion tests of gold since ENM in-situ provides potential and current noise that gives instantaneous corrosion rate ([Eden, 2011](#)). The main advantage of ENM is the in-situ measuring corrosion rate as function of time. On the other hand, using high agitation speeds in ENM could parasite the noise data and that may be considered as a negative point in application for gold leaching studies. It is also important to mention that although ENM technique was used for many different metals such as steel ([Klapper et al., 2013](#)), copper

(Safizadeh and Ghali, 2013), zinc (Zhang et al., 2005), aluminium (Curioni et al., 2013) etc., there is a paucity of in-situ ENM studies on gold leaching.

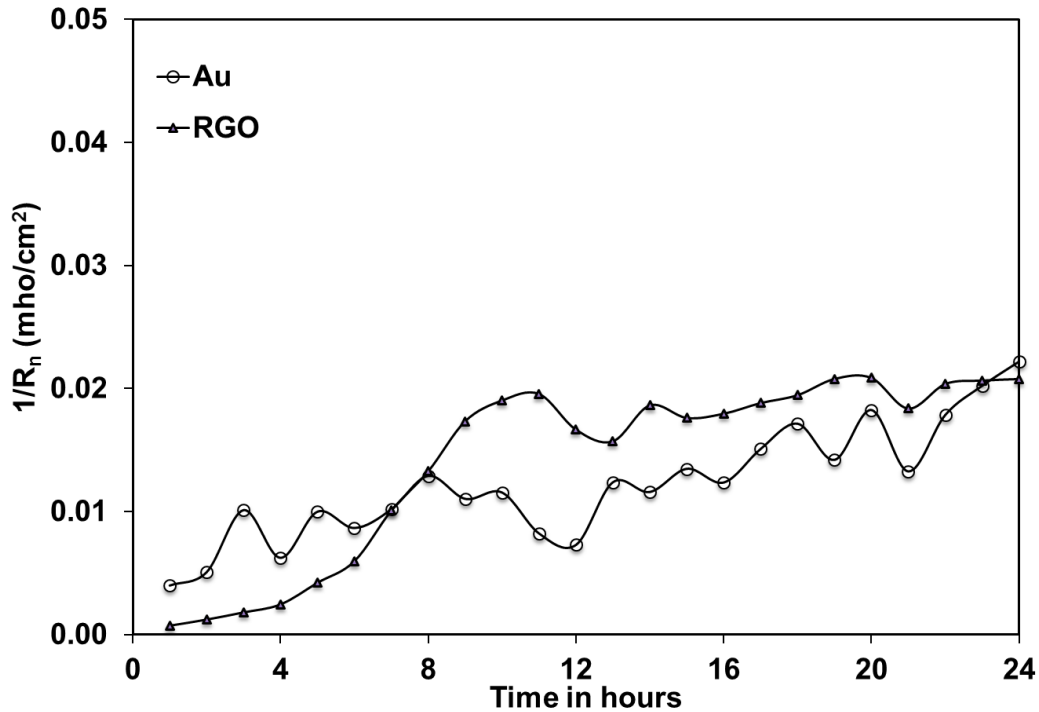


Fig. 5.2 Instantaneous measured corrosion rate ($1/R_n$) for roasted gold ore and pure gold electrodes immersed in NaCN (0.04 M) solution by ENM after potentiodynamic polarization followed by potentiostatic test (2h) in absence of agitation, pH 10.5, 25 °C.

Scanning Reference Electrode Technique Analysis of Au and RGO Electrodes

It has been claimed that each point on the mineral surface (*e.g.* gold) is considered as both an anodic site and a cathodic site and concluded that there is no separation of anodic and cathodic sites on a mineral's surface (Crundwell, 2013). This argument depends on the other closest constituents in an electrolyte. Habashi and Bas (2014) stated the existence of anodic and cathodic zones during the dissolution of minerals with certain experimental results.

The 3-D SRET images of potential differences measured over the surface of pure gold electrode (Au) and roasted gold ore disc electrode (RGO) as a function of immersion time

(1, 8 and 16 h) in 0.04 M NaCN solution are shown in Fig. 5.3. The active pits on the surface of each specimen can be observed. The potential differences were distributed into different zones corresponding to neutral, low and intense anodic and cathodic activities. The most anodic (most active) potential is the lowest point in the down cones and the most cathodic (less active) potential is the maximum point reached in the up cones. According to real time surface evolution of specimens, it is evident that the location of the pits at the surface changes with time. At the beginning of the test, the most active (anodic) potential of Au electrode was $\sim -87 \mu\text{V}$ with respect to saturated calomel electrode (SCE) (Fig. 5.3a) and it was decreased to $-20 \mu\text{V/SCE}$ (Fig. 5.3c) at the end of the experiment after 16 hours. It can be deduced that due to the decrease in most active potentials, less active (most cathodic) potentials on the surface of pure gold electrode were increased. This result suggests that the surface of the gold became passive by the time due to the formation of oxide and/or insoluble cyanide films (Kirk et al., 1978; Nicol, 1980). This was consistent with the potentiodynamic polarization results where pure gold showed a certain passive peak and the current density was sharply decreased to around zero. On the other hand, the most active (anodic) potential of RGO was around $-20 \mu\text{V}$ during 16h. Most cathodic potentials for RGO were found to be higher (Fig. 5.3d) if compared to active (anodic) potentials at the on-set of the test (after 1 hour) but cathodic potential values decreased by $15 \mu\text{V}$ (Fig. 5.3f) with increasing the immersion time (after 16 hours). By the time passed, most active (anodic) and most cathodic (cathodic) potentials of RGO electrode showed a similar trend (Fig. 5.3e and f).

The potential difference between the most active anode and the dominating reactions on cathodic sites has the same trend as the electromotive force (EMF) of the most active corrosion cell and the real EMF should be proportional to the potential difference measured in-situ. Then, “quasi electromotive force” (QEMF) could be used to express the potential difference between the more probable anodic or cathodic reactions based on thermodynamic values on electrode surfaces in cyanide medium. Thus, initiation and propagation of pitting corrosion for the tested specimens can be then identified (Zhang et al., 2006). The QEMF of corrosion cell as a function of immersion time for each specimen in 0.04M NaCN solution at pH 10.5 and 23°C was demonstrated in Fig. 5.4. The QEMF of

Au suddenly decreased $\sim 100 \mu\text{V}$ (from 150 to $45 \mu\text{V}$) in the corrosion cell at the beginning of the immersion time and then became stable $\sim 43 \mu\text{V}$ until the end of the test.

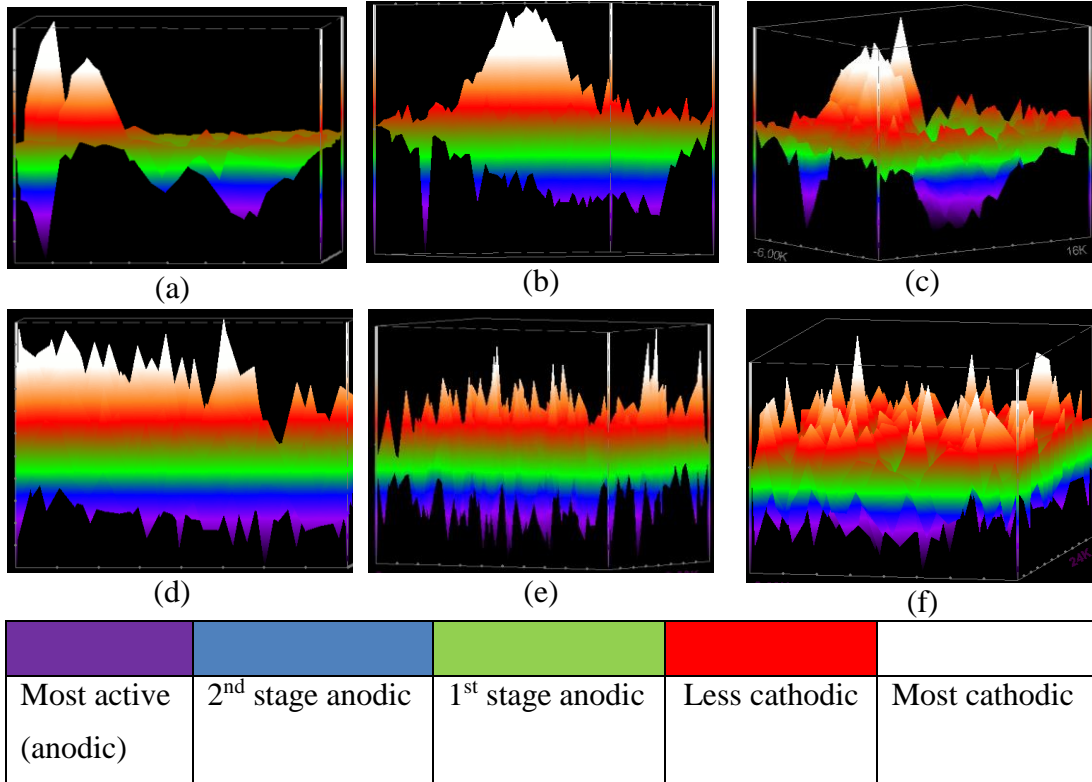


Fig. 5.3 3-D SRET potential images at different immersion times in 0.04M NaCN solution at pH 10.5 and 25°C for (a) Au at 1h, (b) Au at 8 h, (c) Au at 16 h; (d) RGO at 1h, (e) RGO at 8 h and (f) RGO at 16 h.

On the other hand, QEMF of RGO initially decreased by $17 \mu\text{V}$ and then was kept at $38 \mu\text{V}$. Average QEMF values of Au and RGO were found to be 48.4 and $38 \mu\text{V}$, respectively. It is seen that RGO had lower QEMF if compared to Au, suggesting that RGO showed higher corrosion resistance whereas Au specimen was quickly attacked. Considering the QEMF of the different samples (Fig. 5.4) and measuring the depth of the pits of the two specimens, it can be deduced that the Au specimen had the deepest pits. It can be observed that after 8h up to 16h, similar trend in QEMF was observed for both electrodes (Au and RGO). Since the presence of one phase in Au electrode, it gives rise to anodic and cathodic sites. RGO has many phases that could give rise to different

electrochemical cell sites and even passive regions. However, almost same QEMF was obtained for both electrodes at the end of the test. After a 16 hours of exposure time, almost the same QEMF was observed for both of electrodes. SRET results showed that the QEMF is almost the same for anodic and cathodic reactions of pure gold and that of RGO. The cathodic and anodic reactions on gold are the dominating ones than that of silver due to its higher affinity and concentration in roasted gold ore. This result also confirms that the corrosion rate for RGO electrode (in Fig. 5.2) corresponds mainly to the dissolution behaviour of gold. The reproducibility of the QEMF values for Au and RGO electrodes were found to be $\pm 10\%$ and 12% , respectively. These results have indicated that SRET in-situ corrosion measurements without any imposed potential, which is very close to practice, provide significant information on the corrosion behaviour of gold and show the existence and polarisation of anodic and cathodic sites during the leaching of gold.

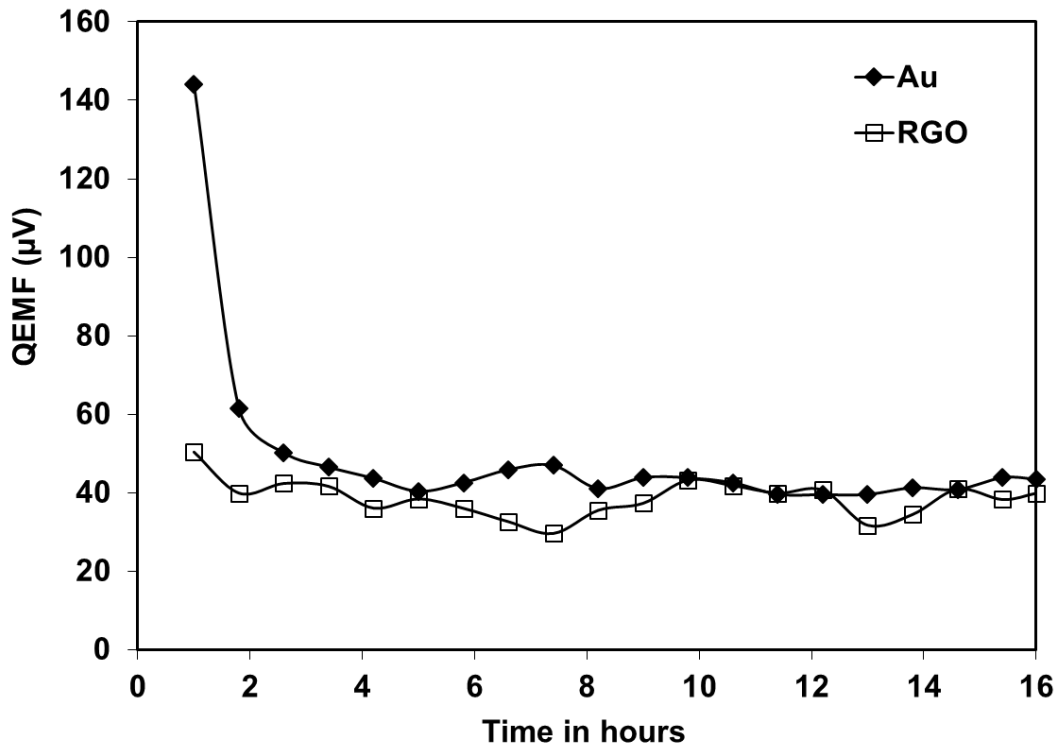


Fig. 5.4 QEMF corrosion cell vs. immersion time in 0.04M NaCN solution at pH 10.5 and 25°C for pure gold (Au) and roasted gold ore (RGO) disc electrodes.

5.3.2 Potentiodynamic Polarization of Au, RGO, and Oxide Mineral Electrodes

Cathodic Polarization

Fig. 5.5 shows the cathodic polarization profiles of electrodes by scanning from E_{corr} to -300 mV at pH 10.5 at 100 rpm agitation in 0.04 M NaCN electrolyte. In addition, cathodic polarization of pure gold was performed by scanning using the reverse direction (from -300 mV to E_{corr} , which was shown as Au* in Fig. 5.5) for comparison. As it is seen, there is an obvious difference in pure gold cathodic polarization curves. Oxygen reduction takes place in cathodic area (Eq. 5.1) with a 605 mV standard potential at pH 10.5. The standard potential of other possible reactions in cathodic section are given vs. standard hydrogen electrode in Eqs. 5.2 and 3 (Aghamirian and Yen, 2005; Ahmed, 1978).

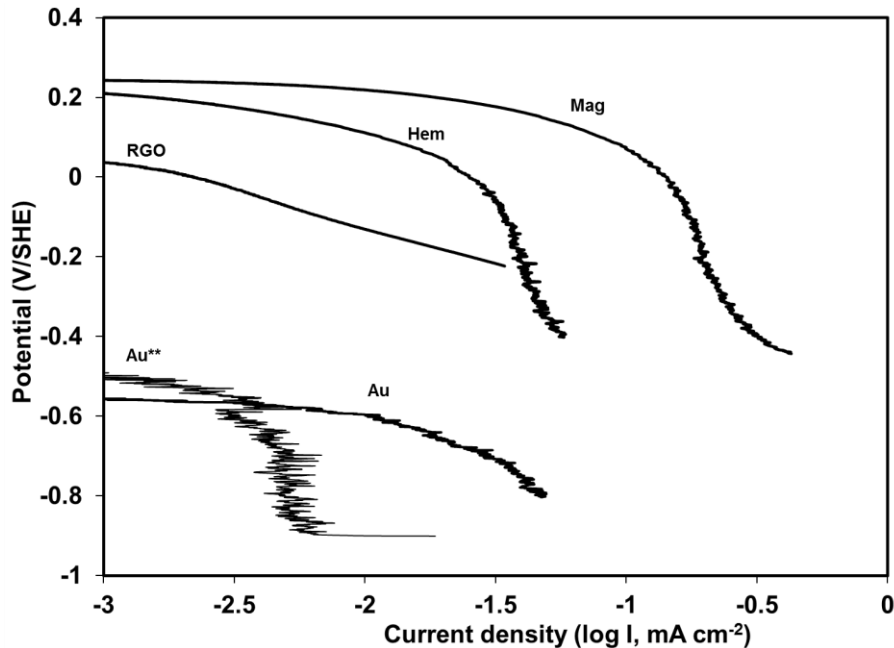
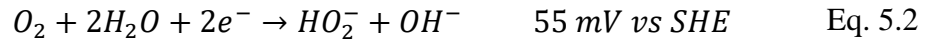
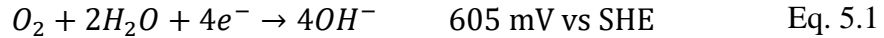


Fig. 5.5 Potentiodynamic cathodic polarization of different electrodes with scan rate of 0.166 mV/s in 0.04M NaCN electrolyte at 100 rpm agitation at atmospheric oxygen, pH 10.5, 25 °C (Au** indicates the cathodic polarization by scanning from -300 mV to E_{corr}).

The difference in conductivity and relative quantities of magnetite and hematite could explain the behaviour of RGO. Also, the presence of soluble and/or insoluble ions, and as a result different behaviours of these ions in the solution could influence the position of RGO electrode. Magnetite, hematite and gold ore at high over-potentials are less active than gold. At low over-potentials, hematite was more active than magnetite. This can suggest that magnetite and hematite are good electrocatalysts for oxygen reduction.

Anodic Polarization

It is seen that gold oxidation starts ~ -0.4 V/SHE (Fig. 5.6). Gold showed three passive peaks at around -0.1 , 0.4 , and 0.7 V with current densities of 0.2 , 2.3 , and 1.8 mA/cm², respectively. AuOH_{ads}, AuCN_{ads}, [Au(III)OH(CN₃)⁻]_{ads}, and Au(OH)₃ products are believed to be responsible for the formation of these passive peaks (Kirk et al., 1978). Furthermore, Bas et al. (2015) characterized gold surface by XPS after polarization tests and found Au¹⁺ and Au³⁺ corrosion products as responsible for the passivation of gold surface.

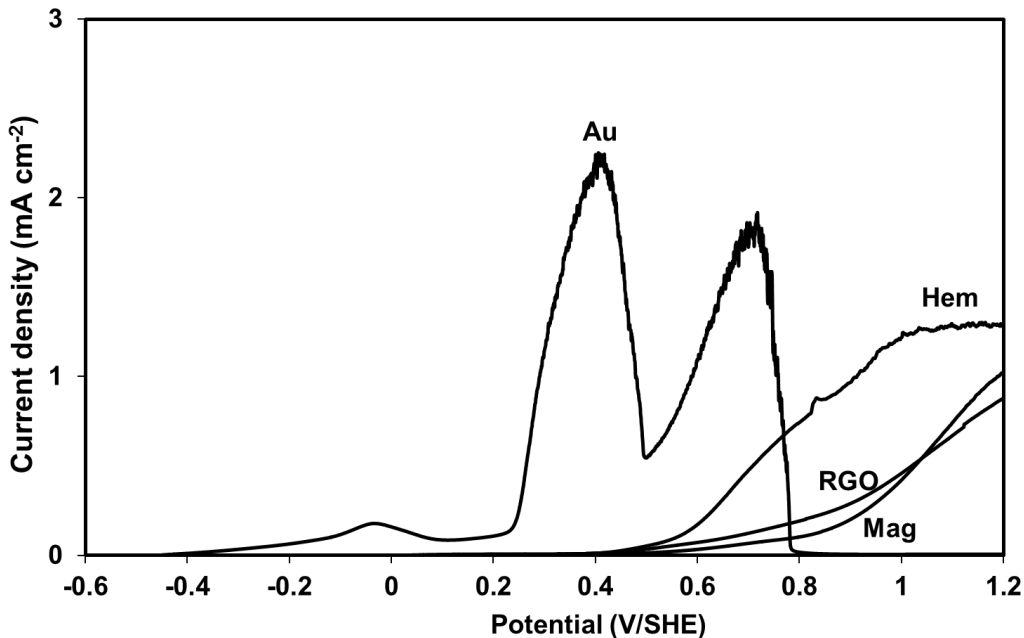
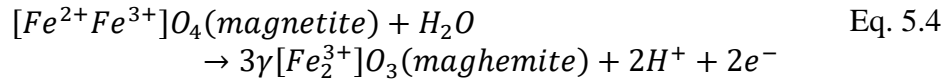


Fig. 5.6 Potentiodynamic anodic polarization of different electrodes with scan rate of 0.166 mV/s in 0.04 M NaCN electrolyte at 100 rpm agitation, pH 10.5 , 25 °C (Au: 1 cm²; other electrodes 4.9 cm²).

In case of RGO electrode, which was prepared using roasted gold ore sample, its current density increased slightly up to 0.75 mA/cm² till the end of the test. The different anodic behaviours of gold and roasted gold ore electrodes could be attributed to the mineralogical composition of gold ore. Potentiodynamic polarization studies in presence of strong agitation gives less information on peak identifications especially for non-pure metal systems. Detection of intermediate species in the double layer needs the presence of a certain quantity of the transient in close contact with the surface. Then, the presence of different soluble and/or insoluble species at the interface has certain influence on detection of different peaks and possess either positive or negative effect on the dissolution behaviour of gold. Dissolution of magnetite, which is a known iron oxide phase, started at more positive potentials if compared to gold. Magnetite (Fe₃O₄) is one of the most common Fe³⁺-containing oxide minerals. Magnetite oxidation (Eq. 5.4) results in the generation of maghemite (γ-Fe₂O₃), metastable spinel polymorph of hematite (White et al., 1994). Hematite (Fe₂O₃), other most found iron oxide mineral, dissolution started earlier and it had higher current density if compared to magnetite. Conductivity of magnetite (Fe₃O₄) is ~ 10⁶ times higher than that of hematite (Fe₂O₃), due to electron exchange between the Fe²⁺ and Fe³⁺ (Greenwood and Earnshaw, 1997).



5.3.3 Effect of Leaching Parameters on Anodic Polarization of RGO Electrode

Influence of NaCN Concentration (0.01-0.04-0.1 M)

Various cyanide concentrations for a maximum gold leaching rate in practice have been reported by many research groups and the range of 0.004-0.05 M NaCN was generally accepted depending on the mineralogy, type of gold ore, and experimental conditions (Fleming, 1999). The influence of NaCN concentration on the polarization of RGO disc electrode at pH 10.5 at 100 rpm agitation is demonstrated in Fig. 5.7. It is seen that current density resulted in an increasing trend with increasing cyanide concentration. Oxidation started earlier at 0.04 M NaCN if compared to other ones. Polarization curves of 0.04 and 0.1 M intersected at 0.9 V having the same current density of 0.35mA/cm², then, higher

current density was obtained at 0.1 M at the end of polarization test. Generally, it can be deduced that 0.04 M NaCN gave higher current density in the potential range of gold dissolution (lower than 0.9 V/SHE). This behaviour in 0.04 and 0.1 M NaCN concentrations could be linked to the presence of soluble species as function of time in the solution. The lower current density obtained at lower cyanide concentration could be linked to the insufficiency of cyanide ions that would react with gold to dissolve. Current density of RGO was increased ~ 4 times with increasing NaCN concentration from 0.01 M to 0.1 M. These findings have revealed that oxidation of RGO commences earlier at higher cyanide concentration and 0.04 M seems to be more significant on dissolution process. On the other hand, it is generally believed that pure gold gives three peaks in cyanide solutions suggesting the passivation of gold surface (Kirk et al., 1980). However, Bas et al. (2015) has found that gold surface becomes relatively more passive and shows less than three passive peaks for lower cyanide concentration (<0.04 M) in tested values. Bas et al. (2015) has reported when gold is under passive conditions, increasing cyanide concentration, increasing pH, and potential have led to more passive behaviour, by using potentiostatic polarization.

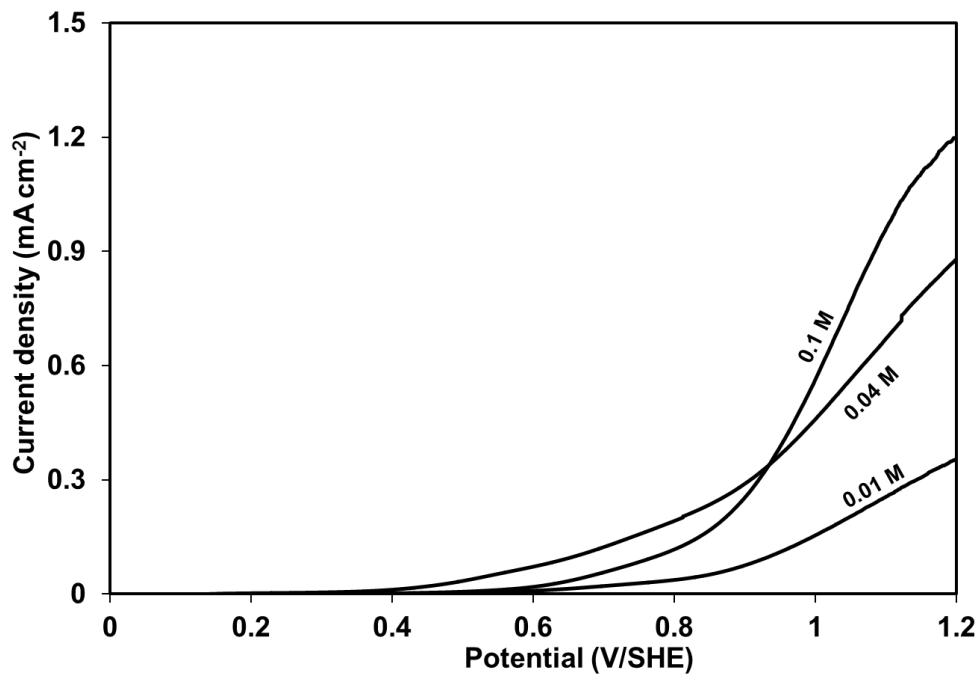


Fig. 5.7 Effect of NaCN concentration on the polarization of RGO with scan rate of 0.166 mV/s at pH 10.5 at 100 rpm agitation, 25 °C.

Influence of pH (10-10.5-11.5)

Hedley and Tabachnik (1968) pointed out the aim of adjusting/monitoring pH in cyanidation is to prevent the loss of cyanide by hydrolysis and by action of carbon dioxide in the air, to neutralize acidic compounds such as ferrous, ferric salts and to improve gold extraction when treating the ores containing tellurides (AuTe_2) which decompose more readily at higher alkalinities. Fig. 5.8 demonstrates the effect of pH on the polarization of RGO electrode in 0.04 M NaCN electrolyte at 100 rpm agitation. Anodic polarization profile was divided into two regions as A (till the potential of 0.9 V) and B (from the potential of 0.9 V to 1.2 V/SHE), since different trends have been observed. In region A, oxidation of roasted gold ore electrode started earlier at lower pH values (10-10.5) if compared to higher pH value of 11.5. Current density increased faster at lower pH values. The slow increasing rate of current density at high pH values (11.5) could be due to the presence of more hydroxides that promote the formation of passivating surface products (Habashi, 2009). However, in region B, a reverse trend was observed if compared to region A. Passing the potential of 0.9 V, current density reached to higher value at pH 11.5 than that of pH 10 and 10.5. This reverse trend in regions of A and B could be linked to the presence of many different mineral phases in roasted gold ore and also difference in quantity of oxygen and free cyanide in the solution. Since gold leaching takes place in the region A (lower potential than 0.9 V), pH 10.5 seems to be more essential and effective value for the leaching of gold from RGO electrode. Furthermore, corrosion rate at pH 10.5 was found to give ~ 1.7 times higher than that of pH 11.5. Mahmoodi et al. (2010) reported that gold extraction was increased by ~ 2% with increasing pH from 9.5 to 10, and became stable in the range of pH 10-11 and finally decreased by increasing the pH from 11 to 12. Barsky et al. (1934) reported the decrease in gold dissolution above pH 11. Then, in this current study, pH 10.5 was selected as the optimum value. However, the optimum pH value for leaching should be selected depending on the type of gold ore, mineralogy and leaching system (Marsden and House, 2006). These obtained results in this tested conditions suggested that the range of pH 10-10.5 was found to be more preferable for gold leaching processes. Similarly, in recent gold galvanic studies depending on the type of gold ore and minerals, pH was maintained at 10.5 and 11 by Aghamirian and Yen (2005) and Azizi et al. (2010), respectively.

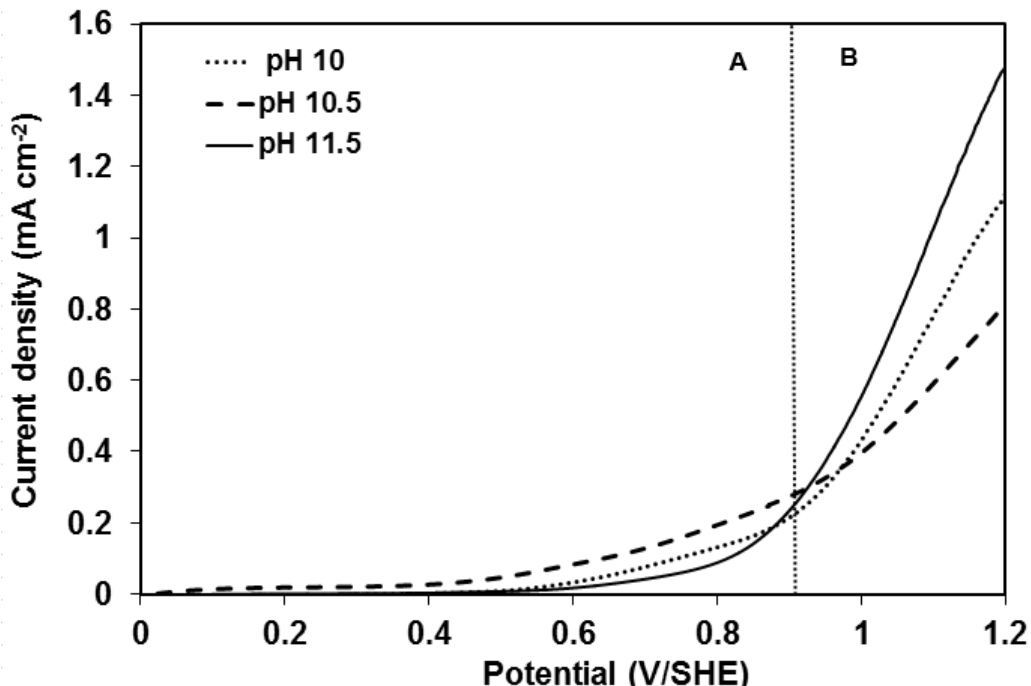


Fig. 5.8 Effect of pH on the anodic polarization of RGO electrode at 0.166 mV/s scan rate in 0.04 M NaCN electrolyte at the agitation of 100 rpm, 25 °C.

In previous study (Bas et al., 2015), authors have found peak current densities of pure gold decreased with increasing pH values (10 to 12) at 100 rpm agitation in 0.04 M NaCN solution. The second peak current density was greatly increased (~ 40 times) at pH 10 if compared to other two pH values. At higher pH values (> 10), first peak current density was found to be very small (~ 0.05 mA/cm²). Additionally, low level of agitation (60 rpm) was tested at pH 11, since agitation is a significant parameter for the electrochemical dissolution of gold. It was found that decreasing agitation from 100 to 60 rpm has resulted in a great increase in the second peak current density which was very close for that of pH 10. The third peak at 60 rpm agitation gave almost the same current density if compared to the 100 rpm agitation.

Influence of Agitation (100-250-400 rpm) on Au and RGO Electrodes

Three passive peaks at -0.1, 0.3, and 0.7 V/SHE were observed as responsible for the passivation of pure gold surface (Fig. 5.9). Current density of second peak was found to be

higher (~5 times) than that of the two other peaks. It was found that current density decreased by increasing agitation from 100 rpm to 400 rpm. In the case of pure gold and clean cyanide solution systems, effect of agitation on the anodic behaviour of gold was examined by some research groups (Kirk and Foulkes, 1980). Principally agitation does not promote the peak formation since the presence of intermediates at the interface becomes more limited. Second peak, known as a less anodic gold dissolution peak, could be passivated due to the oxygen adsorption (Dorin and Woods, 1991), gold oxide formation (Guan and Han, 1994), and by the formation of gold (I) hydroxide according to $\text{Au} + \text{OH}^- \rightarrow \text{AuOH}_{\text{ads}} + \text{e}^-$ (Kirk et al. 1978), or by the conversion of Au(I) to Au (III) was $2\text{CN}^- + [\text{Au(I)OH(CN)}]_{\text{ads}} \rightarrow [\text{Au(III)OH(CN}_3)]_{\text{ads}} + 2\text{e}^-$ (Cathro and Koch, 1964). Moreover, the adsorption of cyanide ions was found to initiate the passivation of second peak (Poskus and Agafonovas, 1995).

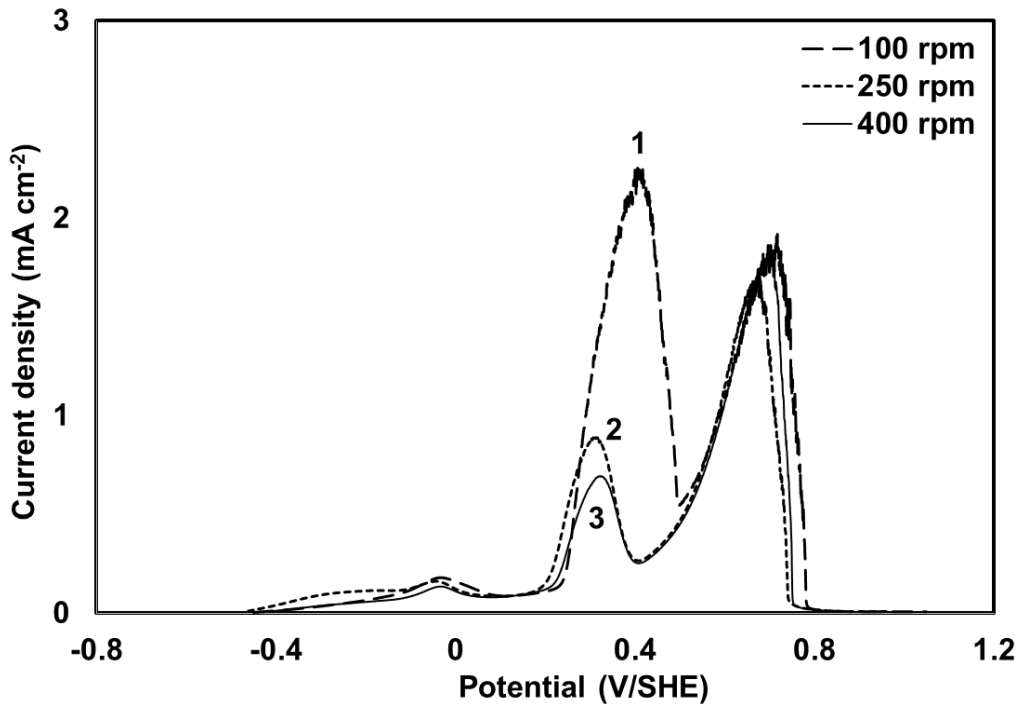


Fig. 5.9 Effect of agitation (1: 100 rpm; 2: 250 rpm; and 3: 400 rpm) on the anodic polarization curve of pure gold (Au) electrode with scan rate of 0.166 mV/s in 0.04 M NaCN solution, pH 10.5, 25 °C.

On the other hand, till now, examining the influence of agitation for electrochemical studies of gold ore systems (i.e. roasted gold ore) in cyanide solution was not much considered. [Fig. 5.10](#) demonstrates the effect of magnetic agitation on the polarization of RGO in 0.04 M NaCN electrolyte at pH 10.5. It is seen that increasing agitation from 100 to 250 rpm, resulted in ~ 3 times (from 0.4 to 1.2 mA/cm²) higher current density at the end of polarization. However, increasing of agitation from 250 to 400 rpm showed around 15% lower current density. The decrease in current density above 250 rpm agitation speed could be explained by the increase in the mineral leaching from roasted gold ore electrode. As a result, higher agitation speeds could favour the release of more soluble and/or insoluble corrosion products that retards the further anodic behaviour of RGO. Also, it could lead to less time for the presence of certain reaction intermediates at the interface. [Azizi et al. \(2010\)](#) examined the influence of rotation speed for a gold and sulphide mineral electrode galvanic corrosion and found that the leaching was progressively decreased at rotation speeds above 400 rpm. It is also important to note that till now, the influence of agitation/rotation speed on mineral electrode leaching has received less attention and needs further detail examinations.

[Kakovskii and Kholmanskikh \(1960\)](#) found that dissolution of gold increases up to a certain agitation speed (150 rpm) then decreases or becomes flat. [Cathro and Walkley \(1961\)](#) examined the effect of agitation on the corrosion rate of gold electrode and reported that increasing agitation has led to the decreasing gold corrosion rate. Similarly, [Aghamirian and Yen \(2005\)](#) reported that high electrode rotation speed reduced the maximum current density as a result of loss of hydrogen peroxide ions. These findings in these tested conditions have revealed that ~ 250 rpm agitation seems to be more effective for mineral electrode dissolution. Duplicate results are reproducible with a 6 % shift at different agitation levels on the anodic polarization of RGO. Then, it is important to underline that agitation provides important information about diffusion, mechanism and the rate of reaction.

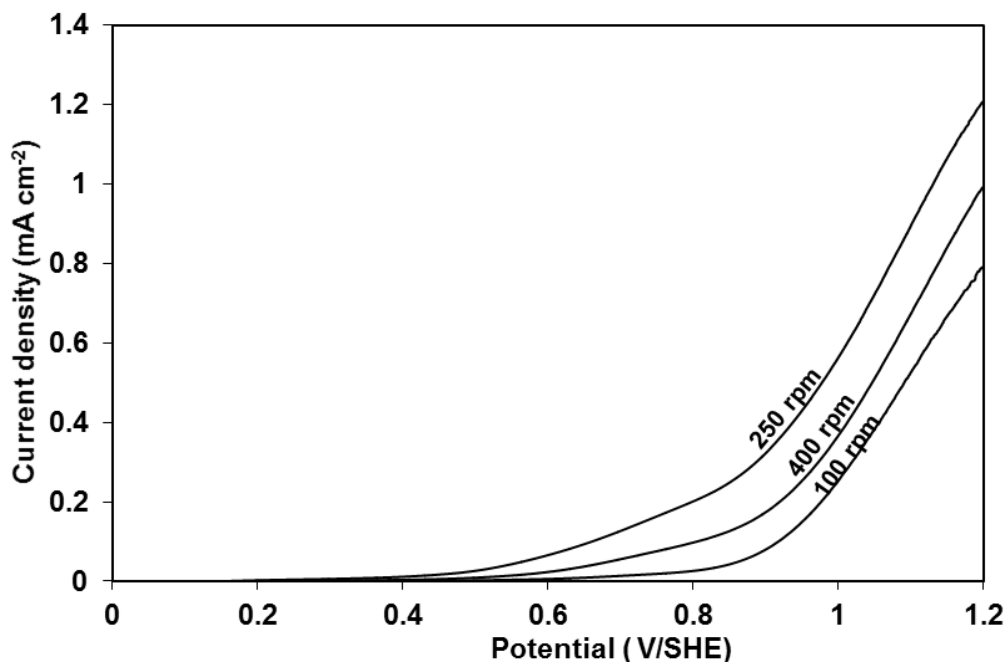


Fig. 5.10 Effect of agitation (100, 250 and 400 rpm) on the anodic polarization curve of RGO with scan rate of 0.166 mV/s in 0.04 M NaCN solution, pH 10.5, 25 °C.

5.3.4 Corrosion Rate of Au, RGO, and Combined Disc Electrodes

In linear polarization tests, potential and current values are plotted and the slope of this curve, denoted as the polarization resistance, R_p , and this value is used to calculate the corrosion current (i_{corr}) utilising the well-known Stern-Geary equation (ASTM G102-89, 2006). Similarly, cathodic Tafel polarization can also be used to calculate corrosion current since anodic Tafel is not suitable due to the presence of passive behaviour in anodic polarization.

In this study, the effect of agitation speed (100, 250, 400 rpm) on the dissolution current (referring to dissolution rate) of pure gold (Au, 1cm²) and roasted gold ore (RGO, 4.9 cm²) electrodes alone and also combined together was examined by only cathodic Tafel polarization and the data obtained was presented in Table 5.2. It is seen that the dissolution current of Au electrode increased by ~ 2 times with increasing agitation speed from 100 to 250 rpm (7.69 to 14.28 μ A). Then, it was decreased by 1.9 times to 7.21 μ A at 400 rpm. On the other hand, the dissolution current of roasted gold ore (RGO) increased by 2.6 times (from 1.19 to 3.13 μ A) with an increase in agitation speed from 100 to 250 rpm, and then

showed a slight increase having of 3.69 μA at 400 rpm agitation (Fig. 5.11). In addition, corrosion current of electrodes was calculated manually and very close values were obtained to that calculated by using EC-Lab software. It can be deduced that increasing agitation speed gave an increase in the rate of dissolution for diffusion controlled systems till a maximum level where the rate remains constant. At this level, the contribution of diffusion is minimized and the rate of dissolution was controlled by chemical reactions in bulk phase or at interface. Furthermore, ~ 4 times lower corrosion current (for different metals) was observed for RGO electrode after 2 and/or 3 times using polishing, if compared to fresh RGO one (not shown). Due to the presence of many different mineral phases in RGO electrode, it has high sensitivity to dissolution. This result suggests the importance of polishing/preparation procedure and recommends also the use of new electrodes (fresh exposed surfaces) and that could be suggested in practice. It is important to note that results were reproducible.

On the other hand, corrosion currents of electrodes were calculated from linear polarization by utilising the Stern-Geary method. Corrosion current of pure gold electrode was found to give close values by Stern-Geary method ($6 \pm 4.13\%$, $14 \pm 3.64\%$, and $7.3 \pm 0.6\%$, at 100, 250 and 400 rpm, respectively). However, certain difference was observed for roasted gold ore (RGO) electrode ($4.9 \pm 4.88\%$, $6.1 \pm 3.08\%$, and $4.7 \pm 4.14\%$ at 100, 250 and 400 rpm, respectively). Since the results obtained in the range of 100-400 rpm agitation speed is significant, then the wide range of agitation speed (0, 50, 600 rpm) was considered for RGO electrode by utilizing both methods. Corrosion currents of 0.162, 0.196, 0.045 μA by Stern-Geary and 0.077, 0.154, 0.071 μA by cathodic Tafel polarization were calculated at 0, 50, 600 rpm, respectively. It can be deduced that when the specimen is not pure, i.e. complex systems, a certain difference is appeared between Stern-Geary and cathodic Tafel slope methods when compared. Furthermore, to test the reproducibility and reliability of cathodic polarization, manual calculation of cathodic Tafel constant (β_c) was used in the calculation of corrosion current by Stern-Geary method and very close values were obtained for pure gold electrode (7.69, 8.1 μA) and roasted gold ore electrode (1.19, 1.52 μA).

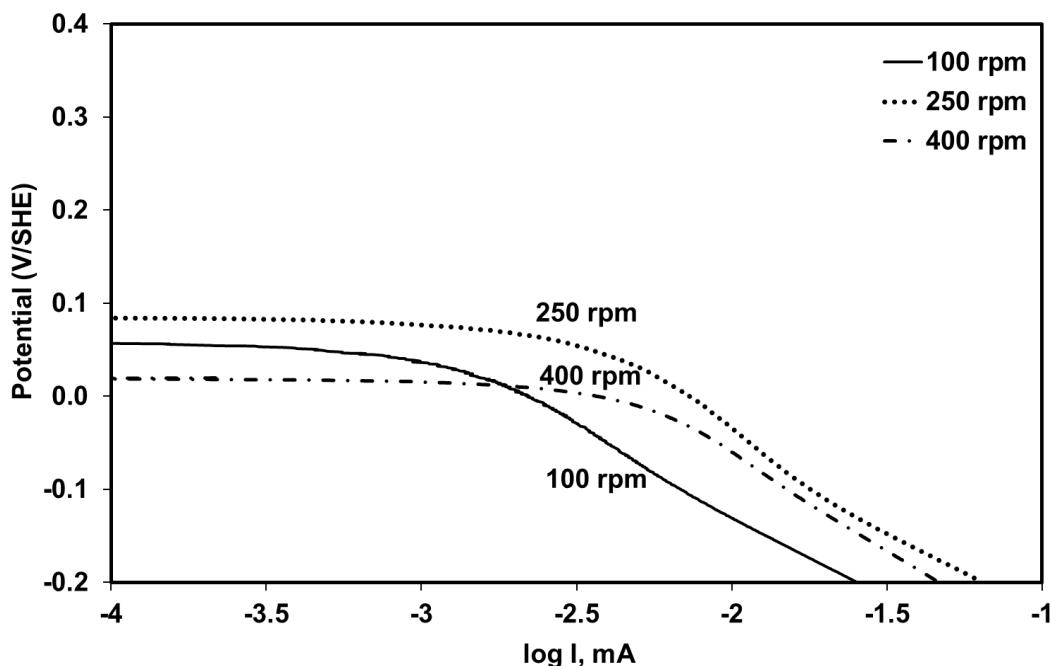


Fig. 5.11 Effect of agitation (100, 250 and 400 rpm) on the cathodic polarization curve of RGO with scan rate of 0.166 mV/s in 0.04 M NaCN solution, pH 10.5, 25 °C.

Table 5.2 Dissolution rate (calculated from cathodic Tafel polarization slope) of electrodes (pure gold (Au) electrode with a surface of 1 cm², roasted gold ore (RGO) electrode with a surface area of 4.9 cm²) (*¹ is calculated by extrapolating Tafel slope to OCP for comparison).

Electrode configuration	Dissolution current (μA)		
	100 rpm	250 rpm	400 rpm
Au (1 cm ²)	7.69 ±1.64% 8.1 ±4.9%* ¹	14.28 ±4.56% 14.48±3.7%* ¹	7.21 ±3.52% 8.73±4.16%* ¹
RGO (4.9 cm ²)	1.19 ±2.63% 1.52±3.30%* ¹	3.13 ±3.27% 3.42±4.88%* ¹	3.69 ±3.94% 3.89±5.10%* ¹
Au connected to RGO	15.42 ±3.84%	18.61 ±3.68%	15.2 ±4.6%

Since cathodic Tafel and Stern-Geary methods gave different results, then it should be questioned which method is more suitable and reliable for the calculation of dissolution rate of gold from RGO. Since cathodic Tafel slope had a good region and provided reproducible results, then it could be proposed that this curve could correspond to gold

mainly. Therefore, to support this idea, the corrosion rate of gold by cyanide leaching at 250 rpm agitation speed was compared to that obtained by cathodic Tafel slope. However, gold content from RGO in the solution in the absence of gold ore slurry after polarization was analysed and found to be lower than the detection limit. Therefore, conventional cyanidation tests of slurry in the absence and in the presence of RGO disc electrode were performed, and the difference in the measured values by AAS was considered as the leaching rate of Au from RGO disc electrode. It is important to note that gold had very close corrosion rates of $3.30 \times 10^{-8} \pm 3.27\%$ mol m⁻² s⁻¹ and $3.07 \times 10^{-8} \pm 7.03\%$ mol m⁻² s⁻¹ obtained by cathodic Tafel slope and that obtained in conventional cyanidation, respectively. It can be noticed that corrosion current of Au (14.28 μA/cm²) and RGO (0.64 μA/cm²) (Table 5.2) shows ~ 30 times only in spite of the higher difference in gold content of the two specimens. This could be potentially linked to the electrolyte composition at the interface, passivation phenomena and electrochemical interactions.

Additionally, the intersection of cathodic and anodic curves was also considered for comparison, and the results were found to be deceptive and incomparable. These findings have confirmed that considering only cathodic Tafel slope scanning from E_{corr} to more cathodic potentials in presence of cyanide ions and atmospheric oxygen provides representative results as in practical cyanidation, especially in presence of a good cathodic Tafel slope.

[Kudryk and Kellogg \(1954\)](#), one of the pioneer works in gold electrochemistry, have reported that the actual leaching rate (current) and potential of gold should correspond closely to the intersection point of the anodic (in absence of oxygen) and cathodic (in absence of cyanide) potential curves, separately. In this regard, [Cerovic et al. \(2005\)](#) considered the dissolution rate of gold from the intersection of cathodic and anodic curves. However, [Dai and Breuer \(2013\)](#) stated that considering only Evans' diagrams did not reflect the leaching rate of gold since the mentioned conception of the electrolyte did not represent the practical conditions. These results and the findings in this work have created a new question to be examined why considering both (anodic and cathodic) Tafel curves, and Stern-Geary method did not give reliable results and not suitable for the estimation of

dissolution rate of gold. The first reason could be linked to the presence of passive behaviour in anodic Tafel slope. Similarly, Stern-Geary method also considers both anodic and cathodic curves. Also, it can be speculated that soluble species (i.e silver, iron) could be dominating in the construction of linear polarization curves of Stern-Geary method. These findings have revealed that considering Tafel slopes and Evans diagrams for both (anodic and cathodic) curves for dissolution rate of gold or roasted gold ore electrodes are misleading and not comparable to that in practical cyanidation results. This conclusion is consistent with the recent findings of [Dai and Breuer \(2013\)](#) which says that leaching of gold starts earlier than the predicted one by Evans' diagrams. It can be deduced that the consideration of the cathodic Tafel slope only is recommended since the corrosion rate especially in roasted gold ore is potentially controlled by the available active surface sites of gold. Then, extrapolation of the cathodic Tafel slope to OCP is the recommended technique.

It is believed that gold dissolution may be affected either in a positive or negative way when it is connected/associated with other minerals/metals ([van Deventer and Lorenzen, 1987](#)). When RGO (4.9 cm² surface area) was electrically connected to Au (1 cm² surface area), corrosion current of metals was increased by 15% (from 13.91 to 16.081 μ A) at 250 rpm agitation if compared to 100 rpm and decreased by 22% to 13.10 at 400 rpm. This result is consistent with the findings for RGO electrode alone. This suggests that gold electrode promoted the gold dissolution possibly from both when electrically connected to mineral disc electrode due to the galvanic interaction. In general, two electrically connected electrodes indicated higher corrosion current due to the increase in surface area and electrochemical interactions. Additionally, in these tests, the effect of slurry on electrically connected electrodes was also tested. Although corrosion currents of gold and other metals were increased ~ 3 times when RGO was connected to Au, ~30% decrease in corrosion current (10.3 μ A) was obtained when they were connected in presence of slurry. Then, it would be critical to use the leaching residue as a new feed material on the dissolution of Au electrically connected to RGO. After the polarization test, solid/liquid separation was done and the residue as solid was collected on the filter paper and then was put into the oven at least 6 h at 105°C. After drying process in oven, it was prepared to use as a new

feed sample, slurry. This finding can be linked to the removal of soluble detrimental ions (e.g. iron species) in the first stage. However, if the tailings of the first slurry was used again as a new feed sample, corrosion current of RGO connected to Au electrode was increased by 1.6 times (16.2 μA). This increase could be explained by the removal of detrimental ions in the first stage and carrying the tailings to the subsequent cyanide leaching and dissolved ions have significant effect on the leaching kinetics.

A brownish-red colour (Fig. 5.12a) was observed on the surface of Au electrode after the test. This was analysed by scanning electron microscopy (SEM) indicating the presence of iron-oxide species (Fig. 5.12b) released from RGO electrode that passivates Au surface. These findings have revealed that released species from mineral electrodes are responsible for the passivation of gold as a retarding effect on gold leaching.

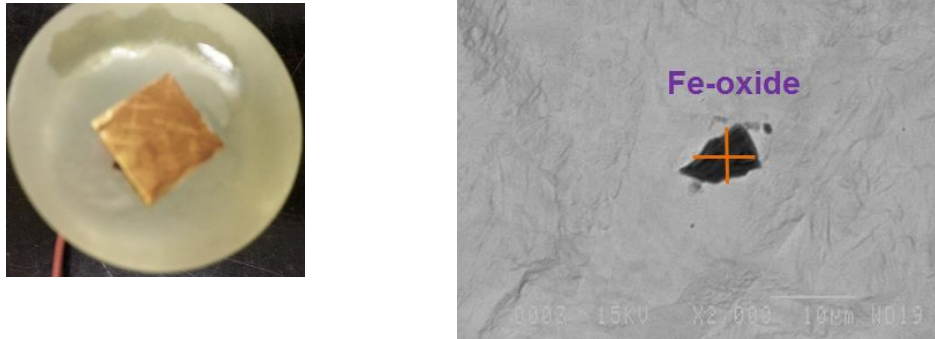


Fig. 5.12 (a) Surface image of Au electrode after combined with RGO electrode test showing the brownish-red colour; (b) SEM image of Au electrode surface.

5.4 Conclusions

The conclusions of this study are summarized as below:

1. In open circuit potential (OCP) tests, the roasted gold ore (RGO) electrode showed a less active behaviour than the gold (Au) electrode. In electrochemical noise measurement (ENM) tests, the corrosion rate of RGO electrode was found to show a plateau after initial 10 h till the end of the test (24 h) while Au electrode showed an increasing trend of corrosion rate. The difference in corrosion potentials of Au and RGO electrodes in OCP

and ENM studies is highly dependent on agitation, oxygen, and different experimental conditions.

2. Employing SRET in-situ results at open circuit potential, as close to practice, Au electrode showed higher quasi electromotive force (QEMF) (150 vs. 50 μ V/SCE) than that of roasted gold ore (RGO) electrode.

3. Potentiodynamic polarization tests showed that:

3.1. Optimum conditions for the leaching of RGO electrode were found to be 0.04 M NaCN concentration, pH 10-10.5, and 250 rpm agitation. The dissolution rate of RGO electrode, pure gold, and also electrically connected electrodes increased up to maximum at 250 rpm then showed a certain decrease. It can be deduced that dissolved ions should have a significant and different synergetic effects on gold leaching that could impact on conductivity, and cyanide concentration of the solution.

3.2. In the presence of slurry, a lower corrosion rate (current density) was obtained for the electrically connected electrodes very possibly due to the presence of surface products that was observed by SEM analysis, leading to the passivation of gold surface. However, a 3 times higher corrosion rate was obtained when the polarization was repeated on the same electrode. The corrosion current of different metals for RGO and Au combination was increased by \sim 2 times, while it was decreased by \sim 30% in the presence of slurry. However, it was increased 1.6-fold if the tailing was used again as a new feed.

3.3. Cathodic (Tafel slope) potentiodynamic polarization curve of gold and roasted gold ore electrodes in presence of atmospheric oxygen and cyanide ions represents the practical leaching kinetics. The reliability of this approach was confirmed by the results obtained via conventional cyanidation.

3.4. Anodic and cathodic Tafel slopes (considering intersection point) and Stern-Geary methods in presence of cyanide and atmospheric oxygen could be misleading to estimate the leaching rate of gold and roasted gold ore potentially due to the passive behaviour in anodic curve.

3.5. Cathodic polarization scanning from E_{corr} to more cathodic potentials provides more representative Tafel slopes and accurate results whilst scanning in the reverse direction is not suitable for gold leaching estimation.

5.5 Acknowledgements

The authors would like to express their sincere thanks and appreciation to Natural Sciences and Engineering Research Council of Canada (NSERC), Barrick Gold Corporation, Hydro-Quebec, for their financial support and participation through R&D NSERC Program. Laval University personnel Mrs. V. Dodier for AAS analysis, Mr. A. Ferland for SEM analysis, and Mr. F. K. Kadiavi are gratefully acknowledged for their help.

Chapter 6

Electrochemical Interactions Between Gold and Iron Oxide Minerals

A Study of the Electrochemical Dissolution and Passivation Phenomenon of Roasted Gold Ore in Cyanide Solutions

Ahmet Deniz Bas^a, Wei Zhang^a, Edward Ghali^a, Yeonuk Choi^b

^aDepartment of Mining, Metallurgical and Materials Engineering, Laval University, Quebec, Canada, G1V 0A6

^bBarrick Gold Corporation, Suite 3700, 161 Bay Street, P.O. Box 212, Toronto, Ontario, Canada, M5J 2S1

*Corresponding author: 4186568657, Fax: 4186565343; (ahmet-deniz.bas.1@ulaval.ca)

Published in Hydrometallurgy, 158, 1-9. DOI: [10.1016/j.hydromet.2015.09.020](https://doi.org/10.1016/j.hydromet.2015.09.020)

Résumé

Cette étude examine les interactions électrochimiques entre l'or et les minéraux de type oxyde étant associé à une (OC) ou deux cellules séparés (TC) en présence ou en l'absence de pulpe. La magnétite a montré des effets négatifs sur la lixiviation de l'or, tandis que la maghémite et l'hématite ont démontré des effets positifs, relativement. La présence de pulpe généralement entraîne à des densités de courant inférieures. Toutefois, la vitesse de la dissolution d'or a triplé ($30 \text{ à } 90 \mu\text{A cm}^{-2}$) lorsque les résidus de pulpe ont été réutilisés comme un nouveau flux dans deux cellules séparés (TC). Ce qui suggère que les ions négatifs ont possiblement été éliminés lors de la première étape. En outre, la densité de courant de l'or a été augmentée de 10 fois par un prétraitement magnétique de minerai d'or grillé. On a constaté que dans les solutions de cyanure saturées avec de l'oxygène atmosphérique, la pente cathodique de Tafel seulement ($8,60 \times 10^{-7} \pm 4,56\% \text{ mol m}^{-2} \text{ s}^{-1}$) prévoit à proximité des vitesses de corrosion d'or à celle cyanuration pratique ($10,57 \times 10^{-7} \pm 1,33\% \text{ mol m}^{-2} \text{ s}^{-1}$), suggérant que la polarisation cathodique est le contrôle de la vitesse d'un. En outre, une nouvelle électrode est composée de quantités égales de magnétite et d'hématite dans une électrode a été développé pour étudier l'influence de ces deux oxydes majeurs de fer sur la lixiviation de l'or, en même temps. 0,04 M NaCN à 100 tr/min d'agitation a été optimale. L'analyse par MEB a révélé la présence de Fe-oxyde et Au-C des produits composites qui pourraient être responsables de la passivation partielle de la surface d'or.

Abstract

This study investigates the electrochemical interactions between gold and its associated oxide minerals either in one (OC) or two separate containers (TC) in presence or absence of slurry. Magnetite showed negative effect on gold leaching, while maghemite and hematite demonstrated positive effect, relatively. The presence of slurry generally resulted in lower current densities. However, when the tailings of slurry was used again as a new feed in two separate containers (TC), the dissolution rate of gold was increased by 3 times (30 to 90 $\mu\text{A cm}^{-2}$), suggesting the removal of detrimental ions in the first stage. Moreover, the current density of gold was enhanced by 10 times by magnetic pre-treatment of roasted gold ore. It was found that in cyanide solutions saturated with atmospheric oxygen, cathodic Tafel slope only ($8.60 \times 10^{-7} \pm 4.56\% \text{ mol m}^{-2} \text{ s}^{-1}$) provides close corrosion rates of gold to that in practical cyanidation ($10.57 \times 10^{-7} \pm 1.33\% \text{ mol m}^{-2} \text{ s}^{-1}$), suggesting that cathodic polarization is the rate controlling one. Furthermore, a new electrode consisted of equal quantities of magnetite and hematite in one electrode was developed to examine the influence of these two major iron oxides on gold leaching, concurrently. 0.04 M NaCN at 100 rpm agitation was found to be optimal. SEM analysis indicated the presence of Fe-oxide and Au-C compound products that could be responsible for partial passivation of gold surface.

Keywords: Gold, Roasted Gold Ore, Magnetite, Hematite, Combined Anode Polarization, Passivation

6.1 Introduction

It has been known that cyanidation is an electrochemical corrosion process (Thompson, 1947), thus the anodic dissolution of gold can be readily studied by electrochemical techniques. In previous electrochemical studies, the dissolution rate of gold has been considered as the intersections of cathodic and anodic Tafel curves (Kudryk and Kellogg, 1954; Cerovic et al., 2005). However, Dai and Breuer (2013) have recently indicated that considering Evan's diagrams could be misleading due to inherent flaws such as oxidation half reaction does not include the influence of oxygen. Additionally, Crundwell (2013) claimed that each point on the mineral surface is considered as both an anodic site and a cathodic site and concluded that there is no separation of anodic and cathodic sites on a mineral's surface. According to these findings, electrochemical studies of gold are still subjects of interest.

During cyanidation, the anodic dissolution of gold may be reduced/retarded in some conditions, and in that case passivation and galvanic interactions phenomena are considered as potential significant electrochemical factors (Lorenzen and van Deventer, 1992a; Mrkusic and Paynter, 1970). Passivation phenomenon of gold has been known since 1907 and assumed that the passivity is due to the formation of a surface film on the surface of gold (Cathro and Walkley, 1961). Passivation of gold has been linked to dissolved species, presence of impurities, gold oxide and hydroxide films, and insoluble sodium aurocyanide film (Kirk et al., 1978; Nicol, 1980; Mrkusic and Paynter, 1970).

It is assumed that gold dissolution may be influenced when gold is in contact with conductive minerals (Lorenzen and van Deventer, 1992a). Aghamirian and Yen (2005) employed potentiodynamic polarization tests in one container and found that pyrite and pyrrhotite showed positive effect on the leaching of gold which is not in agreement with the previous findings (Paul, 1984; Lorenzen and van Deventer, 1992a). However, Filmer (1982) mentioned that gold becomes passive if it is in contact with a conductive mineral, and this was linked to the formation of a passive film on the surface of gold due to the enhanced cathodic current. Van Deventer et al. (1990), and Lorenzen and van Deventer (1992a) examined the polarization of electrically connected gold and sulphide mineral

electrodes either in one or two separate containers where platinum was used as a counter electrode. In case of hematite and gold connection, identical curves were obtained in one and two containers, indicating that only galvanic interactions played a significant role in retarding the dissolution rate of gold. [Azizi et al. \(2010\)](#) found that gold dissolution rate in one container was lower than in two separate containers and this difference was explained by the partial passivation of gold surface by a resistive film of Au₂S and/or metal hydroxides releasing from mineral electrode. Then, it can be deduced that the influence of each mineral could show different effects and generalizing the influence of each mineral may not be correct in all cases and that depends on the anodic and cathodic behaviour of gold and its associated minerals.

Till now, almost all previous electrochemical studies of gold were conducted using only sulphidic gold ores ([van Deventer and Lorenzen, 1987](#); [van Deventer et al. 1990](#); [Lorenzen and van Deventer, 1992a](#); [Aghamirian and Yen, 2005](#); [Cruz et al., 2005](#); [Dai and Jeffrey, 2006](#); [Azizi et al., 2010, 2011, 2012a, 2012b, 2013](#)), and the influence of slurry was not systematically considered. On the other hand, there is a lack of electrochemical studies between gold and oxide minerals. Additionally, since there is an increasing trend on the treatment of refractory gold ores which often requires oxidation such as roasting prior to cyanidation ([Zhou and Fleming, 2007](#)), an increasing request of the gold mining industry for this issue is therefore created. Hence, the objectives of this paper are: (i) to examine the influence of oxide minerals on gold leaching. In this manner, Combined Anode Electrode Polarization “CAP” approach was developed to have a local galvanic cell; (ii) to examine/understand the dominating effect in between galvanic interactions and passivation phenomena on gold leaching either in one container (OC) or two separate containers (TC) in the absence or in the presence of slurry; (iii) to study the effect of two major oxide minerals, concurrently, as function of cyanide concentration and agitation speed. Thus, a new electrode consisted of equal surfaces of magnetite and hematite in one electrode, named as “MagHem-ES”, was developed.

6.2 Experimental Conditions

6.2.1 Material and Preparation of Electrodes

Roasted gold ore sample (80% passing $-75\ \mu\text{m}$ (d_{80})) was received from Barrick Gold Corporation. Mineralogical analysis of the sample indicates that the ore sample consists predominantly of quartz, dolomite, calcite, gypsum, and iron oxides such as hematite, magnetite, maghemite, and with almost non sulphur content. Gold is mainly associated with iron oxides. Metal analysis by atomic absorption spectroscopy (AAS, Perkin Elmer Analyst 800) has shown that gold and silver contents are ~ 8 and ~ 5 g/t, respectively (Bas et al., 2015a).

Sodium cyanide (NaCN) with a $\geq 98\%$ purity was obtained from Thermo Fisher Scientific Company. Electrolyte medium was prepared using distilled water and pH was adjusted to 10.5 by adding 1 M NaOH. Electrolyte was agitated with a magnetic bar (4 cm long and 1 cm diameter) during tests. Pure gold (Au) disc electrode was used as a working electrode while platinum (Pt) as a counter electrode and Ag/AgCl, KCl_{sat} as a reference electrode. $0.25\ \text{cm}^2$ of gold foil (99.9% purity from Sigma Aldrich), as pure gold electrode (Au), was first polished with a fine (MicroCut® 100 Grit Soft) polishing paper and then rinsed in distilled water. Then, it was introduced in aqua-regia for 10 seconds to clean the surface, washed with distilled water and ethanol and finally rinsed with distilled water again, to assure the reproducibility (Kirk et al., 1978).

Roasted gold ore (RGO), magnetite (Mag), hematite (Hem), maghemite (Mgh), and magnetite-hematite (MagHem-ES) disc electrodes with an exposed surface area of $4.9\ \text{cm}^2$ were used, as mineral electrodes. Maghemite was prepared by heating magnetite in oven at $200\ ^\circ\text{C}$ for 3 h as giving a light brown colour to be maghemite (Legodi and Waal, 2007) and this was proved by XRD (Bas et al., 2015b). MagHem-ES consisted of equal surfaces of hematite and magnetite in one electrode. In each case, roasted gold ore, magnetite, hematite was mixed with graphite powder (to increase the conductivity) 3:1 and with few drops of silicone oil, for binding, till a paste was obtained. Graphite powder, which has a particle size of $<45\ \mu\text{m}$, and a 99% purity, was obtained from Sigma-Aldrich. The mixture was manually homogenized during 30 minutes, in general. Then, it was mechanically pressed at 20 tons to have uniform sample surface. After that, disc electrodes were kept

under nitrogen atmosphere over a night. Then, these electrodes connected with an insulated copper wire, cast in acrylic resin.

6.2.2 Electrochemical Procedures

First, electrodes were allowed to stay at open circuit potential (OCP) for 2 minutes before linear polarization tests with a range of ± 25 mV with respect to corrosion potential (E_{corr}). Actually, different stabilization times (up to 30 minutes) were also considered, however the reproducibility was $\pm 4\%$. Then, cathodic polarization tests were performed by scanning from E_{corr} to -300 mV and corrosion current (i_{corr}) was estimated by considering the cathodic Tafel slope only extrapolating from OCP. Anodic polarization tests were performed by scanning from E_{corr} to $+1000$ mV. Tests were performed generally in 0.01 M NaCN electrolyte at pH 10.5 at 100 rpm magnetic agitation at room temperature, saturated with atmospheric oxygen, unless otherwise reported. Scan rate of 0.166 mV/s was selected based on the polarization standards ([ASTM Standard G 5-94, 2006](#)). Corrosion rates of gold by Tafel was compared to cyanide leaching results. In case of cyanide leaching tests, leach solution was prepared using deionised-distilled water at the prescribed concentration of reagent and leached during 3 h. During the experiments, pH was maintained at 10.5 by the addition of 1 M NaOH. Solution was sampled at predetermined intervals and analysed by atomic absorption spectrophotometer (Atomic Absorption Spectroscopy, AAS - Perkin Elmer AAnalyst 800) to determine the gold leaching rate. Electrochemical tests were performed at least in triplicates to assure the reproducibility. In case of slurry tests, to simulate the practical conditions, 35% solid ratio as a slurry of roasted gold ore was considered.

Combined anode electrode polarization “CAP” approach tests, where gold and mineral disc electrodes were electrically connected to each other as anode to establish a local galvanic cell, were performed either in one container (OC) ([Fig. 6.1](#)) or two separate containers (TC). Platinum as a counter electrode and Ag/AgCl, KCl_{sat} as a reference electrode (0.199 V/SHE) were used and all potentials here were reported vs. standard hydrogen electrode (SHE). In case of two separate containers (TC) tests, mineral electrode (having as its open circuit potential) was placed into one of the containers and it was electrically connected

with Au electrode in the other container (that contains platinum as counter electrode) to have a “Au anode connected to non-polarized mineral electrode”. The potential of mineral electrode was measured with a separate reference electrode (SHE) in case of two separate container tests. In certain experiments for comparison, another platinum electrode was also put in the cell of mineral electrode and that was electrically connected to other platinum electrode in the cell of Au to have a “polarized Au-mineral electrode”. Surface characterization tests were carried out on scanning electron microscopy (SEM) (JEOL 840-A) coupled with Energy-dispersive X-ray spectroscopy (EDS).

Combined Anode Electrode Polarization (CAP)

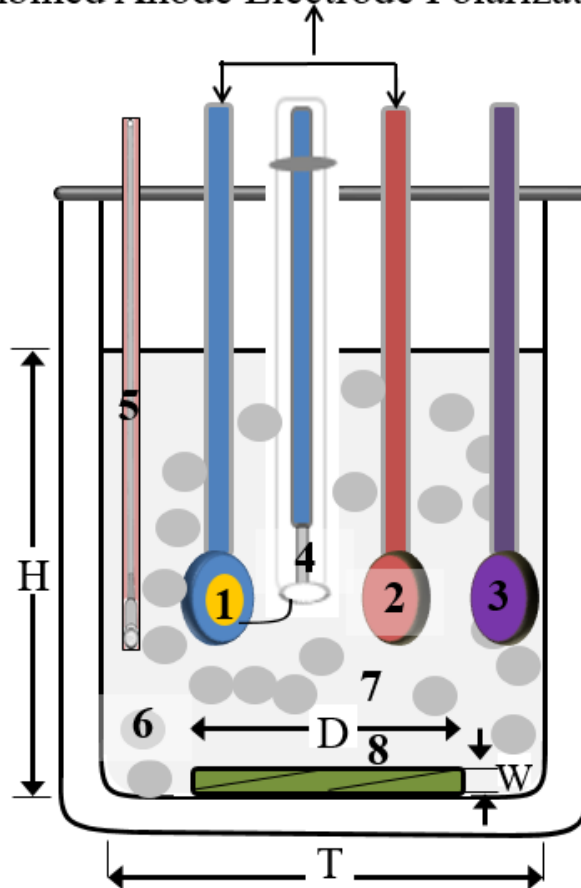


Fig. 6.1 Schematic illustration of one container (OC) electrochemical set-up for combined anode electrode polarization (CAP) tests (1: Au as working electrode; 2: mineral electrode; 3: counter electrode; 4: reference electrode; 5: pH meter; 6: slurry; 7: NaCN electrolyte; 8: magnetic bar ($4 \times 1 \text{ cm}^2$)).

6.3 Results and Discussion

6.3.1 Potentiodynamic Cathodic Polarization of Gold and Roasted Gold Ore

Figs. 6.2a and b shows the influence of oxygen and cyanide on cathodic polarization profiles of pure gold and roasted gold ore electrodes, respectively, by scanning from E_{corr} to -300 mV at pH 10.5 at 100 rpm agitation in 0.01 M NaCN electrolyte. In the presence of cyanide and atmospheric oxygen, the dissolution potential of pure gold was found to be at ~ -550 mV (Fig. 6.2a). To examine the influence atmospheric oxygen on cathodic polarization of gold, bubbling N_2 prior and during the tests was considered. Almost same trends were observed by bubbling N_2 either during and/or prior to tests if compared to that in presence of cyanide and atmospheric oxygen. However, in the absence of cyanide, a very different cathodic Tafel (behaviour) slope with a single wave was obtained and the corrosion potential of gold was shifted to ~ 105 mV, suggesting the formation of hydroxide, whereas Dai and Breuer (2013) observed two waves on pure gold cathodic polarization curve, suggesting the formation of hydrogen peroxide (first wave) and hydroxide (second wave). On the other hand, in case of roasted gold ore, dissolution potential was found to be ~ 50 mV in the presence of cyanide and oxygen. Although the dissolution potential was shifted to more positive potential (~ 280 mV) in presence of N_2 bubbling, almost same cathodic Tafel slopes were observed in both cases. However, in the absence of cyanide, a different cathodic Tafel slope was obtained with a dissolution potential of ~ 190 mV. It is worth noting that the difference in conductivity and relative quantities of magnetite and hematite could explain the cathodic behaviour of RGO. Additionally, the presence of soluble and/or insoluble ions, and as a result different behaviours of the ions in the solution could also influence the position of RGO electrode. Then, it can be deduced that the influence of cyanide on cathodic reaction is highly significant and provides better assumption for corrosion rate.

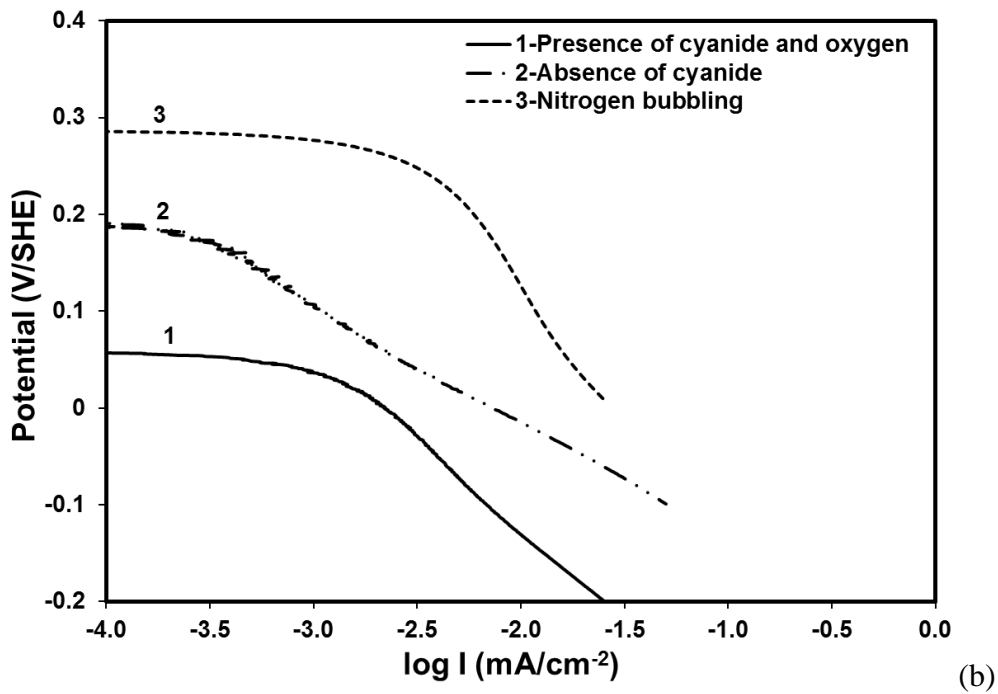
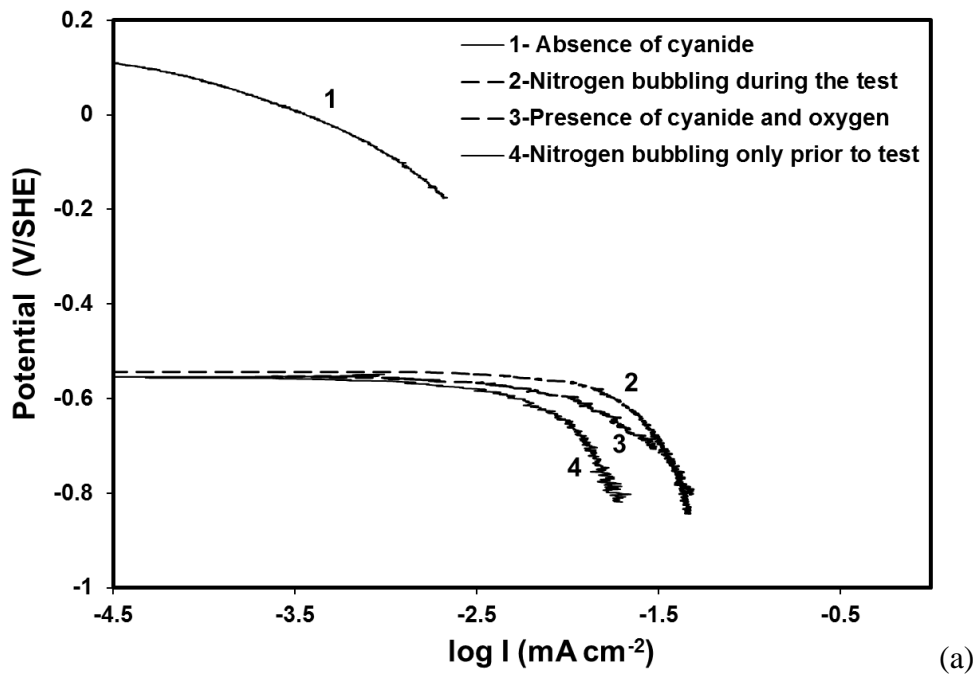


Fig. 6.2 The influence of oxygen and cyanide on cathodic potentiodynamic polarization of pure gold (0.25 cm²) (a) and roasted gold ore (b) electrodes (4.9 cm²) at 0.166 mV/s scan rate in 0.01 M NaCN electrolyte at pH 10.5 at 100 rpm agitation, 25 °C.

In order to estimate the corrosion rate of gold, cathodic Tafel slope only by extrapolating from open circuit potential was considered since there may be passive behaviour in anodic curve, and that was compared to the cyanide leaching result. Then, corrosion rates of pure gold of $8.60 \times 10^{-7} \pm 4.56\%$ mol m⁻² s⁻¹ and $10.57 \times 10^{-7} \pm 1.33\%$ mol m⁻² s⁻¹ were found to be for cathodic Tafel slope only and cyanide leaching, respectively. Similarly, authors have found more representative corrosion rates of gold from roasted gold ore considering only cathodic Tafel curve by extrapolating from open circuit potential ($3.30 \times 10^{-8} \pm 3.27\%$ mol m⁻² s⁻¹) if compared to that of cyanide leaching ($3.07 \times 10^{-8} \pm 7.03\%$ mol m⁻² s⁻¹) (Bas et al., 2015a). Since Tafel curves are generally accepted for an estimation of the corrosion rates of a tested specimen, then the difference in corrosion rates of gold (~ 25%), which is compatible with the findings of Dai and Breuer (2013), could be considered reasonable. Also, it should be noted that the leaching of gold could be retarded by a AuCN film (Jeffrey and Ritchie, 2001). However, the intersection point of anodic and cathodic curves was considered as the corrosion rate of gold (Kudryk and Kellogg, 1954; Cerovic et al., 2015). Recently, Dai and Breuer (2013) have reported that the actual leaching point of pure gold does not match to the intersection of Tafel curves, suggesting that the leaching of gold takes place at higher rate to that of Tafel curves. They concluded that intersection point could be misleading for the estimation of the corrosion rate of gold, since the influence of cyanide is not included in the cathodic curve whereas the influence of oxygen is not included in the anodic curve. These findings have revealed that cathodic slope provides significant information, and has the major controlling effect on the electrochemical behaviour of tested specimen, in this case gold.

6.3.2 Combined Anode Electrode Polarization (CAP) System

Gold-Roasted Gold Ore Electrodes Combined Anode Polarization

In these series of experiments, mineral electrode (e.g. roasted gold ore, hematite, maghemite, and magnetite) is electrically connected to gold electrode to obtain a “Au anode connected to non-polarized mineral electrode”. Roasted gold ore electrode when electrically connected to Au electrode, galvanic dissolution started earlier in one container if compared to that of two separate containers (Fig. 6.3a). In one container (OC) in absence

of slurry, an increasing trend in the galvanic dissolution rate of electrodes was observed with having a slight passive peak at around 0.65 V/SHE. This increase could be explained by the increase in the formation of soluble gold-cyanide complex. In the case of two separate containers, dissolution started later and current densities were found to be greatly lower if compared to that of one container. On the other hand, in the presence of slurry when Au and RGO electrodes were placed into one container, anodic dissolution of gold was influenced in a negative way as a result of two passive peaks at around 0.2 and 0.72 V/SHE with having of lower current densities if compared to that of in absence of slurry. This decrease could be explained by the increase in the amount of soluble species released from slurry. However, in two separate containers in the presence of slurry, the galvanic dissolution of gold showed a very clear passive region with a potential range of 700 mV (from 0.1 to 0.8 V/SHE) and a 1.5 times lower passive current (0.06 to 0.04 mA/cm²) if compared to that of in one container.

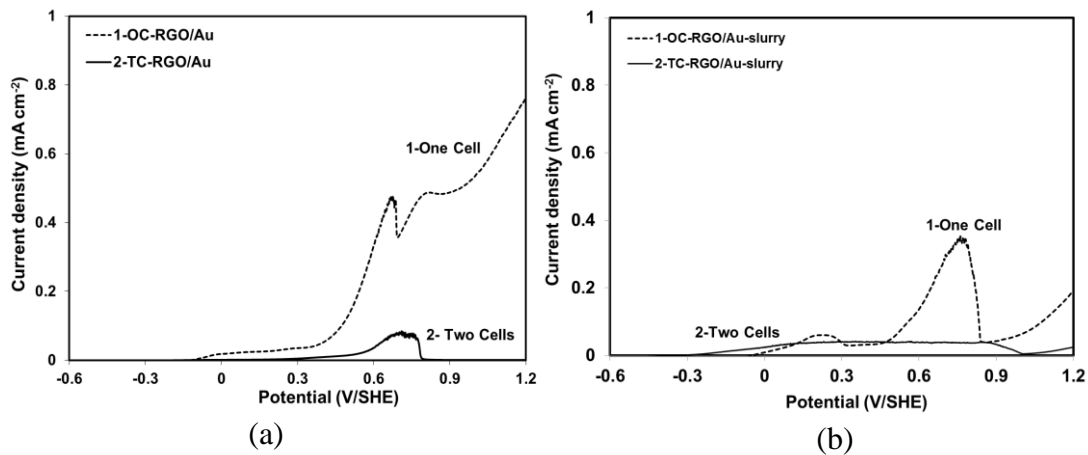


Fig. 6.3 Effect of roasted gold ore (RGO) on gold dissolution either in one or two containers (a) in the absence of slurry, (b) in the presence of slurry (35%), in 0.01 M NaCN solution, atmospheric oxygen, pH 10.5, at 100 rpm magnetic agitation at 0.166 mV/s scan rate, 25. °C

Gold-Hematite Electrodes Combined Anode Polarization

Monitored galvanic currents between gold and hematite either in the presence or absence of slurry as function of time are shown in Figs. 6.4a and b. The dissolution rate of gold was greatly enhanced (from 0.1 to 1.28 mA/cm²) as a result of higher galvanic current density

with no indication of passive peaks when the electrodes were placed in one container in the absence of slurry to that of two separate containers (Fig. 6.4a). That could be attributed to the positive galvanic interactions between hematite and gold and also to the release of ferric ions (powerful oxidant) that may have a positive role in the oxidation of gold. This finding is in agreement with the findings by Filmer (1982) suggesting the positive effect of hematite while Lorenzen and van Deventer (1992b) found that hematite did not show a significant role in gold leaching either in one or two containers. In comparison to magnetite, a 25% increase in current density was obtained with hematite (from 80 to 100 $\mu\text{A}/\text{cm}^2$) in two separate containers in the absence of slurry. On the other hand, in presence of slurry in OC, a similar increasing trend in galvanic current was observed for hematite (Fig. 6.4b). However, in two separate containers (Fig. 6.4b), a similar passive behaviour was observed if compared to that of magnetite (Fig. 6.6b). It can be concluded that hematite showed a promoting effect on the leaching behaviour of gold which is in agreement with the findings of Paktunc et al. (2006) who carried out mineralogical and gold distribution studies of such a gold ore, and demonstrated that the efficient extraction of gold, calcine should be dominantly hematite. The reproducibility of the peak current densities was found to be $\pm 5\%$.

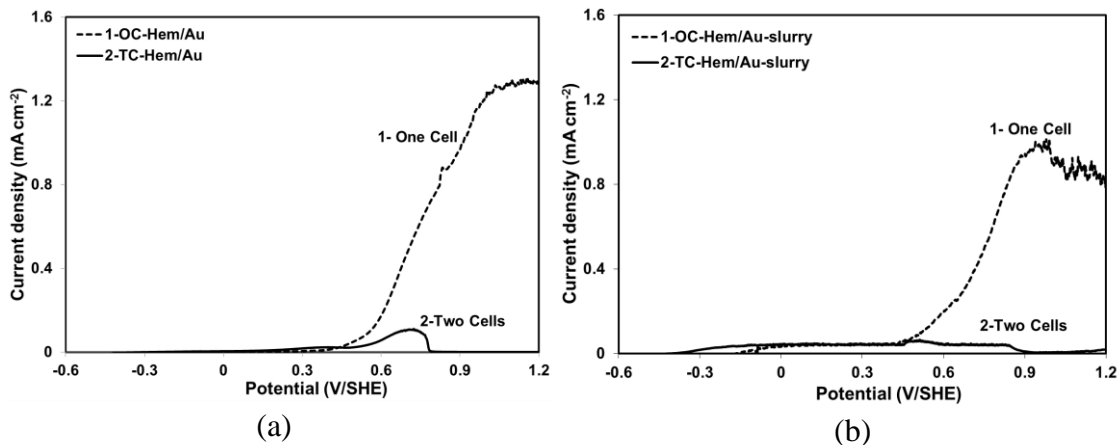


Fig. 6.4 Effect of hematite (Hem) on gold dissolution either in one or two containers (a) in the absence of slurry, (b) in the presence of slurry (35%) in 0.01 M NaCN solution, atmospheric oxygen, pH 10.5, 100 rpm magnetic agitation at 0.166 mV/s scan rate, 25 °C.

Gold-Maghemite Combined Anode Electrode Polarization

Magnetite oxidation (Eq. 6.1) could produce maghemite ($\gamma\text{-Fe}_2\text{O}_3$), metastable spinel polymorph of hematite (White et al. 1994). However, maghemite, with its non-porous property, is problematic for gold dissolution (Marsden and House, 2006).

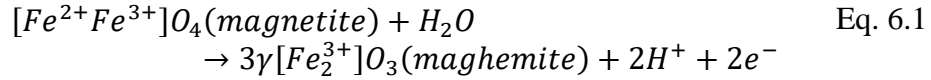


Fig. 6.5 demonstrates the influence of slurry on gold dissolution either in one or two separate containers. As it is seen, the general trend in one container in the absence of slurry (Fig. 6.5a) was found to be very similar with two peaks with higher current densities (up to 3 times) if compared to that of magnetite coupling (Fig. 6.6a). On the other hand, in one container in the presence of slurry, the dissolution rate of gold was obviously enhanced till 0.8 V/SHE, and showed a decrease as a result of the formation of a passive peak. However, in two separate containers in the presence of slurry, the dissolution of gold commenced earlier than in one container. Generally, an increasing trend in current density was observed in TC in the presence of slurry.

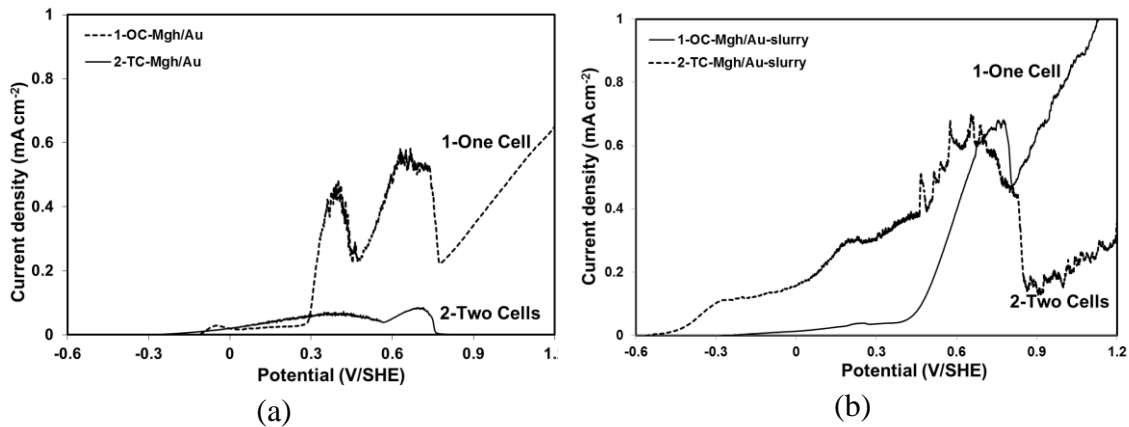


Fig. 6.5 Effect of maghemite (Mgh) on gold dissolution either in one or two containers (a) in the absence of slurry, (b) in the presence of slurry (35%) in 0.01 M NaCN solution, atmospheric oxygen, pH 10.5, 100 rpm magnetic agitation at 0.166 mV/s scan rate, 25 °C.

To note that since it is difficult to distinguish magnetite and maghemite minerals by XRD, another maghemite preparation procedure was also considered to see the effect of

maghemite as function of time (5 hours) and temperature (250 °C) (Paktunc, 2014). However, very close potential and current values were obtained if compared to the first prepared maghemite (at 200 °C for 3 hours) (Bas et al., 2015b).

Gold-Magnetite Combined Anode Polarization

Since the corrosion potential of gold (-0.6 V/SHE) is more active than magnetite (0.210 V/SHE), then a galvanic cell between these two electrodes can be formed when they are electrically connected. The results in Figs. 6.6a and b show the influence of slurry when gold and magnetite electrodes are electrically connected to each other either in one container (OC) or two separate containers (TC). In one container (OC) in the absence of slurry, the initial increase in current density suggests an increase in the formation of soluble gold-cyanide complex, $\text{Au}(\text{CN})_2^-$. As function of time, two passive peaks were observed at 0.45 and 0.75 V/SHE (Fig. 6.6a). These passive peaks in one container could be related to the formation of $\text{Fe}(\text{OH})_3$ passive film as reported earlier by Guo et al. (2005). Mrkusic and Paynter (1970) reported that in presence of magnetite, it is not clear which way the dissolution potential would move. During cyanidation in the presence of magnetite, and when the oxygen partial pressure is increased, it is possible that passive behaviour will be encountered at high dissolution potentials. At 0.75 V/SHE, a passive peak was observed in both cases (OC, and TC), and a 3 times (0.1 to 0.3 mA/cm^2) higher current density was observed in one container if compared to that of two separate containers. The reproducibility of the peak current densities was found to be $\pm 3\%$. However, if these electrodes were placed into two separate containers (TC), the anodic behaviour started later and only one passive peak was obtained at 0.75 V/SHE with a sharp decrease in current density (from 0.3 to 0.075 mA/cm^2) if compared to that of one container (OC). This decrease indicated the negative galvanic interactions between gold and magnetite showing an inhibiting effect on the dissolution of gold. On the other hand, in the presence of slurry, the dissolution rate of gold in OC showed a 4 times decrease (from 0.95 mA/cm^2 to 0.24 mA/cm^2). However, in the presence of slurry in TC, the current density showed a certain passive behaviour with a potential range of ~ 1000 mV (-0.17 to +0.83 mV/SHE). This obvious negative effect on gold dissolution rate could be ascribed to the increase in soluble species into the solution releasing from either mineral electrode or from slurry. Then, it can

be deduced that there is a negative galvanic interaction between gold and magnetite, and the presence of corrosion products are directly affecting the anodic dissolution of gold.

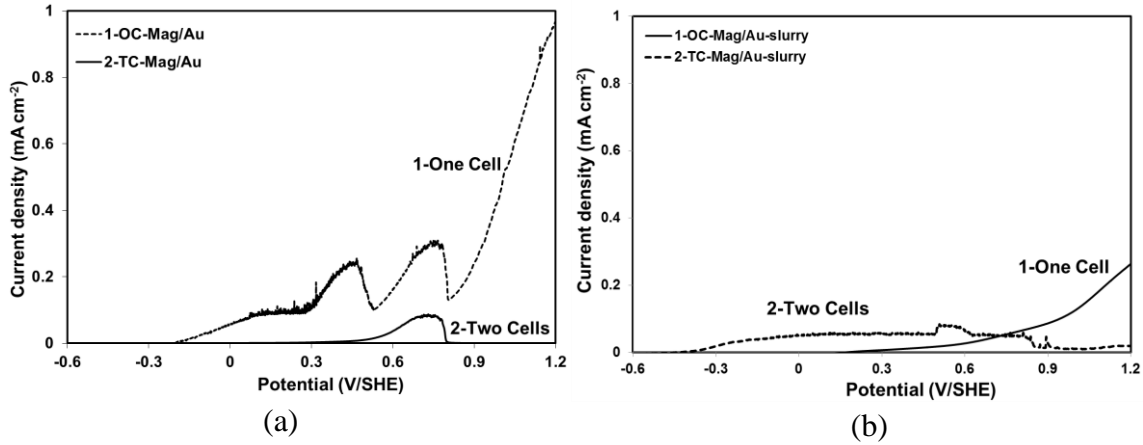


Fig. 6.6 Effect of magnetite (Mag) on gold dissolution either in one or two containers (a) in the absence of slurry, (b) in the presence of slurry (35%), in 0.01 M NaCN solution, atmospheric oxygen, pH 10.5, 100 rpm magnetic agitation, 0.166 mV/s scan rate, 25 °C.

6.3.3 Interpretation of Electrochemical Findings

In some conditions, the leaching of gold could be reduced which is problematic for gold mining industry. From the electrochemical point of view, this could potentially be due to galvanic interactions and/or passivation phenomena.

Due to the presence of certain passive regions (~ 1 V of potential range) in two separate containers, then it is important to examine this behaviour. In two separate containers, when gold electrode was electrically connected to RGO electrode, it was found that dissolution started at around -0.3 V/SHE, and the active behaviour continued up to at 0.15 V (Fig. 6.7). At potential of 0.155 V/SHE, the dissolution of gold was found to be retarded until 0.872 V/SHE by the formation of a barrier on gold surface due to corrosion products, having of $37 \mu\text{A}/\text{cm}^2$ passive current density as illustrated in region B. Then, the anodic behaviour of gold dropped into the trans-passive region (shown as C in Fig. 6.7) and region D possibly indicates the oxygen evolution region.

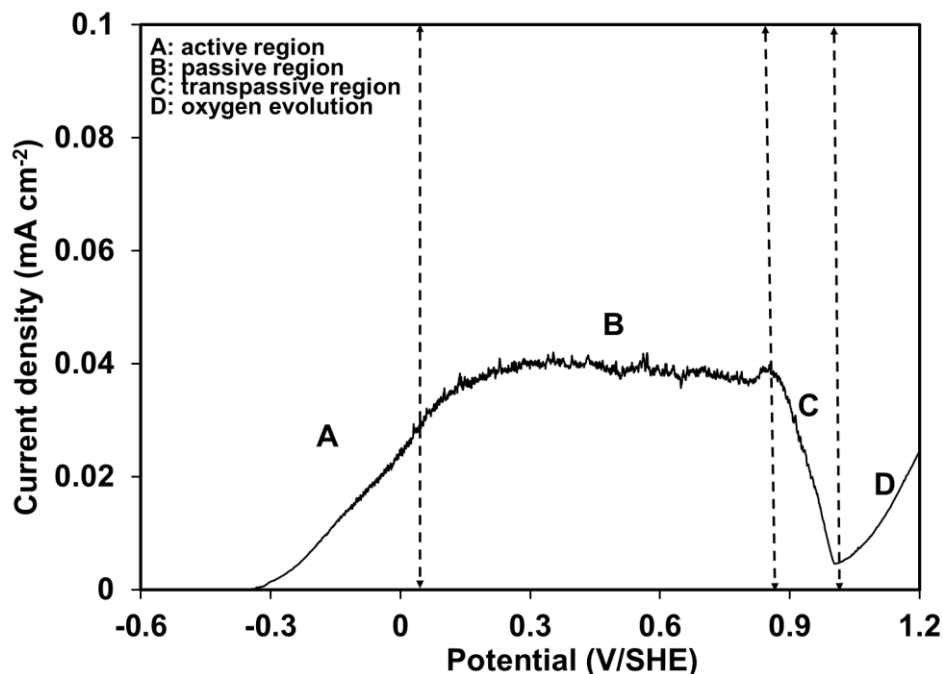


Fig. 6.7 Anodic profile of RGO/Au combined anode polarization in two containers in the presence of slurry in 0.01 M NaCN solution, atmospheric oxygen, pH 10.5, at 100 rpm magnetic agitation at 0.166 mV/s scan rate, 25 °C.

In electrochemical tests, the terms concerning active and passive behaviours could provide significant information on the anodic dissolution behaviour of gold. In this manner, Table 1 shows the terms E_{cp} , i_{cp} , E_{sp} , and i_{sp} that are corresponding to the critical passive potential, the critical passive current density, the starting potential of the trans-passive region and the starting current density of the trans-passive region, respectively. The critical current density for passivation i_{cp} , corresponds to the onset of low corrosion rates since gold passivation is not a perfect conventional one. The starting current density of the trans-passive region i_{sp} , corresponds arbitrarily to the highest corrosion rate before the sudden important increase in corrosion rate. The highest critical passive current was found to be for Au and RGO coupling ($44 \mu\text{A}/\text{cm}^2$), while magnetite coupling gave the lowest one ($35 \mu\text{A}/\text{cm}^2$). On the other hand, hematite coupling resulted in the highest starting current density of the trans-passive region ($33 \mu\text{A}/\text{cm}^2$), while magnetite coupling gave the lowest one ($3.16 \mu\text{A}/\text{cm}^2$). Critical passive potential of hematite coupling was found to be the most active potential of $-270 \text{ mV}/\text{SHE}$, followed by magnetite coupling at $-218 \text{ mV}/\text{SHE}$, and the noble potential

was found to be -150 mV/SHE for RGO coupling. In the passive region, the magnitude of potential was found to be higher for hematite coupling. Then, it can be deduced that hematite showed more promoting effect on the leaching of gold if compared to that of magnetite and roasted gold ore electrodes. This means that passivation is not at least a major controlling factor in certain cases, e.g. in case of hematite.

Table 6.1 Important electrochemical terms on gold polarization with disc electrodes.

Electrode Configuration	E_{cp} (mV/SHE)	i_{cp} ($\mu\text{A}/\text{cm}^2$)	E_{sp} (mV/SHE)	i_{sp} ($\mu\text{A}/\text{cm}^2$)
Au/RGO	-150	39.2	1183	5.01
Au/Mag	-218	35	1152	3.16
Au/Hem	-270	39.8	1279	33

Based on the electrochemical findings in combined anode polarization tests, one of the remaining question is “How does the slurry of roasted gold ore affect on the anodic dissolution of gold?”. Therefore, two different approaches were applied. The first one is the re-use of the tailings of first slurry test as a new feed slurry in the new test. Hence, the tailings of the slurry of first test was collected on a filtered paper and dried in an oven at 105 °C for 6 hours. Then, it was used again as a new feed sample for RGO and Au electrodes combined polarization in two separate containers. It was found that the dissolution rate of gold was increased by 3 times (30 to 90 $\mu\text{A}/\text{cm}^2$) with this pre-treatment step (Fig. 6.8). This increase could be ascribed to the removal of detrimental ions in the first leaching test and resulted in higher dissolution rate with the consideration of tailings of the first test as a new slurry in the second test. Similarly, Lorenzen and van Deventer (1992b) have mentioned that the dissolution current of gold prior to passivation depends on impurities in the solution, which could change the tendency of gold to go to passive state.

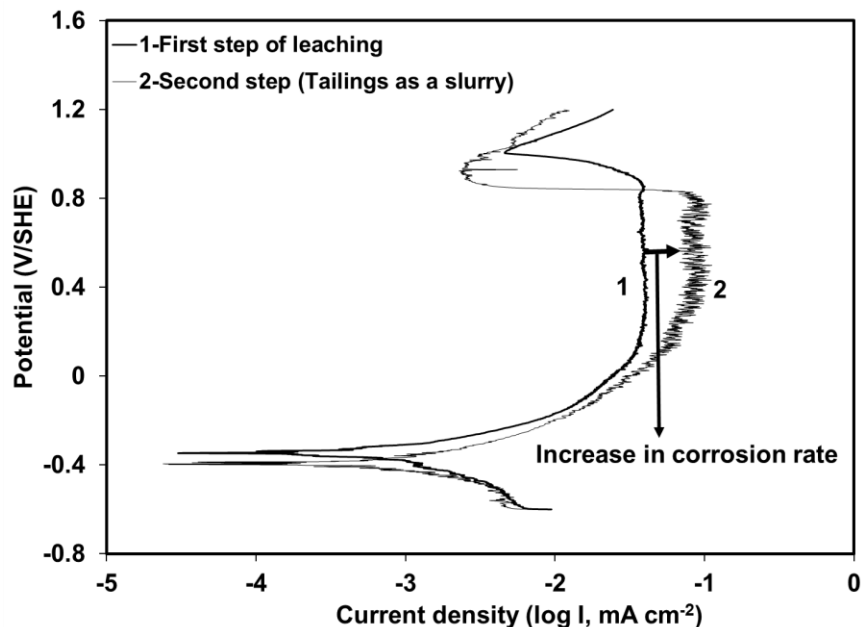


Fig. 6.8 The influence of the treatment of tailings of first slurry test as a new feed slurry on the dissolution behaviour of gold for RGO/Au combined anode polarization in two separate containers in 0.01 M NaCN solution, atmospheric oxygen, pH 10.5, at 100 rpm magnetic agitation at 0.166 mV/s scan rate, 25 °C.

Secondly, to examine the influence of slurry on gold leaching, a systematic approach was considered. In this manner, slurry was added separately only into one of the containers, respectively, e.g. slurry was added only into the container of gold electrode and the other container, where the mineral electrode was placed, was left without slurry. It was found that when slurry was added only into the container of Au electrode (as illustrated 2-TC-RGO/Au(slurry) in Fig. 6.9), dissolution started earlier and a 2 times higher (30 to 60 $\mu\text{A}/\text{cm}^2$) anodic behaviour of gold was recorded if compared to that of the slurry in two separate containers (as illustrated 1-TC-slurry-RGO/Au in Fig. 6.9). This increase is an indication of the increase in the amount of gold and other soluble species that released from slurry. As function of time, when the potential reached to 500 mV/SHE, dissolution was retarded (during 800 mV/SHE) in passive region due to the increase in the presence of detrimental ions in the solution that passivates gold surface. However, when the slurry was placed only in the container of RGO electrode (no slurry in the container of Au electrode), ~ a 2 times higher corrosion rate was recorded if compared to that of the other two different

conditions, and two passive peaks were observed. In these series of tests in two separate containers, where only the container of Au electrode had the counter electrode (Pt), the potential of mineral electrode was found to have its corrosion potential (not shown) which suggests no polarization effect. Hence, the influence of counter electrode (Pt) was considered, and in this manner, another Pt electrode was placed in the cell of RGO electrode and these (counter) electrodes were electrically connected to each other, whereas slurry was added only in the cell of Au electrode (as illustrated 4-TC-Au (slurry + Pt) /RGO (Pt) in Fig. 6.9). In this case, dissolution was started earlier, and resulted in higher current density ($80 \mu\text{A}/\text{cm}^2$) if compared to other three conditions (as illustrated in Fig. 6.9), but however a passive behaviour was also observed till 0.3 V/SHE. Then, this partial passivation of gold surface was found to show active behaviour suggesting the change in surface conditions, and removal of corrosion products from the surface. These findings have revealed that the presence of soluble species in the solution is of prime importance in the retarding or promoting the leaching of gold, and the presence of platinum as a cathode (providing the polarisation of the connected mineral electrode) influences the anodic dissolution of gold.

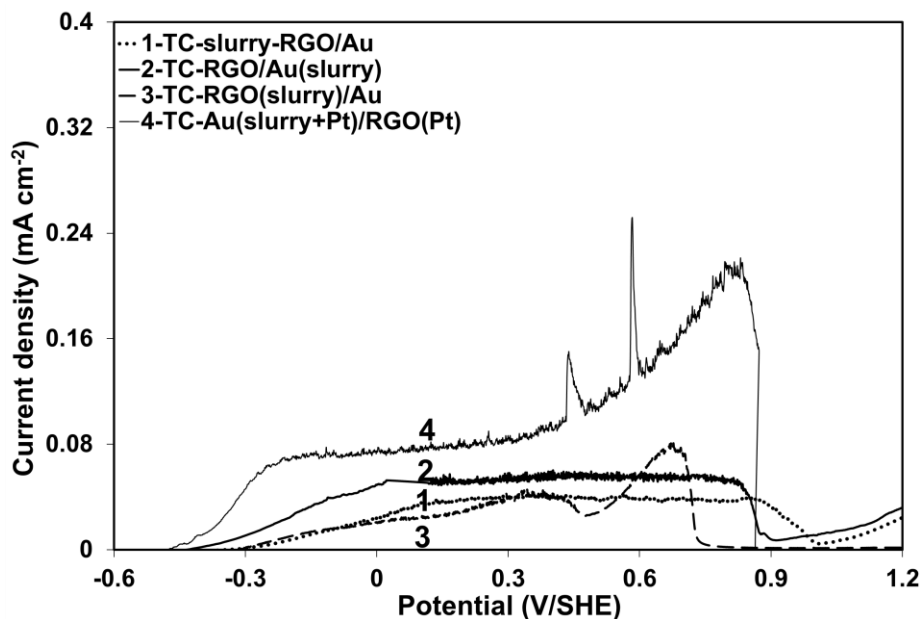


Fig. 6.9 The influence of slurry in two separated containers (TC) for RGO and Au electrode combined polarization in 0.01 M NaCN solution, atmospheric oxygen, pH 10.5, at 100 rpm magnetic agitation at 0.166 mV/s scan rate, 25 °C.

Still, it should be questioned why magnetite showed a retarding effect on the anodic dissolution of gold electrode whereas hematite promoted, relatively. In this case, the removal of iron minerals from roasted gold ore by using a magnet, as a magnetic pre-treatment, was aimed. It is clearly seen that the anodic behaviour of gold gave higher current density (up to 10 times) suggesting increased corrosion rate with a magnetic pre-treatment than the one without magnetic pre-treatment (Fig. 6.10). Additionally, the dissolution of gold commenced earlier when magnetic pre-treatment was applied. The sample, which was removed from roasted gold ore by magnet, was subjected to XRD and XPS analyses to characterize the species. The obtained XRD and XPS results (not shown), however, were not conclusive enough potentially due to low quantity of minerals.

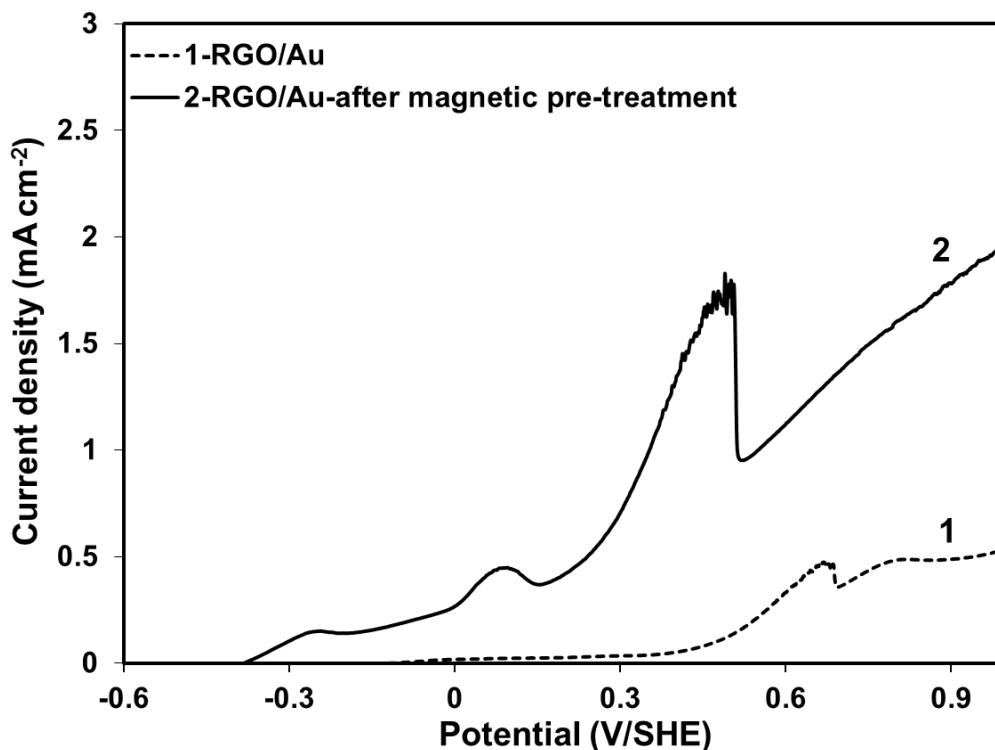


Fig. 6.10 The influence of magnetic pre-treatment on RGO and Au electrode combined polarization in one container in 0.01 M NaCN solution, atmospheric oxygen, pH 10.5, at 100 rpm magnetic agitation at 0.166 mV/s scan rate, 25 °C.

According to these interesting results, a new electrode (MagHem-ES) consisted of equal surfaces of magnetite and hematite in one electrode was generated since it has more resemblance like in practical cyanidation where magnetite and hematite are found together with gold, and was tested as function of cyanide concentration and agitation speed. The effect of NaCN concentration on anodic polarization of Au electrically connected to MagHem-ES electrode is shown in Fig. 6.11. One passive peak at ~ 0.65 V was observed in all tested cyanide concentrations. Peak current density showed a 6-fold increase (0.15 to 0.9 mA/cm^2) with increasing cyanide concentration from 0.01 to 0.04 M while a 1.25-fold increase was observed with increasing cyanide concentration from 0.04 to 0.1 M. This passive peak could be related to the formation of gold hydroxide and/or ferric hydroxide.

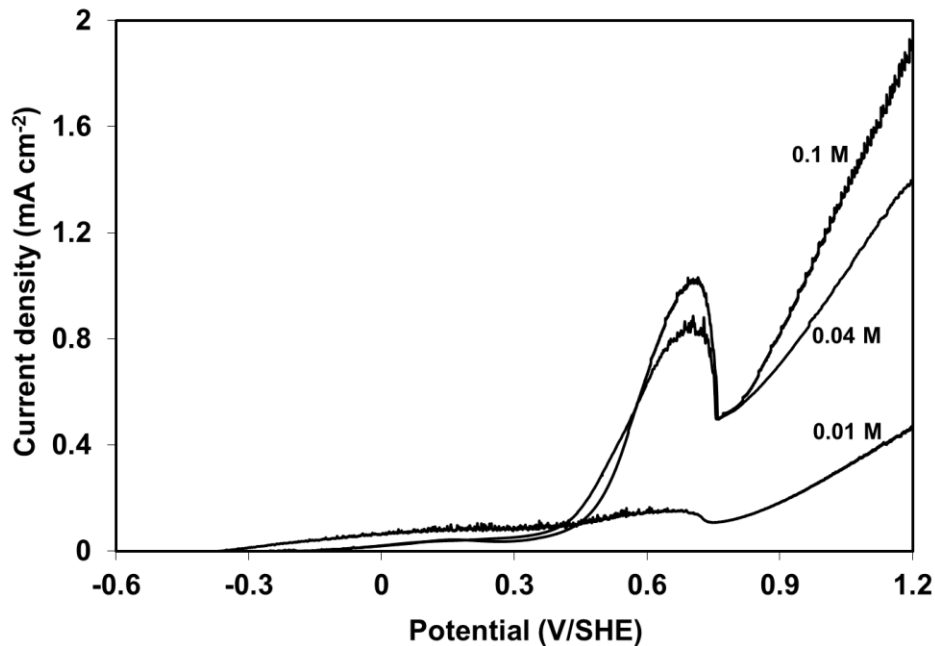
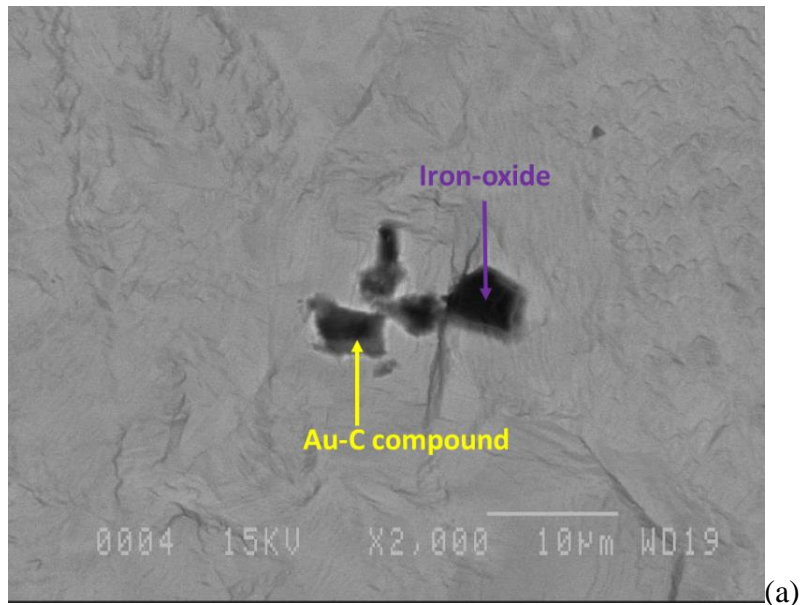


Fig. 6.11 Effect of NaCN concentration on anodic polarization of Au connected to MagHem-ES electrode at 0.166 mV/s scan rate at 100 rpm agitation, pH 10.5, 25 °C.

Fig. 6.12a illustrates Scanning Electron Microscopy (SEM) image of pure gold electrode surface after the polarization test electrically connected to MagHem-ES electrode. According to Energy-dispersive X-ray Spectroscopy (EDS) results, black zone (Fig. 6.12b) was found to be iron-oxide species while grey zone around the black zone (Fig. 6.12c) was

insoluble Au-C compound that potentially could be insoluble AuCN film (Nicol, 1980) (i.e., N atom is not detectable at low concentrations by SEM-EDS). This finding is in accordance with the findings of authors previous results (Bas et al., 2015b) in which similar corrosion products were found on gold surface with galvanic corrosion tests. At the end of polarization test, a 5-fold higher current density was obtained at 0.1 M to that of 0.01 M NaCN suggesting more dissolution behaviour at high cyanide concentration. For comparison, Bas et al. (2015a) did not obtain any passive peak but lower current densities were observed for roasted gold ore electrode alone polarization. Then, it can be deduced that magnetite and hematite have significant and dominating effects on gold leaching and this should be examined case by case. Generally, increasing cyanide concentration resulted in increasing peak densities. These findings have indicated that the release of species from MagHem-ES electrode retard the further dissolution of gold. Duplicate curves with a lower than 6% differences were recorded.



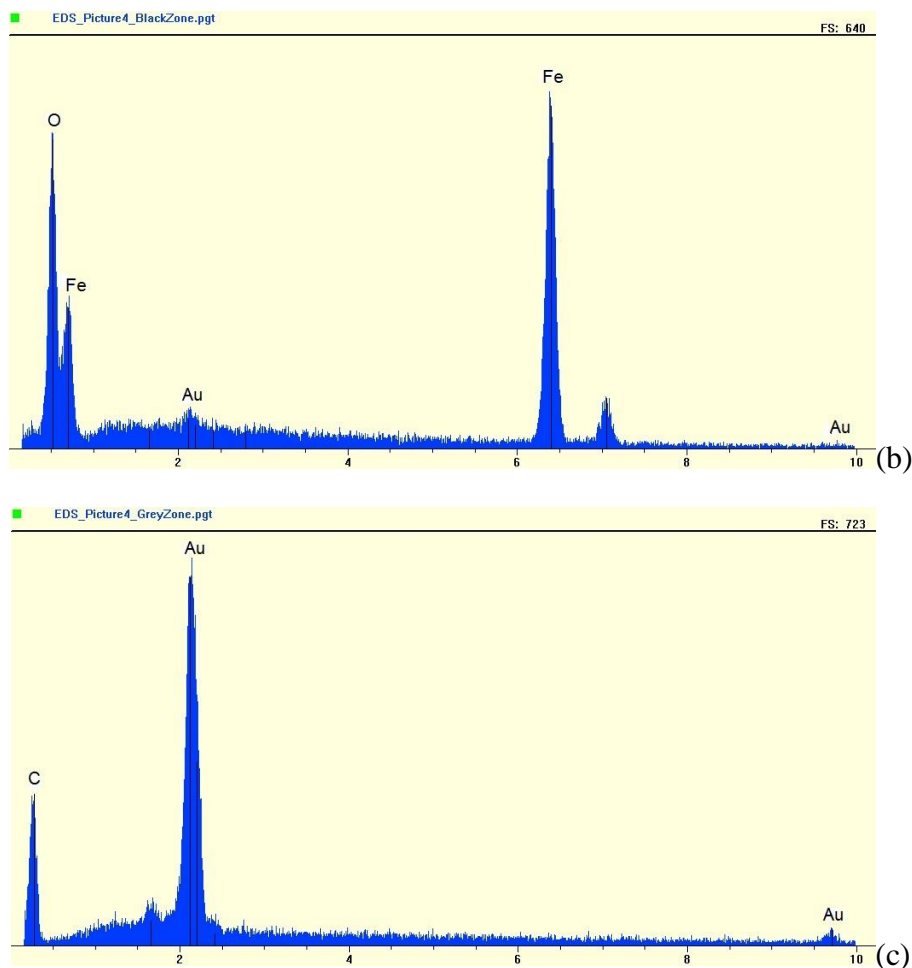


Fig. 6.12 (a) Scanning electron microscopy (SEM), (b) Energy-dispersive X-ray spectroscopy (EDS) of black zone; and (c) EDS of grey zone around black one; on Au electrode after polarization test connected to MagHem-ES at 0.166 mV/s scan rate in 0.4 M NaCN solution, atmospheric oxygen, pH 10.5, at 100 rpm magnetic agitation, 25 °C.

The influence of agitation speed on anodic polarization of Au connected to MagHem-ES electrode is demonstrated in Fig. 6.13. It is seen that two passive peaks, one is very slight at 0.1 V and the other one with a higher current density at 0.65 V were observed with 50, 250, and 400 rpm. However, only one passive peak was observed at 100 rpm agitation at the same potential (0.65 V). Increasing agitation speed from 50 to 100 rpm resulted in a 40% increase in peak current density suggesting the higher dissolution behaviour at 100 rpm agitation while a 20% decrease was obtained by increasing the agitation speed from

100 to 250 and/or to 400 rpm. For instance, diffusion is controlling the rate of dissolution at 50 rpm agitation, giving more passive products that could be the reason of the two peaks. It can be deduced that rate of dissolution was diffusion controlled at lower agitation speed, while it was accelerated mainly by the magnitude of agitation at higher speeds. In these laboratory tests, the optimal agitation speed was found to be 100 rpm for MagHem-ES connected to Au electrode dissolution (Fig. 6.13), whereas ~ 50 rpm rotation speed is generally used for industrial tank leaching processes (Xianhai Mining, 2015). Authors have recently reported 250 rpm agitation as optimal speed with no indication of passive peak for roasted gold ore polarization (Bas et al., 2015a). It has generally been accepted that the leaching rate of gold increases with increasing agitation speed (Jeffrey and Ritchie, 2001). Different optimal agitation/rotation speeds for gold leaching were reported in the literature, e.g. Azizi et al. (2010) demonstrated the maximum gold leaching rate for mineral electrode at 400 rpm electrode rotation speed and observed a progressive decrease above that value, while Kakovski and Kholmanskikh (1960) reported the optimal agitation speed as 150 rpm. The difference in optimal agitation speed is very possibly due to the efficiency and different types of agitation. It can be said also that the presence of different soluble and/or insoluble ions in the solution could have a significant influence on the optimal agitation speed for maximum dissolution behaviour. Then, 100 rpm optimal agitation speed in this current study could be linked to the increased leaching of mineral electrode above 100 rpm agitation, suggesting that the release of species from mineral electrode could partially cover the gold surface (as in Fig. 6.12a) and retard further oxidation of gold.

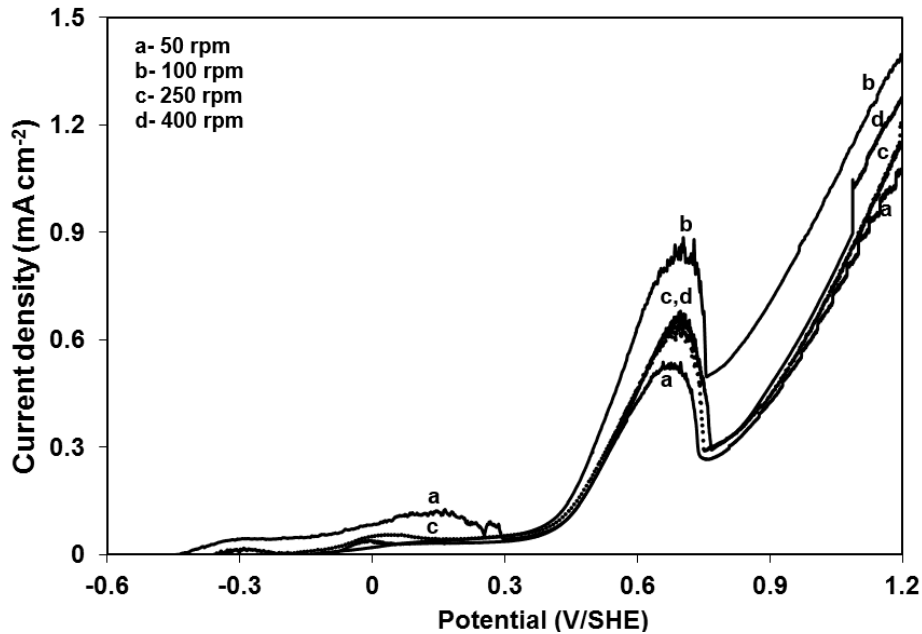


Fig. 6.13 Effect of agitation on anodic polarization of Au connected to MagHem-ES electrode in 0.01 M NaCN solution at 0.166 mV/s scan rate, 25 °C.

The different effects of magnetite and hematite on gold leaching could be ascribed to: (1) the difference in conductivity of these minerals where magnetite is $\sim 10^6$ more conductive if compared to hematite (Greenwood and Earnshaw, 1997); (2) that probably magnetite was cathodically protected in these conditions as a result of the enhanced magnitude of the cathodic current (Filmer, 1982); (3) that in case of hematite, the reduction of oxygen could be proceeded mainly on the surface of gold; (4) the different role of ferrous iron (Fe^{2+}) and ferric iron (Fe^{3+}) ions are suggesting different mechanisms. However, the release of ferric ion, known as a powerful oxidant, into the electrolyte could enhance the dissolution of gold.

6.4 Conclusions

1. Considering the cathodic Tafel slope only by extrapolating to open circuit potential for the estimation of gold leaching rate was successful and corrosion rates for both gold and RGO electrodes were more representative when compared to that of cyanide leaching.

2. The combined anode electrode polarization results showed that:

2.1 When Au electrode was electrically connected with MagHem-ES electrode (consisted of equal quantities of magnetite and hematite in one electrode), a 100 rpm agitation was found to be optimal for a better gold anodic behaviour. The presence of surface products (Fe-oxide, and AuCN) confirmed by SEM are responsible for the passivation of gold surface.

2.2 Hematite, as a part of the combined “Au-hematite anode” system, was found to promote the anodic dissolution behaviour of gold (12% increase in corrosion current (i_{corr})) while magnetite showed negative effect (11% decrease). Two separate containers in the absence of slurry generally showed lower anodic behaviour of gold if compared to that of one container.

2.3 In one container, anodic behaviour of gold was increased as a result of higher current density (up to 10 times) by a magnetic pre-treatment of roasted gold ore electrode before electrically connected to Au electrode, suggesting the removal of some detrimental iron minerals which could lead to a further retard in gold dissolution.

2.4 The presence of slurry resulted in decreasing current densities that indicates lower corrosion rates. However, when the tailings of a slurry was used again as a new feed, the dissolution rate of gold resulted in a 3-fold increase in current density suggesting higher corrosion rate. The release of soluble species into the solution could be the primary factor for inhibiting or passivating the surface of gold.

2.5 In two separate containers (where only one counter electrode was in the cell of Au electrode), the anodic behaviour of gold showed a certain passive behaviour when slurry was in the cell of Au electrode, whereas this passive behaviour was greatly decreased when slurry was not in the cell of Au electrode. When another Pt electrode was placed in the other container (where mineral electrode was placed) and electrically connected Au electrode in presence of slurry, resulted in decreasing passive behaviour and gave higher current densities.

6.5 Acknowledgements

The authors would like to express their sincere thanks and appreciation to Natural Sciences and Engineering Research Council of Canada (NSERC), Barrick Gold Corporation, and Hydro-Quebec for their financial support through R&D NSERC Program. Laval University personnel Mrs. V. Dodier (AAS analysis), Mr. A. Ferland (SEM-EDS analysis), and Mr. F. K. Kadiavi (internship undergraduate student) are gratefully acknowledged for their help.

Chapter 7

Influence of Iron Oxide Slurries on the Dissolution of Gold Electrode

Leaching and Electrochemical Dissolution of Gold in The Presence of Iron Oxide Minerals Associated with Roasted Gold Ore

Ahmet Deniz Bas^{a*}, Fariba Safizadeh^a, Edward Ghali^a, Yeonuk Choi^b

^aDepartment of Mining, Metallurgical and Materials Engineering, Laval University, Quebec, Canada, G1V 0A6

^bBarrick Gold Corporation, Suite 3700, 161 Bay Street P.O.Box 212, Toronto, Ontario, Canada, M5J 2S1

*Corresponding author: 4186568657, Fax: 4186565343; (ahmet-deniz.bas.1@ulaval.ca)

Published in Hydrometallurgy, 166, 143-153. DOI: [10.1016/j.hydromet.2016.10.001](https://doi.org/10.1016/j.hydromet.2016.10.001)

Résumé

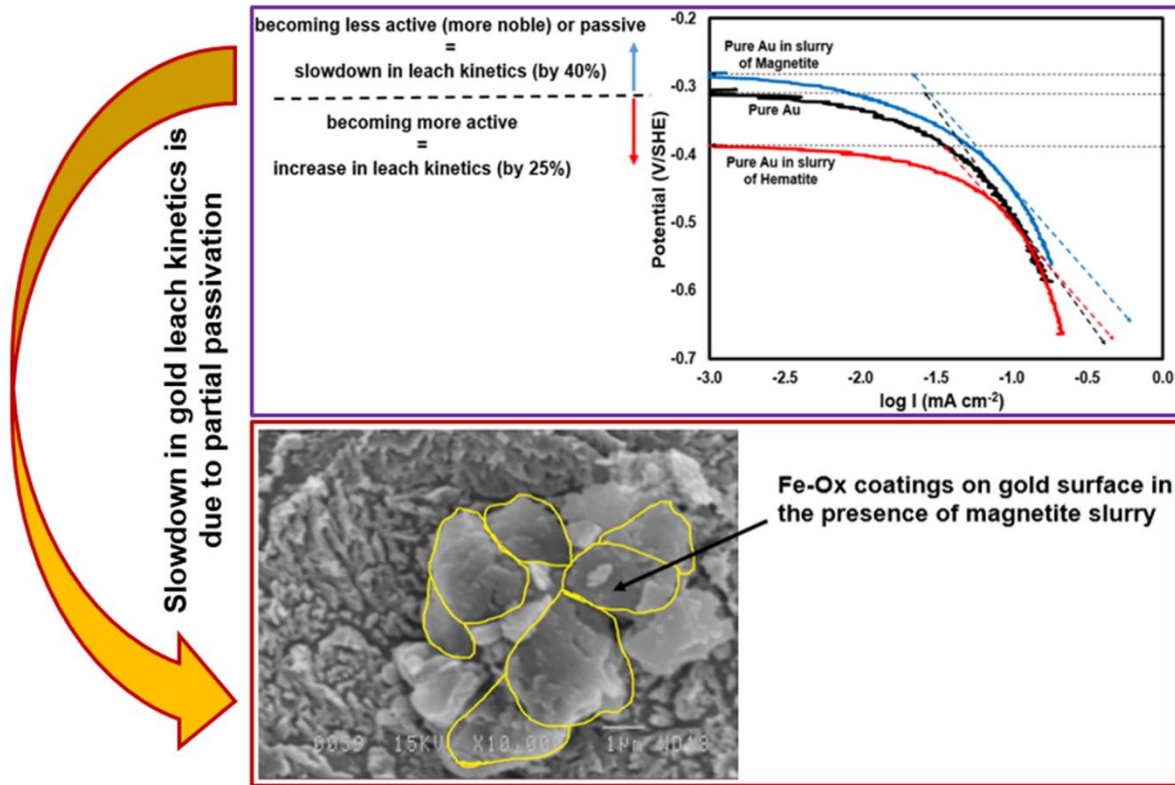
Cette étude examine les interactions électrochimiques entre l'or et le minerai d'or grillé (RGO), avec ses oxydes minéraux associés servant comme pulpe, dans un électrolyte saturé par l'oxygène atmosphérique. La cyanuration conventionnelle a donné à une diminution de ~ 40% de la vitesse de lixiviation de l'or avec de pulpe magnétite, alors que des augmentations de 25% et 10% ont été observées pour hématite et maghémite, respectivement. Ces vitesses de lixiviation de l'or ont été obtenues en appliquant les pentes cathodiques de Tafel seulement. MEB-EDX, dans le cas de la pulpe magnétite, présentait une forte accumulation d'oxydes de fer sur la surface de l'or, ce qui est une indication du ralentissement de la vitesse de lixiviation de l'or. Dans le cas de la pulpe de minerai d'or grillé, des quantités plus faibles d'oxydes de fer ont été détectées avec l'association du revêtement de calcium-magnésium. Les résultats de XPS présentaient également une petite quantité d'or dans la pulpe de particules de magnétite après lixiviation, par exemple, ce qui suggère l'adsorption de l'or par la magnétite, ce qui justifie également le ralentissement de la vitesse de lixiviation de l'or. Les tests de séparation magnétique des résidus de cyanuration contenant 20% Au entrent un 4% (masse-pull) échantillon de concentré magnétique avec 72% non lixivié Au. Minerai d'or grillé, les rejets de la séparation magnétiques et les électrodes de maghémite synthétique présentent un pic cathodique, ce qui indique la réduction de ferriques en ions ferreux, ce qui pourrait être responsable du ralentissement de la cinétique de lixiviation, tandis que le concentré magnétique n'a pas. En outre, lorsque l'oxygène a été barbotée, ce pic a disparu dans le cas du minerai d'or grillé et maghémite synthétique, bien que les rejets de la séparation magnétiques présentaient encore le pic.

Abstract

This study investigates the electrochemical interactions between gold and roasted gold ore (RGO), with its associated oxide minerals serving as slurry, in an electrolyte saturated with atmospheric oxygen. Conventional cyanidation yielded a decrease of ~ 40% in the gold leach rate with magnetite slurry, while increases of 25% and 10% were observed for hematite and maghemite, respectively. These gold leach rates were obtained by applying cathodic Tafel slopes only. SEM-EDS, in the case of magnetite slurry, exhibited a high accumulation of iron oxides on the gold surface, which is an indication of slowdown in the gold leach rate. In the case of roasted gold ore slurry, lower amounts of iron oxides were detected with the association of calcium-magnesium coating. XPS results also exhibited a small amount of gold in the slurry of magnetite particles after leaching, i.e., suggesting the adsorption of gold by magnetite, which also justifies the slowdown in the gold leach rate. Magnetic separation tests of cyanidation tailings containing 20% Au resulted in a 4% (mass-pull) magnetic concentrate sample with 72% non-leached Au. Roasted gold ore, magnetic tailings, and synthetic maghemite electrodes exhibited a cathodic peak, suggesting the reduction of ferric to ferrous ions, which could be responsible for the slowdown of leach kinetics, whereas magnetic concentrate did not. Furthermore, when oxygen was bubbled, this peak disappeared in the case of roasted gold ore and synthetic maghemite, though magnetic tailings still exhibited the peak.

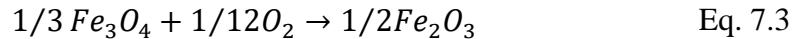
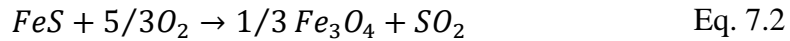
Keywords: Gold, Roasted Gold Ore, Iron oxides, Leaching, Passivation, Electrochemical Dissolution

Graphical Abstract



7.1 Introduction

Due to the rapid depletion of free-milling types of gold ores, it is accepted worldwide that there is an increasing trend in the treatment of refractory gold ores, which often requires oxidation, such as roasting, as a pre-treatment process prior to cyanidation (Adams, 2016; Zhou and Fleming, 2007). Via oxidizing/roasting, pyrite (the most common gold carrier sulphide phase) is made to consist of predominantly hematite, magnetite (Eqs. 7.1-3) and maghemite (Stephens et al., 1990). Paktunc et al. (2006) reported that maghemite associated with gold is problematic for cyanidation as a result of its non-porosity. It has been reported that iron oxides, which are often found to be detrimental in cyanidation (Filmer, 1982; Lorenzen and van Deventer, 1992a), can contain appreciable amounts of gold (30 ppb to 260 ppm) (Paktunc et al., 2006).



Dissolution of gold may be reduced/slowed down in some conditions, and if so, passivation and galvanic interaction phenomena are considered as potentially significant electrochemical factors (Lorenzen and van Deventer, 1992a; Mrkusic and Paynter, 1970). The passivation phenomenon of gold has been known as the formation of a surface film on gold since 1907 (Cathro and Walkley, 1961). Passivation is a commonly used term to explain a phenomenon in many fields, but its meaning could potentially create confusion according to the area of use. In general, two main approaches are considered for the passivation phenomenon: one is defined “as the formation of an adsorbed layer on the tested specimen, e.g. like in stainless steel,” and the second is defined as “a passive film as a diffusion layer of reaction products, e.g., oxides, therefore corrosion rate decreases” (Uhlig, 1963). In a similar manner, Crundwell (2015) identifies passivation, in terms of the corrosion of metals, as the formation of a passive layer composed of metal oxides that lower the rate of dissolution by several orders of magnitude. Hence, the passivation phenomenon should be carefully considered.

The presence of metals/minerals such as silver, iron, arsenic, calcium, and magnesium, which are associated with gold, are important phases that could influence the gold leach rate (Marsden and House, 2006). It has been reported that some ions (silver, lead) in the solution could act to remove the passivation of the gold surface and promote gold dissolution, whereas others (pyrite, copper) slow the kinetics (Lorenzen and van Deventer, 1992b; Deschênes et al., 2000). During cyanidation, not only the individual effects of these metals are important; multi-effects of these minerals, i.e., interactions between many phases, should also be considered (Aghamirian and Yen, 2005; Azizi et al., 2012b). To understand the influence of these minerals on gold dissolution kinetics, different approaches or pre-treatment methods have been considered in the literature to treat these minerals, such as magnetic separation, and diagnostic leach procedures (Lorenzen and van Deventer, 1993; Douglas and Semenyna, 2013). However, in these previous works, conventional cyanidation tests of sulphidic gold ores have mostly been considered. Hence, it is worth mentioning that there is paucity for the electrochemical characterization studies of oxide gold samples after pre-/treatment methods.

In particular, the general goal of this paper is to provide an alternative explanation for the slowdown of the gold leach rate for oxide/oxidised gold ores during cyanidation. Thus far, electrochemical studies of oxide gold ores have received relatively less attention than sulphidic ones because almost all previous electrochemical studies were performed using only sulphidic gold ores (van Deventer and Lorenzen, 1987; van Deventer et al., 1990; Lorenzen and van Deventer, 1992a; Deschênes et al., 2000; Aghamirian and Yen, 2005; Cruz et al., 2005; Dai and Jeffrey, 2006; Azizi et al., 2010, 2011, 2012a, 2012b, 2013). As a result, the treatment of oxidised gold ores by electrochemical techniques and conventional cyanidation has become very essential in recent years. Hence, the objectives of this paper are: (i) to examine the influence of iron oxide minerals on the gold leach rate; (ii) to compare/implement the electrochemical findings in conventional cyanidation results; (iii) to obtain a gold-bearing iron oxide magnetic concentrate and characterize its electrochemical dissolution behaviour; and (iv) to provide an alternative explanation for the slowdown in the gold leach rate supported by surface characterization studies.

7.2 Experimental Conditions

7.2.1 Ore Sample and Iron Oxide Minerals

A roasted gold ore sample (80% passing $-75\ \mu\text{m}$ (d_{80})) was received from Barrick Gold Corporation. Mineralogical analyses of the sample using X-ray diffraction (XRD, Siemens D-5000) and scanning electron microscopy (SEM, JEOL 840-A) indicate that the ore sample consists predominantly of quartz, dolomite, calcite, gypsum, and iron oxides, such as hematite, magnetite, and maghemite, with almost no sulphur content. Microscopic analysis showed that the gold is mainly associated with iron oxides. Metal analysis has shown that the gold and silver contents are ~ 8 and ~ 5 g/t, respectively (Bas et al., 2015a).

Sodium cyanide (NaCN) with a purity of more than 98% was obtained from Thermo Fisher Scientific Company. An electrolyte medium (250 mL) was prepared using distilled water, and the pH was adjusted to 10.5 by adding 1 M NaOH. The electrolyte was agitated with a magnetic bar (4 cm long and 1 cm in diameter) during tests. A pure gold (Au) disc electrode was used as a working electrode, with platinum (Pt) as a counter electrode and Ag/AgCl, KCl_{sat} as a reference electrode. The gold foil with a surface area of $0.25\ \text{cm}^2$ (99.9% purity from Sigma Aldrich), as the pure gold electrode (Au), was first polished with a fine (MicroCut® 100 Grit Soft) polishing paper and then rinsed in distilled water. Then, it was introduced in aqua-regia for 10 seconds to clean the surface, washed with distilled water and ethanol, and finally rinsed with distilled water again to assure the reproducibility (Kirk et al., 1978). The detailed electrode preparation procedure can be found in the author's previous works (Bas et al., 2015a, 2015b).

In these tests, the pure Au electrode was immersed in 0.01 M NaCN electrolyte, and the influence of ore (RGO, 10% solid ratio) and iron oxide minerals, such as magnetite (Mag), hematite (Hem), and maghemite (Mgh) at a 0.5% solid ratio, as a slurry, on gold leaching was tested. Maghemite was prepared by heating magnetite in an oven at $200\ ^\circ\text{C}$ for 3 h, giving it the light brown colour of maghemite (Legodi and Waal, 2007), and this was proved by XRD (Bas et al., 2015c). Due to the difficulty in distinguishing magnetite and maghemite minerals by XRD, another maghemite preparation procedure (heating

magnetite at 250 °C for 5 h) was also considered (Paktunc, 2014), and nevertheless, very close results were obtained (Bas et al., 2015b).

7.2.2 Electrochemical and Leaching Test Procedures

First, electrodes were allowed to stay at open circuit potential (OCP) for 2 minutes before linear polarization tests with a range of ± 25 mV with respect to corrosion potential (E_{corr}). Actually, different stabilization times (up to 30 minutes) were also considered, and the results were found to be highly reproducible (Bas et al., 2015c). Then, cathodic polarization tests were performed by scanning from E_{corr} to -300 mV, and the corrosion current (i_{corr}) was estimated by considering the cathodic Tafel slope, only extrapolating to OCP. Tests were generally performed in the 0.01 M NaCN electrolyte at a pH of 10.5 with 100-rpm magnetic agitation (4 cm long and 1 cm in diameter) at room temperature, saturated with atmospheric oxygen, unless otherwise reported (Bas et al., 2015b). A scan rate of 0.166 mV/s was selected based on the polarization standards (ASTM Standard G 5-94, 2006). Electrochemical tests were performed in at least triplicate to ensure the reproducibility. Corrosion rates of gold by Tafel were compared to cyanide leaching results. In the case of cyanide leaching tests, the leach solution was prepared using deionised-distilled water at the prescribed concentration of reagent and leached for 4 h. In certain experiments, a systematic approach was considered to examine the influence of soluble ions on the gold dissolution rate. In this case, a slurry of RGO (10% solid ratio) was leached over 24 h to have as many soluble ions in the solution as possible and then filtered to obtain only the leached solution, which is considered a stock solution for use in certain experiments and is named “pure Au in the release solution of the RGO slurry” in this manuscript. Note that the initial gold concentration within the released solution of the RGO slurry was subtracted to consider the actual leach rate of gold in these particular experiments in which pure Au was immersed in this released solution of the RGO slurry.

In the case of conventional cyanidation, tests were carried out in a glass reactor over a period of 24 h. The concentration of NaCN in solution was monitored by silver nitrate titration (0.02 mol/L AgNO_3) using p-dimethylamino-benzal-rhodanine (0.02% w/w in acetone) as the indicator. It is important to note that the titration method used herein is a

simple and fast one, although it may overestimate the free cyanide level (Breuer et al., 2011). Sodium cyanide was added to maintain the concentration of titratable NaCN at the predetermined level over the leaching period. Pulp (25% w/w) was stirred with an overhead stirrer at 400 rpm. During all experiments, the pH was maintained at 10.5 by the addition of 1 M NaOH. The solution (10 mL) was sampled at predetermined intervals and analysed by a Microwave Plasma-Atomic Emission Spectrometer (4100 MP-AES by Agilent Technologies) to determine the leach rate of gold and iron. In the termination of leaching tests after 24 h, residues were collected by filtration and then dried in an oven at 105°C for 6 h. Dried residues were then digested in hot aqua-regia (Balaram et al., 2013). MP-AES is a recent methodology that is especially suitable for the detection of gold, even at low concentrations (Shareder et al., 2011).

7.2.3 Magnetic Separation Tests

The tailings of cyanide leaching of roasted gold ore slurry were considered as the feed to magnetic separation. These tests were performed using a Carpco Model MWL-3465 laboratory high-intensity wet magnetic separator with a 40% solid ratio. This magnetic separator was designed specifically for use in research on wet magnetic separation of magnetic minerals, and it was conceived as a laboratory tool. Magnetic separation tests were performed using high range mode at ~3 amperes (A) with 0.1 amp (A) graduations. The magnet has a gap of 2.5 inches between the pole pieces. The maximum magnetic flux produced in the gap in air is 3800 gauss. The separated magnetic concentrate and magnetic tails were put into the oven at 85°C for 6 hours. Then, electrodes were prepared from these samples for potentiodynamic cathodic (from OCP to cathodic or cathodic to OCP) and anodic polarization tests.

7.3 Results and Discussion

7.3.1 The Influence of Cyanidation on the Open Circuit Potential (OCP) of Au

The change in the open circuit potential (OCP) of gold could give an idea about the active behaviour of gold dissolution. Note that the OCP also corresponds to the corrosion/dissolution or leaching potential. Then, the influence of time on gold corrosion potential behaviour in different conditions is shown as prior to leaching and at the end of

leaching (after 4 h) in [Table 7.1](#). It was found that the dissolution potential of the pure gold electrode trended towards a less negative potential, from -0.365 V/SHE to -0.333 V/SHE, at the end of 4 h of leaching. Likewise, when the pure gold electrode was placed in the slurry of roasted gold ore (RGO), the dissolution potential of gold showed close potential with a 10-mV shift to a less negative potential (-0.320 V). During the 4 h of leaching, the highest shifts/changes (~ -80 mV) in the OCP were obtained for hematite and maghemite, while magnetite had the lowest change (~ -18 mV). As seen from [Table 7.1](#), the OCP of pure Au in a slurry of hematite and maghemite shifted to more active potentials by ~ -50 mV and ~ -20 mV, while it shifted to a more noble (less negative) potential by +15 mV in the case of magnetite. This could suggest/explain the positive effect of hematite and the negative effect of magnetite, as illustrated in the examples in [Table 7.2](#).

Table 7.1 Open Circuit Potential (OCP) (V/SHE) of electrodes for 2 minutes prior and after 4 h of leaching.

Electrode type	Corrosion potential (V/SHE)	
	Prior to leaching	End of leaching (after 4 h)
Pure Au	-0.365 \pm 3.012%	-0.333 \pm 5.402%
Pure Au in a slurry of RGO	-0.365 \pm 1.913%	-0.320 \pm 5.004%
Pure Au in a slurry of magnetite (0.5%)	-0.300 \pm 7.852%	-0.318 \pm 6.521%
Pure Au in a slurry of hematite (0.5%)	-0.305 \pm 3.566%	-0.386 \pm 4.283%
Pure Au in a slurry of maghemite (0.5%)	-0.270 \pm 3.727%	-0.355 \pm 5.125%
Pure Au in a slurry of a mixture of Magnetite + hematite (0.5%)	-0.285 \pm 8.674%	-0.310 \pm 4.352%

The shift/change in the dissolution potential of gold during leaching has been reported in the literature. For instance, [Lorenzen and van Deventer \(1992a\)](#) found that the dissolution potential of gold shifted to less negative/active values with a concurrent decrease in dissolution current when gold is immersed in a slurry of sulphide minerals, and this was linked to the retarding effect on the gold dissolution rate. [Bas et al. \(2015a\)](#) reported that the corrosion potential of pure gold and RGO electrodes in the presence of a slurry of roasted gold ore (35%) resulted in less negative potentials if compared to that in the absence of slurry. [Aghamirian and Yen \(2005\)](#) concluded that gold galvanic corrosion could not be estimated using only the potential difference between gold and sulphide minerals.

Although the corrosion potential alone is not sufficient to estimate the dissolution rate of gold, it could still provide significant information regarding the possible active and passive behaviours of the tested specimen.

7.3.2 Corrosion Rate of Au by Cathodic Polarization and Conventional Leaching

In this study, the leach (corrosion) rate of gold was estimated by extrapolation of the cathodic Tafel slope to open circuit potential (Fig. 7.1). It is worth noting that, due to the difficulty in the Tafel extrapolation, two recommended rules as follows are carefully considered as far as possible in this study: i) the extrapolation should start at least 50-100 mV away from E_{corr} , and (ii) at least one of the branches of the polarization curve (cathodic or anodic) should exhibit Tafel over at least one decade of current density (Kelly et al., 2002). However, in this study, it should be underlined that the complete decade is partially observed (~ 55%) for the pure gold and much less in the presence of slurries. It is important to note that, although the slopes are similar, the level of the open circuit potential plays a significant role in the determination of the leach rate of gold.

Table 7.2 Corrosion rates of Au in different conditions (Pure Au electrode: 0.25 cm²).

Electrode type	Considering only the cathodic polarization approach		Conventional cyanidation		
	Corrosion current ($\mu\text{A}/\text{cm}^2$)	Corrosion rate ($\times 10^{-6} \text{ mol m}^{-2} \text{ s}^{-1}$)	Leach rate ($\times 10^{-6} \text{ mol m}^{-2} \text{ s}^{-1}$)	Dissolved Au (mg)	Dissolved Fe (mg)
Pure Au	100	$5.17 \pm 2.45\%$	$4.61 \pm 5.56\%$	0.33	--
Pure Au in a slurry of RGO (10%)	--	--	$7.25 \pm 1.34\%$	0.51	0.12
Pure Au in a slurry of magnetite (0.5%)	66	$3.34 \pm 2.09\%$	$2.63 \pm 3.96\%$	0.186	0.30
Pure Au in a slurry of hematite (0.5%)	200	$10.38 \pm 4.60\%$	$5.76 \pm 11.93\%$	0.40	0.07
Pure Au in a slurry of maghemite (0.5%)	120	$6.26 \pm 9.73\%$	$5.05 \pm 5.42\%$	0.36	0.062
Pure Au in a slurry of a mixture of magnetite + hematite (0.5%)	84	$4.33 \pm 4.50\%$	$4.13 \pm 1.26\%$	0.29	0.140

Note: The slurry of RGO alone test (10%) resulted in 0.092 mg of dissolved Au in the electrolyte.

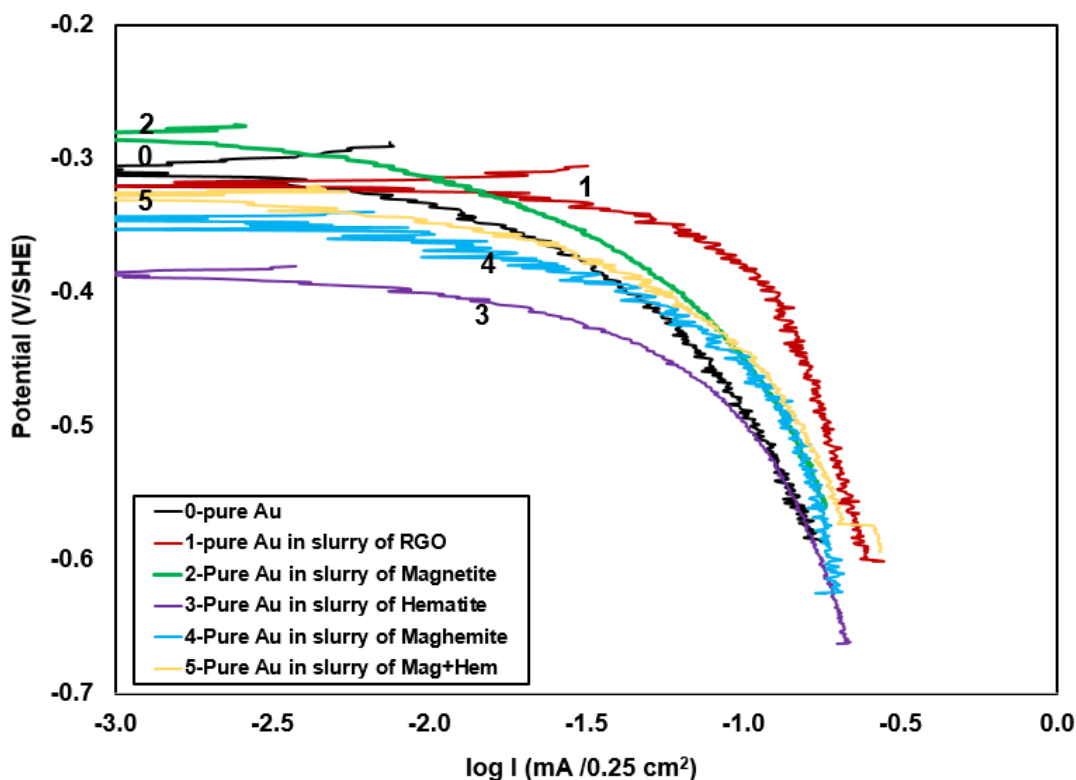


Fig. 7.1 Corrosion rate of Au in 0.01 M NaCN, with a pH of 10.5 and 100-rpm agitation at 25 °C; cathodic polarization curves in different conditions.

As seen from Fig. 7.1, a higher corrosion current, i.e., corrosion rate, was obtained in the case of hematite, whereas the rate was decreased within the magnetite slurry. These findings are in accordance with those obtained in conventional cyanidation results (Table 7.2). A comparison of these two methods for leach rates, corrosion current and dissolved metal are given in Table 7.2. As seen, the leach rate of gold from the pure Au electrode was found to be $4.61 \times 10^{-6} \pm 5.56\%$ mol m⁻² s⁻¹ after 4 h of leaching by conventional cyanidation, whereas it was calculated to be $5.17 \times 10^{-6} \pm 2.45\%$ mol m⁻² s⁻¹ when considering the cathodic Tafel slope. This moderate difference in the two methods is reasonable since the electrochemical method is considered to be just an estimation. In the case of the pure Au electrode immersed in a slurry of roasted gold ore (RGO), a higher gold leach rate, i.e., $7.25 \times 10^{-6} \pm 1.34\%$ mol m⁻² s⁻¹, was obtained by conventional cyanidation. However, for the pure Au electrode in a slurry of RGO, extrapolation of cathodic Tafel according to these two assumptions was not suitable due to the presence of

a diffusion control region and the presence of different phases. As seen from [Table 7.2](#) and [Fig. 7.2](#), there is a difference in the dissolved gold (mg) between the sum of “pure Au alone + the slurry of RGO alone (0.33 mg + 0.092 mg)” and “pure Au in a slurry of RGO (0.51 mg).” This difference could have arisen due to the presence of ferric iron in the electrolyte, which could accelerate the gold dissolution, and also inhomogeneous characteristics of roasted gold ore, which may contribute to the gold dissolution. Additionally, it can be explained by the potential partial passive behaviour of gold in pure systems, which is clearly demonstrated in the literature ([Jeffrey and Ritchie, 2001](#); [Bas et al., 2015d](#)).

Because iron oxides (hematite, maghemite, and magnetite) are the main gold phases in roasted gold ore, their influences as a slurry on gold dissolution are demonstrated in [Table 7.2](#). In the presence of a slurry of magnetite, the rate of gold dissolution was markedly reduced by ~ 40% compared to the pure Au electrode alone, which could mainly be linked to the dissolved species that precipitate on the surface of gold; alternately, the undesired precipitation of Fe(II) could be responsible for this retarding effect. This result is also supported by SEM images showing the high accumulation of iron oxide coatings on the surface of the gold electrode ([Figs. 7.3b, c, and d](#)), which could be responsible for the partial passivation of the gold’s surface. Additionally, as the dissolution potential shifts to less negative values (from -0.333 to -0.318 V) ([Table 7.1](#)), very possibly due to control by limited anodic sites, the dissolution current density decreases (from 100 to 66 $\mu\text{A}/\text{cm}^2$) ([Table 7.2](#)) accordingly, thus indicating the slowdown in the gold dissolution rate in the presence of a magnetite slurry. Note that this negative effect of magnetite on gold dissolution has been extensively examined to ensure reproducibility. Similar negative effects on the gold dissolution rate in cyanide solutions, e.g., 40% in presence of magnetite and 84% in the presence of copper, were previously reported in the literature ([Lorenzen and van Deventer, 1992b](#)). Alternately, hematite and maghemite minerals showed positive effects on the gold dissolution rate (~ 25% and 10%), relatively. This positive behaviour could be explained by the release of ferric ion from hematite as a powerful oxidant that can promote gold dissolution. These findings are also consistent with the author’s previous results by potentiodynamic polarization ([Bas et al., 2015b](#)) and galvanic corrosion tests, showing the positive effect for hematite and maghemite in current density and galvanic

current when the mineral electrodes were electrically connected to the gold electrode (Bas et al., 2015c). It is important to note that, in the case of a “pure Au electrode immersed in a slurry of hematite,” the corrosion rate by the electrochemical method ($10.38 \times 10^{-6} \pm 4.60\%$ mol m⁻² s⁻¹) was found to be too high compared to that obtained by MP-AES (Table 7.2). This could be due to the very low conductive property of hematite and the blocking action of slurry on the surface of the gold electrode. Different behaviours for the same minerals/metals have been reported in the literature, for instance. Filmer (1982), Paul (1984), and Lorenzen and van Deventer (1992a) reported the negative effect of pyrite and pyrrhotite on gold dissolution, while Aghamirian and Yen (2005) reported an increase in galvanic current when these minerals are in galvanic contact with gold.

Estimation of gold corrosion rate by electrochemical tests is a subject of discussion in the literature. The pioneering work in gold electrochemistry by Kudryk and Kellogg (1954), and Cerovic et al. (2005) considered the intersection of cathodic and anodic curves for the calculation of the gold leach rate. However, recent studies by Dai and Breuer (2013), and Bas et al. (2015a, 2015b) reported that considering intersection seems to be misleading since it is unrepresentative of practical conditions, and there is a potential passive behaviour in the anodic curve. Bas et al. (2015a, 2015b) considered only cathodic Tafel slope extrapolation to the open circuit potential, as a new approach, which was found to be representative of the conventional cyanidation.

In roasted gold ore, gold is mainly associated with iron oxide minerals. Then, the leach rate of iron compared to gold could provide significant information about the active and passive behaviours of gold dissolution. Generally, it is important to examine the influence of soluble and insoluble products on gold dissolution; then, in our study, the influence of soluble iron is examined (Table 7.2 and Fig. 7.2). Note that, in the case of pure Au in the released solution of an RGO slurry test (mentioned before in section 7.2.2), labelled as 3 in Fig. 7.2, the gold concentration coming from the released solution is subtracted to calculate the actual initial gold dissolution. A higher gold leach rate was obtained when pure Au was immersed in a slurry of RGO (with a lower iron dissolution, 0.12 mg, as shown in Table 7.2) if compared to that of pure Au in the released solution with an RGO

slurry where the iron dissolution was analysed and found to be higher (0.19 mg, not shown). The increase at the interface in the amount of leached soluble iron ions in the solution is an indication for the slowdown in gold leach rate, suggesting the important role of soluble ions on dissolution kinetics, as though referring to the partial passivation of gold.

Due to the presence of many different mineral phases (complexity) in roasted gold ore, sample solutions were then again analysed after one and two days by MP-AES to monitor if there is an undesired precipitation of gold, but almost the same results were obtained. Because MP-AES is a type of new and recommended tool for gold analysis, and the reproducibility and reliability of metal analyses by MP-AES were also confirmed with a 0.9999 of R^2 for the calibration of Au.

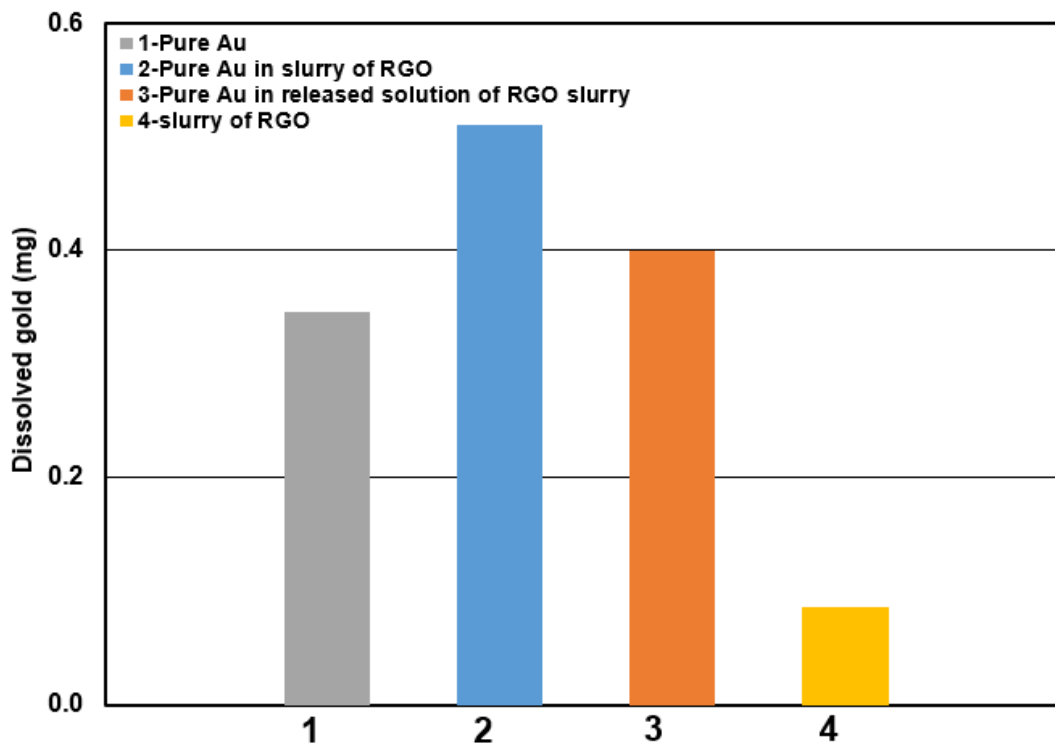


Fig. 7.2 The influence of soluble species on the dissolution kinetics of gold (mg) after 4 h in 0.01 M NaCN, with a pH of 10.5, under 100-rpm agitation, at 25 °C by MP-AES.

7.3.3 SEM-EDS, and XPS studies

When the pure gold electrode was immersed in a slurry of RGO, some spots of iron oxide species as coatings were observed on the gold surface (Fig. 7.3a). A very small number of spots composed of calcium and magnesium coating, together with iron oxide species, was also detected on the gold's surface. XRD results demonstrated the removal or solubilisation of calcite to some extent from slurry of RGO (not shown) which confirms the presence of calcium and magnesium coatings.

Alternately, high accumulations of iron oxide species (as large crystals) were observed by SEM-EDS studies in the case of magnetite slurry (Figs. 7.3b, c, d, and e), whereas very small amounts of iron oxides, just as small spots, were observed for hematite and maghemite slurry tests on the gold's surface. The observed iron oxide coatings at high amounts in the magnetite test are an indication of the decrease in leach rate, as seen in Table 7.2 (Fig. 7.3e). After these tests, the slurry of each iron oxide mineral was collected by filtration for metal analysis. It is important to underline that XPS detected a very small amount of metallic gold in the collected slurry of magnetite (Fig. 7.4), while no gold was detected for hematite, and maghemite. This finding suggests that the dissolved gold from the pure gold electrode in the solution could partially be robbed/adsorbed by magnetite particles, which is a possible mechanism that could slightly influence gold dissolution (Alorro et al., 2010; Parga et al., 2011).

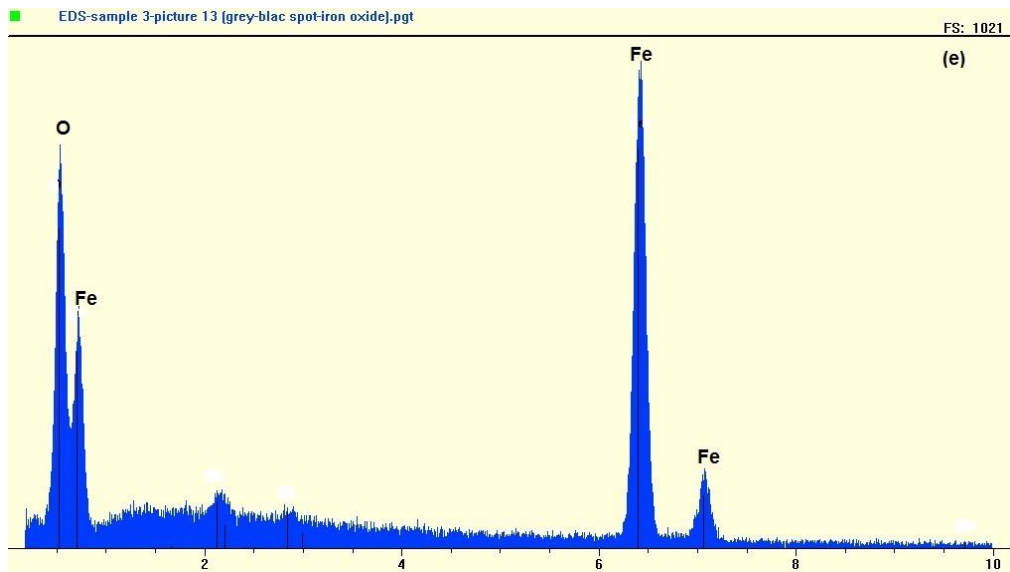
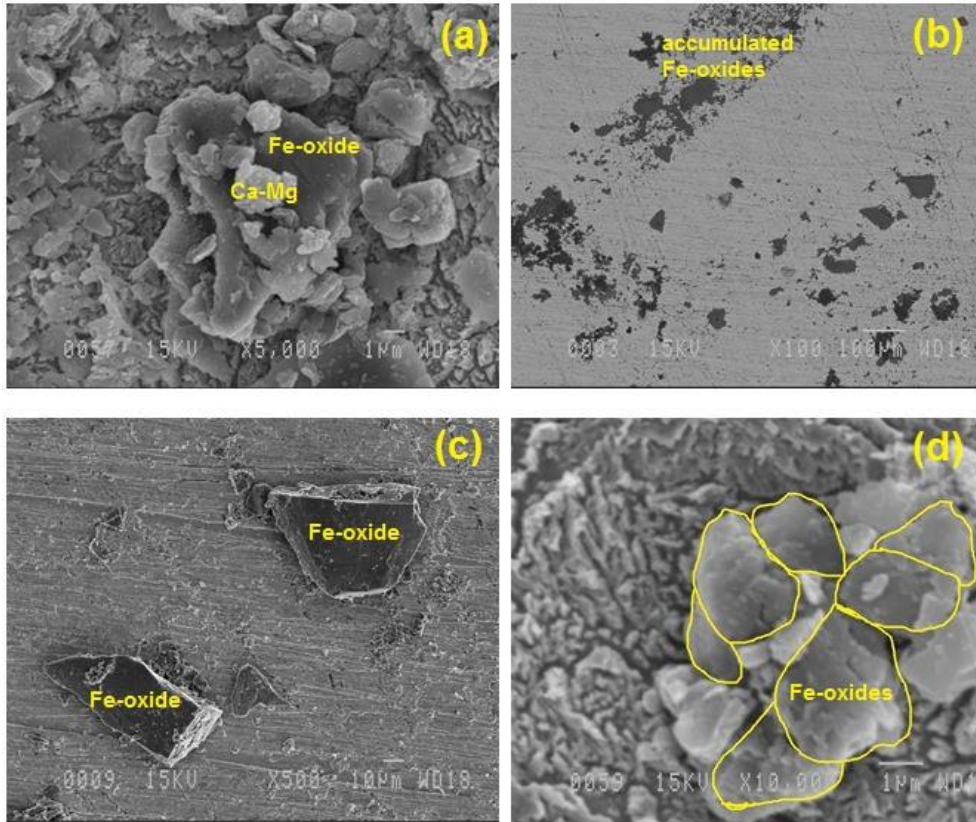


Fig. 7.3 SEM images of coatings on the pure Au electrode after 4 h of leaching; (a) pure Au in a slurry of RGO (x 5000); (b), (c), and (d) pure Au in a slurry of Magnetite (x 100), (x 500); (x 10000), respectively; (e) EDS profile (after the magnetite test) showing Fe-Ox.

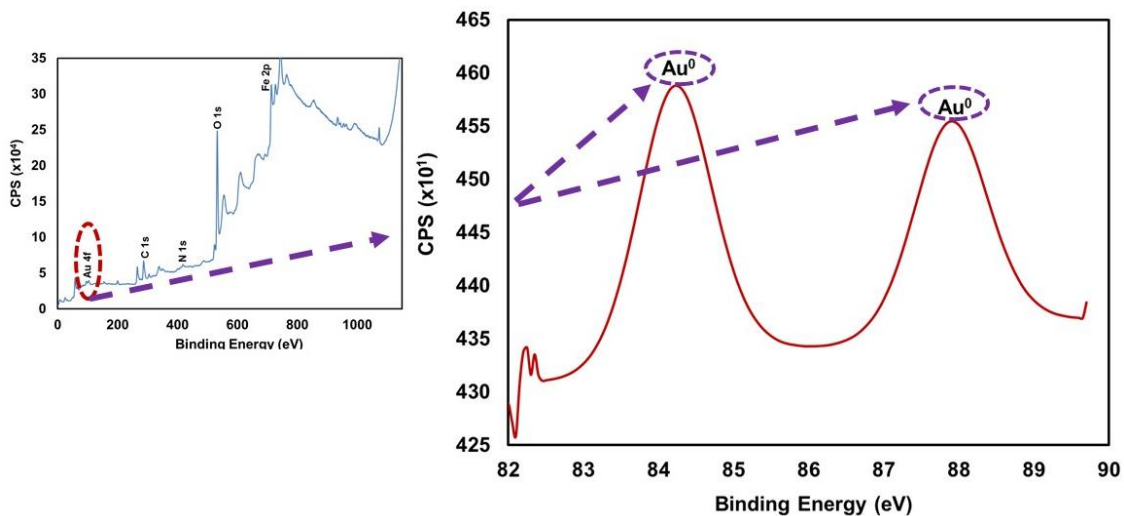


Fig. 7.4 XPS profile of magnetite particles (survey spectrum and Au 4f/2 spectrum).

7.3.4 Cyanidation of RGO and Gold Recovery from Magnetic Concentrate

The addition of suitable lead nitrate concentration is a common and effective practice for increasing the overall gold extraction and reducing the consumption of cyanide. In cyanidation, the use of lead nitrate has been considered in different cases, such as during or combined with the pre-aeration prior to cyanidation. This has been applied mostly for sulphide-bearing gold ores (Deschênes et al., 2000). In this study, to compliment the previous works, the influence of lead nitrate on roasted gold ore has been examined. The addition of lead nitrate showed a slight increase in overall gold extraction and reduced the cyanide consumption by 25% over 24 h of leaching (Table 7.3). The reproducibility of the tests is evaluated at $\pm 1.5\%$. These results are in line with the previous works using sulphidic gold ores. For instance, Deschênes and Wallingford (1995) obtained a similar trend in gold recovery and in cyanide consumption. This result indicates that lead-assisted cyanide leaching could also be effective for roasted gold ores to some extent.

Table 7.3 Influence of lead nitrate on the cyanidation of roasted gold ore, pH: 10.5, NaCN: 0.01 M, 24 h.

Pb(NO ₃) ₂ (g/t)	Au Extraction (%)	NaCN Consumption (kg/t)
0	80.93	0.98
100	82.51	0.73

Previous studies have shown that the iron oxide phase that captures the majority of the gold in tailings is maghemite ($\text{Fe}_{2.67}\text{O}_4$), which is highly magnetic (Paktunc et al., 2006; Douglas and Semenyna, 2013). Hence, a magnetic concentrate could provide significant information for a better understanding of the unrecovered gold. Magnetic separation results have shown that the magnetic concentrate corresponds to 4.29% of the feed material and that 95.71% corresponds to the magnetic tails. Gold distribution results after conventional cyanidation by fire-assay analysis ($\pm 0.24\%$) have shown that 72.014% of gold (4.25×10^{-4} g Au) is in the magnetic concentrate and that 27.986% of gold (1.65×10^{-4} g Au) is in the magnetic tails (Fig. 7.5). Amponsah et al. (2010) performed magnetic separation tests using a similar gold ore sample and reported that gold in the magnetic concentrate corresponds to 79.67%, with 20.33% in the non-magnetic part and a 6.47% mass pull to the magnetic concentrate.

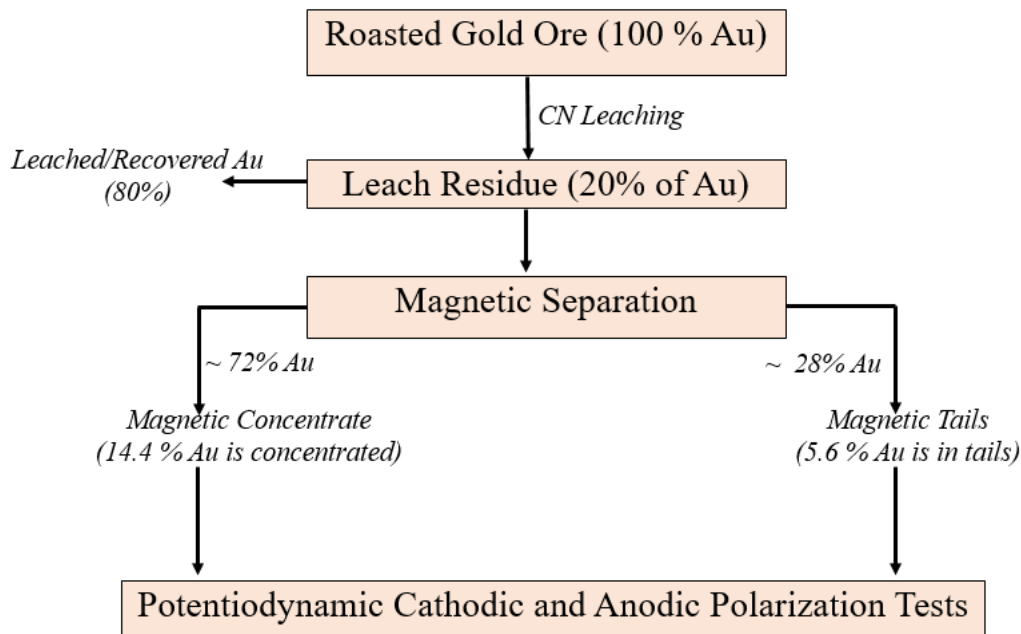


Fig. 7.5 Processing route for maghemite-rich magnetic concentrates.

The efficiency of magnetic separation is essential for the better recovery of gold. For instance, Douglas and Semenyna (2013) obtained an approximately 30-45% magnetic recovery efficiency of the iron oxides present in the leach tailings, resulting in a magnetic

concentrate containing 20-30% of the residual gold. They reported that 35% of those magnetic iron oxides were found to associate with gangue minerals (silicates, quartz, etc.). To provide a higher-grade concentrate, they used a cleaner circuit, but the resulting magnetic cleaner tailings represented a 40-50 per cent loss of gold content.

Characterization tests have been performed to identify the efficiency of magnetic separation test. XPS results have shown that the iron in atomic percentage in the magnetic concentrate is 2.3 times higher (from 3.75% to 1.60%, $\pm 5\%$) than that in magnetic tails, which is in line with the magnetic separation results (Fig. 7.6). In the magnetic concentrate, the Fe-to-As ratio was found to be 3 times greater than that in magnetic tails. In the magnetic tails part, the Ca and Mg percentages were found to be 2 and 1.2 times greater than those of the magnetic concentrate. SEM-EDS results (Fig. 7.7) have also shown that iron oxides (light-white phases) are dominant in the magnetic concentrate, whereas gangue minerals (Ca, Si) are dominant in the magnetic tails, which is in line with the XPS results.

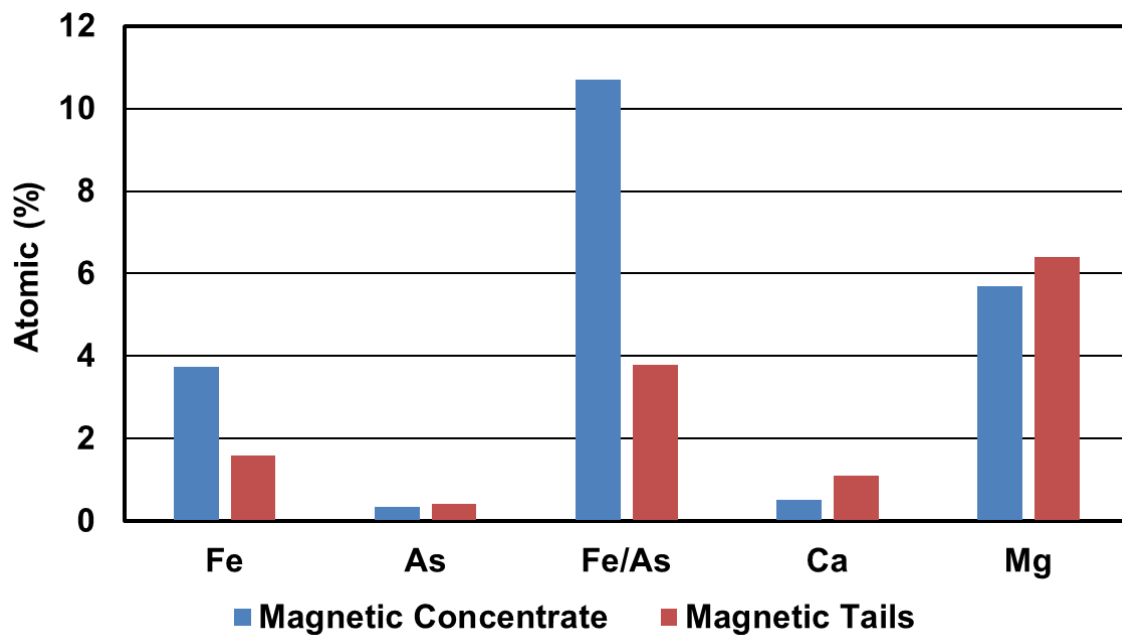


Fig. 7.6 Atomic (%) of elements ($\pm 5\%$) in the magnetic concentrate and magnetic tails by XPS.

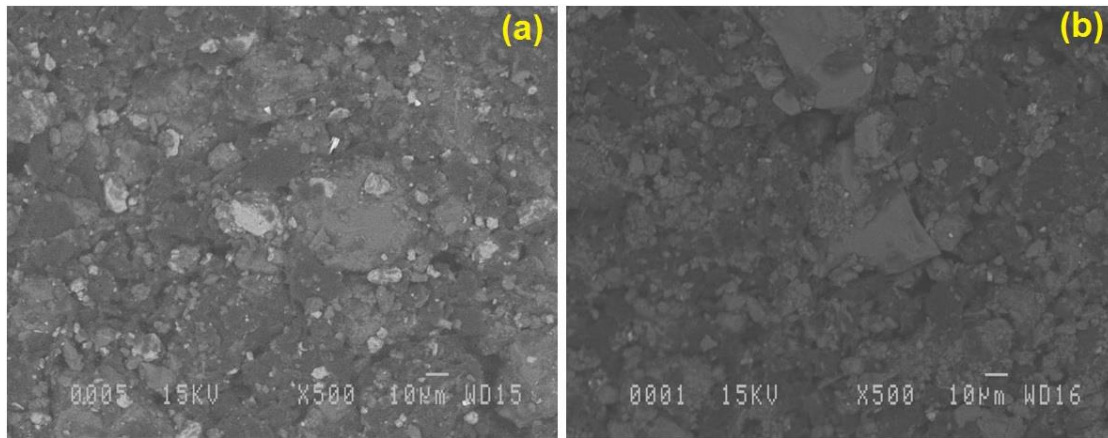


Fig. 7.7 SEM images of the magnetic concentrate (a) and magnetic tails (b). (The light-white phase is Fe-Ox, and the grey phase is Ca and Si).

Moreover, the efficiency of magnetic separation was also tested by XRD analysis. As seen in Fig. 7.8, the magnetic concentrate was mainly found to be composed of magnetic iron oxides, while the magnetic tails part was mainly composed of gangue minerals, such as quartz, calcite, dolomite, and gypsum.

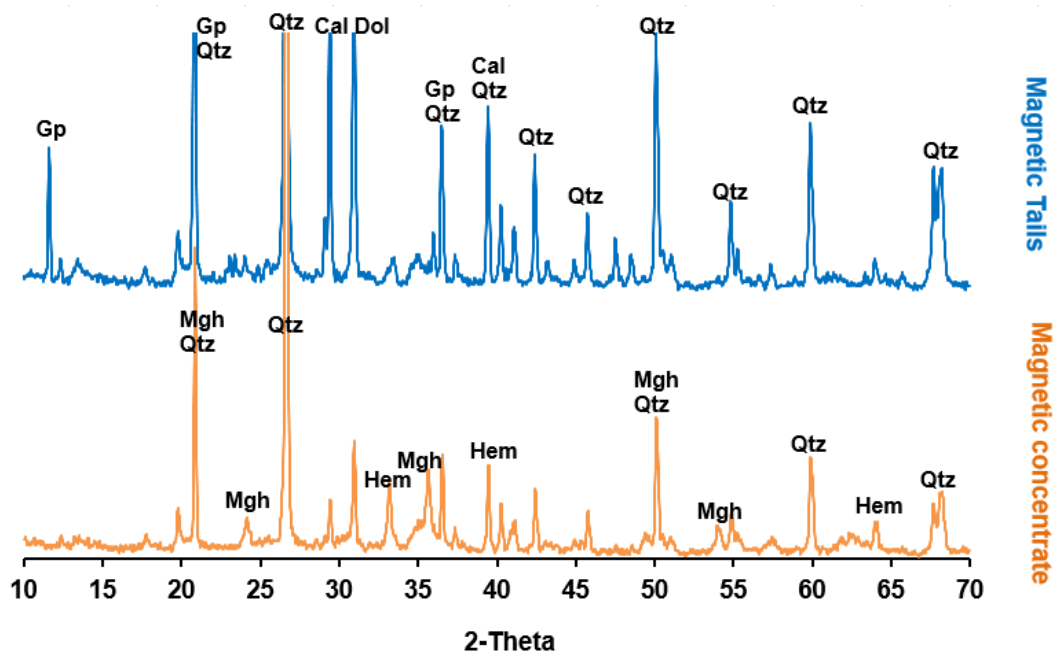


Fig. 7.8 XRD profiles of the magnetic concentrate and magnetic tails (Mgh: Maghemite; Hem: Hematite; Qtz: Quartz; Cal: Calcite; Dol: Dolomite; Gp: Gypsum).

Due to the non-porous property of maghemite, it is not easy to recover the total gold remaining in the tailings. Fosu (2016) used the magnetic concentrate of cyanide leach tailings (which was already roasted) and performed roasting tests as a second stage to recover gold. However, he concluded that gold is still encapsulated by maghemite and not amenable to cyanidation. Then, following the second-stage roasting, he proposed a second-stage magnetic separation for future studies. He noted that a detailed economic evaluation is highly required for gold recovery from the magnetic concentrate. Amponsah et al. (2010) studied the efficiency of magnetic separation of the gold-bearing concentrate at different solid ratios and using different magnets. Note that previous studies using roasted gold ore mainly focused on the efficiency of magnetic separation and that further electrochemical characterization studies were not considered in detail.

7.3.5 Electrochemical Characterization of the Magnetic Concentrate and Tailings

It is important to examine the electrochemical corrosion characteristics of the magnetic concentrate and magnetic tails since the remaining gold is associated with those materials. In this regard, potentiodynamic cathodic and anodic polarization tests of the magnetic concentrate and magnetic tails were performed at least three times (to ensure their reproducibility), and these findings were compared to those of synthetic maghemite (prepared at our laboratory), roasted gold ore (RGO), and pure gold electrodes.

Potentiodynamic Cathodic Polarization of Different Electrodes

Cathodic polarization tests were performed in two different directions: polarization from the open circuit potential (OCP) to the cathodic potential (Fig. 7.9a) and polarization from the cathodic potential to the OCP (Fig. 7.9b). As seen in Fig. 7.9a, one reduction peak at ~ -0.3 V/SHE was observed for roasted gold ore, synthetic maghemite, and magnetic tailings electrodes when polarization was performed from the OCP to the cathodic potential. However, no peak was observed for the magnetic concentrate electrode in the same direction of polarization. This peak can be explained by the reduction of Fe(III) in the oxides to the Fe(II) cyanide complex, which is a possible reaction that could take place according to the Eh-pH diagrams (Osseo-Asare et al., 1984). Alternately, no peak was observed for all the electrodes when polarization was performed from the cathodic potential

to the OCP. Hence, it should be noted that, when polarization is conducted from the OCP to the cathodic potential, it means that the exposed surface of the electrode initially had corrosion behaviour and was then polarized, whereas corrosion behaviour is reached after a certain period when polarized from the cathodic potential to the OCP.

It was found that the OCP of the magnetic concentrate electrode shifted to a more negative/active potential (by 350 mV/SHE) when polarized from the cathodic potential to the OCP. This behaviour can be explained by the positive effect of hematite found in the magnetic concentrate, which is in line with the findings in the beginning (Tables 7.1 and 2).

It is important to characterize the peak formed with synthetic maghemite, magnetic concentrate, and roasted gold ore electrodes (Fig. 7.9a). Oxygen was bubbled to examine the characteristics of this peak. As seen in Fig. 7.10a, the peak that was formed in the presence of atmospheric oxygen for the synthetic maghemite electrode disappeared when oxygen was bubbled into the electrolyte, resulting in a higher corrosion rate. Similarly, this peak also disappeared in the case of the RGO electrode when oxygen was bubbled (Fig. 7.10b), but it resulted in lower current density, which could be linked to the presence of many different phases in the RGO electrode. Alternately, in the case of magnetic tailings where gangue minerals are dominating, this peak was still there even when oxygen was bubbled, suggesting that the peak is very stable in this case. As seen, this peak forms at almost the same potential range in all three conditions, as shown in Fig. 7.10, and therefore this peak is very probably related to the reduction of ferric ions to ferrous ions according to the E-pH diagrams. Generally, it can be deduced that the presence of sufficient oxygen in the electrolyte mostly helps to decrease the negative influence of ferrous ions on gold dissolution.

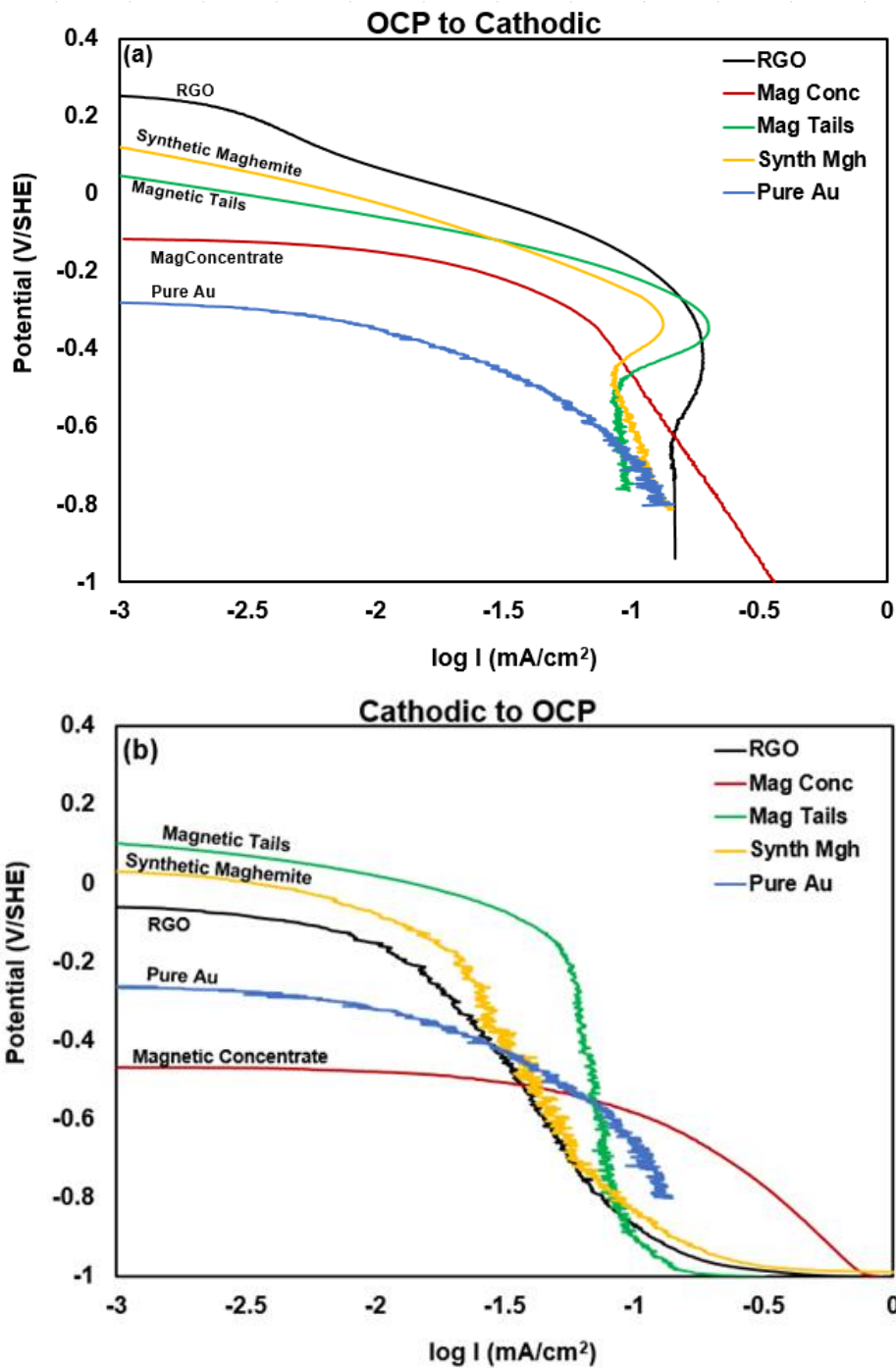
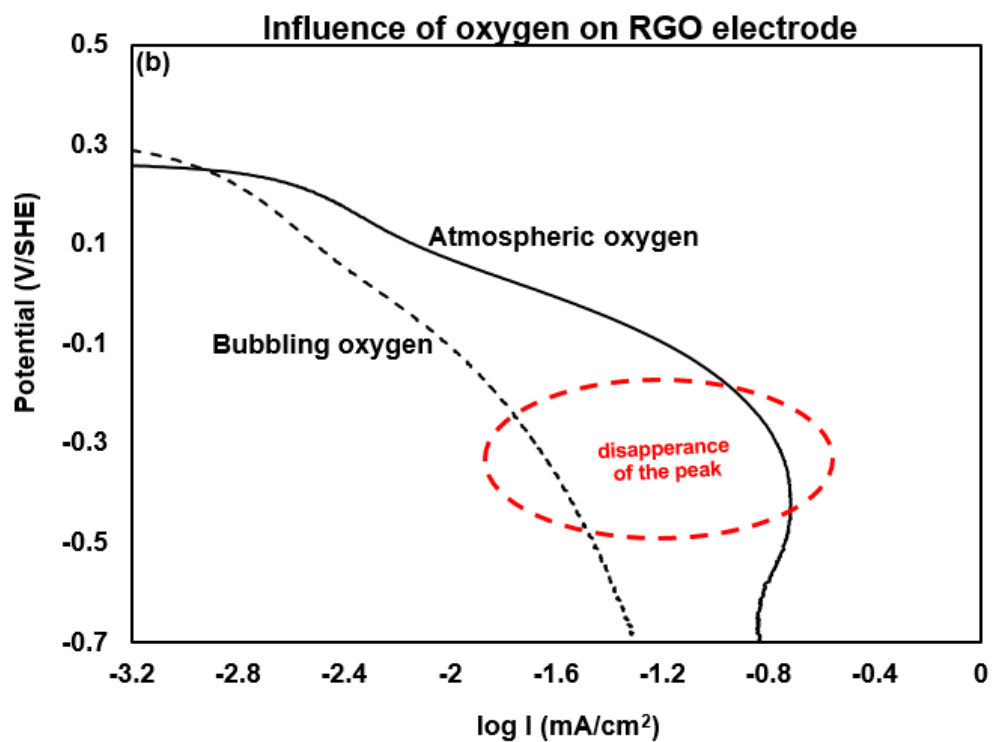
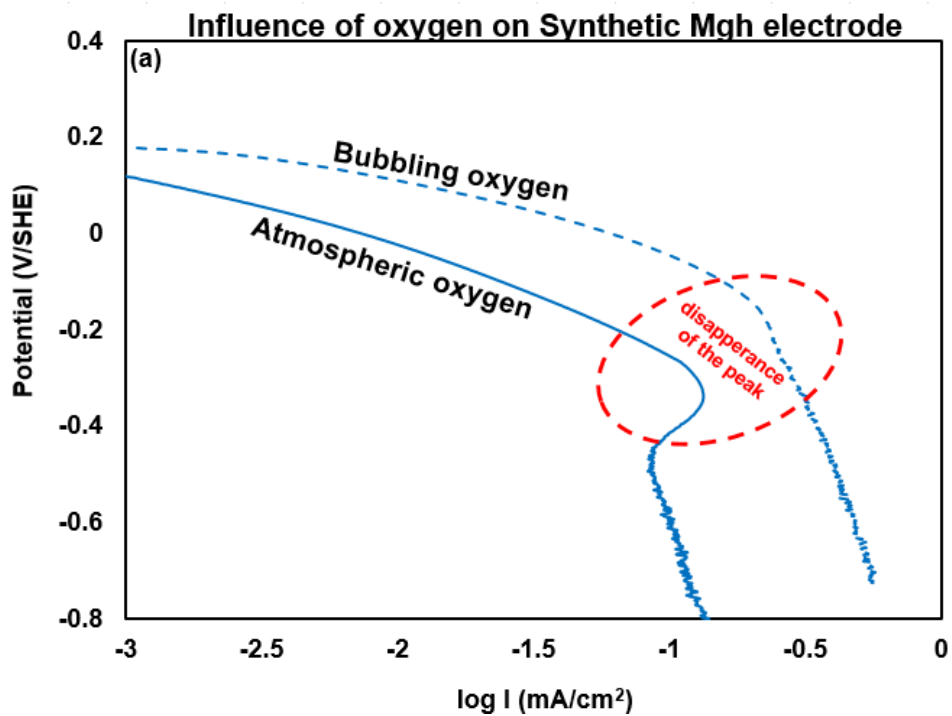


Fig. 7.9 Potentiodynamic cathodic polarization of roasted gold ore (RGO), magnetic concentrate (Mag Conc), magnetic tailings (Mag Tails), synthetic maghemite (Synth Mgh), and pure gold (Au) electrodes with a scan rate of 0.166 mV/s in 0.01 M NaCN electrolyte saturated with atmospheric oxygen at 100-rpm agitation, a pH of 10.5, and 25 °C (Au: 0.25 cm²; other electrodes: 4.9 cm²); (a) polarization from the open circuit potential to the cathodic potential; (b) polarization from the cathodic potential to the open circuit potential.



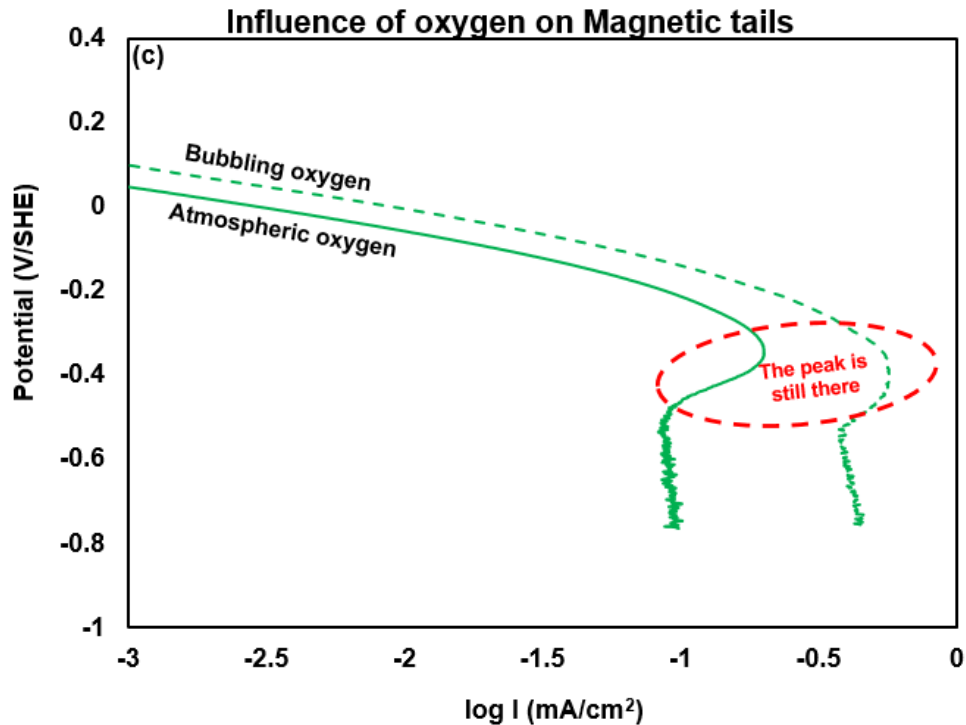


Fig. 7.10 The influence of oxygen concentration (atmospheric and bubbled (dotted line)) on the potentiodynamic cathodic polarization of synthetic maghemite (Synth Mgh) (a), roasted gold ore (RGO) (b), and magnetic tails (c) electrodes from the open circuit potential to the cathode potential with a scan rate of 0.166 mV/s in 0.01 M NaCN electrolyte at 100-rpm agitation, a pH of 10.5, and 25°C.

Potentiodynamic Anodic Polarization of Different Electrodes

Anodic dissolution profiles of different electrodes are shown in Fig. 7.11. Anodic polarization currents were found to be in the order of RGO > Mag Concentrate > Magnetic tails > Synthetic maghemite. Between these electrodes, RGO had the highest current density since it has many different phases, such as iron, gold, and silver, followed by the magnetic concentrate electrode since it is rich in hematite and gold. Alternately, the pure gold electrode showed passive behaviour, which is well reported in the literature. Therefore, for the estimation of the corrosion rate of gold, Bas et al. (2015a, 2015b) showed and suggested that considering the anodic curve only or considering the intersection of the anodic and cathodic curves does not represent the actual leach rates due to this passive behaviour. Similarly, Dai and Breuer (2013) also noted that considering the intersection of

the anodic and cathodic curves results in lower gold corrosion rates when compared to the real industrial application.

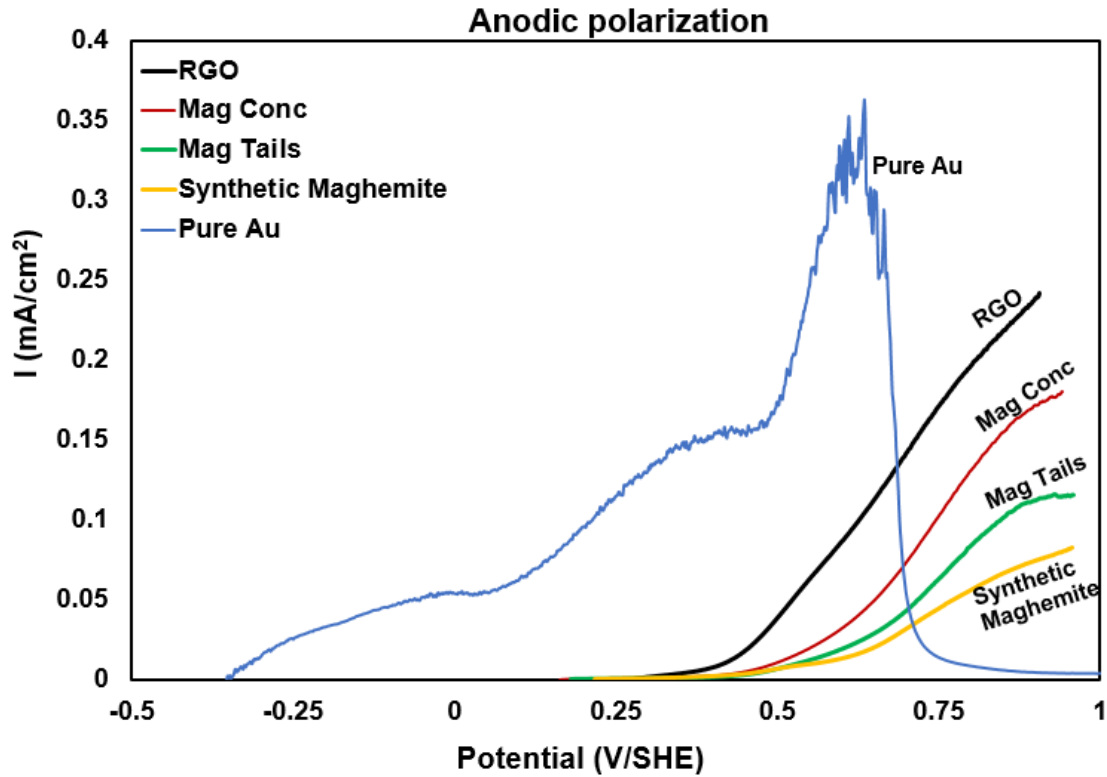


Fig. 7.11 Potentiodynamic anodic polarization of roasted gold ore (RGO), magnetic concentrate (MagConc), Magnetic tails (Mag Tails), synthetic maghemite, and pure gold (Au) electrodes with a scan rate of 0.166 mV/s in 0.01 M NaCN electrolyte saturated with atmospheric oxygen at 100-rpm agitation, a pH of 10.5, and 25 °C (Au: 0.25 cm²; other electrodes: 4.9 cm²).

7.3.6 Influence of Iron Oxides on Gold Dissolution

Magnetite is an $\sim 10^6$ times better conductor than hematite and maghemite (Table 7.4) (Barroso-Bogeat et al., 2014). Hence, the solubility of magnetite in cyanide solutions is expected to be relatively higher compared to hematite, which is in accordance with the findings in this study (Table 7.2). It is well known that oxygen is essential for the dissolution of gold. Then, if the associated mineral with gold is electrically conductive, e.g., magnetite, oxygen reduction can take place over the entire surface of the mineral

electrode, leading to an increase in the magnitude of the cathodic current (Filmer, 1982). As a result, the open circuit potential of gold is shifted to more noble or less active potentials, suggesting the (partial) passivation of the gold's surface. In this case, the rate of gold leaching slows down (Table 7.2). Accordingly, the release of iron oxide species resulted in coatings on the surface of the gold (SEM-EDS results in Fig. 7.3), referring to the partial passivation, which confirms this slowdown in gold leaching.

Table 7.4 Conductivities of iron oxide minerals (Barroso-Bogeat et al., 2014).

Mineral	Conductivity (S.m ⁻¹)
Magnetite (Fe ₃ O ₄)	2.25 x 10 ⁴
Maghemite (Fe _{2.67} O ₄)	2.85 x 10 ⁻⁵
Hematite (Fe ₂ O ₃)	4.76 x 10 ⁻⁴

Alternately, in the case of hematite, which is a lesser conductor, it can be expected that the reduction of oxygen takes place mainly at the surface of gold, so the rate would not be expected to decrease in these conditions (Filmer, 1982). As a result, the open circuit potential of gold is shifted to more active potentials, suggesting the increase in leach kinetics in the case of hematite, and maghemite as well.

It should be underlined that in practice, some part of the gold in roasted gold ore is encapsulated, especially by the maghemite, which is known to be massive and non-porous. During cyanidation, the free-milling part of gold, which is easy to dissolve, could be influenced by the electrochemical properties of maghemite particles. Paktunc et al. (2006) examined such a roasted gold ore and concluded that calcines should dominantly be hematite containing more magnetite as an intermediate product and that the presence of maghemite should be avoided. However, in our lab-scale experimental conditions, iron oxide minerals, i.e., hematite, maghemite, and magnetite, were used as slurry and were mainly in free contact with gold as an electrode, so our experimental conditions could be considered partially representative of the practical conditions mentioned above. It is worth noting that an important part of iron oxide slurries, especially for magnetite, is attached to the magnet, while the rest is found around the gold electrode. However, during the 4 hours

of magnetic agitation, some part of the slurry leaves the magnet and rises to the electrode. This could show that a major influence of slurry presence comes from solved species of magnetite, as well as that of hematite and maghemite slurries. However, the use of electrical agitation could be recommended for future studies. The results in this study have revealed that maghemite, which encapsulates gold in roasted gold ore, normally has a positive effect on gold dissolution when it is in free contact with gold in cyanide solution. It can also be deduced that physical and/or chemical pre-treatment methods are essential to minimize the encapsulation of gold by maghemite.

7.4 Conclusions

1. The leach rate of gold decreased by 40% with magnetite, whereas it increased by 25% and 10% for hematite and maghemite, respectively. The same trends were also obtained within open circuit potential results. Accordingly, the open circuit potential was shifted to less negative potentials ($\sim +15$ mV) for magnetite, while it was shifted to more active potentials (~ -50 and -20 mV) in the case of hematite and maghemite, respectively.
2. The extrapolation of the cathodic Tafel slope only to the open circuit potential (OCP) method for the calculation of the leach rate yields representative results if compared to that of conventional cyanidation for pure gold electrodes. However, in the case of pure Au in the presence of ore and slurry, a difference between these two methods arises due to the presence of many different species/ions in the electrolyte.
3. SEM-EDS findings have confirmed the negative effect of magnetite due to the high accumulation of iron oxides on the gold's surface. Calcium and magnesium spots, together with iron oxides, were observed on the gold's surface in the case of the roasted gold ore slurry test. XPS detected low amounts of gold in magnetite particles, suggesting a decrease in gold dissolution in the case of magnetite.
4. 72% of Au from CN leach tailings (from 20% of the initial Au in tailings) was recovered/concentrated by magnetic separation with a four per cent overall mass pull to

magnetic concentrate. Magnetic separation can be considered an efficient method to identify and recover the gold remaining in tailings.

5. Furthermore, a reduction peak was observed for roasted gold ore, magnetic tails, and synthetic maghemite electrode polarization from the OCP to the cathodic potential, while no peak was found for the magnetic concentrate. In addition, the OCP of the magnetic concentrate was shifted to more active potentials (by 350 mV) when polarized from the cathodic potential to the OCP. Anodic polarization tests indicated that the magnetic concentrate showed the highest corrosion behaviour (anodic current) compared to that of magnetic tails. This peak is possibly due to the reduction of ferric to ferrous cyanide complex, which slows down the reaction rate. Furthermore, it was found that, when oxygen was bubbled, the peak disappeared for synthetic maghemite and roasted gold ore electrodes, whereas magnetic tails still had the peak.

6. It is important to underline that the influence of maghemite slurry on gold dissolution when it is in free contact with the gold's surface is opposite of that observed in practice, where gold is locked inside non-porous maghemite.

7.5 Acknowledgements

The authors would like to express their sincere thanks and appreciation to the Natural Sciences and Engineering Research Council of Canada (NSERC) (36-10-CG101050), Barrick Gold Corporation (03610-CI-103335), and Hydro-Quebec for their financial support through the R&D NSERC Program. Laval University personnel, i.e., V. Dodier (MP-AES analysis), Dr. A. Adnot (XPS analysis and fruitful discussion), A. Ferland (SEM-EDS analysis), and J. Frenette (XRD analysis), are gratefully acknowledged for their help. Thanks are extended to the COREM (Quebec City) personnel for the Fire-assay analysis.

Chapter 8

Conclusions and Recommendations

8.1 Evaluation of Dissolution and Passivation Phenomena

This Ph.D. thesis mainly investigates the reason of slowdown in the dissolution rate of roasted gold ore by electrochemical methods since gold dissolution is an electrochemical corrosion process. Several new contributions of the electrochemical methods and approaches close to extractive metallurgy practice have been proposed by this work, and concluded as follows:

Electrochemical behaviour of pure gold studies have shown that the difference in peak positions and current densities by cyclic voltammetry (without agitation) and potentiodynamic polarization (at 100 rpm agitation) methods, to evaluate the prime importance of agitation on the passivation of gold surface. One of the important contributions of this chapter is that when gold is under passive conditions, increase in cyanide concentration, pH, and potentials adversely affect the gold dissolution, leading to more passive behaviour. The other interesting contribution is the application of Electrochemical Noise Measurement (ENM) in gold studies, since no work was found in the literature for gold using ENM. With its in-situ corrosion rate feature, ENM results have revealed that pure gold electrode showed an increasing trend of corrosion rate while roasted gold ore (RGO) electrode was found to have a plateau after the initial 10 h till the off-set of leaching period (24 h). The formed gold oxide films (I and III) have been determined by XPS studies. These detected gold oxides are the main factors contributing to the passivation of gold surface. These findings have revealed that ENM could be a promising tool for a better understanding to study the anodic dissolution of gold leaching (Chapter 3). Further, as given in Appendix A, the passive behaviour of gold was tested in sulphuric acid medium as compared to that obtained in cyanide solutions. In sulphuric acid medium, gold (I and III) oxide films with much more evident peak densities have been detected by XPS if compared to that in cyanide solutions.

Galvanic interaction studies between gold and iron oxide electrodes by Zero Resistance Ammeter (ZRA) mode have shown that increasing agitation speed (100 to 400 rpm) has led to an increase in galvanic corrosion rate of gold when gold is coupled with roasted gold ore, magnetite, and maghemite disc electrodes. However, hematite showed a maximum

increase in galvanic current, suggesting the increase in gold dissolution, at 250 rpm as compared to that of 400 rpm. In the case of gold and roasted gold ore galvanic coupling tests, XPS studies indicated the presence of silver on gold surface that could lead to partial passivation of the surface. In the case of magnetite and gold electrode tests, SEM analysis demonstrated Fe-oxides and Au-C compound (potentially insoluble Au-CN basic film) on the surface of gold electrode. In galvanic corrosion tests, the tested minerals showed a negative effect on gold leaching in decreasing order: magnetite, magnetite-hematite (MagHem-ES), roasted gold ore. However, maghemite and hematite showed a positive effect, relatively. These results have revealed that formation of corrosion products, passivation, concentration of soluble ions, and diffusion control are responsible for the retarding or promoting effect on gold leaching. This could also be linked to the difference in conductivities of these electrodes (Chapter 4). Further, presented as abstract in Appendix B, another article has also been extracted as complimentary to this publication. In this complimentary work, it was noted that in case of RGO electrode, it is not a perfect passivation, although somewhat a decreasing trend was observed on gold dissolution. The findings have revealed that passivation is not only a laboratory phenomenon, but also it could be responsible for the slowdown of gold dissolution in industrial practice.

Electrochemical behaviour of roasted gold ore (RGO) during cyanidation have shown that the optimal leaching conditions for RGO were found to be 0.04 M NaCN concentration, pH 10-10.5, and 250 rpm agitation speed (Chapter 5). Open circuit potential tests, without imposed potential as in practice, showed that pure gold (Au) electrode gave more active behaviour than that of roasted gold ore (RGO) electrode, which is in line with the electrochemical noise measurement findings as observed in Chapter 3. Cathodic polarisation curve should go directly without cathodic cleaning from corrosion potential to more cathodic ones for both RGO and Au electrodes. SEM analysis indicated the presence of Fe-oxide products could be the main contributor to the passivation of the gold surface. It can be deduced that dissolved ions should have significant and different synergetic effects on gold leaching that could affect conductivity, and cyanide concentration of the solution. Employing Scanning Reference Electrode Technique (SRET) in-situ at open circuit potential, as close to practice, Au electrode was found to have higher quasi

electromotive force (QEMF) (150 vs. 50 $\mu\text{V}/\text{SCE}$) than that of roasted gold ore (RGO) electrode (50 $\mu\text{V}/\text{SCE}$). A new approach has been considered to estimate the corrosion rate of RGO. Considering the anodic curve for Tafel slope or Stern-Geary methods was found to be misleading due to the presence of different constituents. It was found that in cyanide solutions saturated with atmospheric oxygen, cathodic Tafel slope only ($3.30 \times 10^{-8} \pm 3.27\% \text{ mol m}^{-2} \text{ s}^{-1}$) provides representative corrosion rates of gold for RGO to that in practical cyanidation ($3.07 \times 10^{-8} \pm 7.03\% \text{ mol m}^{-2} \text{ s}^{-1}$).

Electrochemical interactions between gold and iron oxide minerals have been examined either in one (OC) or two separate containers (TC) in presence or absence of slurry of roasted gold ore using “**Combined anode electrodes**” approach. Magnetite showed negative effect on gold leaching, while maghemite and hematite demonstrated positive effect, relatively. In two separate containers (where only one counter electrode was in the cell of Au electrode), the anodic behaviour of gold showed a certain passive behaviour when slurry was in the cell of Au electrode, whereas this passive behaviour was greatly decreased when slurry was not in the cell of Au electrode. When another Pt electrode was placed in the other container (where mineral electrode was placed) and electrically connected Au electrode in presence of slurry, resulted in decreasing passive behaviour and gave higher current densities. The release of soluble species into the solution, giving lower current densities, could be the primary factor for inhibiting or passivating the surface of gold. However, when the tailings of slurry was used again as a new feed in two separate containers (TC), the dissolution rate of gold was increased by 3 times (30 to 90 $\mu\text{A cm}^{-2}$), suggesting the removal of detrimental ions in the first stage. It was found that in cyanide solutions saturated with atmospheric oxygen, cathodic Tafel slope only ($8.60 \times 10^{-7} \pm 4.56\% \text{ mol m}^{-2} \text{ s}^{-1}$) provides close corrosion rates of gold to that in practical cyanidation ($10.57 \times 10^{-7} \pm 1.33\% \text{ mol m}^{-2} \text{ s}^{-1}$), suggesting that cathodic polarization is the rate controlling one. Furthermore, a new electrode consisted of equal quantities of magnetite and hematite in one electrode was developed to examine the influence of these two major iron oxides on gold leaching. SEM analysis indicated the presence of Fe-oxide and Au-C compound products could be responsible for partial passivation of gold surface (Chapter 6).

The influence of iron oxide slurries on the dissolution of gold electrodes has been investigated. **Corrosion rate estimation by cathodic Tafel approach** has been compared to that obtained in conventional cyanidation as in practice. Conventional cyanidation yielded a decrease of ~ 40% in the gold leach rate with magnetite slurry, while increases of 25% and 10% were observed for hematite and maghemite, respectively. These gold leach rates were obtained by applying cathodic Tafel slopes only extrapolating to open circuit potential, as shown in Chapters 5 and 6. SEM-EDS, in the case of magnetite slurry, exhibited a high accumulation of iron oxides on the gold surface, which is an indication of slowdown in the gold leach rate. In the case of roasted gold ore slurry, lower amounts of iron oxides were detected with the association of calcium-magnesium coating. The second main contribution is that XPS exhibited a small amount of gold in the slurry of magnetite particles after leaching, i.e., suggesting the adsorption of gold by magnetite, which also justifies the slowdown in the gold leach rate. Other contribution is that magnetic separation tests of cyanidation tailings containing 20% Au resulted in a 4% (mass-pull) magnetic concentrate sample with 72% non-leached Au. Roasted gold ore, magnetic tailings, and synthetic maghemite electrodes exhibited a cathodic peak, suggesting the reduction of ferric to ferrous ions, which could be responsible for the slowdown of leach kinetics, whereas magnetic concentrate did not. Furthermore, when oxygen was bubbled, this peak disappeared in the case of roasted gold ore and synthetic maghemite, though magnetic tailings still exhibited the peak. It is important to underline that the influence of maghemite slurry on gold dissolution when it is in free contact with the gold's surface is opposite to that observed in practice, where gold is locked inside non-porous maghemite (Chapter 7).

A review paper, presented in Chapter 2, has been considered for this project. The key contributions of this review paper are: (1) the evaluation of the electrochemical methods used in gold dissolution studies from past to present; (2) the discussion of the concept of passivation in gold dissolution; (3) the importance of direction in cathodic scanning; and (4) the implication of electrochemical findings in practical cyanidation. The advice of the Editors of Hydrometallurgy Journal have been considered in the preparation of this review paper.

8.2 Recommendations for Future Studies

Based on the findings in this research project, the following perspectives and issues could be considered in future studies:

1. A more detailed magnetic separation of roasted gold ore cyanidation tailings could be considered since maghemite locks up the important portion of the unrecovered gold. It is believed that more detailed electrochemical characterization of magnetic and non-magnetic parts of these tailings would be critical for future studies.
2. Since roasted gold ore, magnetic tailings, and synthetic maghemite electrodes exhibited a cathodic peak and disappeared at high oxygen concentration, then it would be critical to examine the influence of a powerful oxidant, such as hydrogen peroxide.
3. Ultrafine grinding of the magnetic and non-magnetic parts could be a good option to increase the gold leach rate.
4. A new electrode consisted of gold-silver alloy (since gold is often found with silver in nature) electrodes in one anode could be considered.
5. Since hematite promote the leach rate of gold, then it would be critical to have more hematite than having magnetite in roasted gold ore. In this case, roasting procedure could be performed in different conditions which leads to dominantly hematite in the calcine.
6. Electrochemical Impedance Spectroscopy (EIS) study is recommended to examine the influence of iron oxide minerals (magnetite, hematite, and maghemite) as slurry (1% solid ratio; 0.5 g / 200 mL electrode) on the dissolution of a gold electrode during oxidation in cyanide solutions at open circuit potential (OCP). Further, potentiostatic tests at passive potential, e.g. -0.3 V/SHE could also be considered based on the preliminary findings. To note that, EIS characterization of gold in cyanide solutions has received relatively less attention than that in other chemical reagents.

References

- Aballe, A., Bethencourt, M., Botana, F.J., Marcos, M., 1999. Using wavelet transform in the analysis of electrochemical noise data. *Electrochim. Acta* 44, 4805-4816.
- Aballe, A., Bethencourt, M., Botana, F.J., Cano, M.J., Marcos, M., 2001. On the reproducibility of the electrochemical response of AA5083 alloy in NaCl solutions. In: Shaw, B.A., Buchheit, R.G., Moran, J.P. (Eds) *Corrosion and Corrosion Prevention of Low Density Metals and Alloys*, 364-375.
- Adams, M.D., 2005. *Developments in Mineral Processing: Advances in Gold Ore Processing*. Elsevier.
- Adams, M.D., 2016. *Gold Ore Processing: Project Development and Operations*. Second ed. ISBN 978-0-444-63658-4, Elsevier.
- Adnot, A., 2013. XPS analysis of an electrochemically treated Au surface. Department of Chemical Engineering, Laval University. Internal Report sent to Gold Research Group at the Dept. of Mining, Metallurgical and Materials Eng., Laval University, Quebec City, QC, Canada, pp. 1-11.
- Aghamirian, M.M., 1997. Reactivity of sulphide minerals and its effect on gold dissolution and its electrochemical behaviour in cyanide solutions. Ph.D. Thesis. Queen's University, Kingston, Ontario, Canada.
- Aghamirian, M.M., Yen, W.T., 2005. Mechanisms of galvanic interactions between gold and sulphide minerals in cyanide solution. *Miner. Eng.* 18, 393-407.
- Ahmed, S. M., 1978. Electrochemical studies of sulphides, I. The electrocatalytic activity of galena, pyrite and cobalt sulphide for oxygen reduction in relation to xanthate adsorption and flotation. *Int. J. Miner. Process.* 5, 2, 163-174.
- Akcil, A., 2014. Siyanür yönetilebilir bir kimyasal mı? [Is cyanide a manageable chemical?]. *Mining Turkey*, 38, 68-72.
- Alonso-Gómez, A.R., Lapidus, G.T., 2009. Inhibition of lead solubilization during the leaching of gold and silver in ammoniacal thiosulfate solutions (effect of phosphate addition). *Hydrometallurgy* 99, 89-96.
- Alorro, R.D., Hiroyoshi, N., Kijitani, H., Ito, M., Tsunekawa, M., 2010. On the use of magnetite for gold recovery from chloride solution. *Min. Proc. & Ext. Met. Rev.* 31, 4, 201-213.
- Amira, S., Lafront, A.M., Dubé, D., Tremblay, R., Ghali, E., 2007. Electrochemical study of AXJ530 magnesium alloy behavior in alkaline NaCl solution. *Adv. Eng. Mater.* 9, 973-980.

- Amponsah, I., Collins, D., Orlich, J., Cole, J., Brosnahan, D., 2010. Gold recovery from magnetic concentrate at Newmont Carlin Operations, in: Proceedings of Precious Metals '10. UK, pp. 154-174.
- Anderson, C., Dahlgren, E., Huang, H., Miranda, P., Stacey, D., Jeffrey, M., Chandra, I., 2005. Fundamentals and applications of alkaline sulfide leaching and recovery of gold, in: Deschênes, G., Hodouin, D., Lorenzen, L., (Eds.), Proceedings of Treatment of Gold Ores, 44th COM, CIM. Calgary, Alberta, Canada, pp. 145-163.
- Anderson, C.G., 2016. Alkaline sulfide gold leaching kinetics. *Miner. Eng.* 92, 248-256.
- ASTM Standard G 102-89, 2006. Standard practice for calculation of corrosion rates and related information from electrochemical measurements, Annual Book of ASTM Standards, Vol. 03.02, ASTM International, West Conshohocken. PA.
- ASTM Standard G 3-89, 2006. Standard method for conventions applicable to electrochemical measurements in corrosion testing. Annual book of ASTM standards, Vol 03.02. ASTM International. West Conshohocken. PA.
- ASTM Standard G 5-94, 2006. Standard reference test method for making potentiostatic and potentiodynamic anodic polarization measurements. Annual book of ASTM standards, Vol 03.02. ASTM International. West Conshohocken. PA.
- Aylmore, M.G., 2016. Alternative lixivants to cyanide for leaching gold ores, in: Adams, M.D. (Ed.), Gold Ore Processing, Project Development and Operations, second ed., Elsevier, pp. 447-484.
- Azizi, A., Petre, C.F., Olsen, C., Larachi, F., 2010. Electrochemical behavior of gold cyanidation in the presence of a sulfide-rich industrial ore versus its major constitutive sulfide minerals. *Hydrometallurgy* 101, 108-119.
- Azizi, A., Petre, C.F., Olsen, C., Larachi, F., 2011. Untangling galvanic and passivation phenomena induced by sulfide minerals on precious metal leaching using a new packed-bed electrochemical cyanidation reactor. *Hydrometallurgy* 107, 101-111.
- Azizi, A., Petre, C.F., Larachi, F., 2012a. Leveraging strategies to increase gold cyanidation in the presence of sulfide minerals – Packed bed electrochemical reactor approach. *Hydrometallurgy*, 111-112, 73-81.
- Azizi, A., Petre, C.F., Assima, G.P., Larachi, F., 2012b. The role of multi-sulfidic mineral binary and ternary galvanic interactions in gold cyanidation in a multi-layer packed-bed electrochemical reactor. *Hydrometallurgy*, 113-114, 51-59.
- Azizi, A., Olsen, C., Gagnon, C., Bouajila, A., Ourriban, M., Blatter, P., Larachi, F., 2013. Gold passivation: Reconciling cyanidation circuit performances using laboratory testing. *CIM Journal*, 4, 175-182.

- Balaram, V., Vummiti, D., Roy, P., Taylor, C., Kar, P., Raju, A.K. Abburi, K., 2013. Determination of precious metals in rocks and ores by microwave plasma-atomic emission spectrometry for geochemical prospecting studies. *Current Science*, 104, 9, 1207-1215.
- Baron, J.Y., Choi, Y., Jeffrey, M., 2016. Double-refractory carbonaceous sulfidic gold ores, in: Adams, M.D. (Ed.), *Gold Ore Processing, Project Development and Operations*, second ed., Elsevier, pp. 909-918.
- Barroso-Bogeat, A., Alexandre-Franco, M., Fernandez-Gonzalez, C., Macias-Garcia, A., Gomez-Serrano, V., 2014. Electrical conductivity of activated carbon-metal oxide nanocomposites under compression: a comparison study. *Phys. Chem. Chem. Phys.*, 16, 25161-25175.
- Barsky, S.J., Swainson, N., Hedley, N., 1934. Dissolution of gold and silver in cyanide solution. *Am. Inst. Min. Metall. Eng. Trans.* 112, 660-677.
- Bas, A.D., Gavril, L., Ghali, E., 2014. Electrochemical behavior of roasted gold ore (Technical report 2). Submitted to Barrick Gold Corp. p. 70.
- Bas, A.D., Safizadeh, F., Zhang, W., Ghali, E., Choi, Y., 2015a. Active and passive behaviours of gold in cyanide solutions. *Trans. Nonferrous Met. Soc. China* 25, 10, 3442-3453.
- Bas, A.D., Gavril, L., Zhang, W., Ghali, E., Choi, Y., 2015b. Electrochemical dissolution of roasted gold ore in cyanide solutions. *Hydrometallurgy* 156, 188-198.
- Bas, A.D., Zhang, W., Ghali, E., Choi, Y., 2015c. A study of electrochemical dissolution and passivation phenomenon of roasted gold ore in cyanide solutions. *Hydrometallurgy* 158, 1-9.
- Bas, A.D., Ghali, E., Choi, Y. 2015d. A study of electrochemical interactions between gold and its associated oxide minerals, in: *Proceedings of 54th Annual Conference of Metallurgists (COM 2015), The LUCY ROSATO Memorial Symposium, 22-26 August, Toronto, Canada. Paper no 8897.*
- Bas, A.D., Ghali, E., Choi, Y., 2016a. Electrochemical study of gold cyanidation in the presence of roasted gold ore and its associated oxide minerals, in: *Proceedings of XXVIII International Mineral Processing Congress (IMPC 2016) and 55th Annual Conference of Metallurgists (COM 2016), presented at the Electrometallurgy 2016, 11-15 September, Quebec, Canada, Paper #842.*
- Bas, A.D., Safizadeh, F., Ghali, E., Choi, Y., 2016b. Leaching and electrochemical dissolution of gold in the presence of iron oxide minerals associated with roasted gold ore. *Hydrometallurgy* 166, 143-153.

- Bek, R.Y., Kozolapov, G.V., Shuraeva, L.I., Ovchiimikova, S.N., Lazkartzhevskii, P.A., Vais, A.A., 2001. Anodic dissolution of gold in alkali-cyanide solutions: Effect of lead ions. *Russ. J. Electrochem.* 37, 3, 244-249.
- Bek, R.Y., Rogozhnikov, N.A., Kosolapov, G.V., 1997. The kinetics of anodic dissolution of gold in cyanide electrolytes and the interface layer composition. *Russ. J. Electrochem.* 33, 119-125.
- Bevilaqua, D., Acciari, H.A., Benedetti, A.V., Fugivara, C.S., Tremiliosi Filho, G., Garcia Jr, O., 2006. Electrochemical analysis of bioleaching of bornite (Cu_5FeS_4) by *Acidithiobacillus ferrooxidans*. *Hydrometallurgy* 83, 50-54.
- Beyers, E., 1936. Some of the factors which influence the rates of dissolution of gold and silver in cyanide solutions. *J. Chem. Metall. Min. Soc. S. Afr.* 36, 37-89.
- Bodländer, G., 1896. Die Chemie des Cyanidverfahrens: *Z. Angew. Chem.* 9, 583-587.
- Boonstra, B., 1943. Über die Lösungsgeschwindigkeit von Gold in kaliumcyanid-Lösung. *Korros. Metallschutz* 19, 146-151.
- Breuer, P.L., Sutcliffe, C.A., Meakin, R.L., 2011. Cyanide measurement by silver nitrate titration: Comparison of rhodanine and potentiometric end-points. *Hydrometallurgy* 106, 3-4, 135-140.
- Cabri, L.J., Newville, M., Gordon, R.A., Crozier, E.D., Sutton, S.R., McMahon, G., Jiang, D-T., 2000. Chemical speciation of gold in arsenopyrite. *Can. Mineral.* 38, 1265-1281.
- Cardarelli, F., 2008. *Materials Handbook: A Concise Desktop Reference*. Second ed. Springer.
- Cathro, K.J., 1963. The effect of oxygen in the cyanide process for gold recovery, in: *Proceedings AusIMM*, Carlton, Victoria, Australia, 181-205.
- Cathro, K.J., Koch, D.F.A., 1964a. The dissolution of gold in cyanide solutions – An electrochemical study. *Proceedings of Annual Conference of Aust. Inst. Min. Met.* No 210, 111-126.
- Cathro, K.J., Koch, D.F.A., 1964b. The anodic dissolution of gold in cyanide solutions. *J. Electrochem. Soc.* 111, 1416-1420.
- Cathro, K.J., Walkley, A., 1961. *The Cyanidation of Gold*. CSIRO Publication, Melbourne, Australia: CSIRO. Report from the Division of Mineral Chemistry.

- Celep, O., Alp İ., Deveci, H., 2011. Improved gold and silver extraction from a refractory antimony ore by pre-treatment with alkaline sulphide leach. *Hydrometallurgy* 105, 3-4, 234–239.
- Celep, O., Bas, A.D., Yazici, E.Y., Alp, I., Deveci, H., 2015. Improvement of silver extraction by ultrafine grinding prior to cyanide leaching of the plant tailings of a refractory silver ore. *Miner. Process. Extr. Metall. Rev.* 36, 4, 227-236.
- Cerovic, K., Hutchison, H., Sandenbergh, R.F., 2005. Kinetics of gold and a gold-10% silver alloy dissolution in aqueous cyanide in the presence of lead. *Miner. Eng.* 18, 585-590.
- Chimenos, J.M., Segarra, M., Guzman, L., 1997. Kinetics of the reaction of gold cyanidation in the presence of a thallium(I) salt. *Hydrometallurgy* 44, 3, 269-286.
- Choi, Y., 2015. Personal Communication. Barrick Gold Corp., Toronto, Canada. Interview: New frontiers in gold extraction. <http://www.min-eng.com/people/na/157.html>
- Choi, Y.U., Lee, E.C., Han, K.N., 1991. The dissolution behaviour of metals from Au/Cu and Ag/Cu alloys in acidic and cyanide solutions. *Metall. Trans.* 22B, 755-764.
- Choudhary, L., Wang, W., Alfantazi, A., 2016. Electrochemical corrosion of stainless steel in thiosulfate solutions relevant to gold leaching. *Metall. Mater. Trans. A* 47, 314-325.
- Ciftci, H., Akcil, A., 2010. Effect of biooxidation conditions on cyanide consumption and gold recovery from a refractory gold concentrate. *Hydrometallurgy* 104, 142-149.
- Cottis, R., Turgoose, S., 1999. Electrochemical Impedance and Noise. Corrosion Testing Made Easy, in: Syrett, B.C., (Ed.), NACE International, Houston, TX., pp.5-14.
- Cottis, R.A., 2001. Interpretation of electrochemical noise data 57, 3, NACE Int. 265-285.
- Crundwell, F.K., 2013. The dissolution and leaching of minerals: Mechanisms, myths and misunderstandings, *Hydrometallurgy* 139, 132-148.
- Crundwell, F.K., 2015. The semiconductor mechanism of dissolution and the pseudo-passivation of chalcopyrite. *Can. Metall. Quart.* 54, 3, 279-288.
- Crundwell, F.K., Godorr, S.A., 1997. A mathematical model of the leaching of gold in cyanide solutions. *Hydrometallurgy* 44, 147-162.
- Cruz, R., Luna-Sanchez, R.M., Lapidus, G.T., Gonzalez, I., Monroy, M., 2005. An experimental strategy to determine galvanic interactions affecting the reactivity of silver mineral concentrates. *Hydrometallurgy* 78, 198-208.

- Curioni, M., Cottis, R.A., Thompson, G.E. 2013. Application of electrochemical noise analysis to corroding aluminium alloys. *Surf. Interface Anal.* 45, 1564-1569.
- Dai, X., Jeffrey, M.I., 2006. The effect of sulfide minerals on the leaching of gold in aerated cyanide solutions. *Hydrometallurgy*, 82, 118-125.
- Dai, X., Breuer, P.L., 2013. Leaching and electrochemistry of gold, silver, and gold-silver alloys in cyanide solutions: Effect of oxidant and lead (II) ions. *Hydrometallurgy* 133, 139-148.
- Davis, G.O., Kolts, J., Sridhar, N., 1986. Polarization effects in galvanic corrosion. *Corrosion*, 42, 329-336.
- De Faria, D.L.A., Venâncio Silva, S., de Oliveira, M.T., 1997. Raman micro spectroscopy of some iron oxides and oxyhydroxides, *J. Raman Spectrosc.* 28, 873–878.
- Deschênes, G. 2016. Advances in the cyanidation of gold, in: Adams, M.D. (Ed.), *Gold Ore Processing, Project Development and Operations*, second ed., Elsevier, pp. 429-445.
- Deschênes, G., Guo, H., Xia, C., Pratt, A., Fulton, M., Choi, Y., Price, J., 2012. A study of the effect of djurliete, bornite and chalcopyrite during the dissolution of gold with a solution of ammonia-cyanide. *Minerals* 2, 459-472.
- Deschênes, G., Lastra, R., Brown, J.R., Jin, S., May, O., Ghali, E., 2000. Effect of lead nitrate on cyanidation of gold ores: progress on the study of the mechanism. *Miner. Eng.* 13, 12, 1263-1279.
- Deschênes, G., Wallingford, G., 1995. Effect of oxygen and lead nitrate on the cyanidation of a sulphide bearing gold ore. *Miner. Eng.* 8, 923-931.
- Dimov, S.S., Chryssoulis, S.L., Sodhi, R.N., 2003. Speciation of surface gold in pressure oxidized carbonaceous gold ores by TOF-SIMS and TOF-LIMS. *Appl. Surf. Sci.* 203-204, 644-647.
- Dimov, S., Hart, B., 2014. Quantitative analysis of sub-microscopic and surface preg-robbed gold in gold deportment studies. in: *Proceedings of XXVII International Mineral Processing Congress, IMPC 2014, Santiago, Chile*. Paper #1408.
- Dorin, R., Woods, R., 1991. Determination of leaching rates of precious metals by electrochemical techniques. *J. Appl. Electrochem.* 21, 419-424.
- Douglas, W., Semenyna, L., 2013. Magnetic recovery of gold-bearing iron oxides at Barrick Goldstrike's roaster, in: *Proceedings of World Gold Conference 2013, Brisbane, QLD, Australia*, pp. 79-85.

- Dunne, R., Staunton, W.P., Afewu, K., 2013. A historical review of the treatment of preg-robbing gold ores - What has worked and changed, in: Proceedings of World Gold Conference 2013, Brisbane, QLD, Australia, pp. 99-110.
- Eden, D.A., 2011. Electrochemical Noise, Chapter 86, in: Revie, R. W. (Ed.), Uhlig's Corrosion Handbook, third ed., John Wiley & Sons, Inc., pp. 1167-1177.
- Eisenmann, E.T., 1978. Kinetics of the electrochemical reduction of dicyanoaurate. *J. Electrochem. Soc.* 125, 5, 717-723.
- Ellis, S., Senanayake, G., 2004. The effects of dissolved oxygen and cyanide dosage on gold extraction from a pyrrhotite-rich ore, *Hydrometallurgy* 72, 39 – 50.
- Elsner, L., 1846. Über das Verhalten verschiedener Metalle in einer wässrigen Lösung von Cyankalium. *J. Prakt. Chem.* 37, 441-446.
- Evans, D.H., Lingane, J.J., 1963. The chronopotentiometric reduction of oxygen at gold electrodes. *J. Electroanal. Chem.* 6, 283-299.
- Feldmann, R.M.W., Breuer, P.L., 2015. An investigation of gold leaching in the presence of hydrogen peroxide using rotating disc electrodes, in: Proceedings of World Gold Conference 2015, J. S. Afr. Inst. Min. Metall. pp. 289-304.
- Filmer, A.O., 1982. The dissolution of gold from roasted pyrite concentrates. *J. S. Afr. Inst. Min. Metall.*, 90-94.
- Fink, C.G., Putnam, G.L., 1950. The action of sulfide ion and of metal salts on the dissolution of gold in cyanide solutions. *Miner. Eng.* 187, 952-955.
- Finkelstein, N.P., 1972. The chemistry of the extraction of gold from its ores, in: R.J. Adamson (Ed.), Gold Metallurgy in South Africa, Chamber of Mines of South Africa, CTP Book Printers, Johannesburg, pp. 284-351.
- Fleming, C., 1999. Leaching of gold ores. Lakefield Research Limited, Canada.
- Fontana, M.G., Greene, N.D. 1978. Corrosion engineering. McGraw-Hill Company.
- Fosu, B. 2016. Experimental investigation of recovering gold from maghemite-rich gold magnetic concentrates by roasting. MSc Thesis. Colorado School of Mines, USA. p.144.
- Franks, D.M., 2015. Mountain Movers: Mining Sustainability and the agents of change. Routledge, Taylor and Francis Group, London and Newyork. ISBN: 978–0415711715.

- Gamry Potentiostat Manual, 2012. Reference 3000™, Potentiostat/Galvanostat/ZRA Operator's Manual. Revision 6.0, August 27, 2012, 988-00014.
- Ghali, E., 2010. Corrosion Resistance of Aluminium and Magnesium Alloys, Understanding, Performance and Testing. Wiley & Sons Inc.
- Gilroy, D., Conway, B.E., 1965. Kinetic theory of inhibition and passivation in electrochemical reactions. *J. Phys. Chem.* 69, 4, 1259-1267.
- Greenwood, N.N., Earnshaw, A., 1997. Chemistry of Elements, second ed. Butterworth Heinemann.
- Guan, Y., Han, K.N., 1994. An electrochemical study on the dissolution of gold and copper from gold-copper alloys. *Metall. Mater. Trans. B* 25B, 817-827.
- Guo, B., Peng, Y., Espinosa-Gomez, R., 2015. Effects of free cyanide and cuprous cyanide on the flotation of gold and silver bearing pyrite. *Miner. Eng.* 71, 194-204.
- Guo, H., Deschênes, G., Pratt, A., Fulton, M., Lastra, R., 2005. Leaching kinetics and mechanisms of surface reaction during cyanidation of gold in the presence of pyrite and stibnite. *Miner. Metall. Process* 22, 2, 89-95.
- Gupta, C.K., Mukherjee, F.K., 1990. Hydrometallurgy in Extraction Processes, Volume II. CRC Press.
- Guzman, L., Segarra, M., Chimenos, J.M., Cabot, P.L. Espiell, F., 1999. Electrochemistry of conventional gold cyanidation. *Electrochimica Acta* 44, 2625-2632.
- Habashi, F., 2009. Gold History Metallurgy Culture. Métallurgie Extractive Québec, Canada.
- Habashi, F., 1966. Theory of cyanidation. *Trans. Soc. Min. Eng. AIME* 235, 236-239.
- Habashi, F., 1967. Kinetics and mechanisms of gold and silver dissolution in cyanide solutions. Bulletin 59, Montana Bureau of Mines, CO, U.S.
- Habashi, F., 2016. Gold-An historical introduction, in: Adams, M.D. (Ed.), Gold Ore Processing, Project Development and Operations, second ed., Elsevier, pp. 1-20.
- Habashi, F., Bas, A.D., 2014. Evidence of the existence of anodic and cathodic zones during the dissolution of minerals and metals. *Hydrometallurgy* 144-145, 148-150.
- Hackerman, N., 1959. Kinetics of dissolution processes, in: Gatos, H.G., Faust, J.W., Lafleur, W.A. (Eds.), Surface Chemistry of Metals and Semiconductors, John Wiley and Sons, Inc., New York, N.Y., pp. 313-325.

- Han, K.N., Guan, Y., 1995. The dissolution behavior of metals from Au/Ag/Cu-alloys, in: Proceedings of the XIX International Mineral Processing Congress – Physical & Chemical Processing – vol 2, SME, pp. 245-250.
- Hedley, N., Tabachnick, H., 1968. Mineral Dressing Notes No 23, Chemistry of Cyanidation. American Cyanamid Company, New Jersey, USA.
- Holmes, P.R., Crundwell, F.K., 2013. Polysulfides do not cause passivation: Results from the dissolution of pyrite and implications for other sulfide minerals. *Hydrometallurgy* 139, 101-110.
- Jara, J.O., Bustos, A.A., 1992. Effect of oxygen on gold cyanidation: Laboratory results. *Hydrometallurgy* 30, 195-210.
- Jeffrey, M.I., 1997. A kinetic and electrochemical study of the dissolution of gold in aerated cyanide solutions: the role of solid and solution phase purity. PhD. Thesis. Curtin University, Australia.
- Jeffrey, M.I., Chandra, I., Ritchie, I.M., Hope, G.A., Watling, K., Woods, R., 2005. Innovations in gold leaching research and development, in: Innovations in Natural Resource Processing, Proceedings of the Jan D. Miller Symposium, Salt Lake City, UT, United States, pp. 207-222.
- Jeffrey, M.I., Ritchie, I.M., 2000a. The leaching of gold in cyanide solutions in the presence of impurities: I. The effect of lead. *J. Electrochem. Soc.* 147, 3257-3262.
- Jeffrey, M.I., Ritchie, I.M., 2000b. The leaching of gold in cyanide solutions in the presence of impurities: II. The effect of silver. *J. Electrochem. Soc.* 147, 3272-3276.
- Jeffrey, M.I., Ritchie, I.M., 2001. The leaching and electrochemistry of gold in high purity cyanide solutions. *J. Electrochem. Soc.* 148, 4, D29-D36.
- Jeffrey, M.I., Watling, K., Hope, G.A., Woods, R., 2008. Identification of surface species that inhibit and passivate thiosulfate leaching of gold. *Miner. Eng.* 21, 443-452.
- Jiang, X., Nestic, S., Huet, F., Kinsella, B., Brown, B., Young, D., 2012. Selection of electrode area for electrochemical noise measurements to monitor localized CO₂ corrosion. *J. Electrochem. Soc.* 159, 7, C283-C288.
- Jin, S., May, O., Ghali, E., Deschênes, G., 1998. Investigation on the mechanism of the catalytic effect of lead salts on gold dissolution in cyanide solutions, in: Proceedings of Third International Conference on Hydrometallurgy (ICHM'98), China, pp. 666-679.

- Jones, D.A., 1992. Principles and prevention of corrosion. Macmillan Publishing Company. 167-196.
- Kakovskii, A., Kholmanskikh, Yu.B., 1960. Investigation of the kinetics of cyaniding copper and gold. *Izvest. Akad.Nauk SSSR, Otdel. Tekh. Nauk. Met. i Toplivo*, No.5, 207-218.
- Kameda, M., 1949. Fundamental studies on dissolution of gold in cyanide solutions. II: On equations of reactions and effects of cyanide strength and other variables on dissolution rate. *Science Reports of the Research Institutes, Tohoku University, Series A, Physics, Chemistry and Metallurgy*, vol. 1, pp. 223-230.
- Kasaini, H., Kasongo, K., Naude, N., Katabua, J., 2008. Enhanced leachability of gold and silver in cyanide media: Effect of alkaline pre-treatment of jarosite minerals. *Miner. Eng.* 21, 1075-1082.
- Kelly, R.G., Sculy, J.R., Shoesmith, D.W., Buchheit, R.G., 2002. *Electrochemical techniques in corrosion science and engineering*. ISBN, 0203909135, 9780203909133, CRC Press.
- Kirk, D.W., Foulkes, F.R., 1980. Anodic dissolution of gold in aqueous alkaline cyanide solutions at low overpotentials. *J. Electrochem. Soc.* 127, 1993-1997.
- Kirk, D.W., Foulkes, F.R., Graydon, W.F. 1978. A study of anodic dissolution of gold in aqueous alkaline cyanide. *J. Electrochem. Soc.* 125, 1436-1443.
- Kirk, D.W., Foulkes, F.R., Graydon, W.F., 1980. Gold passivation in aqueous alkaline cyanide. *J. Electrochem. Soc.* 127, 1962-1969.
- Kiss, L., 1988. *Kinetics of Electrochemical Metal Dissolution*. ISBN 9780444989642, Elsevier.
- Kissinger, P.T., Heineman, W.R., 1983. Cyclic voltammetry. *J. Chem. Educ.* 60, 9, 702-706.
- Klapper, H.S., Goellner, J., Burkert, A., Heyn, A., 2013. Environmental factors affecting pitting corrosion of type 304 stainless steel investigated by electrochemical noise measurements under potentiostatic control. *Corros. Sci.* 75, 239-247.
- Kolotyркин, Y.M., 1958. Electrochemical behaviour and anodic passivity mechanism of certain metals in electrolyte solutions. *Z. Electrochemie* 62, 6-7, 664-669.
- Kondos, P., Deschênes, G., Morrison, R.M., 1995. Process optimization in gold cyanidation. *Hydrometallurgy* 39, 235-250.

- Kudryk, V., Kellogg, H.H., 1954. Mechanism and rate-controlling factors in the dissolution of gold in cyanide solutions. *Trans. AIME J. of Metals* 6 (5), 541-548.
- La Brooy, S.R., Linge, H.G., Walker, G.S., 1994. Review of gold extraction from ores. *Miner. Eng.* 7(10), 1213-1241.
- Lafont, A-M., Zhang, W., Ghali, E., Houlachi, G., 2010a. Electrochemical noise studies of the corrosion behavior of lead anodes during zinc electrowinning maintenance. *Electrochim. Acta* 55, 6665-6675.
- Lafont, A-M., Safizadeh, F., Ghali, E., Houlachi, G., 2010b. Study of the copper anode passivation by electrochemical noise analysis using spectral and wavelength transforms. *Electrochim. Acta* 55, 2505-2512.
- Lafont, A-M., Zhang, W., Jin, S., Tremblay, R., Dube, D., Ghali, E., 2005. Pitting corrosion of AZ91D and AJ62x magnesium alloys in alkaline chloride medium using electrochemical techniques. *Electrochim. Acta* 51, 489-501.
- Legodi, M.A., de Waal, D., 2007. The preparation of magnetite, goethite, hematite and maghemite of pigment quality from mill scale iron waste. *Dyes and Pigments*, 74(1), 161-168.
- Li, J., Zhong, T., Wadsworth, M.E., 1992. Application of mixed potential theory in hydrometallurgy. *Hydrometallurgy* 29, 47-60.
- Lin, H.K., Chen, X., 2001. Electrochemical study of gold dissolution in cyanide solution. *Miner. Metall. Process* 18, 147-153.
- Lorenzen, L., van Deventer, J.S.J., 1992a. Electrochemical interactions between gold and its associated minerals during cyanidation. *Hydrometallurgy*, 30, 177-194.
- Lorenzen, L., van Deventer, J.S.J., 1992b. The mechanism of leaching of gold from refractory ores. *Miner. Eng.* 5, 1377-1387.
- Lorenzen, L., 1992. A fundamental study of the dissolution of gold from refractory ores. Ph.D. Thesis, University of Stellenbosch, South Africa.
- Lorenzen, L., van Deventer, J.S.J., 1993. The identification of refractoriness in gold ores by the selective destruction of minerals. *Miner. Eng.* 5, 3, 1013-1023.
- Lorösch, J., 2001. Process and environmental chemistry of cyanidation. Degussa AG, Frankfurth am Main.
- Loto, C.A., 2012. Electrochemical noise measurement technique in corrosion research. *Int. J. Electrochem. Sci.* 7, 9248-9270.

- Luna, R.M., Lapidus, G.T., 2000. Cyanidation kinetics of silver sulfide. *Hydrometallurgy* 56, 171-188.
- Lund, V., 1951. The corrosion of silver by potassium cyanide solutions and oxygen. *Acta Chim. Scand.* 5, 555-567.
- MacArthur, D.M., 1972. A study of gold reduction and oxidation in aqueous media. *J. Electrochem. Soc.* 119, 672-676.
- Mahmoodi, A., Noaparast, M., Aslani, S., Ghorbani, A., 2010. The arghash gold ore sample treatment. *Iran. J. Sci. Technol. B*, 34 (B5), 577-589.
- Marsden, J.O., House, C.L. 2006. *The Chemistry of Gold Extraction*. Society for Mining Metallurgy and Exploration, USA.
- May, O., Jin, S., Ghali, E., Deschênes, G., 2005. Effects of sulfide and lead nitrate addition to a gold cyanidation circuit using potentiodynamic measurements. *J. Appl. Electrochem.* 35, 131-137.
- McCarley, R.L., Bard, A., 1992. Surface reactions of Au(III) with aqueous cyanide studied by scanning tunnelling microscopy. *J. Phy. Cem.* 96, 7410-7416.
- McCarthy, A.J., Coleman, R.G., Nicol, M.J., 1998. The mechanism of the oxidative dissolution of colloidal gold in cyanide media. *J. Electrochem. Soc.* 145, 408-414.
- McMullen, J., Thompson, R., 1989. Practical use of oxygen for gold leaching in Canada, in: *Randol Gold & Silver Recovery Innovations: Phase IV Workshop*, Sacramento, California, USA. Randol International, Golden, CO, pp. 9-100.
- Mills, T., 1951. An electrochemical study of the dissolution of gold and silver in cyanide solutions. Ph.D. Thesis, University of Melbourne, Australia.
- Mrkusic, D.P., Paynter, J., 1970. The recovery of gold from sulphidic and arsenical ores mainly from the Barberton area. Johannesburg, National Institute for Metallurgy, Report 911.
- Mughogho, D.T., Crundwell, F.K., 1996. Gold dissolution in dilute cyanide solutions, in: Woods, R., Doyle, F.M., Richardson, P. (Eds.), *Electrochemistry in Mineral and Metal Processing, IV*, USA, pp. 275-307.
- Muir, D.M., 2011. A review of the selective leaching of gold from oxidised copper–gold ores with ammonia–cyanide and new insights for plant control and operation. *Min. Eng.* 24, 576-582.

- Mussatti, D., Mager, J., Martins, G.P., 1997. Electrochemical aspects of the dissolution of gold in cyanide electrolytes containing lead, in: Dreisinger, D.B., (Ed.), Proceedings of Aqueous Electrotechnologies: Progress in Theory and Practice, The Minerals, Materials Society, pp. 247-265.
- Nicol, M., Fleming, C., Paul, R., 1987. The chemistry of the extraction of gold, in: Stanley, G.G. (Ed.), The Extractive Metallurgy of Gold. second ed., South African Institute of Mining and Metallurgy. Johannesburg. S. Africa., pp. 831-905.
- Nicol, M.J., 1980. The anodic behavior of gold. *Gold Bulletin* 13, 105-111.
- Oltra, R., Maurice, V., Akid, R., Marcus, P., 2007. Local probe techniques for corrosion research, CRC press.
- Osseo-Asare, K., Xue, T., Ciminelli, S.T., 1984. Solution chemistry of cyanide leach systems. In Kudryk, V., Corrigan, D.A., Liang, W.W. (Eds.), Proceedings of Precious Metals: Mining, Extraction and Processing. Warrendale, PA: TMS. 173- 196.
- Paktunc, D., 2014. Personal communication. CANMET, Ottawa, Canada. (October 10, 2014).
- Paktunc, D., Kingston, D., Pratt, A., McMullen, J., 2006. Distribution of gold in pyrite and in products of its transformation resulting from roasting of refractory gold ore. *Can. Mineral.* 44, 213-227.
- Pan, T.P., Wan, C.C., 1979. Anodic behaviour of gold in cyanide solution. *J. Appl. Electrochem.* 9, 653-655.
- Papavinasam, S., 2011. Corrosion inhibitors, in: Revie, R.W. (Ed.), Uhlig's Corrosion Handbook, third ed., The Electrochemical Society Series, Wiley, pp. 1021-1032.
- Parga, J.R., Valenzuela, J.L., Vasquez, V., 2011. Analysis of the adsorption of gold and silver on magnetic species formed in the electrocoagulation process. Proceedings of 140th Annual Meeting of TMS, Wiley Publishing, Canada, pp. 267-275.
- Paul, R.L., 1984. The role of electrochemistry in the extraction of gold. *J. Electroanal. Chem.* 168, 147-162.
- Poskus, D., Agafonovas, G., 1995. Adsorption of cyanide-containing species from potassium cyanide solutions on gold electrodeposits. *J. Electroanal. Chem.* 393, 1-2, 105-112.
- Princeton Applied Research, 2014. Electrochemical instruments, corrosion. (accessed 28.07.2014) <http://www.ameteki.com/applications/corrosion/galvanic-corrosion>.

- Puddephatt, R.J. (1978). The Chemistry of Gold, in: Clarke, R.J.H., Topics in Inorganic and General Chemistry, Monograph 16. Elsevier, Amsterdam. pp. 49-75.
- Qian, L., Tao, J., Yong-bin, Y., Guang-Hui, L., Yu-feng, G., Guan-zhou, Q., 2010. Co-intensification of cyanide leaching gold by mercury ions and oxidant. *Trans. Nonferrous Met. Soc. China* 20, 1521-1526.
- Reyez-Cruz, V., Ponce-de-León, C., González, I., Oropeza, M.T., 2002. Electrochemical deposition of silver and gold from cyanide leaching solutions. *Hydrometallurgy* 65, 187-203.
- Riggs, O.L., 1973. Theoretical aspects of corrosion inhibitors and inhibition, in: Corrosion Inhibitors, Nathan C.C. (Ed.), NACE Publication, Texas, pp. 7-27.
- Rogozhnikov, N.A., Bek, R.Y., 1987. Double-layer capacity and the zero-charge potential of a gold electrode in cyanide solutions. *Elektokhimiya* 23, 10, 1440-1443.
- Safizadeh, F., Ghali, E., 2013. Electrochemical noise of copper anode behavior in industrial electrolyte using wavelet analysis. *T. Nonferr. Metal. Soc.* 23, 1854-1862.
- Sandenbergh, R.F., Miller, J.D., 2001. Catalysis of the leaching of gold in cyanide solutions by lead, bismuth and thallium. *Miner. Eng.* 14, 1379-1386.
- Sawaguchi, T., Yamada, T., Okinaka, Y., Itaya, K., 1995. Electrochemical scanning tunneling microscopy and ultra-high vacuum investigation of gold cyanide adlayers on Au(111) formed in aqueous solution. *J. Phys. Chem.* 99, 14149-14155.
- Scully, J.C., 1966. The fundamentals of corrosion. Pergamon Press.
- Senanayake, G., 2008. A review of effects of silver, lead, sulfide and carbonaceous matter on gold cyanidation and mechanistic interpretation. *Hydrometallurgy* 90, 46-73.
- Shareder, D., Vanclay, E., Hammer, M., Taylor, C., 2011. An innovative new plasma source for elemental analysis using atomic spectroscopy. Gulf Coast Conference, Galveston Island, TX, October 11-12.
- Sheveleva, L.D., Kakovskii, I.A., 1979. Lead compounds and dissolution of gold in cyanide solutions. *Tsvetnye Metally* 7, 100-102.
- Shreir, L.L., Jarman, R.A., Burstein, G.T., 1994. Corrosion: Metal/environment reactions. Third ed., ISBN: 978-0-08-052351-4, Butterworth.
- Simon, G., Huang, H., Penner-Hahn, J.E., Kesler, S.E., Kaol, S., 1999. Oxidation state of gold and arsenic in gold-bearing arsenian pyrite. *Am. Mineral.* 84, 7-8, 1071-1079.

- Stephens, T., 1988. The use of pue oxygen in the leaching process in South Africa gold mines, in: Perth International Gold Conference. Randol International, Golden, CO, pp. 191-196.
- Stephens, J.D., Bryan, S.R., Rothbard, D.R., 1990. Characterization of solid solution gold in pyrite and metallurgical treatment products by SIMS. In D.M. Hansen, D.N. Halbe, E.O. Petersen & W.J. Tafuri (Eds.), Proceedings of Gold '90 Symposium, Salt Lake Utah, AIME, USA. pp. 333-339.
- Stern, M., Geary, A.L., 1957. Electrochemical polarization. I. A theoretical analysis of the shape of a polarization curves. *J. Electrochem. Soc.* 104, 33-63.
- Sun, X., Guan, Y.C., Han, K.N., 1996. Electrochemical behaviour of the dissolution of gold-silver alloys in cyanide solutions. *Metall. Mater. Trans.* 3B, 355-361.
- Surface Science Western, Application Note. Characterization of passivating coatings on gold grains from carbon in leach (CIL) residue sample by TOF-SIMS, Ontario, Canada. Retrieved on 15 August 2014 from <http://www.surfacesciencwestern.com/industrial-solutions/mining-and-mineralogy/application-notes/>.
- Tan, H., Feng, D., van Deventer, J.S.J., Lukey, G.C., 2006. An electrochemical study of gold cyanidation in the presence of carbon coatings. *Hydrometallurgy* 84, 14-27.
- Tan, Y.J., Bailey, S., Kinsella, B., 1996. The monitoring of the formation and destruction of corrosion inhibitor films using electrochemical noise analysis (ENA). *Corros. Sci.* 38, 10, 1681-1695.
- Taylor, A., 2013. Developments in the processing of refractory & complex gold ores. Presented at AusIMM Bendigo Technical Meeting, 2013, Melbourne, Australia.
- Thompson, N.G., Payer J.H., 1998. DC Electrochemical Test Methods, NACE Internationals.
- Thompson, N.G., Syrett, B.C., 1992. Relationship between conventional pitting and protection potentials and a new, unique pitting potential. *Corrosion* 48, 8, 649-659.
- Thompson, P.F., 1947. The dissolution of gold in cyanide solutions. *J. Electrochem. Soc.* 91, 1, 41-71.
- Thurgood, C.P., Kirk, D.W., Foulkes, F.R., Graydon, W.F., 1981. Activation energies of anodic gold reactions in aqueous alkaline cyanide. *J. Electrochem. Soc.* 128, 8, 1680-1685.
- Tshilombo, A.F., 2000. Influence of silver alloying and impurities on the dissolution of gold in alkaline cyanide solutions. MSc Thesis. University of Pretoria, South Africa.

- Tshilombo, A.F., Sandenbergh, R.F., 2001. An electrochemical study of the effect of lead and sulphide ions on the dissolution rate of gold in alkaline cyanide solutions. *Hydrometallurgy* 60, 55-67.
- Uhlig, H.H. 1963. Corrosion and corrosion control. Canada: John Wiley & Sons, Inc.
- Van Den Berg, R., Petersen F.W., 2000. Inhibition of pregrobbing phenomenon in gold ores, in: Sanchez, M.A., Vergara, F., Castro, S.H. (Eds.), Proceedings of the V International Conference on Clean Technologies for the Mining Industry, Santiago, Chile, pp. 329-338.
- Van Deventer, J.S.J., Lorenzen, L., 1987. Galvanic interactions during the leaching of gold, in: Davies, G. A. (Ed.), Separation Processes in Hydrometallurgy, pp. 49-57.
- Van Deventer, J.S.J., Reuter, M.A., Lorenzen, L., Hoff, P.J., 1990. Galvanic interactions during the leaching of gold in cyanide and thiourea solutions. *Miner. Eng.* 3 (6), 589-597.
- Wadsworth, M.E., 2000. Surface processes in silver and gold cyanidation. *Int. J. Min. Proc.* 58, 351-368.
- Wadsworth, M.E., Zhu, X., 2003. Kinetics of enhanced gold dissolution: activation by dissolved silver. *Int. J. Miner. Process.* 72, 301-310.
- Weichselbaum, J., Tumilty, J.A., Schmidt, C.G., 1989. The effect of sulfide and lead on the rate of gold cyanidation, in: Proceedings of The AusIMM Annual Conference, Perth/Kalgoorlie, Melbourne, Australia, pp. 221-224.
- Wet, J.R.D., Pistorius, P.C., Sandenbergh, R.F., 1997. The influence of cyanide on pyrite flotation from gold leach residues with sodium isobutyl xanthate. *Int. J. Min. Proc.* 49, 3-4, 149-169.
- White, A.F., Peterson, M.L., Hochella, M.F.Jr., 1994. Electrochemistry and dissolution kinetics of magnetite and ilmenite. *Geochim. Cosmochim. Ac.* 58, 8, 1859-1875.
- Wierse, D.G., Lohrengel, M.M., Schultze, J.W., 1978. Electrochemical properties of sulfur adsorbed on gold electrodes, *J. Electroanal. Soc.* 92, 121-131.
- Xianhai Mining, 2015. http://www.xinhaimining.com/en/product_11_41.html, (accessed on 05-06-2015).
- Xue, T., Osseo-Asare, K., 2001. Anodic behaviour of gold, silver, and gold-silver alloys in aqueous cyanide solutions, in: Young, C.A. Twidwell, L.G., Anderson, C.G., (Eds.), Cyanide: Social, Industrial and Economic Aspects, TMS, Warrendale, pp. 563-576.

- Yang, X., Moats, M.S., Miller J.D., 2010a. Using electrochemical impedance spectroscopy to investigate gold dissolution in thiourea and thiocyanate acid solutions. *ECS Trans.* 28, 6, 213-221.
- Yang, X., Moats, M.S., Miller, J.D., 2010b. The interaction of thiourea and formamidine disulfide in the dissolution of gold in sulfuric acid solutions. *Miner. Eng.* 23, 698-704.
- Yang, X., Moats, M.S., Miller, J.D., 2010c. Gold dissolution in acidic thiourea and thiocyanate solutions. *Electrochim. Acta* 55 (11), 3643-3649.
- Yannopoulos, J.C., 1991. The extractive metallurgy of gold. Van Nostrand Reinhold, New York.
- Zhang, Z., Leng, W.H., Cai, Q.Y., Cao, F.H., Zhang, J.Q., 2005. Study of the zinc electroplating process using electrochemical noise technique. *J. Electroanal. Soc.* 578, 357-367.
- Zhang, J., Shen, S., Cheng, Y., Lan, H., Hu, X., Wang, F., 2014. Dual lixiviant leaching process for extraction and recovery of gold from ores at room temperature. *Hydrometallurgy* 114-145, 114-123.
- Zhang, W., Jin, S., Ghali, E., Tremblay, R., Shehata, M., Es-Sadiqi, E., 2006. Corrosion behaviour of AZ91D and AJ62x magnesium alloys in chloride media. *Adv. Eng. Mater.* 8 (10), 973-980.
- Zheng, J., Ritchie, I.M., La Brooy, S.R., Sing, P., 1995. Study of gold leaching in oxygenated solutions containing cyanide-copper-ammonia using a rotating quartz crystal microbalance. *Hydrometallurgy* 39, 277-292.
- Zhou, J., Fleming, C.A., 2007. Gold in tailings - Mineralogical characterization and metallurgical implications, in: Proceedings of World Gold Conference 2007, 22-24 October, Cairns, Australia, AusIMM, pp. 311-317.
- Zlatev, R., Valdez, B., Stoytcheva, M., Ramos, R., Kiyota, S., 2011. Solution Conductivity Influence on Pitting Corrosion Studies by SVET. *Int. J. Electrochem. Sci.* 6, 2746-2757.
- Zurilla, R.W., Yeager, E., 1969. Oxygen electrode kinetics of gold. Technical Report: Electrochemistry Research, Laboratory, Case Western Reserve University, Cleveland, Ohio.

Appendix A Passive Behaviour of Gold in Sulphuric Acid Medium

Wei Zhang^{a*}, Ahmet Deniz Bas^a, Edward Ghali^a, Yeonuk Choi^b

^aDepartment of Mining, Metallurgical and Materials Engineering, Laval University, Quebec, Canada, G1V 0A6

^bBarrick Gold Corporation, Suite 3700, 161 Bay Street P.O.Box 212, Toronto, Ontario, Canada, M5J 2S1

Published in: *Trans. Nonferrous Met. Soc. China*, Elsevier, 25, 6, 2037-2046.

DOI: [10.1016/S1003-6326\(15\)63813-4](https://doi.org/10.1016/S1003-6326(15)63813-4)

Résumé

Le phénomène de passivation d'or (Au) en médium d'acide sulfurique est encore pas bien compris ; par conséquent, le comportement anodique de l'or pur par rapport au platine (Pt) en solution de H₂SO₄ a été examiné par différentes techniques électrochimiques pour un aperçu approprié. Les études de voltammétrie cyclique ont montré deux pics d'oxydation et un pic de film de réduction pour Au, tandis qu'une réaction de dégagement d'oxygène pour Pt. L'augmentation de la concentration de H₂SO₄ (0,5 à 1 mol / L) a doublé le pic de la densité de courant de l'or. L'augmentation de l'agitation a favorisé une zone passive sur l'Au, alors qu'il était négligeable sur Pt par des études potentiodynamiques. Les études potentiostatique (2 h) aux trois potentiels anodiques passifs dans 1 mol / L de H₂SO₄ ont montré que l'admittance d'Au a été plus faible à 1,4 V. Les mesures de bruit électrochimique pendant les périodes de désintégration (16 h) après la polarisation ont montré que le film mince passif formée lors de la polarisation potentiostatique a été dissout.

Abstract

Passive phenomenon of gold (Au) in sulphuric acid medium is still not well understood; hence anodic behaviour of pure Au as compared to platinum (Pt) in H₂SO₄ solutions was examined by different electrochemical techniques for an appropriate insight. Cyclic voltammetry studies showed two oxidation peaks and one film reduction peak for Au, while one oxygen evolution reaction for Pt. Increasing H₂SO₄ concentration (0.5 to 1 mol/L) caused 2 fold increases in peak current density of Au. Increase in agitation promoted passive zone on Au, while it was negligible on Pt by potentiodynamic studies. Potentiostatic studies (2 h) at three anodic passive potentials in 1 mol/L H₂SO₄ showed that the admittance of Au was found to be the lowest at 1.4 V. Electrochemical Noise Measurements during the decay periods (16 h) after polarization showed that the formed thin passive film during potentiostatic polarization has been dissolved.

Keywords: gold, passivation, sulphuric acid, electrochemical noise

Appendix B Electrochemical Study of Gold Cyanidation in the Presence of Roasted Gold Ore and Its Associated Oxide Minerals

Ahmet Deniz Bas^{a*}, Edward Ghali^a, Yeonuk Choi^b

^aDepartment of Mining, Metallurgical and Materials Engineering, Laval University, Quebec, Canada, G1V 0A6

^bBarrick Gold Corporation, Suite 3700, 161 Bay Street P.O.Box 212, Toronto, Ontario, Canada, M5J 2S1

Published in: 55th Annual Conference of Metallurgists (COM 2016), Electrometallurgy 2016 Symposium, Proceedings of XXVIII IMPC-Quebec, Canada, September 11-15, paper no 842.

Résumé

Le traitement de l'oxyde, par exemple les minerais d'or oxydés a reçu relativement moins d'attention que ceux sulfurés, récemment, le traitement des minerais d'or d'oxyde devient indispensable. Dans cette étude, l'influence du minerai d'or grillé (RGO) du minerai en suspension (à 35% ratio solide) lors de la dissolution électrochimique de l'or a été examinée à l'aide d'or pur et de minéraux d'oxyde de fer (hématite, maghémite et magnétite) comme électrodes à disque par zéro-résistance mode ampèremètre, soit dans un ou deux cellules séparés. La présence du minerai en suspension a diminué les courants galvaniques, c'est-à-dire, les vitesses de corrosion en raison de la libération et l'augmentation de la quantité d'espèces solubles et / ou insolubles qui pourraient retarder davantage le comportement anodique de l'or. Les courants galvaniques plus élevés ont été observés dans deux cellules séparés que dans un cellule indiquant l'importance primordiale des interactions galvaniques. Les résultats de MEB-EDX ont observé des revêtements de fer hydro / oxyde sur la surface d'or en cas de test de magnétite. Toutefois, en cas de l'électrode de RGO, la passivation n'est pas une parfaite, bien que la tendance légèrement décroissante a été observée lors de la dissolution de l'or. Ces résultats ont révélé que la passivation est non seulement un phénomène de laboratoire, mais aussi il pourrait être responsable du ralentissement de la dissolution de l'or dans la pratique industrielle.

Abstract

Treatment of oxide, e.g. roasted gold ores has received relatively less attention than sulphidic ones and recently, handling of oxide gold ores is becoming essential. In this study, the influence of roasted gold ore (RGO) slurry (at 35% solid ratio) on the electrochemical dissolution of gold has been examined using pure gold and iron oxide minerals (hematite, maghemite, and magnetite) as disc electrodes by zero-resistance ammeter mode either in one or two separate containers. The presence of slurry decreased galvanic currents, i.e. corrosion rates due to the release and increase in the amount of soluble and/or insoluble species that could retard further the anodic behaviour of gold. Higher galvanic currents were observed in two separate containers than that in one container indicating the primary importance of galvanic interactions. SEM-EDS results observed iron hydro/oxide coatings on gold surface in case of magnetite test. However, in case of RGO electrode it is not a perfect passivation, although somewhat decreasing trend was observed on gold dissolution. These findings have revealed that passivation is not only a laboratory phenomenon, but also it could be responsible for the slowdown of gold dissolution in industrial practice.

Keywords: Roasted gold ore, gold, cyanide, magnetite, maghemite, hematite

Appendix C Complimentary Activities during the Doctoral Formation

During the doctoral period, I have been involved in some activities such as:

C.1) I've been awarded the "[MetSoc's 2016 Gordon M. Ritcey Ph.D. Award](#)" by Hydrometallurgy Section of MetSoc of CIM, the first person from Laval University to receive this award.

C.2) I worked as "[Poster Chair](#)" in the Organising Committee of the 55th Annual Conference of Metallurgists (COM 2016) & 28th International Mineral Processing Congress (IMPC 2016) which was held in Quebec City, 11-15 September, 2016.

C.3) With the invitation of Dr. Barry Wills of MEI (Minerals Engineering International) (also Editor-in-Chief of Minerals Engineering), I have been interviewed as being the first in "[Rising Stars](#)" interview series.

C.4) I have done a series of [interviews](#) on metal extraction, [which](#) all can be [found](#) on MEI Online. For instance, Dr. [Yeonuk Choi](#), Director of Strategic Technology Solutions, at Barrick Gold Corporation, and [Engin Ozberk](#) (Past President of MetSoc) of the International Minerals Innovation Institute. I also wrote a technical report entitled "Field Trip to Gold Mines by Laval University and 25th CMPNOQ" published by [CIM Magazine](#), February issue, 2014.

C.5) I have also participated in two papers which are related to the metallurgy subjects:

i) Fathi Habashi, [Ahmet Deniz Bas](#), 2014. Evidence of the existence of anodic and cathodic zones during the leaching of minerals and metals. Hydrometallurgy, 144-145, 148-150. (DOI: [10.1016/j.hydromet.2014.02.002](#)).

ii) Fathi Habashi, [Ahmet Deniz Bas](#), 2016. Electrochemistry and mineral dissolution, 55th Annual Conference of Metallurgists, Electrometallurgy 2016 Symposium, Proceedings of XXVIII IMPC-Quebec, Canada, September 11-15, paper no 921.

C.6) I supervised three undergraduate students, involving closely with their laboratory test work during their internship periods.

Appendix D Scientific Publications

1. [Ahmet Deniz Bas](#), Edward Ghali, Yeonuk Choi. A review on electrochemical dissolution and passivation of gold during cyanidation in presence of sulphides and oxides. Revised version submitted to *Hydrometallurgy Journal*.
2. [Ahmet Deniz Bas](#), Fariba Safizadeh, Edward Ghali, Yeonuk Choi, 2016. Leaching and electrochemical dissolution of gold in the presence of iron oxide minerals associated with roasted gold ore. *Hydrometallurgy* 166, 143-153. (DOI:10.1016/j.hydromet.2016.10.001)
3. [Ahmet Deniz Bas](#), Wei Zhang, Edward Ghali, Yeonuk Choi, 2015. A study of the electrochemical dissolution and passivation phenomenon of roasted gold ore in cyanide solutions. *Hydrometallurgy*, 158, 1-9. (DOI:10.1016/j.hydromet.2015.09.020)
4. [Ahmet Deniz Bas](#), Liliana Gavril, Wei Zhang, Edward Ghali, Yeonuk Choi, 2015. Electrochemical dissolution of roasted gold ore in cyanide solutions. *Hydrometallurgy*, 156, 188-198. (DOI:10.1016/j.hydromet.2015.07.003)
5. [Ahmet Deniz Bas](#), Fariba Safizadeh, Wei Zhang, Edward Ghali, Yeonuk Choi, 2015. Active and passive behaviours of gold in cyanide solutions. *Transactions of Nonferrous Metals Society of China*, 25, 10, 3442-3453. (DOI: 10.1016/S1003-6326(15)63981-4)
6. Wei Zhang, [Ahmet Deniz Bas](#), Edward Ghali, Yeonuk Choi, 2015. Passive behaviour of gold in sulphuric acid medium. *Transactions of Nonferrous Metals Society of China*, 25, 6, 2037-2046. (DOI:10.1016/S1003-6326(15)63813-4)

Conference Presentations

- 1 [A. D. Bas](#), E. Ghali, and Y. Choi, 2016. Electrochemical study of gold cyanidation in the presence of roasted gold ore and its associated oxide minerals, 55th Annual Conference of Metallurgists, Electrometallurgy 2016 Symposium, Proceedings of XXVIII IMPC-Quebec, Canada, September 11-15, paper no 842.
2. [A. D. Bas](#), E. Ghali, and Y. Choi, 2015. A study of electrochemical interactions between gold and its associated oxide minerals, The LUCY ROSATO Memorial Symposium, 54th Annual Conference of Metallurgists (COM 2015), The Metallurgy and Materials Society of CIM, Toronto, Canada, August 23-26, paper no 8897.